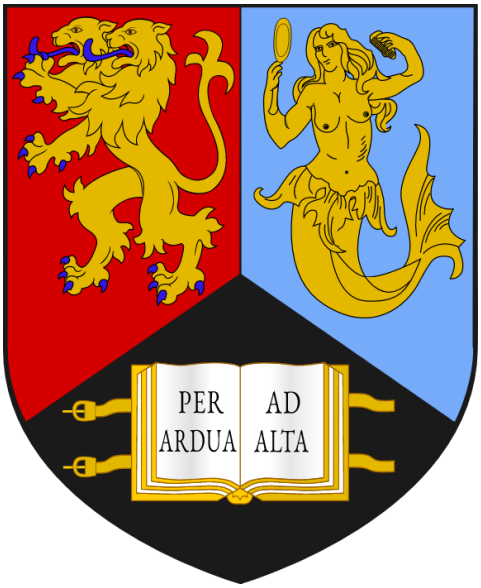

Optimising CAR-T cells for enhanced activity in the tumour microenvironment

Institute of Immunology and Immunotherapy

College of Medical and Dental Sciences

University of Birmingham

Nicola McJannett

2024

Acknowledgements

First and foremost, to my supervisor, Carmen, for your exceptional guidance, support and patience, which I relied on constantly throughout my PhD. To my colleague and mentor, Sarah Booth, for her encouragement and teaching me the CAR T ways. Both Carmen's and Sarah's time, energy, and perseverance over the last 4 years has been unwavering. My sincere thanks and gratitude to you both.

To our now Roche colleagues: Frank, thank you for your support and guidance during the first two years of my PhD and Stone, and thank you for sharing your invaluable knowledge.

Thank you, Nora, for all our tea breaks and for making the lab a livelier place.

To Robert and Sarah Martin, your funding made this research and PhD possible. I am so very grateful for the opportunity you afforded me. I hope this and my future work proves worthy of your generosity. I enjoyed our meetings, and I hope you did too.

Thank-you to Birmingham Genomics team, Birmingham metabolomics team and Birmingham Children's hospital for their work, and expertise that contributed this PhD.

To Joost Van Meerwijk, Cecile Apert, Anoop Chandran, and all my colleagues in Toulouse and in Adaptimmune, thank you for introducing me to academia and industry, and setting me up for all I have done since my time with you all was invaluable.

To my Mum - Lucy, Dad - Neal, and Brother -James, my indebted thanks for looking after me physically and mentally throughout every aspect of my career so far. To Tom, my thanks and love for always being there, no matter what, and patiently believing in me. All your love and support has kept me moving forward. Thank you forever.

Thank you, Helena, for all our meals out, games nights and mini breaks that brought me laughter and sanity during this time.

To all the people who I couldn't name but have supported me the last 4 years - thank you.

Abstract

Acute myeloid leukaemia is a cancer of the myeloid cells in the bone marrow. AML alters the bone marrow niche, creating an immunosuppressive microenvironment. AML increases tryptophan metabolism and cystine uptake. T-cells require sufficient nutrients to function. Due to a lack of clinical activity, CAR T-cell therapies are currently only used in a limited number of cancers. We hypothesised that the lack of nutrients in the AML microenvironment supresses CAR T-cell function.

This work discusses how the availability of tryptophan and cystine affected T-cell and CAR T-cell proliferation. We designed CAR T-cells with the overexpression of tryptophan or cystine transporters, SLC7A5 and SLC7A11, respectively. We first demonstrated that the addition of SLC7A5 and SLC7A11 to Jurkat CAR T-cells provided increased metabolic rates in low tryptophan and cystine environments, respectively. The addition of SLC7A5 and SLC7A11 to CAR T-cells increased tryptophan and cystine uptake, respectively. CAR T-cells with SLC7A5 or SLC7A11 overexpression had increased proliferation in low tryptophan and cystine environments, respectively. The CAR T-cells with overexpression of SLC7A5 and SLC7A11 improved cancer clearance in murine models. Performing RNA sequencing of CAR-T cells following interaction with tumour cells, we showed a significant alteration of pathways associated with T-cell activation, metabolism, and migration, caused by the addition of the transporters to the CAR T-cells. These results demonstrate that the addition of SLC7A5 and SLC7A11 could improve CAR T-cell function in low amino acid environments.

Contents

Table of Figures

Table of Abbreviations

Table 1: List of Abbreviations

Abbreviations	**Explanation**
4-1BB	Tumour necrosis factor ligand superfamily member 9
Akt	protein kinase B
AML	Acute Myeloid Leukaemia
APCs	Antigen Presenting Cells
APL	Acute promyelocytic leukaemia
ARG2	Arginase-2
ATCC	American Type Culture Collection
ATP	Adenosine triphosphate
BAM15	N5,N6-bis(2-fluorophenyl)-[1,2,5]oxadiazolo[3,4-b]pyrazine-5,6-diamine
B-cells	B-Lymphocytes
BCR	B-cell receptors
BM-MSCs	Bone Marrow Mesenchymal Stromal Cells
BRCA1	Breast Cancer gene 1
BRCA2	Breast Cancer gene 2
BSA	Bovine Serum Albumin
CAF	Cancer Associate Fibroblasts
CAR	Chimeric Antigen Receptor
CCL3	Chemokine Ligand 3
CCR7	C-C chemokine receptor type 7
CD	Cluster differentiation
CFSE	CarboxyFluorescein Succinimidyl Ester
CHOP	C/EBP homologous protein
c-myc	Cellular myelocytomatosis oncogene
CRS	Cytokine release syndrome
CRUK	Cancer Research UK
CSF2	Colony Stimulating Factor-2
CTLA-4	Cytotoxic T-Lymphocyte Associated 4
CXCR4	C-X-C chemokine receptor type 4
DAMPS	Danger-Associated Molecular Patterns
DC	Dendritic cell
DMSO	Dimethyl Sulfoxide
DN	Double Negative
DNA	Deoxyribonucleic acid
DP	Double Positive
E2F2	Early region 2 binding factor 2
ECAR	Extracellular Acidification Rate
ECL	Enhanced Luminol-Based Chemiluminescent
ECM	Extra Cellular Matrix
EDTA	Ethylenediaminetetraacetic acid
ELISA	enzyme-linked immunosorbent assay
ERG1	Early growth response protein 1

FACs	Flow-assisted cell sorting media
FBS	Foetal bovine serum
FDA	Food and Drug Administration
FOXP3	Forkhead box P3
GCN2	general control nonderepressible 2
GLUT1	Glucose transporter 1
GVHD	Graft Versus Host Disease
H3K9me	Histone H3 lysine-9 methylation
HLA	human leukocyte antigens
HSV-tk	Herpes Simplex Virus Thymidine Kinase
ICAM-1	Intracellular Adhesion Molecule 1
ICANS	Immune effector Cell-associate Neurotoxicity Syndrome
ICOSL	Inducible T-cell Costimulatory Ligand
IDO	Indoleamine 2,3-dioxygenase
IFN-α	Interferon alpha
IFN-γ	Interferon-Gamma
IL	Interleukin
IL7R	Interleukin-7 receptor
JAK	Janus Kinase
LAG3	Lymphocyte Activating Gene 3
LAT1	Large neutral Amina acid Transporter 1
Lck	Lymphocyte-specific protein Tyrosine Kinase
LFA-1	Lymphocyte Function Associate-1
LINC01281	long intergenic non-protein coding RNA 1281
LSC	Leukemic Stem Cells
LTA	Lymphotoxin-α
MACs	Magnetic assisted cell sorting
MAPK	mitogen-activated protein kinase
MDSC	Myeloid-Derived Suppressor Cells
MHC	Major Histocompatibility Complexes
mRNA	Messenger ribonucleic acid
mTEC	Medullary thymic epithelial cells
mTOR	Mammalian target of rapamycin
NDFIP2	Nedd4 Family Interacting Protein 2
NICE	National Institute for Health and Clinical Excellence
NSCLC	Non-small Cell Lung Cancer
OCR	Oxygen Consumption Rate
OX-40	Tumour Necrosis Factor Receptor Superfamily Member 4
PAMPs	Patterns on the surface of pathogens
PBMC	Peripheral blood mononuclear cells
PBS	Phosphate buffered saline
PD-1	Programmed Death-1
PD-L1	Programmed death-ligand 1
PI3K	Phosphoinositide 3-kinase

PRRs	Pattern Recognition Receptors
PVDF	Poly-1,1-difluoroethene
qPCR	Quantitative polymerase chain reaction
RDH10	Retinol dehydrogenase 10
RIPA	Radio immunoprecipitation assay buffer
ROS	Reactive oxygen species
scFv	Single Chain Variable Fragment
SLC3A2	Solute Carrier Family 3 Member 2
SLC7A11	Solute carrier family 7 member 11
SLC7A5	Solute carrier family 7 member 5
SLFN5	Schlafen 5
SLS	Scientific Laboratory Supplies
STAT4	Signal transducer and activator of transcription
T-cells	T-Lymphocytes
TCEP	Tris(2-carboxyethyl) phosphine)
TCR	T-cell receptors
TECs	Tumour Endothelial Cells
TGF-β	Tumour Growth factor-β
Th1	T helper 1
TIL	Tumour Infiltrating T-cells
TIM3	T-cell Immunoglobulin and Mucin Domain-containing Protein 3
TME	Tumour Microenvironment
TNF-α	Tumour necrosis factor-alpha
Treg	Regulatory T cells
V(D)J	Variable, Diversity and Joining Regions
V(D)J	variable, diversity, and joining
WHO	World Health Organisation
xCT	Cystine/glutamate transporter
ZAP70	Zeta-chain-associated protein kinase 70

1. Introduction

1.1 The Immune system

1.1.1 Introducing the Immune System

The immune system's most known function is to prevent infection by identifying and removing non-self-material such as pathogens. However, the immune system has many additional roles that are just as important, including removing dead cells, removing aberrant cells, preventing autoimmune responses, preventing foetal rejection during pregnancy and wound healing (Julier et al., 2017).

The immune system components include primary lymphoid organs, secondary lymphoid organs, lymphoid vessels, immune cells, cytokines, and antibodies. The primary lymphoid organs are the bone marrow and thymus, where immune cells develop, differentiate and mature. Secondary lymphoid organs such as the spleen, tonsils, lymph nodes, liver, and skin, are locations of extensive immune cell cross-talk and activation against pathogens. The immune system components must be highly coordinated to perform all the above-mentioned roles successfully and mount an effective immune response.

During evolution, the immune system developed in life forms in two stages: innate immunity around 1 billion years ago and adaptive immunity only some 450 million years ago (Martins et al., 2023, Marshall et al., 2018). The mechanisms of innate immunity are always present, circulating throughout the body, allowing for rapid and effective recognition and removal of most harmful materials within minutes or hours of their arrival. However, if the innate immune system is insufficient and cannot clear the harmful material by itself, it induces the activation of the adaptive immune system (Mirchandani et al., 2014, Iwasaki and Medzhitov, 2015).

1.1.2 Innate immunity

The innate immune system provides rapid non-specific responses and can be split into four components. The first components and lines of defence against infection are physical barriers to pathogen entry into the host, such as the skin, epithelial layers, and mucosal membranes. The next component of the innate immune system is physiological barriers, which eliminate pathogens through adverse conditions such as low pH and phagocytic cell enzymes found in stomach acid and saliva. The third component of the innate immune system is inflammatory barriers. These barriers are induced during cell stresses, including infection, resulting in the release of intracellular components that are recognised as markers of tissue damage and are known as danger-associated molecular patterns (DAMPs). These DAMPs activate the complement cascade, marking cells for destruction by other immune cells, recruiting immune cells to the site, and causing cell lysis. The DAMPs can be recognised by pattern recognition receptors (PRRs) on the surface of innate immune cells, causing innate immune cell activation. These inflammatory barriers can also be triggered by circulating innate immune cells, such as neutrophils, mast cells, eosinophils, and basophils, that will identify pathogens through PRRs that bind to pathogen-associated molecular patterns (PAMPs) on the surface of pathogens and then the innate immune cells release pro-inflammatory cytokines. These PRRs allow the innate immune system to recognise a wide range of pathogens as the PAMPs they recognise are commonly conserved small surface molecules found on the surface of a wide range of pathogens but are not present on host cells. The final component is phagocytosis, performed by specialised innate immune cells such as monocytes and neutrophils. Using the same

identification process described above, these cells identify the pathogens, internalise, and eliminate them by digestion, as depicted in Figure 1.

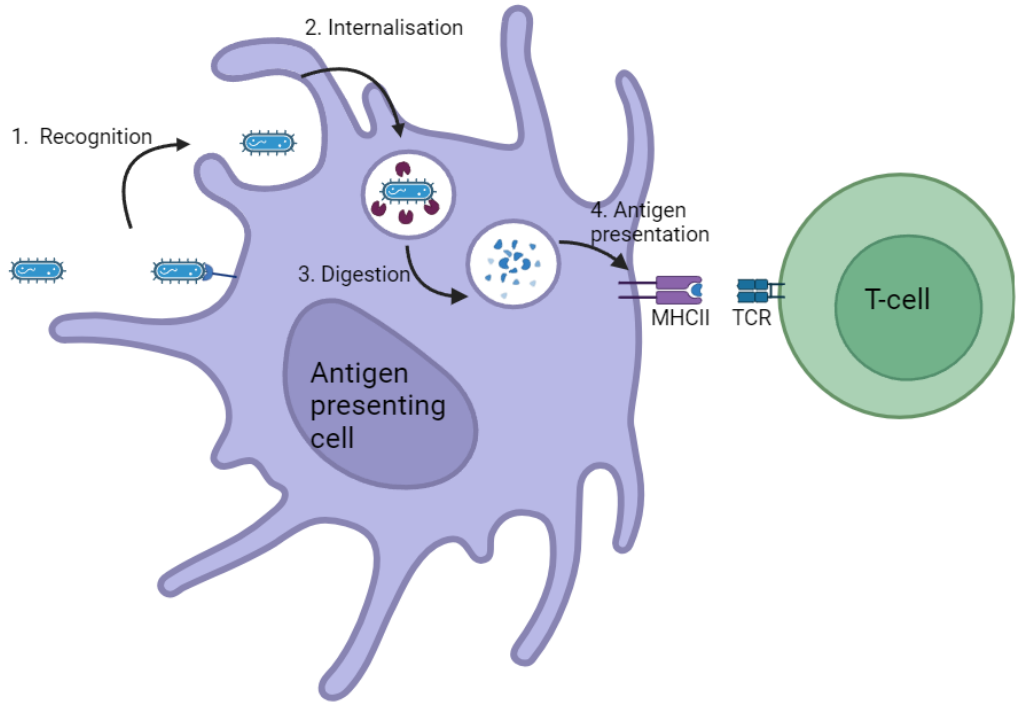

Figure 1: Antigen processing and presentation
Major histocompatibility complex two (MHCII), T-cell receptor (TCR). Diagram created in BioRender.

This process of phagocytosis also allows the innate immune cells to process protein fragments from the pathogen, known as antigens and present them to the adaptive immune system (Munz, 2011). This cross-talk between the two immune systems is crucial for an effective immune response to pathogens that cannot be eliminated by the innate immune system alone.

When activated, monocytes differentiate into macrophages and dendritic cells (DCs), which are collectively called antigen-presenting cells (APCs). APCs are immune cells that express class two major histocompatibility complexes (MHCII) designed to effectively present these engulfed pathogen derived antigens to the adaptive immune system for screening, as shown in Figure 1.

1.1.3 Adaptive immunity

The adaptive immune system comprises two cell types derived from a common lymphoid cell progenitor: B-lymphocytes (B-cells) and T-lymphocytes (T-cells). These lymphocytes have receptors allowing each cell to recognise a specific antigen and produce a tailored response to that antigen. These receptors differ for B-cells and T-cells; B-cells have B-cell receptors (BCRs), and T-cells have T-cell receptors (TCRs). These cells have a screening process to identify their specific antigen and then mount a response to that antigen, which is a much slower process than that of the innate immune system. This slower response means the adaptive immune system can take days or weeks to establish a meaningful response to a pathogen. However, once the adaptive immune system has been exposed to a pathogen, it develops memory cells that react faster and develop a stronger response to that antigen upon re-exposure.

B-cells are immune cells that develop in the bone marrow, migrate into the bloodstream, and typically reside in secondary lymphoid organs. When activated against specific target antigens, such as proteins on pathogens or toxins pathogens have produced, B-cells differentiate into effector B-cells, memory B-cells, or regulatory B-cells. Effector B-cells can produce proteins known as immunoglobulins. These immunoglobulins bind to the specific target antigens, covering them and marking them for phagocytosis, known as opsonisation. Immunoglobulins can also activate the complement system, causing cell lysis and immune cell recruitment. Effector B-cells also release important cytokines for the recruitment, activation, and differentiation of other immune cells, and they can act as APCs. Memory B-cells are essential for providing quicker responses during re-exposure to an antigen by allowing faster effector B-cell clonal expansion and immunoglobulin production. Conversely, regulatory B-cells inhibit the immune response by producing immunosuppressive cytokines.

T-cells are immune cells that start developing in the bone marrow but migrate to the thymus to undergo extra development and maturation. Like B-cells, upon T-cells recognising a specific antigen, they differentiate into cytotoxic, memory, helper and regulatory T-cells. Cytotoxic T-cells, when activated, release cytokines that induce cell death upon the target cells. Helper T-cells are required for most adaptive immune responses and have several subgroups that provide different responses using various signalling pathways. Depending on the subgroup of T helper cells, the signalling proteins presented to the immune cells will differ, promoting different types of innate and adaptive immune cells to be activated, shaping the response to the target antigens. Memory T-cells, like memory B-cells, provide a swifter immune response when re-exposed to an antigen. Regulatory T-cells (Treg) recognise host cells to prevent autoimmune responses and regulate immune responses to prevent chronic inflammatory diseases (Vignali et al., 2008).

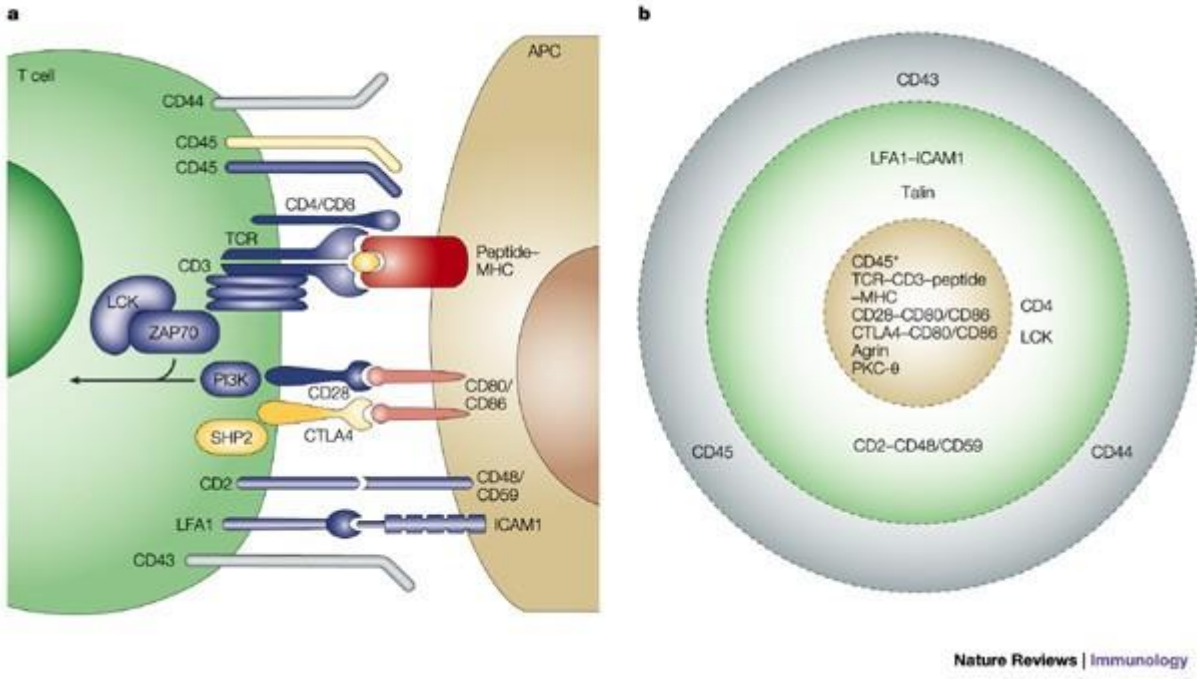

Figure 2: Diagram of the interactions required to form the immunological synapse.
Taken from (Huppa and Davis, 2003)

1.1.6 T-cell co-stimulation

The conditions in which T-cells are activated can determine the differentiation pathway the naïve T-cells will take. T-cells can also be put into a state of anergy or apoptosis in response to the binding of their TCR to a complementary MHC-antigen complex.

As depicted in Figure 4, whilst present on the cell surface, the TCR (transmembrane region, a constant region and a variable region) is associated with a CD3 molecule, which is used to begin a signalling cascade through zeta-chain-associated protein kinase 70 (Zap70). However, this signalling will only occur during a TCR-antigen MHC complex interaction if the T-cell forms an immunological synapse, which is composed of the TCR-antigen MHC complex and surrounding complexes that provide essential costimulatory interactions, enabling the T-cell to activate successfully.

As depicted in Figure 4, the immunological synapse stabilises the cell-to-cell interaction and provides supporting signals to promote T-cell activation. The immunological synapse includes the interaction of adhesion receptors and costimulatory signals, as shown in Figure 4. As previously mentioned, CD28 on T-cells bound to CD80/CD86 on APCs provides essential signalling to support the signals received from the bound TCR. Some of the well-established interactions at this immunological synapse, as shown in Figure 4, include lymphocyte function associate-1 (LFA-1) on T-cells complexed with intracellular adhesion molecule 1 (ICAM-1) on APCs, CD4/CD8 interaction with the MHC complex and, CD45 interaction with the lymphocyte-specific protein tyrosine kinase (Lck) (Shah et al., 2021a). The CD28 to CD80/CD86 interaction provides essential costimulatory signalling through protein tyrosine kinase phosphorylation, which promotes T-cell survival, activation, and interleukin-2 (IL-2) production (Ogawa et al., 2013). The LFA-1-ICAM-1 provides prolonged TCR-MHC binding, ensuring sufficient interaction time for the transmission of activation signalling (Ma et al., 2022). During the binding of the TCR-MHC complex, CD45 promotes the phosphorylation of the molecule Lck, allowing the protein tyrosine kinase ZAP70 to bind to CD3 (Rossy et al., 2012). CD4 or CD8 cooperatively bind to the antigen-MHC complex with the TCR, enabling increased TCR docking and a more robust interaction between the antigen-MHC complex compared to the interaction between TCR and the antigen-MHC complex alone (Rushdi et al., 2022, Jiang et al., 2011).

1.1.4 TCR generation

T-cells start in the bone marrow as common lymphoid progenitor cells that migrate to the thymus, where the majority of their development occurs. These early development stage thymocytes are known as double negative (DN) T-cells as they do not express cluster differentiation 4 (CD4) or CD8 on their surface, which are upregulated later in the maturation process and are mutually exclusively expressed on all adult T-cells. CD4 and CD8 are important co-receptors that bind to MHC complexes, stabilising the TCR MHC complex. CD4 binds to MHC class 2 (present on APCs), and CD8 binds to MHC class 1 (present on all nucleated cells). The thymus is a primary lymphoid organ in the thoracic cavity and has two regions: the cortex and the medulla. The intersection of these two regions is known as the cortico-medullar junction (Shah and Zuniga-Pflucker, 2014).

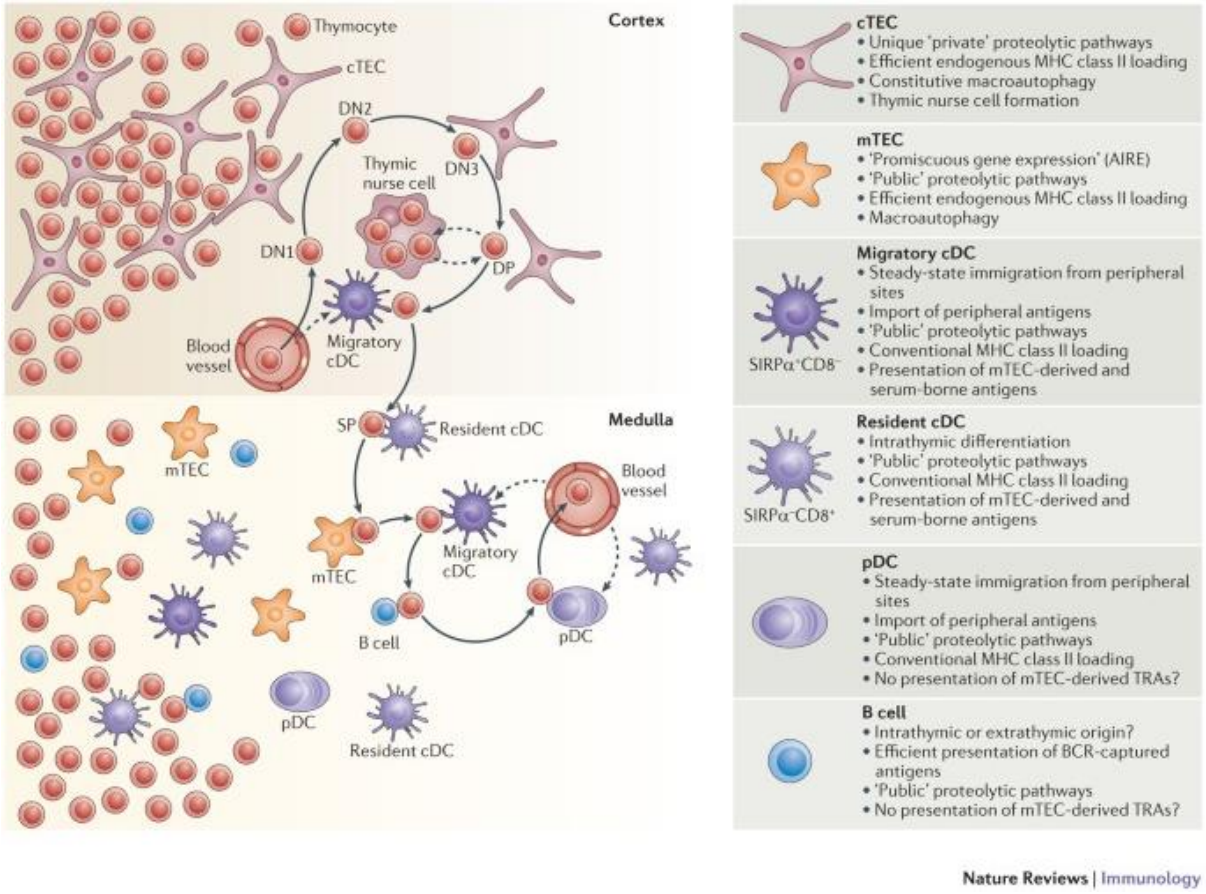

Figure 3: T-cell development and cell to cell interactions in the thymus.
Taken from (Klein et al., 2014)

The cortico-medullary junction is where the common lymphoid progenitors enter the thymus. The common lymphoid progenitors migrate to the cortex, become thymocytes and start developing their TCR by randomly generating a pre-TCRβ chain through rearrangement of the variable (V), diversity (D), and joining (J) regions called V(D)J regions of the gene segments by V(D)J recombinase. V(D)J recombinase recognises deoxyribonucleic acid (DNA) sequence elements located next to each of the V(D)J regions, known as recombinant signal sequences (Schatz and Swanson, 2011). This pre-TCRβ chain binds with a pre-TCRα chain and CD3 molecule to form a pre-TCR. Pre-TCRs can interact with cortical thymic epithelial cells for the first stage of screening, known as β-selection, which occurs at DN3, as shown in Figure 2 (Klein et al., 2014). The thymocytes with TCR β chains that are determined to be correctly interacting with the MHC complex will receive anti-apoptotic signalling, proliferate, and pass to the next stage of development (Kreslavsky et al., 2012). Without this successful binding, the thymocytes will die of apoptosis as these cells require anti-apoptotic signalling to survive. After β-selection, the thymocytes upregulate CD4 and CD8 expression and are known as double-positive (DP) cells. These DP cells undergo the V(D)J recombination for the TCR α chain to complete their TCR. Then, with their completed TCR, these thymocytes migrate through the cortex, interacting with cortical thymic epithelial cells undergoing positive selection. Positive selection ensures that the completed TCR has a sufficient binding affinity to the MHC and will upregulate the chemokine receptors, allowing these cells to migrate to the medulla. Once in the medulla, the thymocytes downregulate either CD4 or CD8 expression, locking them in as single positive cells that either interact with all cells or only APCs. Again, any thymocytes which cannot fulfil this requirement will undergo apoptosis due to a lack of anti-apoptotic signalling. These single positive cells then begin the process of negative selection. The negative selection phase eliminates TCRs that are reactive to self-peptides.

In the thymic medulla, the thymocytes interact with medullary thymic epithelial cells (mTEC), which can express proteins from a broad range of peripheral cells, enabling them to express a broad range of self-peptides to the thymocytes. The interaction of mTEC and thymocytes is the next selection process, known as negative selection. This time, the strength of the interaction between the TCR and self-peptide MHC complex must land within the Goldilocks threshold region; it must not be too strong or too weak, as shown in Figure 4. If the interactions are too weak, the thymocytes will not provide enough interaction with the MHC complex to screen the peptides effectively and, therefore, die due to neglect, as depicted in Figure 3. Interactions that are too strong indicate that the thymocytes are unsuitable as they would be self-reactive, leading to autoimmune responses if they were let out into circulation. Therefore, thymocytes that do exceed this threshold will either be differentiated into regulatory T-cells or undergo apoptosis.

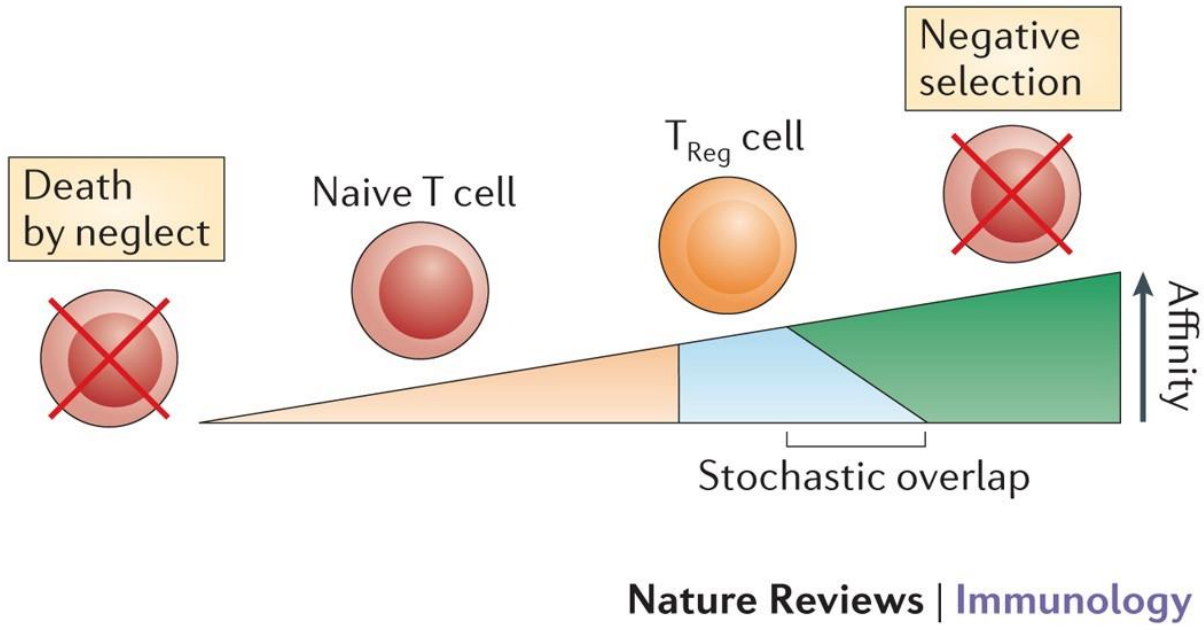

Figure 4: Diagram of negative selection goldilocks threshold region required for T-cell selection.
Taken from (Klein et al., 2014).

After negative selection, the thymocytes become naive T-cells and can migrate to secondary lymph organs and circulate throughout the body, ready for surveillance and, ultimately, activation.

1.1.5 Antigen recognition and T-cell activation

Each TCR can recognise only one specific antigen through specific antigen binding. As described above, during their development, these cells undergo rigorous selection processes that define the acceptable strength of the interactions these receptors can have with their targets. Therefore, the MHC molecules, whilst bound to the target antigen, will form complexes of sufficient strength with a TCR that is reciprocal for that antigen, fulfilling the first requirement during the start of the activation process for the T-cell. The stimulation solely of an antigen or the MHC complex is insufficient to elicit the activation of T-cells; the antigen-MHC complex needs to interact with the BCR or TCR. However, TCR stimulation must occur alongside costimulatory signalling, such as through CD80/CD86 on an APC to CD28 on T-cells for successful T-cell activation (Chambers and Allison, 1997).

1.1.7 T-cell differentiation

Naïve T-cells, when they leave the thymus to circulate the body, can differentiate into several types of T-cells with different functions, proliferative capacity, metabolism, ability to self-renew, and cytotoxicity against their target. This differentiation is determined by a few factors, including the strength of the activating stimulation, engagement of the costimulatory elements, the immune cells present, the amino acids, and the cytokines present during activation (Shah et al., 2021a, Lee et al., 2013, Martinez-Mendez et al., 2022).

Naïve T-cells can differentiate into effector T-cells, effector memory T-cells, central memory T-cells, resident memory T-cells, stem cell memory T-cells, and regulatory T-cells.

Effector memory T-cells persist in peripheral organs and vascular circulation to protect against future infections. Central memory T-cells persist in lymphoid organs and vascular circulation to protect against future infections. Resident memory T-cells are located in mucosal tissues and provide a first line of defence from infection (Thom et al., 2015). Stem cell memory T-cells protect against future infections for decades after the initial antigen exposure (Fuertes Marraco et al., 2015).

Effector $CD8^+$ T-cells, upon activation, eliminate target cells through target cell interactions via the expression of Fas ligand, which stimulates death in Fas-expressing cells. $CD8^+$ T-cells secrete cytotoxic granules containing a variety of cytotoxic molecules such as perforins, granzymes, cathepsin C and granulysin (Raskov et al., 2021). These cytotoxic proteins create pores in the target cell membrane and cause DNA fragmentation, leading to target cell death (Smyth et al., 2001).

Effector $CD4^+$ T-cells are divided into subgroups called T helper 1 (Th1), Th2, Th9, Th17, Th22, and T Follicular Helper Cells (Tfh). Each of these $CD4^+$ T-cells produces a different profile of cytokines (Golubovskaya and Wu, 2016). Th1 cells clear viruses and intracellular bacteria. Th2 cells recruit other immune cells to protect against parasites. Th17 cells protect against extracellular bacteria. Tfh cells reside in secondary lymphoid organs and assist the function of specialised microstructure called germinal centres that specialise in B-cell responses (Xia et al., 2023). The final phenotype discussed here is regulatory T-cells that suppress the immune response to inhibit autoimmune or over-reactive immune responses to maintain immune homeostasis (Apert et al., 2022, Wong et al., 2021).

homeostasis (Apert et al., 2022, Wong et al., 2021).

1.1.8 Mechanisms of T-cell homeostasis

An essential part of the immune response is immune homeostasis. Immune responses must be strong enough to eliminate pathogens but not react to self-antigens, balancing tolerance with over-reactive responses. The immune system must also eliminate cancer cells, originating solely from host cells without reacting to healthy cells, balancing cancer elimination and autoimmunity. Immune homeostasis starts during immune cell development, known as central tolerance. Innate immune cells' pattern recognition receptors only recognise antigens not expressed on host cells. Adaptive immune cells go through a selection process to remove any self-reactive cells or divert them to be regulatory T-cells. However, even if some self-reactive adaptive immune cells escape the selection process, peripheral tolerance can divert these cells' differentiation into a regulatory phenotype or eliminate them (Wong et al., 2021).

Self-reactive naïve T-cells that escape thymic development without being converted into regulatory T-cells when activated can still be differentiated into induced regulatory T-cells (Campbell et al., 2020). Differentiation into induced regulatory T-cells occurs if the T-cells TCR is activated with sub-optimal co-stimulation and in the presence of cytokines Tumour growth factor-β (TGF-β) and IL-2 (Li et al., 2023). Tregs will inhibit self-reactive T-cells through 4 mechanisms of action, including inhibitory cytokine secretion, cytolysis, metabolic disruption, and modulation of dendritic cell function. Secretion of inhibitory cytokines such as IL-10, IL-35, and TGF-β inhibits phagocyte function, suppresses T-cell proliferation, and differentiates T-cells into Tregs (Ness et al., 2021). Tregs cause cytolysis through the secretion of Granzyme B (Loebbermann et al., 2012, Ulbar et al., 2020). Tregs metabolically disrupt T-cell function by upregulating amino acid-depleting enzyme arginase II to reduce the environmental arginine

availability, an amino acid crucial for T-cell proliferation (Lowe et al., 2019). Tregs modulate DC function by upregulating Cytotoxic T-Lymphocyte Associated protein 4 (CTLA-4), a receptor with a higher affinity for CD80/CD86 than CD28. The binding of CD80/CD86 by CTLA-4 down-regulates CD80/CD86 expression, preventing T-cell CD28 co-stimulation and thus inhibiting T-cell activation (Chen et al., 2017).

Activated T-cells upregulate immune checkpoint receptors that, when stimulated, cause T-cell exhaustion. T-cell exhaustion is where immune checkpoint receptors are activated, or repeated antigen exposure leads to the inhibition of T-cell activation, differentiation, and function (Scharping et al., 2021). T-cell exhaustion is a part of normal T-cell homeostasis to prevent overactive immune responses. There are many regulatory immune checkpoint inhibitors, such as Programmed death-1 (PD-1), Lymphocyte-activating gene 3 (LAG3), and T-cell immunoglobulin and mucin domain-containing protein 3 (TIM3). PD-1 is an immune checkpoint upregulated on activated T-cells, and its ligand, programmed death-ligand 1 (PD-L1), is expressed on APCs, non-hematopoietic cells and tumours (Freeman et al., 2000, Li et al., 2021). PD-L1 binding to PD-1 causes inhibition of T-cell function by clustering directly with TCR, inhibiting TCR phosphorylation and signalling (Yokosuka et al., 2012, Takehara et al., 2021). LAG3 is a CD4 homolog that binds to peptide-bound MHC class 2 molecules, preventing the stabilisation of the TCR MHC class interaction (Maruhashi et al., 2018). TIM3 ligands are soluble lectin galectin-1 and carcinoembryonic antigen-related cell adhesion molecule-1. The downstream signalling of TIM3 is not well elucidated, but it is known that TIM3 is recruited during immune synapse formation and, if activated, will reduce the synapse stability (Wolf et al., 2020, Clayton et al., 2014).

The immune checkpoint receptors that these therapies target are not always exclusive to T-cells. PD-1 is expressed on natural killer cells, tumour-associated macrophages, tumour cells, and B-cells (Kim and Ha, 2021). LAG-3 is expressed on DCs (Huo et al., 2022). Although these immune checkpoint receptors are designed to prevent excessive immune reactions, these mechanisms have been abused by the tumour microenvironment (TME) to promote tumour growth and suppress anti-tumour immune activity.

Tolerogenic DCs differentiate from monocytes when they come into direct contact with regulatory and activated helper T-cells in the presence of IL-10 and TGF-β (Zhang et al., 2020b). Tolerogenic DCs have low expression of costimulatory molecules and high anti-inflammatory cytokine expression. Tolerogenic DCs differentiate naïve T-cells into regulatory T-cells via IL-10 and TGF-β.

These mechanisms of homeostasis are often taken advantage of by cancers to ensure their survival.

1.2 Cancer

1.2.1 Introduction to Cancer

Cancer is an extensive and varied group of diseases categorised by uncontrolled division of cells. Cancer is the second leading cause of premature death worldwide (Bray et al., 2021). Cancer is a non-communicable disease, and each individual has different risk factors such as genetics, age, carcinogen exposure, and weight that can contribute to the percentage chance of whether an individual develops cancer. Cancer can occur in almost any cell in the body and thus has a variety of causes, symptoms, and severity. Therefore, there is no common solution to the treatment of all cancers. However, currently, most cancers are treated using a combination of surgical removal of the cancer, radiotherapy, and chemotherapy. Since cancer is the second leading cause of death worldwide, it is clear that these three treatment options do not always provide a sufficient solution. Therefore, researchers, in the hope of improving outcomes, have continued to develop a range of alternative treatments to replace or to be used in conjunction with pre-existing treatments. Recently, these treatments have become more specific to the type of cancer they target. One example of this is hormone therapies; breast cancers and prostate cancers rely heavily on hormones for their growth, so there are hormone therapies that suppress hormone production or inhibit hormone signalling to shrink the cancer before surgery or be used to prevent relapse after surgery (Cold et al., 2022, Liu et al., 2021). However, these treatments would not affect cancers that do not rely heavily on these hormones for their growth.

1.2.2 Oncogenesis

DNA damage occurs daily as a consequence of exposure to exogenous agents (ultraviolet light, asbestos, viral insertion), endogenous agents (reactive oxygen species (ROS), nitrogen oxygen species), and erroneous DNA synthesis (nucleotide misincorporations during

replication or repair) (Schumacher et al., 2021). However, despite the damage cell DNA is exposed to, DNA sequences have high replicative fidelity between cells and their daughter cells, and mutation is rare because of the extensive mechanisms of protection in place. The mechanisms prevent DNA damage, prevent DNA alteration, repair DNA damage, and maintain conservation during replication, and if the DNA damage is deemed irreparable, cells will undergo apoptosis. However, in rare cases, these protection mechanisms fail, and cells with a mutation can continue to grow and proliferate, passing the mutation on to their daughter cells. These mutations can be benign and not affect the cell phenotype or function, known as carrier mutations. However, mutations known as driver mutations make the cells more prone to developing into cancerous cells (Mack et al., 2020).

There is no single mutation or series of mutations that cause cancer; even within the same type of cancer, the progression of mutations varies, as they are non-communicable diseases that occur due to random mutations. During progression towards cancer, a healthy cell acquires chance or inherited genetic mutations that induce genomic instability and mutation through genetic mutations that negatively impact the efficacy of the cell's DNA repair machinery. When a cell's DNA repair machinery is damaged, the cell and its daughter cells enter an evolution-like process. These cells acquire random genetic mutations at an increased rate and undergo natural selection to determine which mutations survive. The tumour protein 53 gene, which encodes the p53 protein that inhibits the cell cycle to enable DNA repair and apoptosis of cells with DNA damage, is commonly mutated in many cancers (Olivier et al., 2010, Grob et al., 2022). The breast cancer gene 1 (BRCA1) and BRCA2 genes help repair DNA by arresting the cell cycle, and the inheritance of mutations in these genes is well described as leading to increased rates of breast cancer and prostate cancer in populations with these mutations (Yarden et al., 2002, Andreassen et al., 2021).

The progression of normal cells to cancerous cells is a heterogeneous multistep process of genetic mutations that provide the cells with several universal characteristics they require to be cancerous. These characteristics, known as the "Hallmarks of cancer", were first compiled by Hanahan and Weinburg (Hanahan and Weinberg, 2000). They were a list of 6 traits that most, if not all, cancers acquire during development. Hanahan and Weinburg expanded this to 10 hallmarks in 2011 (Hanahan and Weinberg, 2011). These hallmarks are sustaining proliferative signalling, evading growth suppressors, activating invasion and metastasis, enabling replicative immortality, inducing angiogenesis, resisting cell death, avoiding immune destruction, deregulating cellular energetics, genome instability and mutation, and tumour-promoting inflammation. Together, these characteristics enable uncontrolled replication and the evasion or inhibition of all processes that would suppress that replication.

1.2.3 Elimination equilibrium escape

Despite cells that have the potential to become cancerous cells being generated in the body regularly, the immune system recognises them as abnormal cells and eliminates them before they become cancer. The immune system's role in cancer clearance has been apparent from early reports of spontaneous cancer clearance in patients with bacterial infections (McCarthy, 2006, Ottaiano et al., 2021). However, the immune system's mechanisms to eliminate cancerous cells are not always effective. Consequently, these cells may either develop an equilibrium with the immune system or manage to escape it entirely and develop into cancer (Dunn et al., 2004). Benign tumours are cancerous cells that develop an equilibrium with the immune system so the cancer cannot expand or metastasise, but the immune system cannot eliminate the cancerous cells.

1.2.4 Development of the tumour microenvironment

During the growth of cancer, a tumour microenvironment develops. The tumour microenvironment consists of stromal cells, endothelial cells, extracellular matrix, cytokines and immune cells. During cancer development, tumours become either "hot" or "cold" tumours. This label of hot or cold refers to the presence of immune cells in the tumour; a tumour with many immune cells is "hot", whereas tumours without immune cell infiltration are called "cold" tumours (Newman et al., 2020). The presence of the immune system in tumours, such as tertiary lymphoid structures (hubs of immune cell interactions formed at sites of persistent inflammation), correlates with improved patient outcomes (Zhao et al., 2021). However, immune cell presence is not always an indicator of improved outcomes, as high regulatory T-cell populations in the tumour microenvironment correlate with a poor prognosis (Bergsland et al., 2022).

Many factors generated by tumour cells lead to the development of the tumour microenvironment. Tumour endothelial cells (TECs) are endothelial cells that encourage angiogenesis in the tumour microenvironment in response to the tumour cells inducing hypoxia (Kondoh et al., 2013, Mao et al., 2019). Hypoxia causes T-cell dysfunction and exhaustion (Liu et al., 2020, Bannoud et al., 2021). TECs can alter the type of immune cells entering the tumour microenvironment, favouring regulatory T-cell infiltration compared to activated $CD8^+$ T-cells by increasing cell adhesion molecule production, such as endothelial adhesion molecule and cell barrier molecule. These cell adhesion molecules can also inhibit the function of activated T-cells that have infiltrated into the tumour microenvironment (Markel et al., 2006, Chae et al., 2018).

The TME interactions with fibroblasts, connective tissue cells that support and connect tissue within the body, cause them to alter their function to support cancer survival, resulting in

fibroblast differentiation into cancer-associated fibroblasts (CAF) (Mayer et al., 2023). In ovarian cancer, the cancer cells produce TGF-β, which causes CAF to secrete cytokines that promote glycolysis in cancer cells (Curtis et al., 2019).

The extracellular matrix (ECM) is material secreted by cells that provides structural support to cells. It is well-documented in cancer that the ECM is dysregulated and poorly structured, enabling a cancer-supporting niche that increases tumour cell survival signalling and migration into the vascular system (Paszek et al., 2014, Han et al., 2016, Cheung et al., 2024). The production of a high-density extracellular matrix can limit immune cell migration into the cancer cell sites and reduce immune cell proliferation (Kuczek et al., 2019). CAF modulate the ECM composition, resulting in poorer prognosis, such as the production of lysyl oxidase enzyme by CAF in gastric and breast cancer that crosslinks collagen I—the increase of collagen I by CAF results in increased metastasis and poorer prognosis (Li et al., 2019, Ramos et al., 2022). CAF secrete matrix metalloproteinase-9 that degrades elastin, collagens and the chemokines that attract T helper cells (Taguchi et al., 2014, Denney et al., 2009).

Immunosuppressive cytokines such as IL-10 and TGF-β are produced by cancer-associated fibroblasts, and regulatory T-cells (Jarnicki et al., 2006, Takahashi et al., 2017). TGF-β can convert naïve T-cells into induced Treg, prevent DC recirculation into lymph nodes by downregulating C-C motif chemokine 7 (CCR7) on DC, and convert fibroblasts into CAF (Yoon et al., 2021).

IL-35 is an immunosuppressive cytokine that is produced by Tregs and cancer cells that is upregulated in the tumour microenvironment, suppresses T-cell proliferation, and promotes Treg function (Collison et al., 2007, Sullivan et al., 2020, Ren et al., 2023). IL-35 promotes tumour metastasis (Huang et al., 2017, He et al., 2021).

1.2.5 Metabolic switch and nutrition depletion

Cancers alter their metabolism, switching from oxidative phosphorylation to glycolysis to provide enough energy, substrates, and nutrients to sustain their excessive levels of proliferation. This altered metabolic state was defined as deregulating cellular energetics by the hallmarks of cancer, as stated by Hanahan and Weinberg 2011 (Hanahan and Weinberg, 2011). Although glycolysis has a lower glucose-to- Adenosine triphosphate (ATP) efficiency rate, cancer cells often switch to glycolysis and instead upregulate glucose transporters such as glucose transporter 1 (GLUT1) and sodium-glucose co-transporter-2, to increase glucose uptake to compensate for the lower efficiency (Zambrano et al., 2019, Zhou et al., 2020a). The increased glucose uptake by cancer cells restricts glucose availability to T-cells, which is essential to effector T-cell proliferation, ultimately leading to reduced effector T-cell proliferation and cytokine production (Chang et al., 2013, Fu et al., 2023).

This metabolic switch also alters the availability of certain amino acids in the tumour microenvironment. Many cancers increase arginine uptake by increasing arginine transporter cationic amino acid transporter 1, which promotes cancer cell proliferation and survival (Lu et al., 2013, Werner et al., 2019, You et al., 2022). Cancers also upregulate arginine enzymes, such as arginase II (Arg2), which further depletes the microenvironment of arginine, resulting in the development of an immunosuppressive environment as immune cells rely on arginine for proliferation and survival (Mussai et al., 2015a, De Santo et al., 2018).

Glutamine is another amino acid essential to many tumours proliferation and survival. Glutamine is the most abundant amino acid in blood and tissues. Usually, glutamine is used for oxidative phosphorylation. However, in cancers, glutamine is used to produce glutathione and nicotinamide adenine dinucleotide phosphate, all of which are used to protect against ROS (Gregory et al., 2019). Glutamine ROS clearance capabilities are important as cancer cells'

constant proliferation causes increased ROS production. Glutamine is also used to generate asparagine, which is used for the biosynthesis of nucleotides (Krall et al., 2016, Nilsson et al., 2020). Therefore, without glutamine, cancer cells cannot proliferate (Gwangwa et al., 2019).

1.3 Immunotherapies

Immunotherapies have generated considerable interest in the research community as they promote the patient's immune system to recognise and eliminate cancer. These can be potent tools, but each type of immunotherapy has complications that must be acknowledged.

1.3.1 Immune checkpoint inhibitor therapy

Immune checkpoint inhibitor therapies, such as anti-PD-1, anti-CTLA-4 and anti-LAG3 therapies, block the T-cell surface receptors involved in immunosuppressive signalling. Blocking these receptors prevents the tumour microenvironment from inhibiting T-cell function, restoring T-cell function.

These therapies have shown great success, and combinations of immune checkpoint therapies have been approved by the Food and Drug Administration (FDA) for multiple cancers and have become part of first-line therapies for several cancers (Lu et al., 2022). Nivolumab (anti-PD1) and Ipilimumab (anti-CTLA-4) were approved for use in metastatic melanoma in 2015, renal clear cell carcinoma and colorectal cancer in 2018, hepatocellular carcinoma, non-small cell lung cancer (NSCLC), and urothelial mesothelioma in 2020 (Lu et al., 2022). These treatments have excellent response rates; in renal cancer, the use of Nivolumab and Ipilimumab have a 75% higher overall survival than Sunitinib (the previous first-line treatment for renal cancer) (Motzer et al., 2018, Kooshkaki et al., 2020).

Anti-LAG3 immunotherapy, Relatlimab, became the first anti-LAG3 therapy to be FDA-approved for metastatic melanoma and is in further clinical trials to be used in NSCLC (NCT01968109) (Chocarro et al., 2022). Several anti-LAG3 therapies are currently in clinical trials for various cancers, as LAG3 is a promising candidate for becoming an immune checkpoint inhibitor (NCT03489369, NCT02658981).

1.3.2 Cytokines

Cytokines are crucial to directing immune cell responses and can promote anti-tumour activity; therefore, the modulation of cytokine availability as immunotherapies has been researched. The FDA has approved two cytokine therapies: IL-2 and Interferon-α (Berraondo et al., 2019). IL-2 was approved by the FDA in 1998 and can be used to treat renal carcinoma and metastatic melanoma (Atkins et al., 1999, Fyfe et al., 1995). IFN-α was approved for use in 2011 and approved for the treatment of hairy cell leukaemia, renal cell cancer, follicular non-Hodgkin lymphoma, Kaposi's sarcoma and melanoma (Herndon et al., 2012). These therapies are used in conjunction with other therapies, such as chemotherapy.

1.3.3 Cancer vaccines

There are three types of cancer vaccines: pre-defined antigen, ex vivo anonymous antigen and in situ anonymous antigen vaccines (Lin et al., 2022). In ex vivo anonymous antigen vaccines, cancerous tissue is extracted and loaded into patient APCs to be injected back into the patient. In in-situ cancer vaccines, the cancer is induced to release antigens through immunogenic cell death, leading to APC recruitment and activation. In pre-defined antigen vaccines, antigens are pre-selected and determined by cancer-specific mutations; these can be antigens shared across many patients or antigens specific to one patient. The cancer vaccines developed so far have been shown to typically have a favourable safety profile (Chia et al., 2012, Fritah et al., 2022). However, the cancer vaccine's efficacy in activating a meaningful immune response against their target cancers without triggering an autoimmune response is currently under further development (Hollingsworth and Jansen, 2019).

1.3.4 TIL therapy

Adoptive T-cell therapy involves the isolation of the patient's tumour infiltrating T-cells (TIL), expanding the TIL, and injecting TIL back into the patient. This type of treatment has had some positive results in tumours with TIL present, and there are many TIL therapies in clinical trials

against a variety of solid tumours (NCT01993719, NCT05087745, NCT05098197, NCT06084299) (Stevanovic et al., 2015, van den Berg et al., 2020). The TIL isolated from the tumour have T-cells of multiple TCRs, reducing the risk of antigen escape and lowering toxicities due to them being isolated from the patient's cells. However, TIL therapy is unsuitable for many patients as the amount of TIL present in cancers is highly variable. Moreover, the patient's cancer may not be suitable for the surgery necessary to isolate the TIL due to the patient's health or cancer location, and the expansion of TIL can be a complex process without guarantee of success (Zhao et al., 2022b). TIL therapy can be combined with other immunotherapies to enhance the TIL anti-tumour activity, such as the combination of TIL with anti-PD-1 to prevent TIL exhaustion or the addition of IL-12 with TIL therapy to enhance cytotoxicity (Hall et al., 2022, Jones et al., 2022).

1.3.5 Therapies targeting amino acid depletion in cancer

One method to target cancers is to disrupt the cancer metabolism. Cancers are dependent on external sources of amino acids for survival as their altered metabolism can result in cancers being unable to synthesise non-essential amino acids.

One example of altered cancer metabolism that is targetable for therapies is the upregulation of amino acid transporters to increase amino acid uptake. Large neutral amino acid transporter 1 (LAT1), also known as SL7A5, is a transporter for many amino acids, including tryptophan, tyrosine, phenylalanine, methionine, valine, and isoleucine. LAT1 is upregulated in many cancers as cancers need high amino acid uptake to maintain their high rates of proliferation and have been linked to a poorer prognosis, such as in renal cell carcinoma, adenocarcinoma, and colorectal cancer (Higuchi et al., 2019, Shibasaki et al., 2023, Yanagisawa et al., 2014). JPH203 and SKN103 are LAT1 inhibitors. SKN103 has been shown to reduce cancer cell line growth in in vitro models (Kongpracha et al., 2017). JPH203 has been

shown to reduce cancer growth in solid cancer murine models with high LAT1 expression and biliary tract cancer patients had a 60% response rate (Hafliger et al., 2018, Okano et al., 2020).

Another example is asparaginase, an enzyme that depletes the non-essential amino acids asparagine and glutamine. Many cancers depend heavily on asparagine and glutamine metabolism for survival as a nitrogen source for nucleic acid synthesis and regulation of cellular redox (Altman et al., 2016, Xu et al., 2022b, Krall et al., 2021). Asparaginase derived from Erwinia Chrysanthemi bacteria is FDA-approved for acute lymphoblastic leukaemia and has shown positive responses in patients with acute myeloid leukaemia (AML) (Keating, 2013, Emadi et al., 2018b).

1.4 CAR T-cells

1.4.1 CAR T-cells

Chimeric antigen receptor (CAR) T-cells are a personalised immunotherapy that involves isolating patient T-cells, genetically modifying them to target the patient's cancer and then re-introducing those T-cells into the patient. The CAR is a TCR-like receptor designed to allow T-cells to recognise the cancer and lead to anti-tumour T-cell activity. The CAR typically comprises four regions: a single chain variable fragment (scFv), a hinge region, a transmembrane domain, and an intracellular signalling domain (Yoo and Harapan, 2021). The scFv is comprised of heavy and light chain variable regions that recognise the cancer antigens. The hinge region provides flexibility, increasing interactions between CAR T-cells and their targets. The transmembrane domain anchors the receptor into the plasma membrane and transports signalling from the scFv to the intracellular signalling domain. The intracellular signalling domain comprises the CD3ζ, which triggers the signalling cascade that activates the CAR T-cell (Salter et al., 2018). As the CAR technology has been improving since its initial development in the 1980s, additional components have been added, such as costimulatory domains Tumour Necrosis Factor ligand superfamily member 9 (4-1BB), Tumour Necrosis Factor Receptor Superfamily Member 4 (OX-40), CD27 and CD28, to provide improved responses (Gross et al., 1989, Kuwana et al., 1987). CAR T-cells with CD28 have been shown to have a higher proliferative response to target cells, whereas CAR T-cells with the addition of 4-1BB have increased persistence (Ying et al., 2019). The design of the CAR molecule is crucial not only to the recognition of the cancer by the T-cells but also to the efficacy of the CAR T-cells' response to the cancer, such as mitigating T-cell exhaustion (Gumber and Wang, 2022).

The hypothesis behind this treatment is not only that it could provide a targeted treatment to eliminate cancers but also that as they are made of the host's immune system, the CAR T-cells have the ability to provide long-term surveillance to prevent relapse.

1.4.2 CAR T-cell successes

CAR T-cells have succeeded in treating B-cell malignancies such as diffuse large B-cell lymphoma and acute lymphoblastic leukaemia and were approved as a treatment by the FDA in 2017 (Schuster et al., 2017). In the UK, the National Institute for Health and Clinical Excellence (NICE) has approved three CAR T-cell therapies for third-line use, two in primary mediastinal B-cell lymphoma and one in diffuse large B-cell lymphoma (Wilkinson, 2023). In the US, 6 CAR T-cell treatments are approved by the FDA: 4 targeting CD19 and 2 targeting the B-cell maturation antigen (Chen et al., 2023). These treatments have provided effective therapy to patients who have exhausted other treatment possibilities, with overall 5-year survival rates of 86% being reported (Srour et al., 2020). These results vastly improved on the previous survival rates for acute lymphoblastic leukaemia, which had a 5-year survival rate of 40% (Anagnostou et al., 2020).

1.4.3 CAR T-cell failures

However, despite these promising results and considerable amounts of research being undertaken across a wide range of cancers, there have yet to be further CAR treatments approved outside of haematological malignancies. The tumour microenvironment is one barrier to achieving these results that is currently being investigated (Rafiq et al., 2020). The tumour microenvironment and repeated antigen exposure prevent the host's immune system from effectively eliminating the cancer and pose significant obstacles to CAR T-cell anti-tumour activity, exhaustion, and persistence (Kong et al., 2023).

CAR T-cells have high rates of associated toxicities affecting patients' tolerances to this treatment, such as anaemia, nausea, hypotension, headache, vomiting, diarrhoea, tremor, neutropenia, tachycardia, encephalopathy, thrombocytopenia, cytokine release syndrome (CRS) and immune effector cell-associated neurotoxicity syndrome (ICANS) (Locke et al., 2019). The most serious of these CAR T-cell-associated toxicities are CRS and ICANS. CRS is a systemic inflammatory response that increases IL-6, IL-10 and Interferon-Gamma (IFN-γ) serum levels. CRS symptoms can be varied, ranging from fever, fatigue, and nausea to organ failure, seizures, and acute heart failure (Shimabukuro-Vornhagen et al., 2018). CRS occurs in many CAR T-cell therapy patients between hours and up to 14 days after infusion (Jain et al., 2023, Porter et al., 2015). ICANS is an inflammatory response that increases inflammatory cytokines such as IL-6 and IL-8 in the blood-cerebrospinal fluid (Santomasso et al., 2018). Symptoms can include attention deficits, language deficits, impaired levels of consciousness, and seizures (Sterner and Sterner, 2022). These toxicities have inhibited the progress of CAR T-cell use by preventing higher therapeutic dosages, as a higher disease burden is linked with the severity of toxicities. An extensive release of cytokines causes cytokine release syndrome, resulting in fatigue, fever, diarrhoea, headache, myalgia, hypotension, cardiac dysfunction, organ failure, and progression to death.

1.4.4 Considerations during CAR T-cell design

Current limitations of CAR T-cells that must be considered during CAR T-cell design are antigen escape, on-target off-tumour effects, CAR T-cell trafficking, CAR T-cell tumour infiltration, survival and function in the tumour immunosuppressive microenvironment, and CAR T-cell-associated toxicities (Sterner and Sterner, 2021, Wei et al., 2019).

The target antigens used for CAR T-cell targets must have sufficient coverage across the cancerous cells, which can be difficult as cancers are often very heterogeneous. The target

antigen must also be highly specific, only being expressed on the cancer cells so that the CAR T-cells do not kill healthy, non-cancerous cells that just happen to express that antigen. The homogenous expression of an antigen exclusively found on cancer cells can be problematic since cancer cells originate from host tissues, so compromises must often be made. CD19 is the antigen used to target B-cell malignancies with great success, but CD19 is also a marker expressed on all B-cells; consequently, anti-CD19 CAR T-cell therapy results in long-term B-cell aplasia (Kochenderfer et al., 2010, Gabelli et al., 2024). This B-cell aplasia causes hypogammaglobulinemia and agammaglobulinemia, causing increased infection risk in these patients. However, this is considered an acceptable risk, and the use of subcutaneous immunoglobulin replacement has been shown to reduce the infection risk of these patients (Arnold et al., 2020).

Target antigen expression must be stable to ensure target antigen downregulation does not render CAR T-cell treatment ineffective. After treatment with anti-CD19 CAR T-cells, 30-60% of patients relapse, and 10-20% of relapsed patients are CD19 negative (Xu et al., 2019). These patients have CD19 antigen loss through loss-of-function mutations within the CD19 exons, preventing persisting anti-CD19 CAR T-cells from eliminating the cancerous cells (Orlando et al., 2018). Multi-antigen-target CAR T-cells or treatment using multiple types of CAR T-cells have been proposed to avoid antigen escape. However, these multi-antigen-target CAR T-cells are limited by on-target off-tumour responses; finding a singular suitable target can be difficult for many cancers (Han et al., 2019).

The tumour microenvironment inhibits CAR T-cell trafficking, infiltration, survival and function. To overcome a lack of CAR T-cell trafficking and infiltration into a tumour, some researchers have injected the CAR T-cells intratumorally to bypass CAR T-cell trafficking and

tumour infiltration with success in both safety and anti-tumour activity (NCT01837602) (Tchou et al., 2017).

1.4.5 CAR T-cell safety

Safety measures have been designed into CAR T-cells to protect patients against CAR T-cell therapy-related toxicities. The first safety measure in CAR T-cell design is choosing an appropriate antigen to prevent off-tumour responses or to anticipate and manage any off-tumour immune responses that would occur. Another hypothesis to limit on-target off-tumour responses currently showing promising results in pre-clinical research is altering the CAR T-cell binding affinity to the target antigen. This affinity-tuning of the CAR for its antigen limits CAR T-cell activation against low-level physiological antigen expression in healthy cells but enables activation against high antigen-expressing cancer cells (Liu et al., 2015, Vander Mause et al., 2023).

A vast improvement in the safety of CAR T-cell products is the insertion of safety switches. Safety switches currently have three varieties: suicide, activation, and inhibition switches, which can modulate CAR T-cell death, CAR T-cell activation, and CAR expression (Yu et al., 2019, Moghanloo et al., 2021). The safety switches that have been sufficiently researched for clinical trials are mainly suicide switches.

A suicide switch, called inducible caspase-9, has been successfully used in adoptive cell therapies previously in haploidentical stem-cell transplants; patients expressing graft versus host disease (GVHD) received the caspase-9 activating molecule AP1903, reversing GVHD as 90% of the transplanted T-cells were removed within 30 minutes (Di Stasi et al., 2011). Inducible caspase-9 has been used in CAR T-cell constructs in clinical trials, successfully eliminating CAR T-cells when necessary (Yu et al., 2022, Del Bufalo et al., 2023).

Cells expressing herpes simplex virus thymidine kinase (HSV-tk) will convert the non-toxic pro-drug ganciclovir into toxic competitive inhibitors of DNA polymerase, causing inhibition of DNA synthesis leading to cell death (Chen et al., 2014). Insertion of HSV-tk into CAR T-cells allows CAR T-cell elimination upon exposure to ganciclovir in a dose-dependent manner (Casucci et al., 2018). However, clinical trials using this switch in CAR T-cells have yet to be completed (NCT04097301).

Other possible safety measures include those used to counteract or manage the side effects of CAR T-cell therapy. Immunosuppressive treatments such as corticosteroids and Tocilizumab can be used to manage CAR T-cell-induced CRS and ICANS (Jain et al., 2023). The pre-emptive use of Tocilizumab has been proven to reduce the onset and severity of CRS and ICANS (Caimi et al., 2021).

1.5 CAR T-cells future

1.5.1 Autologous vs Allogeneic CAR T-cells

Currently, autologous CAR T-cells are the only FDA-approved CAR T-cell products available. The prevailing consensus was that the risk of an autologous CAR T-cell product would be lower than that of an equivalent allogeneic product. Autologous CAR T-cells are derived from the patient's cells, therefore resulting in a lower risk of GVHD (Zhang et al., 2023c). However, autologous CAR T-cells are subject to lengthy manufacturing times before the patient receives treatment, and the T-cell fitness may not be optimal (Watanabe et al., 2022). Conversely, allogeneic CAR T-cells are derived from a healthy third party, providing T-cells with increased fitness and reduced patient waiting times. Despite these positives, these allogeneic CAR T-cells have a higher risk of donor rejection.

Allogeneic CAR T-cells are currently mostly in early development in clinical trials. However, some surprisingly positive preliminary results have shown higher efficacy of allogeneic CAR T-cells than autologous CAR T-cells without increasing the toxicity profile. This indicates there is potential that patients may tolerate this therapy better than autologous CAR T-cells (Zhang et al., 2023c, Bader, 2023, Martinez Bedoya et al., 2021, Shahzad et al., 2021, Hu et al., 2024).

1.5.2 Addressing CAR T-cells in the tumour microenvironment

“Armoured” CAR T-cells has been a name given to CAR T-cells with additional proteins, antibodies, or cytokine expression alongside their CAR molecule to protect the CAR T-cells from the immunosuppressive effects of the tumour microenvironment (Hawkins et al., 2021).

Inducing CAR T-cell co-expression of pro-inflammatory cytokines is a compelling hypothesis as they have the possibility to not only increase CAR T-cell efficacy but also stimulate surrounding immune cells.

One example of this is using IL-12 in combination with CAR T-cells. IL-12 is a pro-inflammatory cytokine that binds to the IL-12 receptor, which activates signal transducer and activator of transcription (STAT4), promoting naïve T-cell differentiation into pro-inflammatory T helper cells (Sun et al., 2015). CAR T-cells with cell surface tethered IL-12 expression have been shown to have the potential to increase T-cell anti-tumour responses without systemic toxicities (Jones et al., 2022).

One example of CAR T-cell design to tackle CAR T-cell exhaustion is CAR T-cells that excrete an anti-PD-1 ligand antibody to inhibit exhaustion signalling through PD-1 on CAR T-cells. These anti-PD-1 excreting CAR T-cells have been shown to have reduced exhaustion rates and increased tumour clearance in mouse models (Suarez et al., 2016).

1.6 Acute myeloid leukaemia

1.6.1 Introduction to AML

AML is a name given to a group of heterogeneous leukaemia's that stem from malignancies of myeloid lineage stem cells. AML cases often present as genetic evolutions of pre-existing myeloproliferative or myelodysplastic neoplasms, which carry a risk of progressing into AML (Jain et al., 2024). The difference between these diseases has been defined by the percentage of abnormal myeloid cells, known as blasts, in their bone marrow and peripheral blood (Estey et al., 2022). The classification of AML was most recently updated by the World Health Organisation (WHO) to define patients with above 10% of blasts with recurrent genetic abnormalities in their blood or bone marrow. This cut-off is 20% when the AML has a fusion mutation of BCR: ABL1 to prevent overlapping diagnosis criteria with chronic myeloid leukaemia (Huber et al., 2023).

AML's primary peak of incidence is above 65 years of age. However, AML also has a small peak incidence in 0-4 years of age (Deschler and Lubbert, 2006, Schraw et al., 2022). AML has increased incidence in correlation to inherited genetic abnormalities that affect the bone marrow, such as Fanconi anaemia (Alter, 2014) and Shwachman-Diamond syndrome (Myers et al., 2020). Increased AML incidence is correlated with many environmental factors, such as cigarette smoking, maternal alcohol consumption, radiation exposure, asbestos exposure, and arsenic exposure (West et al., 2000, Shu et al., 1996, Kumar et al., 2023). Unfortunately, current treatments for many cancers, such as radiation and chemotherapy, have many side effects and can lead to increased cancer risk, as cells that already have inherited oncogenic mutations during treatment will undergo the positive selection for resistance to cancer cell treatments (Puglisi et al., 2020, Sun et al., 2022).

AML patients have impaired blood cell development, causing symptoms such as frequent infections, nausea, haemorrhage, swelling in limbs, weight loss, and fatigue, adversely affecting the patient's quality of life (De Kouchkovsky and Abdul-Hay, 2016, Chae et al., 2024).

Patients with AML exhibit heterogeneous cytogenetic mutations that can be classified into favourable, intermediate, and adverse prognostic groups. These groups have a 5-year survival rate of 64%, 42%, and 20%, respectively (Herold et al., 2020). The incidence of AML is currently increasing, which has been attributed to multiple factors such as chemotherapy and radiation therapy use that, as described earlier, can induce relapse (Dong et al., 2020b). An example of a favourable prognostic factor is an AML the chromosomal translocation, t(8;21)(q22;q22). This fusion inhibits the function of the runt-related transcription factor 1 from binding to DNA, which regulates osteoblast proliferation and differentiation. This translocation results in a more favourable treatment response and prognosis compared to other translocations associated with AML (Christen et al., 2019, Tang et al., 2020). An example of an adverse prognostic factor is AML containing t(6;9)(p23;q34) chromosomal mutation, a rare mutation resulting in a fusion of DEK and NUP214 proteins known to alter DNA coiling associated with genes involved with DNA damage responses and proliferation. This mutation leads to poor response to chemotherapy, resulting in an adverse prognosis for the patient (Diaz-Beya et al., 2020, Kayser et al., 2020).

1.6.2 The immunosuppressive microenvironment of AML

The bone marrow is a specialised niche enabling blood cell formation, protecting hematopoietic stem cells from overstimulation and the trafficking of cells into the bloodstream (Frobel et al., 2021, Heil et al., 2021). Therefore, to maintain these roles, the bone marrow niche requires an intricate series of interactions between the extracellular

matrix, hematopoietic cells, blood vessel endothelial cells, mesenchymal cells, progenitor cells and sinusoids (Dolgalev and Tikhonova, 2021, Tikhonova et al., 2019).

AML disrupts this bone marrow niche and exploits it to develop the AML tumour microenvironment that inhibits immune responses and the success of treatments. The components of and how to target the AML tumour microenvironment are under scrutiny to develop new and improve AML treatment options (Hino et al., 2022, Menter and Tzankov, 2022, Tettamanti et al., 2022, Bakhtiyari et al., 2023).

AML disrupts the bone marrow niche by altering the AML blasts interactions with the surrounding cells, creating an immunosuppressive environment (Ayyadurai et al., 2022).

AML upregulates the excretion of oncoprotein Mucin 1, which promotes the expansion of myeloid-derived suppressor cells (MDSC), which supress the immune response (Pyzer et al., 2017, Fultang et al., 2019).

AML cells target other immune cells more directly through overexpression of CD47, which inhibits macrophage phagocytosis and prevents immune presentation of cancer cell proteins to the adaptive immune system (Wang et al., 2021a). CD47 overexpression is associated with a poorer prognosis in AML (Majeti et al., 2009, Pan et al., 2022).

One mechanism AML uses to suppress the T-cell immune response is through the promotion of T-cells immune checkpoint markers that cause T-cell exhaustion, inhibiting the T-cell anti-cancer responses. In the presence of AML, T-cells upregulate immune checkpoint molecules such as PD-1, LAG3 and CTLA-4, which inhibit T-cell function (Chen et al., 2020, Radwan et al., 2020). These immune checkpoint markers' expression is associated with reduced overall survival in AML (Chen et al., 2020, Radwan et al., 2020).

To further suppress the T-cell immune response, AML cells recruit regulatory T-cells through C-X-C chemokine receptor 4 (CXCR4) expression (Wan et al., 2020). AML further increase regulatory T-cell presence in the AML niche by promoting the differentiation of T-cells into regulatory T-cells through the upregulation of ligands such as inducible T-cell costimulatory ligand expression (ICOSL) and PD-L1, which promote Forkhead box protein 3 (FoxP3) expression through altering the phosphoinositide 3-kinase-Akt pathway (Wan et al., 2020, Han et al., 2018, Dong et al., 2020a). AML patients have higher plasma concentrations of the immunosuppressive cytokine IL-10, which promotes T-cell differentiation into regulatory T-cells (Wu et al., 2012, Stevens et al., 2023). Regulatory T-cells in AML predict a poor prognosis (Zhao et al., 2020, Bruck et al., 2020).

One major contributor to the immunosuppressive abilities of the AML tumour microenvironment is the relationship of AML cells with bone marrow mesenchymal stromal cells (BM-MSC). AML-derived BM-MSCs have the ability to inhibit immune cell proliferation and immune cell secretion of pro-inflammatory cytokines (Towers et al., 2024). BM-MSCs induce resistance against chemotherapy, reducing apoptosis in response to chemotherapy by transferring their mitochondria to AML cells (Saito et al., 2021). AML-derived BM-MSC release higher levels of IL-10, which promotes T-cell differentiation to Treg as described earlier (Diaz de la Guardia et al., 2017).

Another way that AML inhibits treatment efficacy is by developing resistence to the treatment. One example of this is, AML down-regulating human leukocyte antigens (HLA) expression after hematopoietic cell transplant (Jan et al., 2019, Toffalori et al., 2019). Hematopoietic cell transplant relies on injecting donor immune system cells into the patient to identify and kill the cancer. However, HLA encodes the MHC genes required for immune

cells' ability to detect the cancer cells. Therefore, loss of HLA hides the AML cells from the immune systems survaliance rendering further HCT treatments ineffective.

1.6.3 Metabolism in the AML microenvironment

One component of tumours and their microenvironment that is an expanding area of interest is understanding amino acid metabolic vulnerabilities developed in tumours during their conversion from healthy cells to malignancy, which has been valuable in the development of new therapies (Fultang et al., 2021). AML is well known to reprogram their metabolism to enable their excessive growth. Treatments targeting the mechanisms that cancers use to acquire the nutrients they need have been shown to reduce the burden of the cancer (Folger et al., 2011, Gregory et al., 2019, Pardieu et al., 2022, Hafliger et al., 2018). Examples include treatments that target cancers uptake of amino acids.

AML depends on the uptake of the essential amino acid methionine for survival and cell proliferation, leading to methionine depletion in patient plasma (Muscaritoli et al., 1999, Cunningham et al., 2022). AML upregulates S-adenosyl-methionine production, a methionine derivative catalysed by the isoenzymes methionine adenosyl transferase family. The importance of methionine to AML has become a target of several therapies, such as Pinometostat (EPZ-5676), which is a competitive small molecule inhibitor for a methionine derivative s-adenyl-methionine (Stein et al., 2018, Lonetti et al., 2020). S-adenyl-methionine binds to H3 lysine-9 methylation, a methyltransferase that controls the gene transcription required for leukemic fusion genes. Patients tolerate Pinometostat well, but clinical results have not shown a meaningful response in cancer clearance (Stein et al., 2018).

AML proliferation is dependent on the uptake of amino acid arginine (Mussai et al., 2015a, Cunningham et al., 2022). AML blasts are reliant on extracellular arginine uptake to maintain

this dependence. The use of therapeutics to take advantage of this, such as BCT-100, a pegylated human recombinant arginase to deplete extracellular arginine, inhibits AML blast proliferation (Mussai et al., 2023, Fenwick et al., 2024).

1.6.4 The importance of tryptophan and cytsine in AML

Tryptophan uptake and metabolism have been identified as potential targets because tryptophan is essential to many tumours (Fultang et al., 2021). Cancers convert tryptophan into kynurenine, which promotes T-cell differentiation into regulatory T-cells and deprives T-cells of tryptophan (Curti et al., 2007, Brincks et al., 2020, Bracho-Sanchez et al., 2019). Tryptophan metabolism also creates a tryptophan-starved environment, leading to amino acid starvation signals and increasing T-cell apoptosis (Fallarino et al., 2002, Lee et al., 2002, Siska et al., 2021). Cancer cells can create a microenvironment that suppresses and eliminates effector T-cells, including CAR T-cells, through tryptophan metabolism (Arandi et al., 2018, Towers et al., 2024). AML blasts increase their expression of indoleamine 2,3-dioxygenase (IDO), an immunomodulatory enzyme known to be a rate-limiting step of tryptophan metabolism into the kynurenine pathway (Wells et al., 2021). This depletion of the essential amino acid tryptophan and conversion into the kynurenine pathways downstream derivatives causes immunosuppressive effects on T-cells, resulting in a reduction in T-cell proliferation and generation of regulatory T-cells (Yang et al., 2022b, Wu and Zhu, 2021, Bracho-Sanchez et al., 2019). Expression of IDO and kynurenine levels are both well-documented to be correlated with a poorer prognosis (Hara et al., 2016, Mabuchi et al., 2016, Arandi et al., 2018, Kierdorf et al., 2022, Muller-Thomas et al., 2020). To target this, *in vitro* studies of IDO inhibitors such as Indoximod have shown increased effector T-cell proliferation and reduced regulatory T-cell generation (Brincks et al., 2020). Indoximod has been described as well tolerated by patients in combination with chemotherapy Cytarabine and Idarubicin but

further study of this combination in AML have yet to be published (NCT02835729) (Soliman et al., 2014, Emadi et al., 2018a).

Cancers overexpress the cystine transporter SLC7A11, decreasing the availability of cystine in patient plasma (Zhao et al., 2018, Pardieu et al., 2022). Cystine is a non-essential amino acid but is essential for activated T-cell function as T-cells cannot synthesise cysteine, which is required for DNA and protein synthesis, rendering it vital for T-cell proliferation and survival (Edinger and Thompson, 2002, Garg et al., 2011, Han et al., 2024). Therefore, reduced cystine availability due to cancer cell uptake reduces T-cell function. AML upregulates xCT expression, an importer of cystine, the oxidised dimer of the semi-essential amino acid cysteine (Zhao et al., 2018, Pardieu et al., 2022). Cysteine is required even in leukemic stem cells (LSC), which are progenitor cells which AML can arise from, for their glutathione production, which in turn is required for their ATP production in AML (Jones et al., 2019, Cramer et al., 2017). Cystine depletion using cyst(e)inase has been shown to suppress tumour growth without off-target effects in murine models (Cramer et al., 2017). AML cancers' uptake of cystine is so significant that AML patients have cystine depletion in their plasma (Zhou et al., 2020b). Inhibition of SLC7A11 by sulfasalazine induces AML cell death and augmented anti-leukaemia activity when used in combination with chemotherapy (Pardieu et al., 2022)

1.6.5 Current Treatment

The current first-line treatment for AML with FLT3 mutations is a continuous infusion of 2 chemotherapies: Cytarabine for 7-days and Daunorubin for 3-days (Dombret and Gardin, 2016). Several clinical trials have been performed to assess the effectiveness of different dosages and add additional agents to this combination. This treatment has an overall survival below 50% (Lancet et al., 2021, Garg et al., 2020, Othus et al., 2023).

1.6.6 CD33 in AML

CD33 is a sialic acid-binding immunoglobulin-like lectin that is upregulated during the myeloid commitment of hematopoietic progenitors and remains expressed for their lifespan. Therefore, CD33 is expressed on all myeloid-derived cells; the only exception is granulocytes, which down-regulate their CD33 expression to low levels. CD33 is expressed in 80-90% of AML cases (Ehninger et al., 2014, Liu et al., 2022). This makes CD33 an ideal target for AML, as the FDA has already approved an anti-CD33 antibody bound to calicheamicin known as Gemtuzumab Ozogomicin used in combination with standard chemotherapies. Gemtuzumab Ozogomicin binds to CD33 positive cells, is internalised and then causes DNA damage leading to cell death (van Der Velden et al., 2001). Adding CD33 targeting treatment reduces patient relapse and improves overall survival (Swaminathan and Cortes, 2023).

The ability of CD33 to be used as a target for AML treatments has been developed into an anti-CD33 CAR T-cell with successful anti-leukemic activity in patient-derived xenograft models (Qin et al., 2021). These treatments have been taken to phase 1 trial for both adult and paediatric AML (NCT03971799, NCT05672147, and NCT05984199). The clinical trial results show no dose-limiting toxicities but no meaningful anti-cancer activity at the first dose level (Tambaro et al., 2021).

There also has been interest in generating anti-CD33 CAR cells outside of T-cells. Developments in anti-CD33 CAR natural killer cells have demonstrated safety at phase 1 trial (NCT05008575) (Huang et al., 2023).

1.7 Aims and objectives of the thesis

This thesis aims to improve anti-CD33 CAR T-cell therapies in AML and their anti-tumour function. Previous members of this laboratory have also designed CAR T-cells with increased expression of the arginase enzymes arginase I and arginase II, which increased CAR T-cells' proliferation and anti-tumour activity in the AML microenvironment (Panetti et al., 2023). As identified in the introduction, the amino acid depletion in the tumour microenvironment is crucial to T-cell function. However, currently there has been very few studies looking at the alteration to CAR T-cell design to aid amino acid uptake that could protect CAR T-cells from the amino acid depletion present in tumour microenvironments. Therefore, we hypothesised that improving amino acid uptake of crucial amino acids could improve CAR T-cell function in the tumour microenvironment.

The amino acids we decided to target were cystine and tryptophan as these amino acids have been shown to be crucial to tumour survival and their depletion has been shown to significantly reduce T-cell function. AML is known to upregulate tryptophan degrading enzymes that produce immunosuppressive compounds (Wells et al., 2021). AML uses extracellular cystine uptake to prevent ROS accumulation and inhibit ferroptosis (Cunningham et al., 2024).

How the availability of these amino acids affect T-cells function is discussed in more detail in chapter 3 but one example is that both tryptophan and cystine are required for mammalian target of rapamycin (mTOR) activity that is required for T-cell activation and the maintenance of the activated state (Ma et al., 2023b). To improve uptake of these amino acids by CAR T-cells, we designed anti-CD33 CAR T-cells with increased amino acid transporters SLC7A5 or SLC7A11 expression. SLC7A11 imports cystine. SLC7A5 uptakes tryptophan as well as the amino acids methionine, histidine, leucine, and tyrosine.

2. Material and Methods

2.1 Research Project Ethics

The study received ethical approval from the Regional Ethics Committee.

2.2 Media composition

Table 1: Compositions of media

Media	Reagent	Concentration	Supplier
R10%	RPMI-1640	-	Sigma
	Foetal Bovine Serum (FBS)	10%	Sigma
	L-Glutamine	2mM	Gibco
	Penicillin-streptomycin	100U/mL	Gibco
	Sodium Pyruvate	1mM	Gibco
	Hepes	5mM	Gibco
	Non-essential amino acids 100X	1%	Gibco
Tryptophan free media	RPMI1640 without L-Tryptophan	-	PAN Biotech
	Dialysed FBS	10%	Gibco
	L-Glutamine	2mM	Gibco
	Penicillin-streptomycin	100U/mL	Gibco
	Sodium Pyruvate	1mM	Gibco
	Hepes	5mM	Gibco
	Non-essential amino acids 100X	1%	Gibco
	β-mercaptoethanol	0.1%	Gibco
Cystine free media	RPMI 1640 without L-Cystine	-	PAN Biotech
	Dialysed FBS	10%	Gibco
	L-Glutamine	2mM	Gibco
	Penicillin-streptomycin	100U/mL	Gibco
	Sodium Pyruvate	1mM	Gibco
	Hepes	5mM	Gibco
	Non-essential amino acids 100X	1%	Gibco
Freezing Media	FBS	-	Sigma
	Dimethyl Sulfoxide (DMSO)	10%	Sigma
Phoenix Ampho Medium	Dulbecco's Modified Eagle Medium (DMEM)	-	Sigma
	FBS	10%	Sigma
	L-Glutamine	2mM	Gibco
	Sodium Pyruvate	1mM	Gibco
T-cell media	RPMI 1640		Sigma
	FBS	10%	Sigma
	Human serum	1%	Gibco
	Penicillin streptomycin	100U/mL	Gibco
	L-glutamine	2 mmol/L	Gibco
	Hepes	5mM	Gibco
	Sodium pyruvate	1 mmol/L	Gibco
	non-essential amino acids	1%	Gibco
	β-mercaptoethanol	0.1%	ThermoFisher

			Scientific
	IL-2	100U/ml	Peprotech
MACs	Dulbecco's Phosphate-buffered Saline (PBS)	-	Sigma
	Bovine serum albumin (BSA)	0.5%	Merk
	Ethylenediaminetetraacetic acid (EDTA)	2mM	ThermoFisher
FACs	Dulbecco's Phosphate-buffered Saline	-	Sigma
	FBS	10%	Sigma

2.3 Cell line culturing

HL60, THP1 and Jurkat cell lines were obtained from American Type Culture Collection (ATCC) and validated using short DNA tandem repeats. All these suspension cell lines were routinely cultured in R10% media, RPMI 1640 (Sigma), 10% Foetal bovine serum (Sigma), 2mM L-Glutamine (Gibco), 100U/mL Penicilin-streptomycin (Gibco), 1mM sodium pyruvate (Gibco), 5mM Hepes (Gibco), and 1% non-essential amino acids (Gibco), in T75 flasks at 37°C 4% CO_2. They were passaged at a 1:10 ratio when the cell lines reached 70-80% cell density. The cell lines were routinely tested for mycoplasma by PCR analysis. Cell line expression of CD33 was assessed by flow cytometry, as depicted in Figure 5. Cell lines were washed with flow-assisted cell sorting media (FACs), incubated for 20 minutes at 4°C with CD33 BV421 (Biolegend), rewashed with FACs media and then stained with Propidium Iodide in FACs and read by flow cytometry (Beckman Coulter).

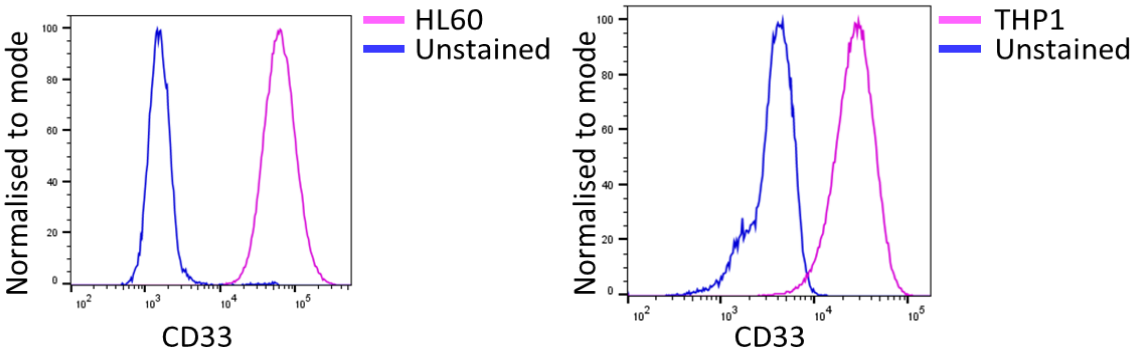

Figure 5: CD33 expression on HL60 and THP1 determined by flow cytometry.

2.4 Cell line viability

AML cell lines HL60, K562, KGIA, U937, NOMO, and THP1 were cultured in R10%, Tryptophan free or cystine free media for 72 hours. After 72 hours, cells were harvested, washed with FACs media, stained with propidium iodide, and assessed for viability using flow cytometry.

2.5 Tryptophan and cystine uptake

The concentration of tryptophan and cystine was measured in the patient's serum and conditioned media. Conditioned media was generated from supernatant harvested at the end of *in vitro* assays by harvesting and then centrifuging the cell culture at 300g for 5 minutes. The supernatant would then be collected. Conditioned media was stored at -80°C from the day of harvest until the day of the experiment.

The concentration of tryptophan was measured using a tryptophan Assay kit (Alpha Diagnostic).

To measure the cystine concentration, the cystine must first be reduced to cysteine using 20mM 2-carboxyethylphosphine to reduce the cystine into cysteine. The resulting cysteine was measured using the Human Cysteine (enzyme-linked immunosorbent assay) ELISA kit (BlueGene Biognosis Ltd). Both were carried out as per the manufacturer's instructions.

2.6 Isolation of PBMCs from whole blood and blood products

Peripheral blood mononuclear cells (PBMCs) were isolated from healthy apheresis cones obtained from NHS Blood and Transplant Blood Bank (Birmingham). The blood products were first diluted in RPMI (Sigma) to four times the original volume of the cone and layered on top of Lymphoprep™ (StemCell technologies). Alternatively, PBMCs isolated from healthy

controls were diluted to double the original volume and layered on top of Lymphoprep™. All blood products were processed on the same day as they were received.

The blood and Lymphoprep™ mixture were centrifuged for 20 minutes at 800xg at room temperature with the brake off. The PBMC layer was collected and washed in RPMI at 300xg for 10 minutes. If the pellet was red after this wash, indicating that the PBMC layer collected was contaminated with red blood cells, an additional step to remove the red cells was carried out. The pellet would be resuspended in Puregene Red Blood Cell lysis buffer (Qiagen) and incubated for 5 minutes at room temperature. Once the PBMCs were not contaminated with red blood cells, they were washed twice with RPMI for 10 minutes at 300xg.

2.7 Isolation of T-cells from PBMCs

The PBMCs were washed in magnetic assisted cell sorting buffer (MACs), which comprises PBS (Gibco), 0.5% bovine albumin serum (Merk), and 2 mM EDTA (ThermoFisher). To enrich T-cells from the PBMC mix, the washed PBMCs were resuspended in MACs buffer at 30µl per 10^7 cells with Pan T-cell isolation Microbeads (Miltenyi Biotec), a T-cell negative selection kit, at 20µl per $1x10^7$ cells and incubated for 20 minutes at 4°C. Post incubation, the cells were passed through a pre-washed LS magnetic column (Miltenyi Biotec) on a QuadroMACs Separator (Miltenyi Biotec). Up to $1x10^8$ cells were sorted per LS column. The column was washed three times with 3ml MACs buffer for the LS column to ensure all non-bound cells passed through the column. The negative fraction, which is comprised solely of T-cells, was collected. The isolated T-cells could be used immediately or stored at $10x10^6$ cells per millilitre of freezing media [DMSO (Bioworld), 10% FBS] in cryovials at -80°C.

2.8.1 Proliferation assay using anti-CD3 anti-CD28 stimulation

T-cell proliferation assays were performed to determine the effect of amino acid depletion on proliferation. The conditional medias used for these assays were R10%, R10% with 0.1% β-mercaptoethanol, tryptophan-free media (PAN Biotech) and cystine-free media (PAN Biotech). The composition of each media has been described in Table A. Where indicated for tryptophan and cystine-free media, there was an addition of 50µM of tryptophan (Scientific laboratory supplies [SLS]) or cystine (SLS) to the corresponding amino acid-free media.

Healthy T-cells were washed in PBS and stained with 1µM of the cell tracker carboxyfluorescein succinimidyl ester (CFSE) (ThermoFisher Scientific) per $1x10^6$ cells for 30 minutes at room temperature. Post incubation, $1x10^5$ CFSE labelled cells were washed three times in RPMI-1640 (ThermoFisher) and incubated for 10 minutes at room temperature before they were aliquoted into plates. The T-cells were put into plates that had been coated with anti-CD3 Monoclonal antibody (eBioscience™) in 200µl in the required media as described above with anti-CD28 monoclonal antibody (eBioscience™) and 100U/ml IL-2 (Peprotech).

The plated T-cells were incubated at 37°C, 5% CO2 for 3 days. The T-cells were washed with stained CD4-APC and CD8-APC-Cy7 (Bioscience) for 20 minutes at 4°C. T-cells were washed and stained with Propidium Iodide viability stain (Invitrogen) and read by flow cytometry on the CytoFLEX Flow Cytometer (Beckman Coulter). Flow cytometry data was analysed using the FlowJo software (BD Biosciences).

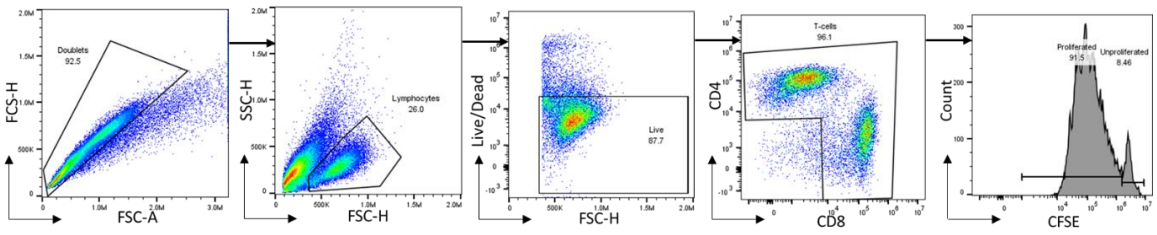

Figure 6: Example of gating used to identify proliferating populations when investigating proliferation by CFSE.

2.8.2 Proliferation assay using tumour cell stimulation

CAR T-cells were plated with THP1 cells or patient AML cells at a ratio of 5 CAR T-cells to 1 target cells. The plated T-cells and CAR T-cells with THP1 cells were incubated at 37°C, 5% CO_2 for 3 days. The CAR T-cells plated with patient AML cells were incubated at 37°C, 5% CO_2 for 7 days. The CAR T-cells were stained with CD34- APC (Biolegend) and CD33 BV421 (Biolegend). Both CAR T-cells were washed and stained with Propidium Iodide viability stain (Invitrogen) and read by flow cytometry on the CytoFLEX Flow Cytometer (Beckman Coulter). Flow cytometry data was analysed using the FlowJo software (BD Biosciences).

2.9 Assessing T-cell activation

Plates were pre-coated with anti-CD3 Monoclonal antibody (1µg/ml)(eBioscienceTM) overnight before the addition of T-cells, anti-CD28 monoclonal antibody (1µg/ml)(eBioscienceTM) and 100U/ml IL-2 (Peprotech).

To assess IFN-γ, the plate was incubated at 37°C 5% CO_2 for 20 hours, then Golgi stop (BD Biosciences) was added, and the plates were returned to the incubator for 4 hours. The T-cells were harvested and washed with FACs buffer, then stained with CD8 FITC (Biolegend), CD4- PE (Biolegend), and CD69 PE Cy7 (Biolegend) in FACs buffer for 20 minutes at 4°C in the dark. After washing again with FACs, the cells were fixed with fixative buffer (Biolegend) and washed twice with Permeabilisation buffer (Biolegend). After permeabilisation, the cells were stained with IFN-γ APC (BioLegend) for 20 minutes in the dark at room temperature. The cells were then assessed by flow cytometry (Beckman Coulter).

To assess activation markers, the plate was incubated at 37°C 5% CO_2 for 72 hours, the cells were harvested, washed with FACs buffer and stained with CD8 FITC (Biolegend), CD4 PE (Biolegend), CD69 APC (Biolegend), and CD25 BV421 (Biolegend) for 20 minutes at 4°C in the

dark. Post-staining, the cells were washed and stained with propidium iodide and read by flow cytometry (Beckman Coulter).

2.10 Metabolic analysis of CAR-Jurkat

CAR-Jurkat were cultured for 3 hours in R10% with or without β-mercaptoethanol, tryptophan-free media, and cystine-free media. The CAR Jurkat were plated and incubated for 1 hour at 37°C at $1x10^5$ cells per well respectively on Cell Tak-coated (Corning) Agilent Seahorse XFe96 cell culture microplates (Agilent Technologies) in 175µl per well XF RPMI (#103576-100, Agilent Technologies) with 5mM glucose, 2mM L-Glutamine and 1mM sodium pyruvate and 5mM HEPES.

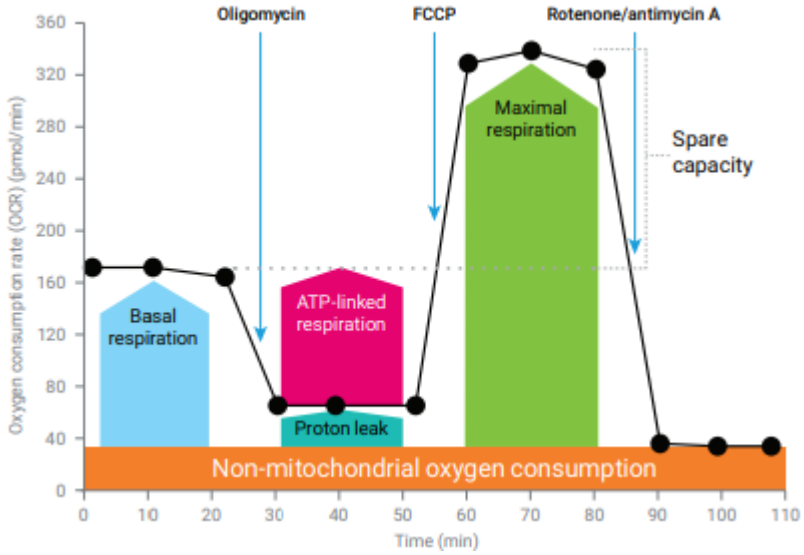

Figure 7: Oxygen consumption rate by time

Post incubation, the cells were analysed using the Seahorse XFe96 extracellular flux analyser. The Seahorse analyser uses 4 cycles with the injection of 4 drugs to measure the oxygen consumption rate (OCR) and extracellular acidification rate (ECAR). These 4 cycles have a 3-minute mix and 3-minute measure period. In between each cycle, to investigate the mitochondrial function, there is the addition of one inhibitor, added in the order listed here: 2µg/ml oligomycin, 3µM N5,N6-bis(2-fluorophenyl)-[1,2,5]oxadiazolo[3,4-b]pyrazine-5,6-

diamine (BAM15), 2µM rotenone with 2µM antimycin A as demonstrated in Figure 7. All work and analysis related to metabolic analysis using the seahorse analyser was done with the support of Dr. Jonathon Barlow of the Birmingham Metabolomics team.

2.11 Viral production

The Phoenix Ampho packaging cell line (ATCC) was cultured in Phoenix antibiotic-free Ampho medium (DMEM, 10% FBS, 1mM sodium pyruvate and 200mM Glutamine). This cell line was seeded and cultured in sterile T150 flasks at $3x10^6$ cells per flask. To passage the Phoenix Ampho cell line, the cells were trypsinised with TrypLE (Gibco) for a maximum of 5 minutes at 37°C to dissociate the cells from the flask. The cells were washed and returned to a flask. The day before the transfection of the Phoenix Ampho cell line, they are passaged as described and returned to the flask at $4x10^6$ cells per flask so that they would reach a 50-80% confluency for the next day. Once the Phoenix Ampho had reached 50-70% confluency, the supernatant was gently removed, and a new 9ml of Ampho media was added with the transfection mix. The transfection mix per flask included 12µl of validated CAR-plasmid constructs (Genscript), 12µl of pCL-Ampho retroviral packaging vector (Bio-techne), 120µl FuGENE 6 transfection reagent (Promega) and 3480µl OptiMEM (Gibco). pCL-Ampho contains the gag, pol and env coding regions which create the viral core protein structure, the reverse transcriptase and the envelope (Naviaux et al., 1996). Fugene 6 contains cationic polymers that interact with both the plasmid and the cell membrane of the Phoniex Ampho to promote uptake (Hasan et al., 2021). One of the three CAR-plasmid constructs were used to transduce the cells, which are depicted in Figure 8. The plasmids were designed by Carmela DeSanto, Livingstone Fultang, and Francis Mussai inserting the sequencing coding for SLC7A11 and SLC7A5 in this laboratories original CAR construct coding for anti-CD33 CAR. The plasmid was manufactured by Genscript (sequencing supplementary data 1 and 2). The anti-CD33 CAR

construct contains several sections surrounded by long terminal repeat sequences on either side of the transcription zone (Figure 8). All of the constructs contain a truncated CD34 tag, an F2A self-signal peptide, anti-CD33 scFv, a CD8-derived hinge/trnasmembrane region, a 4-1BB co-intracellular signalling domain, and a CD3 ζ-chain signalling domain. The anti-CD33 SLC7A5 construct additionally contains the SLC7A5 sequence after the 4-1BB code. The anti-CD33 SLC7A11 construct additionally contains the SLC7A11 sequence after the 4-1BB code.

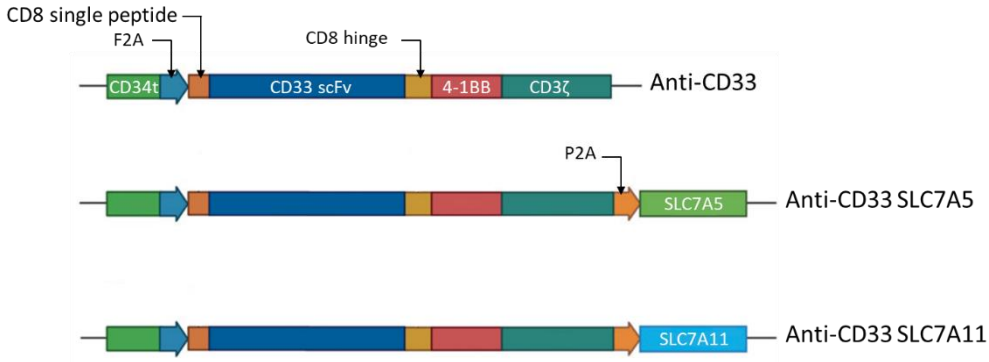

Figure 8: Anti-CD33, anti-CD33 SLC7A5, and anti-CD33 SLC7A11 cassettes depicting the components of the CAR constructs

This mix was rested at room temperature for 30 minutes before addition to the Phoenix Ampho to enable the formation of DNA-FuGENE complexes. The transfected Phoenix Ampho cells were incubated for 24 hours at 37°C, 4% CO_2. To prevent FuGENE toxicity, 24 hours after transfection, the supernatant containing the transfection mix was discarded after 24 hours, and new Ampho media was added to replace this. The transfected Phoenix Ampho cells were incubated for 24 hours at 37°C, 4% CO_2. On day 2, after transfection, the supernatants were harvested off the Phoenix Ampho and centrifuged at 3000g for 5 minutes. The final resulting supernatant was the retroviral media used to transfect the T-cells.

The day before harvesting the supernatant from the Phoenix Ampho cells, 6-well non-tissue culture plates were coated in 2ml of PBS with 30µg/ml RetroNectin (Takara Clontech) and

incubated at room temperature overnight. After overnight incubation, the RetroNectin was removed from the plates, 2ml of the retroviral media, harvested from the transfected Phoenix Ampho cells, was added to each well, and the plates were centrifuged at 2000g for 2 hours. The supernatant was removed, and the retroviral-coated plates were ready for T-cell or Jurkat transduction.

2.12 Transduction of T-cells

On the same day as the Phoenix Ampho cell line transfection, the healthy T-cells acquired from Lymphoprep and MACs sorting as described above were activated with anti-CD3/anti-CD28 Dynabeads (Gibco) (2 beads per cell) for 2 hours and incubated for 48 hours in T-cell media which is comprised of RPMI 1640 (Sigma), 10% FBS, 1% Human serum, 1% Penicillin streptomycin, 1% L-glutamine, 1% Hepes, 1% Sodium pyruvate, 1% non-essential amino acids, 0.1% β-mercaptoethanol, 300U IL-2) at a concentration of $1x10^6$ cells per ml. The activated T-cells were then washed and added to T-cell media with 100U/ML IL-2 and rested for 30 minutes before they were plated in 2ml containing $2x10^6$ T-cells per well on the retroviral coated plates described above. The T-cells were then incubated at 37°C, 5% CO_2 for 24 hours. The plates were filled with 4ml of T-cell media per well and incubated for 72 hours at 37°C, 5% CO_2. To check the transduction efficiency, the cells are stained with CD34-APC (Biolegend) and live dead stained with propidium iodide viability stain (Invitrogen) and read by flow cytometry on day 4 on the CytoFLEX Flow Cytometer (Beckman Coulter). The cytometry data was then analysed using the FlowJo software (BD Biosciences). Additional staining was performed alongside CD34 with CD8 FITC (Biolegend) and CD4 PE (Biolegend).

2.13 Transduction of Jurkat

The suspension Jurkat cell line (ATCC) used to generate Jurkat-CAR was designed to model the T-cell transduction preliminarily. The Jurkat were harvested and plated on the retroviral coated plates at $0.5x10^6$/ml without activation. The Jurkat transduction then continued in the same way as the T-cell transduction.

2.14 Purification of CAR products

Once transduced, the CAR T-cells required purification to ensure only the desired transduced population remained. The transduced cells were washed with MACs buffer, counted and resuspended in MACs buffer at 300µl per 10^8 cells with CD34 anti-human microbeads (Miltenyi Biotec) at 100µl per 10^8 cells and incubated for 30 minutes at 4°C. Post incubation, the cells were washed and resuspended in 2mL MACs buffer and passed through an MS column (Miltenyi Biotec) on a QuadroMACs Separator (Miltenyi Biotec). Up to 10^8 cells could be sorted per MS column. The column was washed 3 times with 500µl MACs buffer to ensure all non-bound cells passed through the column. The positive fraction was collected, as this positive fraction should comprise solely of transduced cells.

2.15 Western blot

The cells isolated for Western blot were washed in PBS, counted, and resuspended in 100µl of RIPA++, which comprised of Pierce RIPA Buffer (Thermo Scientific), 4% EDTA-free protease inhibitor (Roche) and 10% PhosSTOP phosphatase (Sigma). This isolates proteins from cells without the proteins being degraded by the enzyme present in the cells. The cells were then vortexed every 5 minutes during a 20-minute incubation at 4°C. Post incubation, the cells were centrifuged at 13,000g for 20 minutes at 4°C and the resulting supernatants were then collected. To quantify the protein concentration, 2µl of the supernatant was added to 98µl

Coomassie Plus Protein assay reagent (Thermo Scientific) in a 96-well flat bottom plate (Corning) and incubated for 5 minutes at room temperature in the dark. The plate was then read at 595nm on a microplate reader (Bio-rad). A standard curve of known protein concentrations was generated to determine the protein level in the samples.

The samples were added to each mix at the same concentration with a ratio of 1:4 of sample to Laemmli buffer loading dye (Bio-Rad). RIPA 1X Buffer was added to make the volume across each sample equal. The protein mixes were then incubated at 95°C for 5 minutes to denature the proteins. The mix was then loaded onto the Pre-cast 4-20% Midi protein gel (Bio-Rad) with a 10-250kDa pre-stained protein standard (BioLabs), and the gel was run in 1X Tris/Glycine/SDS Buffer (Bio-rad) at 150V for 1 hour. The proteins were transferred onto Trans-Blot Turbo 0.2µm poly-1,1-difluoroethene (PVDF) membrane (Bio-rad) over 7 minutes using a Trans-Blot Turbo machine (Bio-Rad). The protein-loaded PVDF membrane was blocked with PBS, 5% Bovine serum albumin (BSA) fraction V (Roche) for 1 hour.

The membrane was stained with PBS, 5% BSA containing the appropriate primary antibodies diluted per the manufacturer's instruction overnight on a shaker at 4°C. The primary antibody was removed from the membrane by washing 3 times with PBS, 0.1% Tween 20 (VWR Life Science) on a shaker for 10 minutes at room temperature. The membrane was covered with an appropriate Horse-Radish Peroxidase secondary antibody (Cell signalling) in PBS 5% BSA for 45 minutes on a shaker at room temperature. The membrane was washed in the same manner as described above 3 times to remove excess secondary antibody. The Amersham enhanced luminol-based chemiluminescent (ECL) western blotting detection reagent (Cytiva) was added to the membrane for 1 minute at room temperature before the excess ECL was drained off and the membrane was exposed using chemiluminescence by the ChemiDocMP

system (Bio-rad). After analysis, the membrane was washed in the same manner as described above, and the membrane was ready for the next probing primary antibody.

2.16 CAR T-cell proliferation and phenotyping

CAR T-cell proliferation and assays were performed to determine the effect of amino acid depletion on CAR T-cell proliferation and phenotype. The conditional medias used for these assays were R10% with or without β-mercaptoethanol, tryptophan-free media and cystine-free media. The compositions of each media have been described in Table 1. Low tryptophan and low cystine media contain 25% R10% and 75% of their corresponding depleted media.

For proliferation assays, CAR T-cells were washed in PBS and stained with 1µM of the cell tracker CFSE (ThermoFisher Scientific) per $1x10^6$ cells for 30 minutes at room temperature. Post incubation, CFSE labelled CAR T-cells were washed three times in RPMI-1640 (ThermoFisher) and incubated for 10 minutes at room temperature. The $1x10^5$ CAR T-cells were plated on 96-well plates in 200µl of the appropriate media with 100U/ml IL-2. The plated CAR T-cells were incubated at 37°C, 5% CO_2 for 3 days. On day 3, they were washed with stained CD4-APC and CD8-APC-Cy7 (Bioscience) with Propidium Iodide viability stain (Invitrogen) and read by flow cytometry on day 3 on the CytoFLEX Flow Cytometer (Beckman Coulter). All flow cytometry data was analysed using the FlowJo software (BD Biosciences).

For phenotype assays, the CAR T-cells were harvested, washed in PBS, and stained with CFSE for 20 minutes at 4°C. Post incubation, the cells were washed with FACs, stained with CD3 PE-Cy7 (Biolegend) for 20 minutes at 4C, then washed and stained with Propidium Iodide in FACs and read by flow cytometry.

The CAR T-cells were plated with THP1 at a 5 CAR T-cell to 1 THP1 cell ratio. The CAR T-cells were re-stimulated with THP1 cells on days 3 and 6 for repeat exposure to target cells. The

mix to assess exhaustion markers: CD3 PE-Cy7 (BioLegend), LAG3 FITC (BioLegend), PD-1 PE (BioLegend), CD69 BV421 (Biolegend) and TIM3 APC-Cy7 (BioLegend). The mix to assess phenotypic markers: CD3 PE-Cy7 (BioLegend), CD45RO FITC (BioLegend), CD45RA APC-Cy7 (BioLegend), CD62L PE (BioLegend), and CCR7 BV421 (BioLegend).

2.17 Murine xenografts

Axis Bioservices was employed to conduct all animal studies described in this thesis. All experimental protocols were approved and monitored by Axis Bioservices Animal Welfare and Ethical Review Board (I2AE50C0) in compliance with the UK Home Office Animals (Scientific Procedures) Act 1986, the United Kingdom National Cancer Research Institute guidelines for the welfare of animals in cancer research, and the ARRIVE guidelines.

To assess the effectiveness of the CAR T-cells in an *in vivo* model, 10-14-week-old NOD/Shi-scid/IL-2R SCIDγnull (NSG) mice were used. $1x10^6$ cells of the HL60 AML cell line were injected into the tail vein of the mice. A bone marrow biopsy was taken to confirm the HL60 had engrafted, the sample was stained for CD45 CD33 by flow cytometry, and a 5-10% engraftment was considered successful. Anti-CD33 CAR T-cells were generated from 3 healthy donors and used in this experiment. The successfully engrafted mice would then be injected with $2.5x10^6$ anti-CD33 CAR T-cells were injected.

2.18 Sequencing

Purified populations of unmodified and modified CAR T-cells were cultured in 75% amino acid free media 25% R10 for 72 hours in the presence of THP1 cells. Post incubation the CAR T-cells were isolated by flow assisted cell sorting (Beckman coulter) using CD34-APC (Biolegend). The RNA was extracted using the RNeasyPLus Micro Kit (Qiagen). The samples were then handled by the Birmingham Genomics team for the rest of the sample processing

steps. Illumina TruSeq RNA sample preparation kit v2 was used to prepare a library and the library was sequenced using the HighSeq 500 platform (Illumina) using Truseqv3 chemistry reagents over 76 cycles. The data analysis was performed by Birmingham University Genomics team members Boris Noyvert and Yi Pan. The sequences were aligned using the STAR RNA-Seq aligner software to the GRCh37 human genome.

2.19 Statistical analysis

The statistical analysis employed in this study primarily consisted of unpaired parametric t-tests to compare differences between groups, unless otherwise specified in the respective figure legends. These tests were chosen for their ability to assess whether the means of two independent groups differ significantly under the assumption of normal distribution.

All statistical analyses were conducted using GraphPad Prism 10 (GraphPad Software), a widely used platform for performing rigorous statistical tests and generating high-quality graphical representations of data. This software facilitated the visualization and interpretation of experimental results, ensuring statistical robustness and reproducibility.

Where necessary, additional statistical tests, including two-way ANOVA for multiple group comparisons, were used to analyse more complex experimental designs. Data are presented as mean ± standard deviation unless otherwise stated, and statistical significance was defined as $p < 0.05$.

3. T-cells in amino acid-restricted environments

3.1 Overview

In AML, amino acid metabolism is altered to support cancer progression; for example, AML blasts upregulate SLC7A11 expression to increase cystine uptake and IDO expression to metabolise tryptophan (Zhao et al., 2018, Arandi et al., 2018). T-cells require the amino acids tryptophan and cystine to proliferate and clear target cells optimally; therefore, the reduced availability of these amino acids reduces T-cell function (Dimeloe et al., 2017, Fultang et al., 2021). Cancer treatments using CAR T-cells have produced remarkable clinical responses with B-cell leukaemia and lymphoma (Chow et al., 2018, Zhang et al., 2020a). However, many challenges limit CAR T-cells' therapeutic efficacy in other cancers (Pearson et al., 2022, Shah et al., 2021b). Barriers to effective CAR T-cell therapy include low patient suitability due to rapid disease progression, modest anti-cancer activity, finding appropriate target antigens, loss of target antigen, and high-level toxicities at low dose levels (Tambaro et al., 2021, Pearson et al., 2022). There is a need to continue improving CAR T-cell expansion and persistence upon injection into patients to ensure effective and sustained anti-cancer responses (Ritchie et al., 2013, Baumeister et al., 2019). To enhance the efficacy of AML targeting CAR T-cells, we speculated that increasing their ability to compete for the amino acids when there are limited amounts available would improve CAR T-cells' adaptation to the tumour microenvironment. From investigating the literature and previous work performed in this lab it was decided to investigate how altering CAR T-cells' ability to uptake tryptophan and cystine could affect their function in AML. To begin this work, we must first understand how T-cells are affected by low tryptophan and cystine environments.

3.2 Objectives

In this chapter, we aim to:

- To investigate the effect of cystine and tryptophan on T-cell activation and proliferation.
- To investigate the effect of cystine and tryptophan on CAR T-cell proliferation
- To investigate the effect of cystine and tryptophan uptake on CAR Jurkat transduced with anti-CD33 SLC7A5 and anti-CD33 SLC7A11 CAR constructs.
- Assess whether the modified constructs affect the CAR Jurkat activation in response to the target antigen.
- Assess whether the modified constructs increase the CAR Jurkat activation in low tryptophan and cystine environments.

3.3 Results

3.3.1 Cystine and tryptophan essential for T-cell function

Cell viability and proliferation were assessed in low amino acid environments to examine the effect of cystine and tryptophan depletion on T-cells.

CFSE labelled T-cells were cultured in cystine or tryptophan free media with and without the addition of cystine or tryptophan, respectively, for 72 hours, and their proliferation was measured by flow cytometry. The proliferation of T-cells in cystine and tryptophan-depleted media was significantly reduced when compared to T-cells in R10% ($p=0.0003$ and $p=0.0002$, respectively) (Figure 9A and B). Adding 50µM of cystine or tryptophan to the respective amino acid-depleted media restored T-cell proliferation compared to T-cells in depleted media, $p=0.0005$ and $p=0.0093$, respectively (Figure 9B).

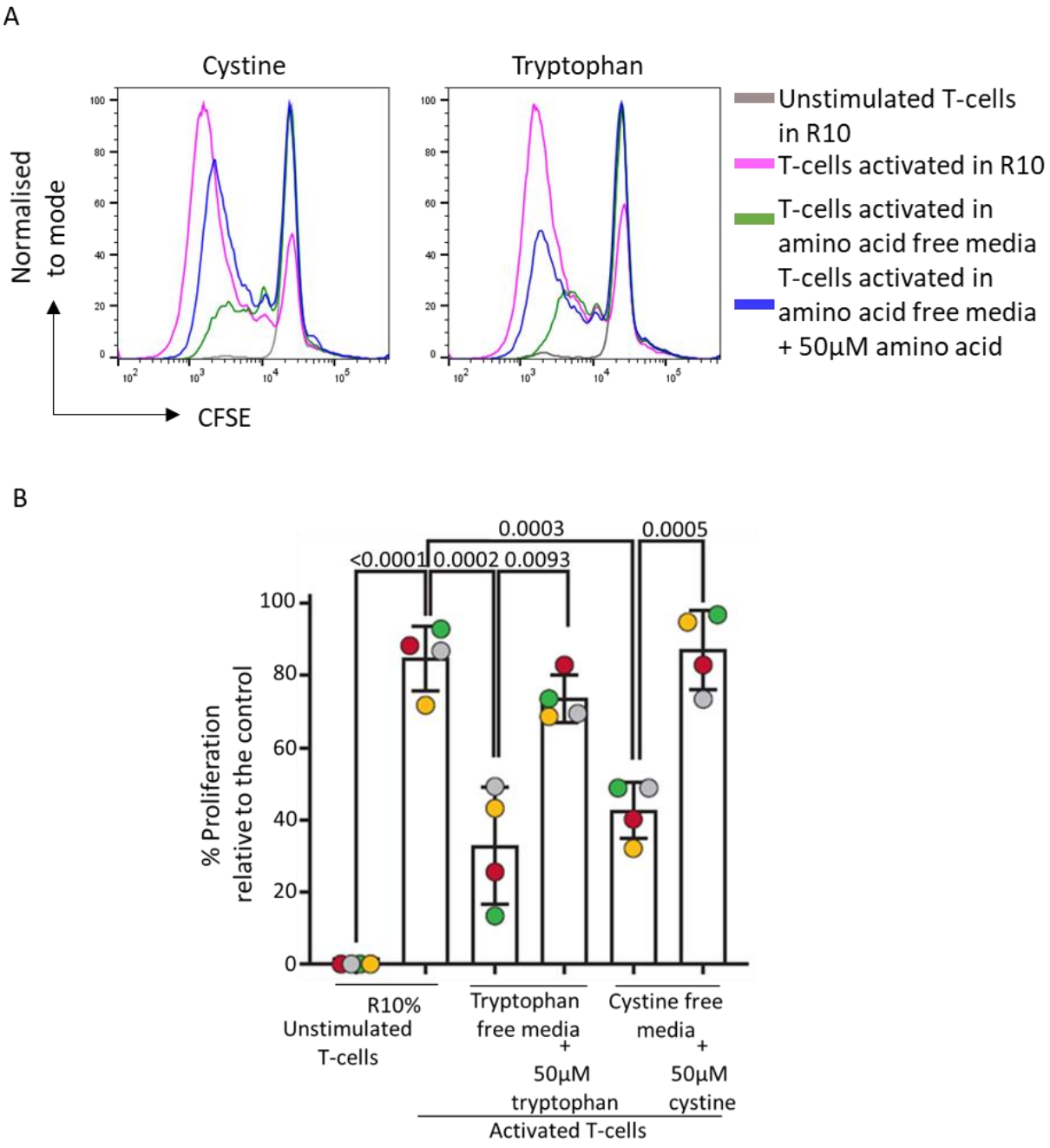

Figure 9: Depletion of Cystine and Tryptophan causes reduced T-cell proliferation.

(A) Representative dot plots and histograms demonstrating T-cell proliferation after 72 hours of culture with cystine and tryptophan free media. (B) The percentage of T-cell proliferation in amino acid deplete media. Anti-CD3/CD28 dynabeads activated T-cells were stained with CFSE prior to culture and the proliferation was assessed by flow cytometry. Statistical analysis was performed using unpaired parametric t-test. Each point represents an independent experiment (n=4).

The IFN-γ production and the upregulation of activation markers CD69 and CD25 were measured on CD4 and CD8 T cells, to understand if cystine and tryptophan depletion affected T-cell activation and function. The CD3 molecules on T-cell surface were masked due to their prior engagement in the activation process (anti-CD3 beads used the same clone as the flow antibody), preventing their use for identifying T-cells. As a result, alternative markers, anti-CD4 and anti-CD8 antibodies, were utilized to accurately distinguish T-cell populations. IFN-γ release was assessed 24 hours post-T-cell activation in the amino acid deplete media. T-cells were activated in cystine or tryptophan-depleted media for 20 hours. Next, the GolgiStop (Monensin) was added to inhibit the release of intracellular IFN-γ. After 4 hours, the intracellular level of IFN-γ was assessed by flow cytometry (Figure 10A).

IFN-γ production was increased at 24 hours in activated T-cells in R10% in $CD4^+$ and $CD8^+$ T-cells (p=0.0140, p=0.0045, p=0.0073 and p=0.0053, respectively). Tryptophan and cystine depletion did not significantly affect $CD4^+$ T-cells or $CD8^+$ T-cells intracellular production of IFN-γ after 24 hours of activation compared to the T-cells activated in R10% (p=ns) (Figure 10B and C).

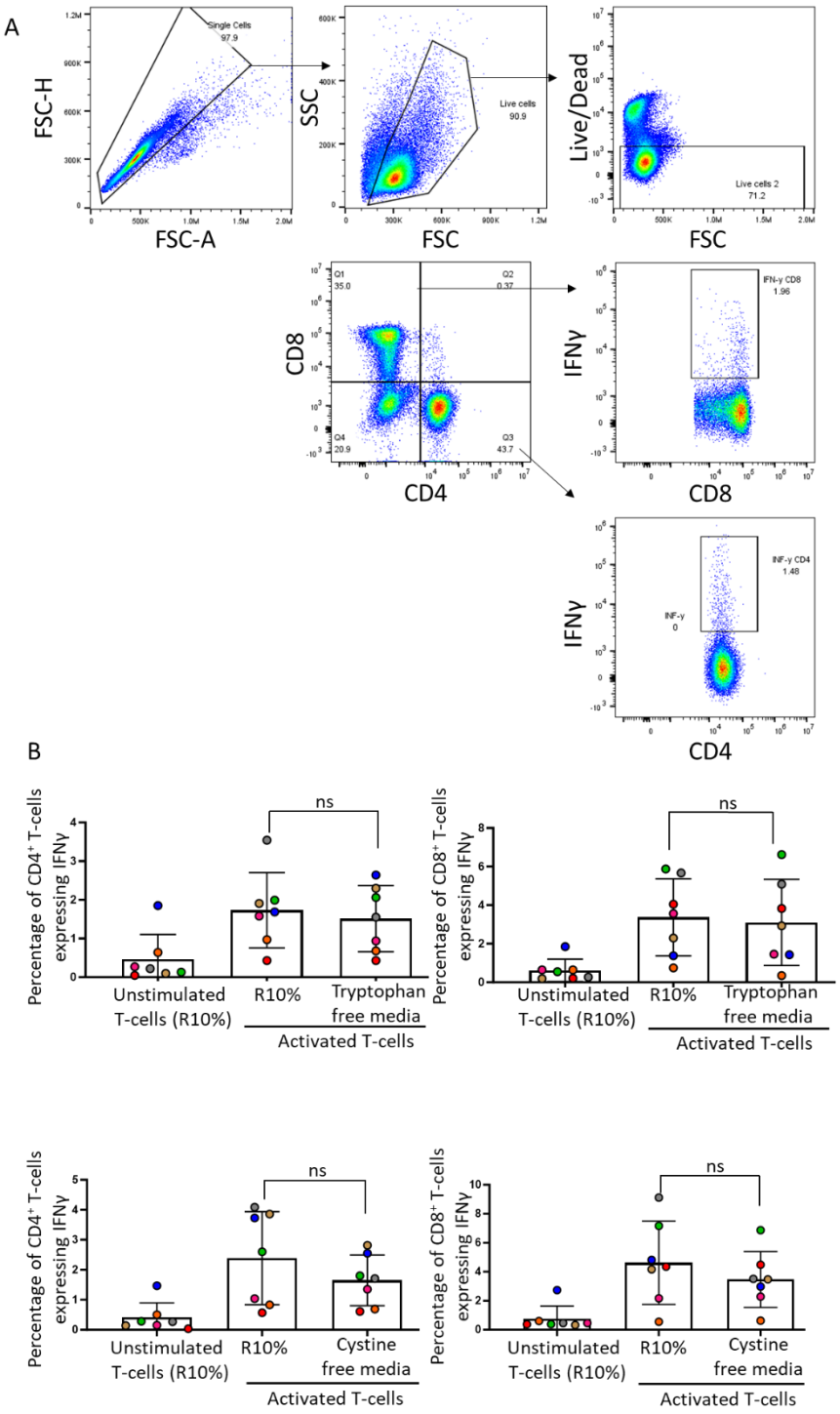

Figure 10: The effect of cystine and tryptophan depletion on T-cell IFN-γ production.

T-cells were activated by anti-CD3/CD28 dynabeads and cultured in tryptophan or cystine free media for 24 hours. After 20 hours, GolgiStop (Monensin) was added to prevent the release of IFN-γ. INF-γ and CD69 expression were measured by flow cytometry. (A) Representative dot plots of the gating strategy used to isolate INF-γ positive T-cells. (B) Percentage of CD4+ and CD8+ T-cells expressing IFN-γ in tryptophan free media. (C) Percentage of CD4+ and CD8+ T-cells expressing IFN-γ in cystine free media. Statistical analysis was performed using unpaired parametric t-tests. Each dot represents an independent experiment (n=7).

CD69 is an early marker of T-cell activation that begins to be transcribed within minutes of stimulation, and the CD69 protein is upregulated on the T-cell surface within 2 hours of activation. However, CD69 transcription stops after 4-6 hours post-stimulation, leading to CD69 surface expression being downregulated between 48-72 hours post-activation (Reddy et al., 2004).

To investigate whether low amino acid conditions altered the expression levels of CD69 on activated T-cells, T-cells were cultured with CD3/CD28 antibodies in tryptophan and cystine-free media for 24 hours, and CD69 expression was assessed by flow cytometry. When amino acid availability is limited, T cells experience metabolic stress, leading to reduced expansion and impaired functionality. We analysed the percentage of CD69 positive T-cells and the intensity of the CD69 expression on the same cell population. The percentage of live CD69 positive T-cells did not change over time in the both experimental conditions (data not shown) instead the intensity of CD69 expression showed significant change.

As expected, CD3/CD28 stimulation significantly upregulated CD69 on T cells compared to unstimulated cells. At 24 hours, there is no significant difference in CD69 expression observed on activated $CD4^+$ or $CD8^+$ T-cells in both cystine ($p=0.8471$ and $p=0.6751$) or tryptophan free media ($p=0.4602$ and $p=0.7561$) (Figure 11).

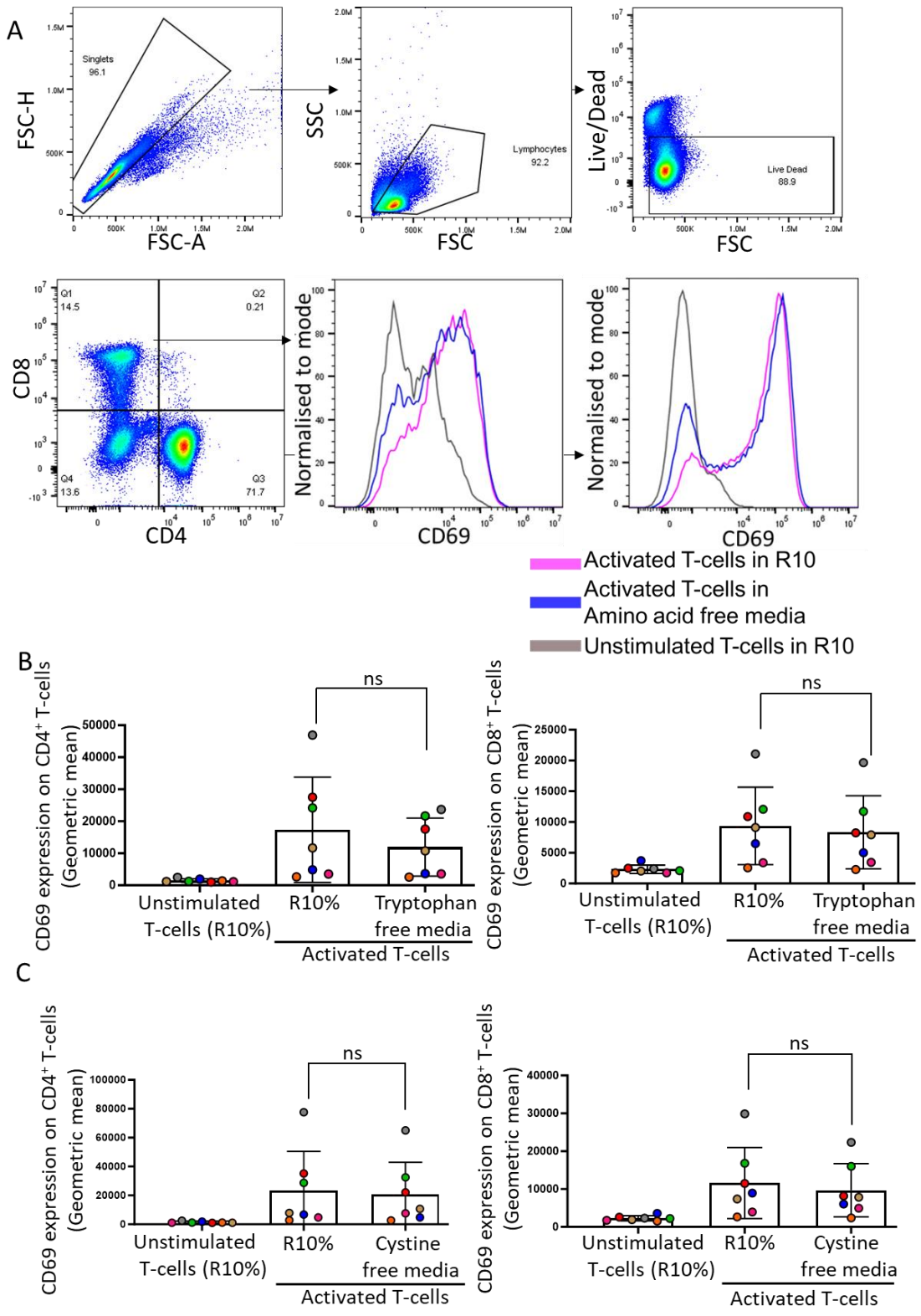

Figure 11: Cystine and tryptophan depletion do not affect T-cell CD69 expression after 24 hours.

Geometric mean of T-cells in tryptophan and cystine free media. (A) Dot plots representative of the gating used to identify the T-cell population which was then assessed for its geometric mean of CD69. (B) Geometric mean of CD4+ and CD8+ T-cells in tryptophan free media. (C) Geometric mean of CD4+ and CD8+ T-cells in cystine free media. Statistical analysis was performed using unpaired parametric t-tests. Each colour of point represents an independent experiment (n=7).

As expected, CD69 expression in T-cells cultured in R10% had lower CD69 expression at 72 hours compared to their CD69 expression at 24 hours. $CD8^+$ T-cells CD69 expression was not significantly different from unstimulated T-cells.

Interestingly, at 72 hours, stimulated $CD4^+$ and $CD8^+$ T-cells had a significantly higher CD69 expression when cultured in cystine-free media ($p=0.0219$ and $p=0.0074$, respectively) and tryptophan-free media ($p=0.0263$ and $p=0.0029$ respectively) compared to the activated T-cells in R10% (Figure 12B and C).

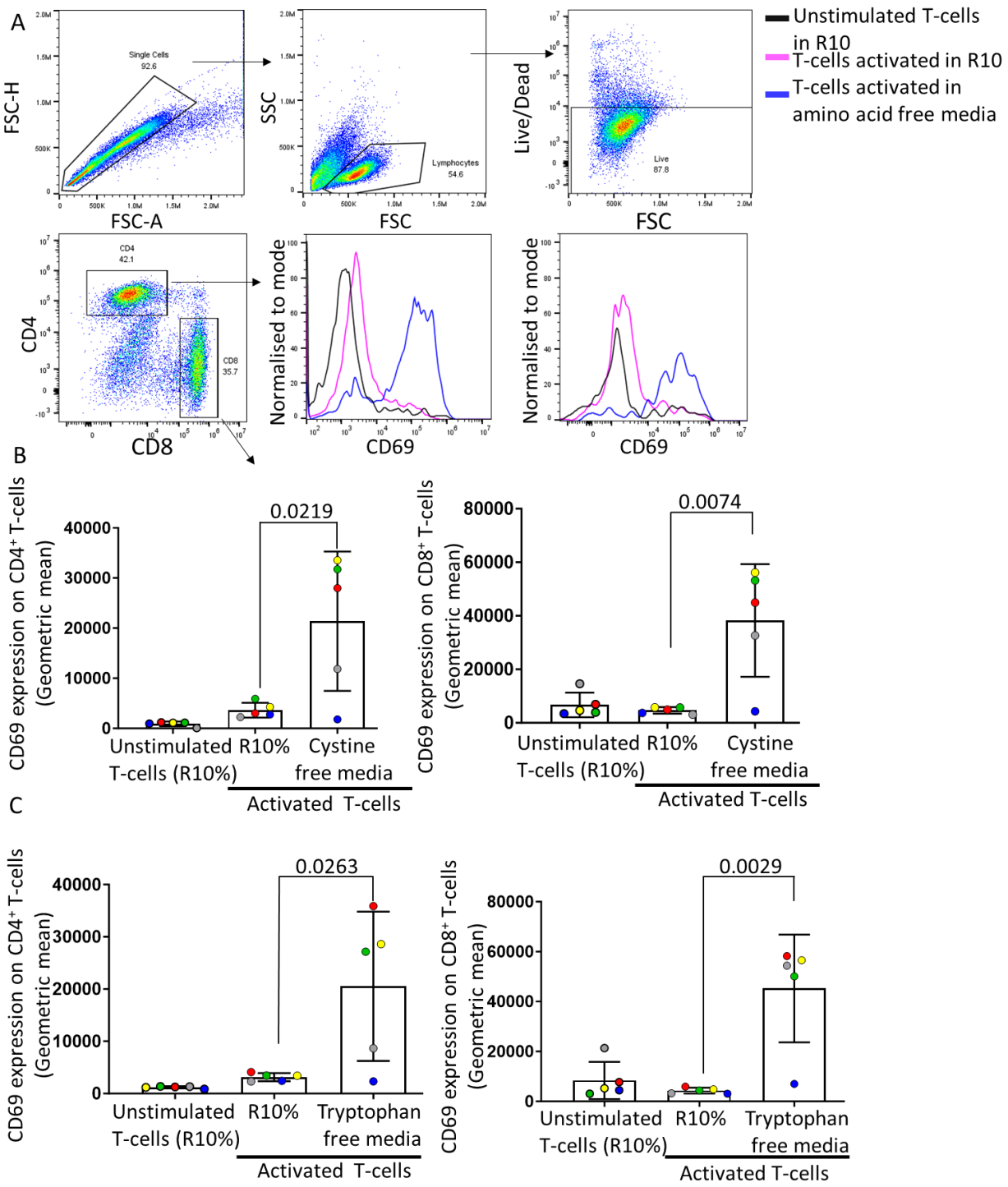

Figure 12: Depletion of tryptophan and cystine alters T-cell CD69 expression after 72 hours.

T-cells activated and cultured for 72 hours in tryptophan and cystine free media were analysed by flow cytometry. (A) Dot plots representive of the gating used to identify the T-cell population which was then assessed for its geometric mean of CD69 and CD25 expression. (B) The geometric mean of CD69 expressed on live CD4+ and CD8+ T-cells cultured in cystine free media (n=5). (C) The geometric mean of CD69 expressed on live CD4+ and CD8+ T-cells cultured in tryptophan free media. Statistical analysis was performed using unpaired parametric t-test. Each point represents an independent experiment (n=5).

Additionally, we analysed the expression of CD25, a protein involved in the assembly of the high-affinity IL-2 receptor and is a crucial marker of T-cell activation. CD25 is upregulated 24 hours post T-cell stimulation, with expression peaking at 72 hours (Reddy et al., 2004).

Stimulated $CD8^+$ T-cells cultured in cystine and tryptophan free media ($p=0.0499$ and $p=0.0458$, respectively) had a significantly lower CD25 expression after 72 hours compared to stimulated T-cells in R10% (Figure 13B). Stimulated $CD4^+$ T-cells cultured in cystine-depleted and tryptophan-depleted media ($p=0.0628$ and $p=0.0968$, respectively) did not have significantly lower CD69 expression (Figure 13C). This data shows that cystine and tryptophan depletion significantly inhibit the activation of $CD8^+$ T-cells.

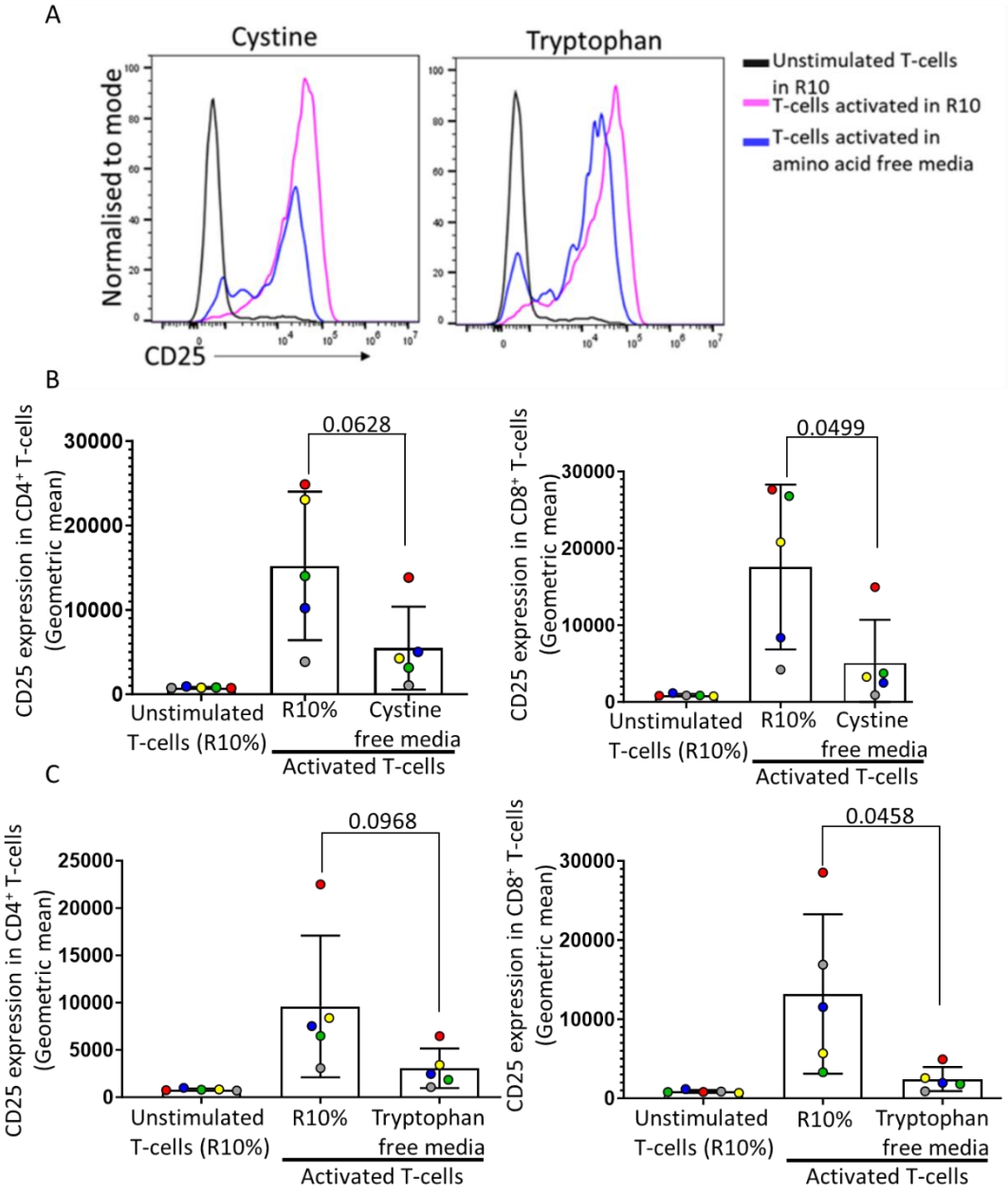

Figure 13: Depletion of tryptophan and cystine decreases T-cell CD25 expression.

T-cells activated and cultured for 72 hours in tryptophan and cystine free media were analysed by flow cytometry. (A) Histogram of the CD25 geometric mean present on live CD4+ T-cells. (B) Summaries of the CD25 geometric mean present on live CD4+ and CD8+ T-cells cultured in cystine deplete free (n=5). (C) Summaries of the CD25 geometric mean present on live CD4+ and CD8+ T-cells cultured in tryptophan free media. Statistical analysis was performed using unpaired parametric t-test. Each colour point represents an independent experiment (n=5).

3.3.2 Cystine and tryptophan are essential for CAR T-cell function

Following the evidence that cystine and tryptophan depletion affected T-cell activation and proliferation, we investigated if low amino acid environments could also affect CAR T-cell activity. The Phoenix Ampho retroviral cell line was transfected with vectors that contained an anti-CD33 CAR construct.

After 24 hours of incubation, the virus-containing supernatant was harvested and immobilised onto RetroNectin-coated plates using spinfection. The anti-CD33 CAR construct contains several sections surrounded by long terminal repeat sequences on either side of the transcription zone (Figure 8A). The first section contains a truncated CD34 tag, an F2A self-cleaving peptide (Philip et al., 2014). The CAR section of the construct included a CD8-derived signal peptide to localise the CAR into the cell membrane, the anti-CD33 scFv with a CD8 hinge region to allow flexibility needed for antigen recognition, CD3 ζ-chain signalling domain to enable signal transmitting and T-cell activation, and a 4-1BB co-stimulation domain which improves anti-tumour activity and CAR T-cell persistence.

T-cells were isolated from healthy apheresis cones via Lymphoprep and magnetic-assisted cell sorting before activation with anti-CD3/CD28 Dynabeads for 48 hours. The activated T-cells were added to the virally coated plates for 96 hours. Post incubation, the transduced T-cells were harvested, and the transduction efficiency was assessed by flow cytometry using the CD34 tag inserted into the CAR T-cell construct (Figure 14A). The same CD34 tag was used to isolate the transduced CAR T-cell population from the non-transduced population (Figure 14B).

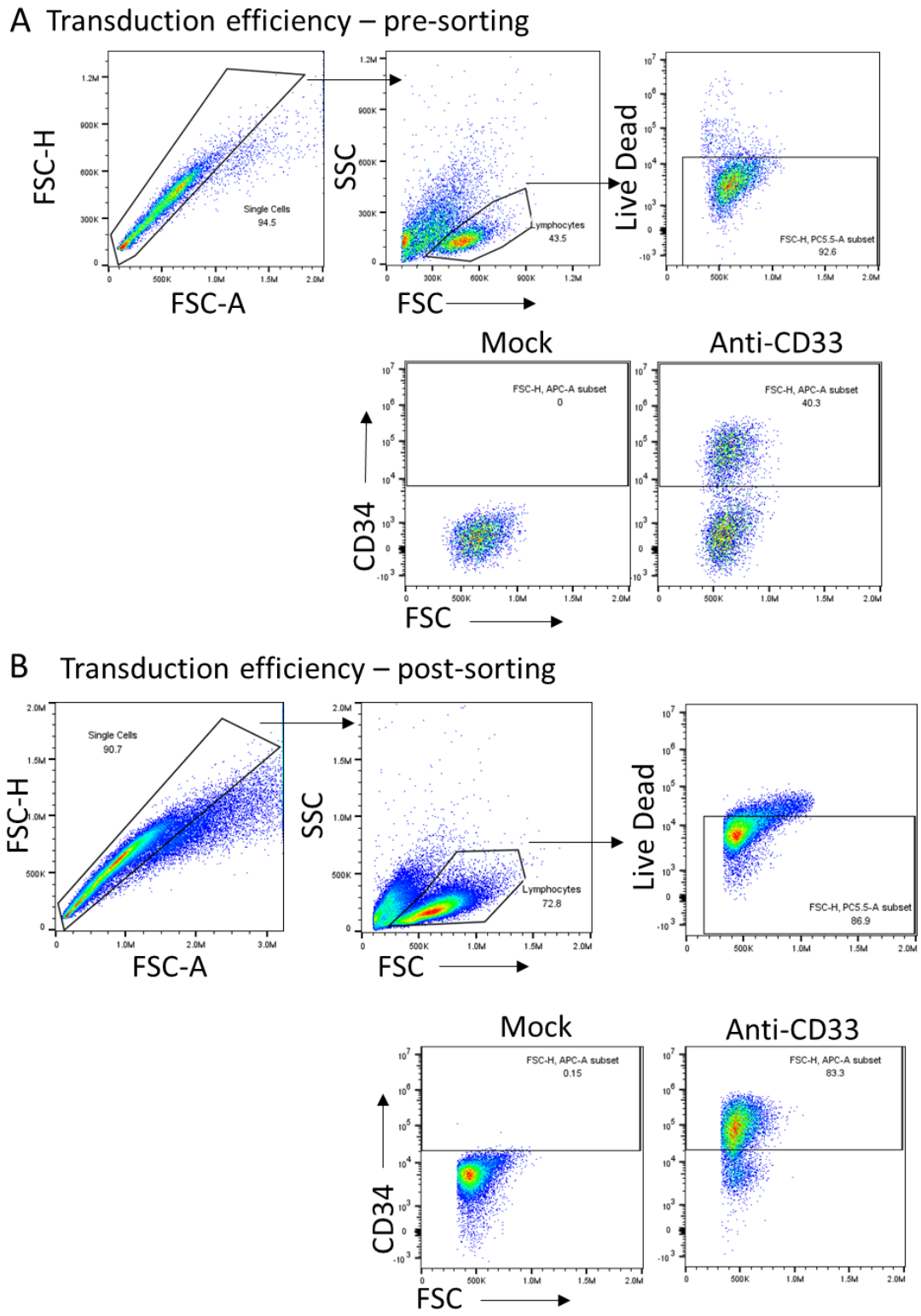

Figure 14: Transducing and sorting anti-CD33 CAR T-cells
(A) Representative dot plots demonstrating the transduction efficiency of anti-CD33 CAR T-cells pre-sorting. (B) Representative dot plots demonstrating the transduction efficiency of anti-CD33 CAR T-cells post-sorting.

The enriched CAR T-cells were cultured with $CD33^+$ THP1 in R10%, tryptophan-depleted, or cystine-depleted media. CAR proliferation was measured by flow cytometry after 72 hours. Across all three donors tested, the anti-CD33 CAR T-cell proliferation was significantly decreased in tryptophan-depleted and cystine-depleted media compared to the CAR T-cells cultured in R10% ($p>0.05$) (Figure 15A and B).

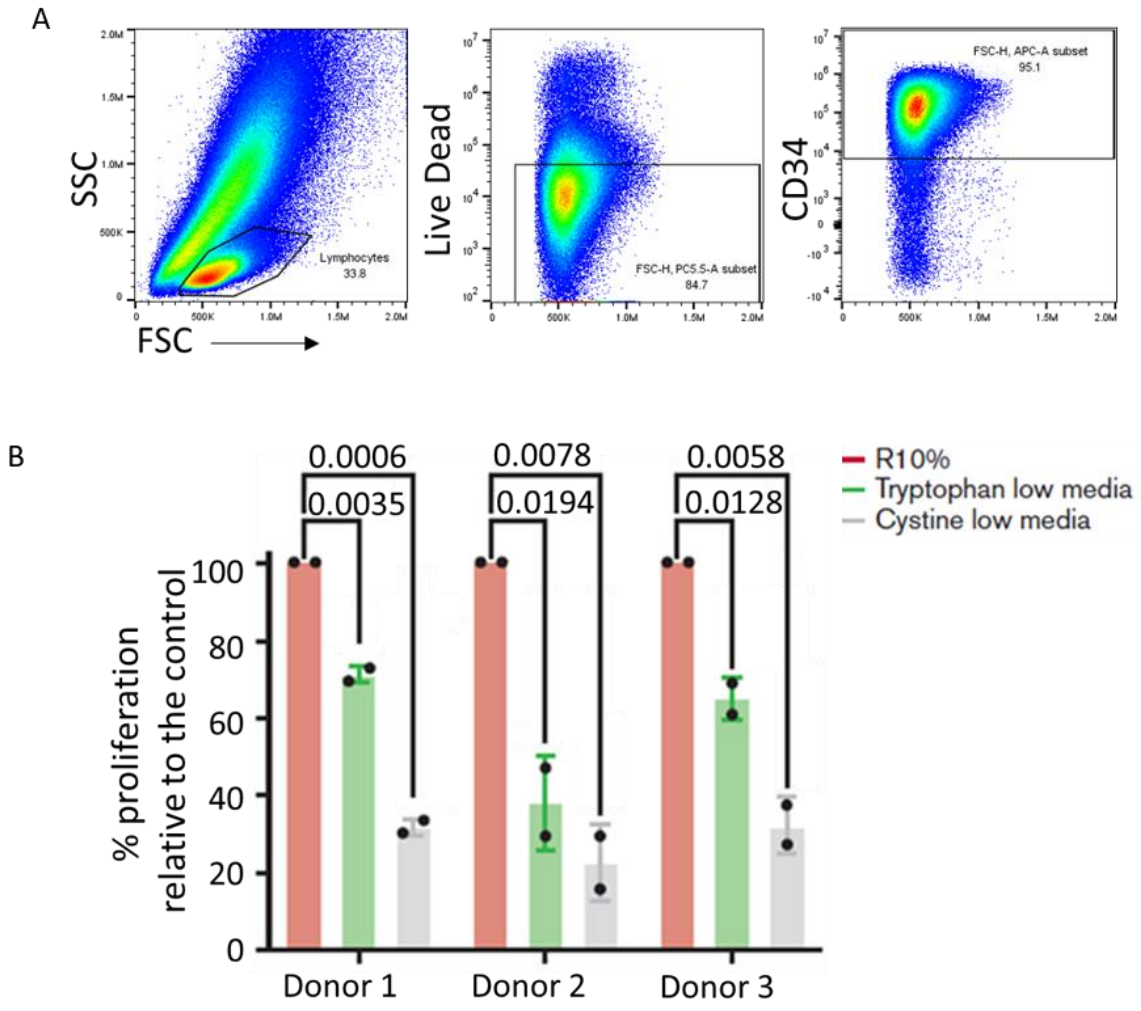

Figure 15: Anti-CD33 CAR T-cells are affected by amino acid depletion
(A) Representative dot plots demonstrating the gating used to identify anti-CD33 CAR T-cell population. (B) Anti-CD33 CAR T-cells were cultured with THP1 cells in low amino acid media for 72 hours and then read by flow cytometry to assess proliferation by count. Statistical analysis performed was unpaired parametric t-tests. Each donor represents an independent experiment n=3 with 2 technical repeats per donor.

3.3.3 Transducing anti-CD33 Jurkat

Following these results, we decided to add the amino acid transporters for tryptophan (SLC7A5) and cystine (SLC7A11) to the original CAR anti-CD33 construct transcriptome (Figure 8). The hypothesis was that these modified CAR T-cells would better compete with any surrounding cells to access their respective amino acids in the low amino acid conditions.

Unlike the anti-CD33 construct, the two transporter CAR T constructs have an additional P2A self-cleaving peptide to remove the CAR sequence from the transporter sequence and either a SLC7A5 or SLC7A11 gene to provide the CAR T-cells with the appropriate transporters (Figure 8).

Firstly, the CAR constructs were transduced into Jurkat cells, a T-cell leukaemia cell line widely used as a T-cell analogue, to create CAR Jurkat. The retroviral cell line, Phoenix Ampho cells, were transfected with the CAR vectors, and 24 hours later, the supernatant was used to transduce the Jurkat cell lines. The CAR Jurkat cells were identified using a truncated CD34 tag inserted into the CAR construct that would be expressed on the surface of transduced cells. Successfully engineered Jurkat cells were isolated by positive selection using anti-CD34 magnetic beads, and flow cytometry was used to assess population purity (Figure 16A-B).

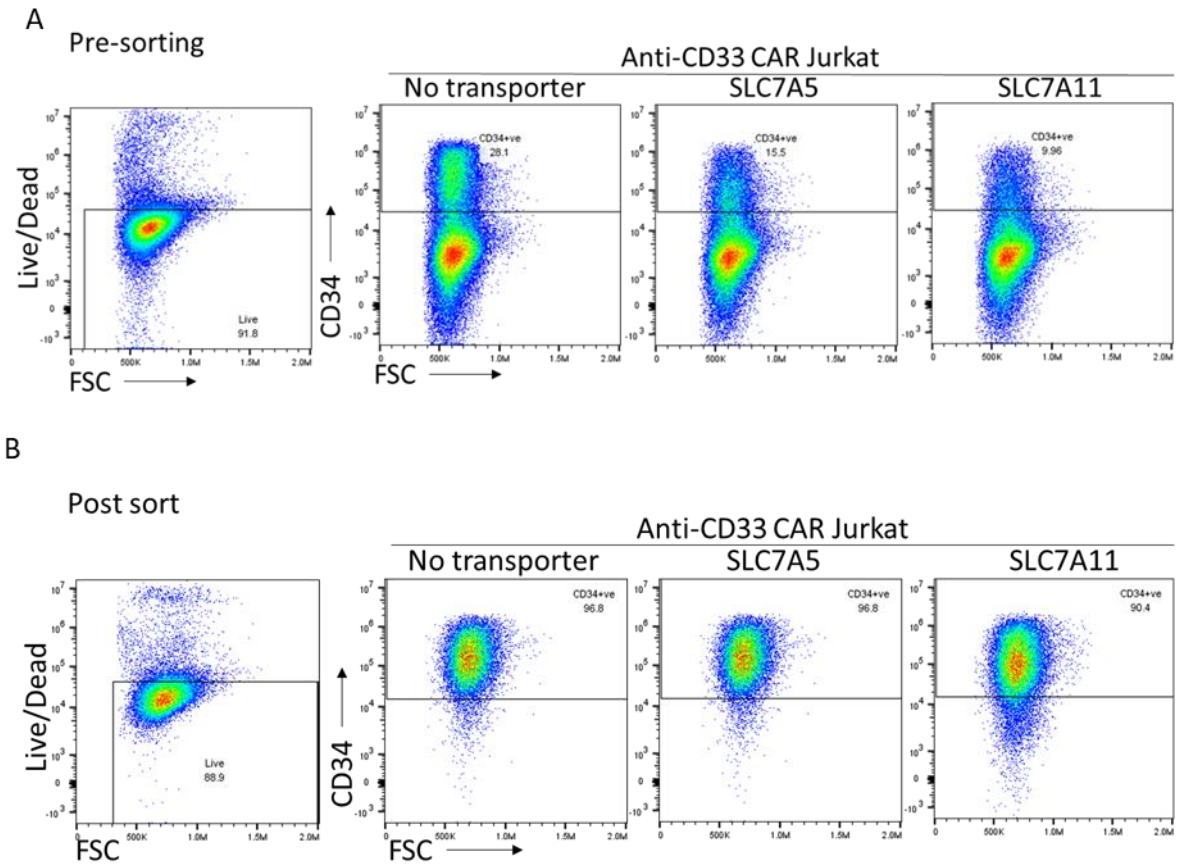

Figure 16: Transduction of CAR T-cells.

(A) At day 3 the efficiency of transduction was assessed by measuring the CD34 expression on transduced T cells by flow cytometry. The live/death marker propidium iodide was added to exclude death population. Representative dot plots has been shown. (B) After assessing the percentage of CAR on T cells, the CAR-T were enriched using a CD34 magnetic beds and the cells were staining to verify the purity of CAR-T. Representative dot plots of each CAR-T show a similar frequency of CD34 positive cells.

To ensure SLC7A5 and SLC7A11 transporter expression in the modified CAR Jurkat, the expression of their respective transporters was assessed by western blot, using β-actin as a loading control. SLC7A5 expression was higher in anti-CD33 SLC7A5-Jurkat CAR compared to unmodified anti-CD33 Jurkat CAR (Figure 17). SLC7A11 expression was higher in anti-CD33 SLC7A11 Jurkat CAR compared to anti-CD33 CAR Jurkat (Figure 17). To measure the surface expression of SLC7A5 and SLC7A11 transporters on the CAR Jurkat cells following transduction the cells were stained with specific antibodies. However, to measure transporter expression by flow cytometry was not possible due to lack of clear staining obtained with the antibodies available. Therefore, western blot was determined to be the most suitable assay to assess protein expression of the transporters.

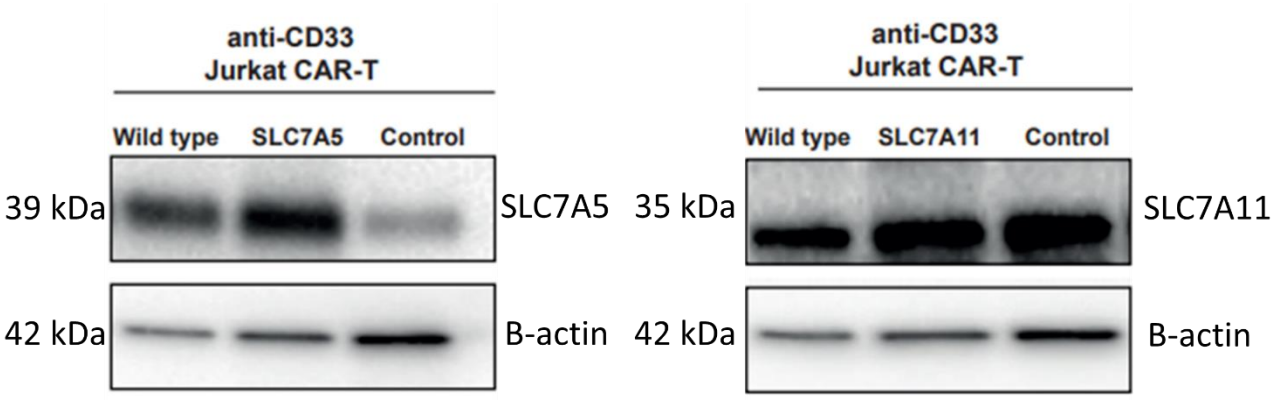

Figure 17: The successful transduction of Jurkat CAR.
Jurkat cell line were cultured for 48 hours in plates coated with retrovirus harvested from Phoenix AMPHO cells that had been transduced with our CAR containing retrovirus. Post incubation the Jurkat were harvested and analysed by flow cytometry and western blot. (A) Jurkat CAR cell assessed by western blot for expression of SCL7A5, SLC7A11, and β-actin. THP1 were used as a positive control. The protein size is indicated next to each band.

3.3.4 Assessing AML recognition and early activation in modified CAR Jurkat

Firstly, we assessed whether the modified CAR Jurkat cells had an altered ability to recognise and respond to the tumour target. THP1 and HL60 leukaemia cell lines were used for the following experiments due to their high surface expression of CD33, our target antigen (Figure 5). The three types of CAR Jurkat cells were co-cultured with decreasing concentrations of the $CD33^+$ cell lines. After 48 hours of culture, the cells were harvested and analysed by flow cytometry for the expression of the activation marker CD69. Like T-cells, the Jurkat cell line upregulates CD69 during activation, and this upregulation is used, as shown in the literature, to model CAR antigen-specific responses in Jurkat (Bloemberg et al., 2020).

All CAR Jurkat showed a significantly increased expression of CD69 following antigen presentation (Figure 18). The level of CD69 expression decreased incrementally with the decreasing ratio of CAR-Jurkat: target cells demonstrating a dose-dependent response.

Without stimulation, the addition of the SLC7A5 transporter to the anti-CD33 CAR Jurkat did not alter the baseline expression of CD69 ($p=0.9281$) compared to unmodified CAR Jurkat (Figure 18B). In response to the target antigen stimulation, anti-CD33 SLC7A5 CAR Jurkat CD69 expression significantly increased compared to unmodified CAR Jurkat ($p=0.0257$) (Figure 18B).

There is a significant increase in CD69 expression on CAR Jurkat following the co-culture of the increasing concentration of $CD33^+$ cell lines comparing the anti-CD33 CAR T-cells with anti-CD33 SLC7A5 CAR T-cells ($p=<0.0001$) and with anti-CD33 SLC7A11 CAR T-cells ($p=0.0007$).

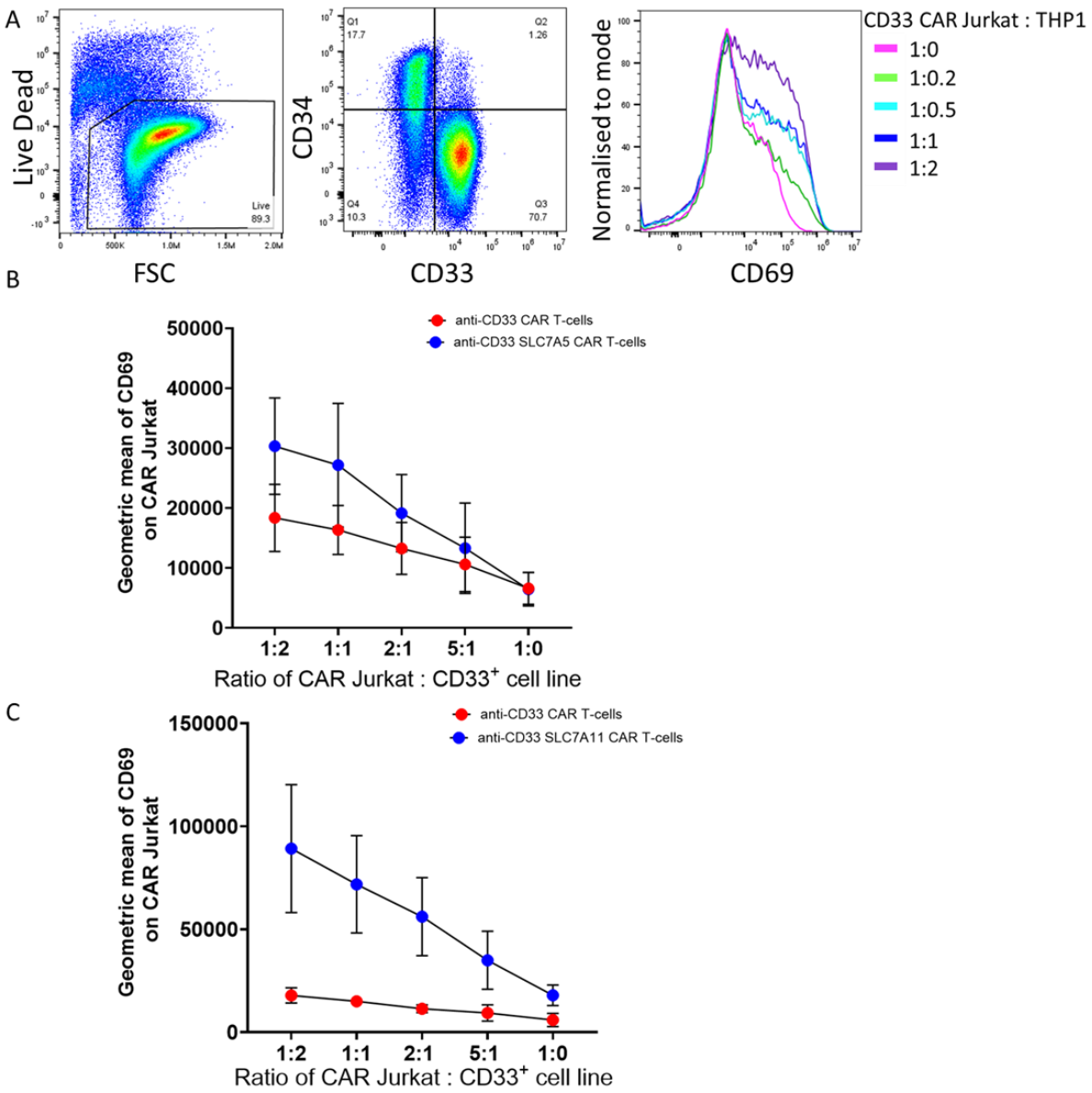

Figure 18: CAR Jurkat are responsive to target cells

CAR Jurkat were co-cultured with CD33+ cell line HL60 (square) or THP1 (circle) at a range of effector to target concentrations. These included the ratios of 1:2, 1:1, 2:1, and 5:1 CD33+ cell to CAR Jurkat cultured for 48 hours in R10. (A) Representative dot plots demonstrating the gating strategy used to isolate the desired population. (B and C) The geometric mean of the CD69 expression of the CAR Jurkat after 48 hours. Two-way ANOVA were used to determine statistical significance. Each point represents the mean of five individual experiments. Red circle anti-CD33 CAR T-cells. The blue circle represents the modified anti-CD33 CAR T-cells.

3.3.5 Metabolomics of modified CAR Jurkat

To understand how the insertion of SLC7A5/SLC7A11 can influence Jurkat CAR metabolism, we cultured the 3 CAR Jurkat in different conditions. As described in Figure 17A and B, both tryptophan and cystine, through various metabolic and signalling pathways, are used for protein synthesis and provide signalling that promote T-cell proliferation, activation, differentiation and survival (Fallarino et al., 2002, Mak et al., 2017, Han et al., 2024, Rashidi et al., 2020). Additionally, cystine can be converted to glutathione, which reduces ROS synthesis (Figure 19 A) (Siska et al., 2016).

Furthermore, tryptophan inhibits a stress response mediated through GCN2 that, in tryptophan depletion, causes T-cell apoptosis (Rashidi et al., 2020). Tryptophan is converted into purine nucleotide rings that are essential for DNA, RNA and membrane lipid synthesis (Figure 19B). However, the enzyme IDO, expressed in AML, will break down tryptophan into the kynurenine pathway, which causes inhibitory signals for T-cell proliferation and activation and promotes Treg differentiation (Munn et al., 1999, Komrokji et al., 2019, Yang et al., 2022b).

T-cell proliferation and activation alter the metabolic pathways of T-cells, resulting in altered glycolytic and mitochondrial metabolism (Sena et al., 2013). Tryptophan and cystine abundance promotes mTOR activity, which induces the transcription factor c-myc, which in turn promotes glycolysis (Ma et al., 2023b). A seahorse XF analyser Agilent system was used to quantify the metabolomic rate of cells by measuring the dissolved oxygen concentration and extracellular pH, which were measured across multiple time points. The addition of inhibitors of the electron transport chain, oligomycin, BAM15, Rotenone, and Antimycin A, allows the measurement of different aspects of mitochondrial respiration and glycolysis,

that together enable the assessment of the basal mitochondrial respiration rate and the glycolytic rate (Figure 19 C).

A

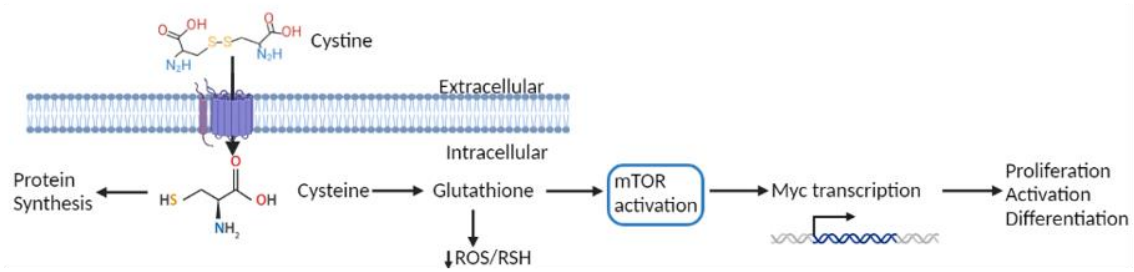

B

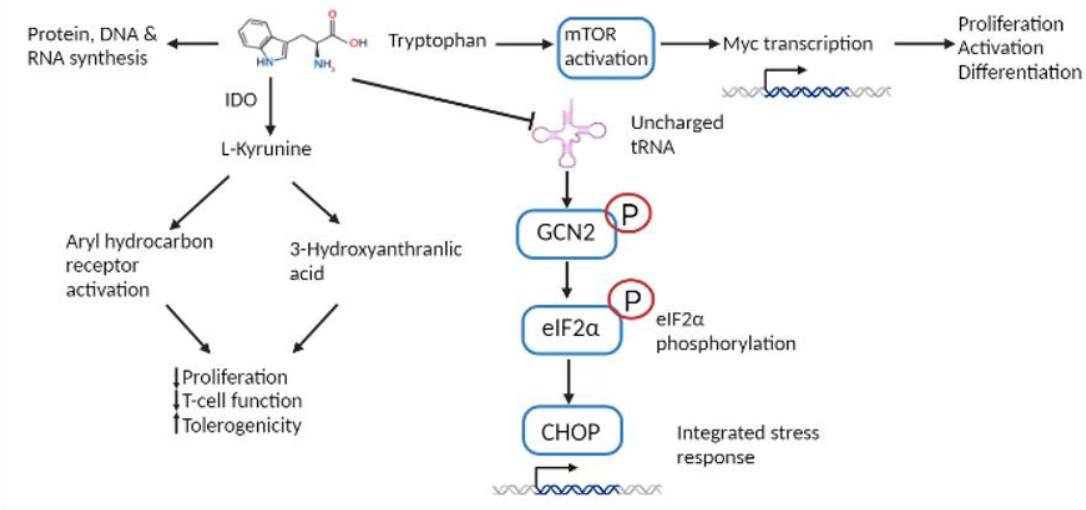

C

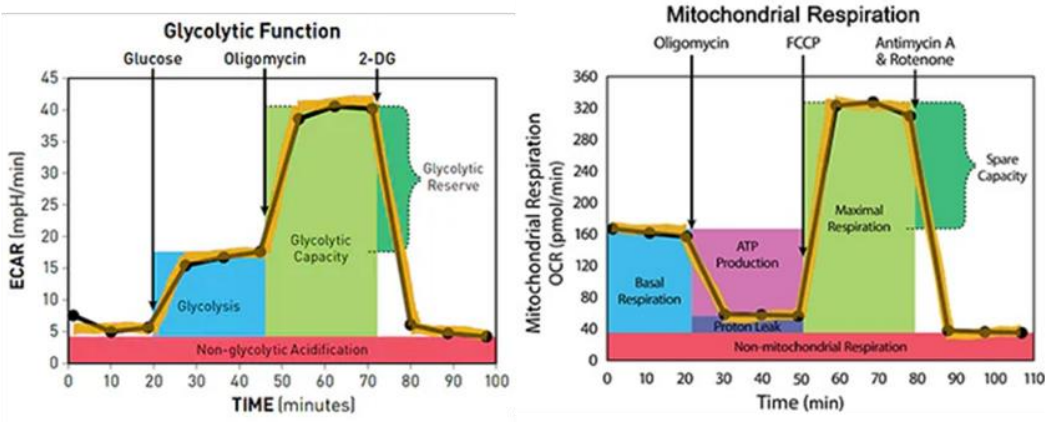

Figure 19: Cystine and Tryptophan are involved in T-cell metabolism.
(A) Cystine metabolism in T-cells. Diagram created using Biorender.com
(B) Tryptophan function and metabolism in T-cells. Diagram generated using biorender.com.
(C) Representative diagrams demonstrating how the seahorse XF analyser Agilent systems calculate glycolysis and mitochondrial respiration. Diagrams sourced from Aligent.com

The CAR Jurkat were cultured in R10%, tryptophan, and cystine-depleted media. After three hours, the cells were assessed for respiration rates using the seahorse XF analyser. This experiment was repeated four times. The results showed that a higher rate of oxygen was consumed by both the anti-CD33 SLC7A5 and anti-CD33 SLC7A11 CAR Jurkat, compared to the anti-CD33 CAR Jurkat across the total assay (Figure 20 A and B). Anti-CD33 SLC7A5 Jurkat had an increased glycolytic proton efflux rate compared to the anti-CD33 CAR Jurkat (Figure 20 C). Anti-CD33 SLC7A11 CAR Jurkat had an increased basal mitochondrial respiration rate compared to the anti-CD33 CAR Jurkat (Figure 20 C). Both anti-CD33 SLC7A5 CAR Jurkat and anti-CD33 SLC7A11 CAR Jurkat had a significantly higher ATP production rate when under starved conditions (Figure 20 C).

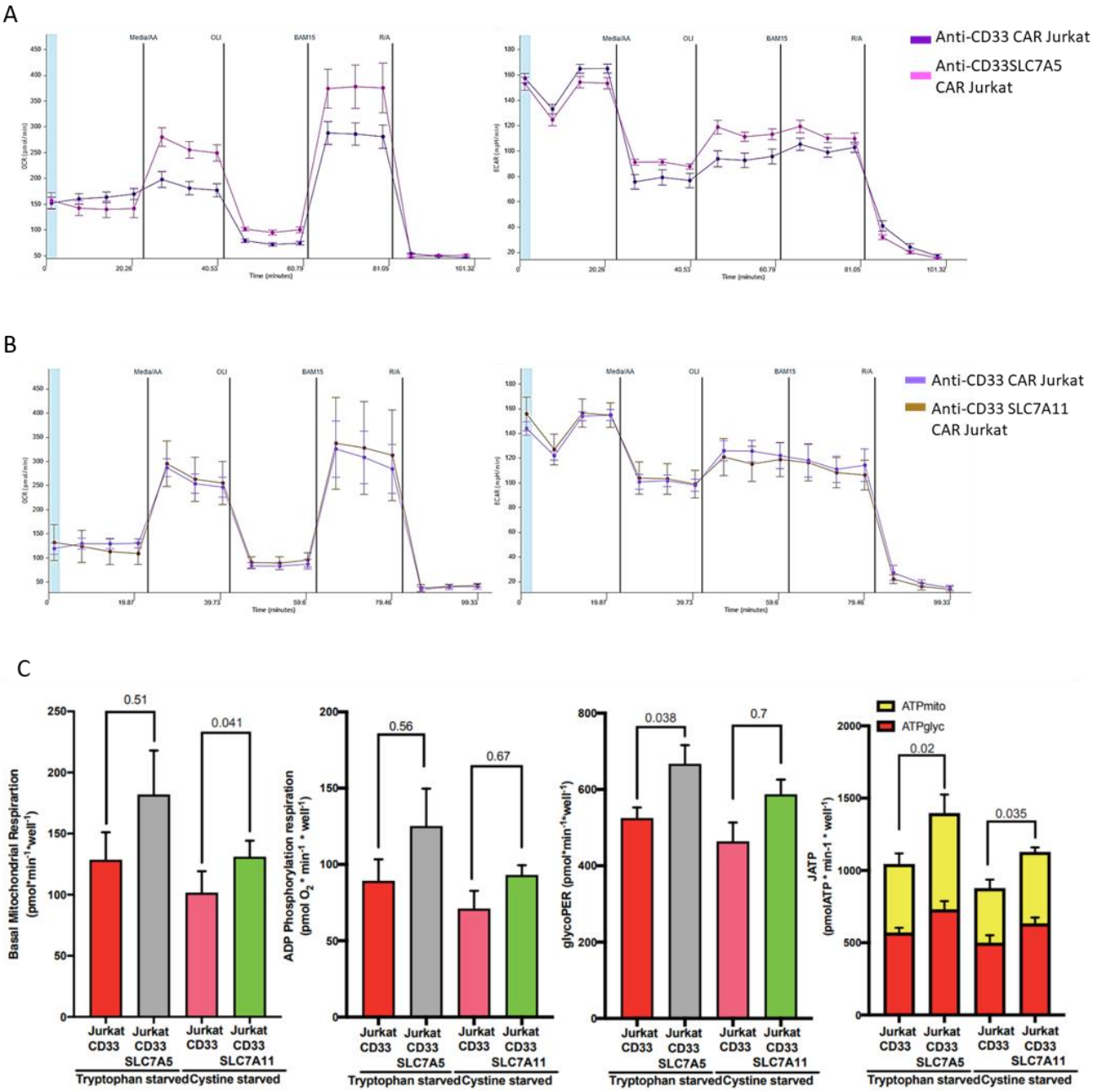

Figure 20: Metabolomics of CAR Jurkat under starved conditions

The CAR Jurkats were cultured in R10% or amino acid depleted media for 3 hours and then transferred to the seahorse XF analyser Algilent. (A and B) Representative OCR and ECAR diagrams demonstrating the raw data gathered from the seahorse XF analyser from anti-CD33 SLC7A5 and anti-CD33 SLC7A11 CAR Jurkat, respectively. (C) The graphs showing the analysed data from the seahorse XF analyser demonstrating the respirations rates of glycolysis, basal mitochondrial rate, and ATP production levels. Biological replicates were used to perform experiments (n=4). Seahorse analysis was done with the support of Jonathon Barlow of the Birmingham metabolomics team.

3.4 Discussion

This chapter demonstrated how low tryptophan and cystine environments can affect the proliferation and function of T-cells and anti-CD33 CAR T-cells. The results in this chapter demonstrated the design of CAR constructs that attempt to mitigate the effects of low cystine and tryptophan environments. The final section of this chapter demonstrated the transduction of Jurkat using the modified CAR constructs and the altered metabolomics, which these CAR constructs facilitated in low amino acid environments.

During T-cell activation, the transporters SLC7A5 and SLC7A11 are upregulated as the amino acids they transport are required for T-cell function (Srivastava et al., 2010, Hayashi et al., 2013, Garg et al., 2011, Zhang et al., 2023b).

As anticipated in the literature, healthy activated T-cells cultured *in vitro* in low tryptophan or low cystine conditions had significantly decreased proliferative capacity. The addition of cystine and tryptophan to the respective low amino acid media recovers the T-cell proliferation.

Activated $CD8^+$ and $CD4^+$ T-cells highly express IFN-γ. IFN-γ has many roles in immunity as it can improve T-cell anti-tumour activity, increase immune cell trafficking, induce T-cell mediated killing and increase tumour antigenicity through increasing MHC expression (Zhang et al., 2019). IFN-γ expression by activated $CD4^+$ T-cells is lower than $CD8^+$ T-cells, but $CD4^+$ T-cell derived IFN-γ can still be involved in direct T-cell mediated killing and supports $CD8^+$ T-cell function, including $CD8^+$ T-cell IFN-γ production (Green et al., 2013). Culturing activated $CD4^+$ and $CD8^+$ T-cells in low cystine or low tryptophan media did not reduce IFN-γ expression 24 hours after activation compared to activated $CD4^+$ and $CD8^+$ T-cells cultured in R10%.

CD69 suppresses autoimmune responses and is often used as an early marker of T-cell activation as it is upregulated on the T-cell surface within 2-3 hours of T-cell activation, peaking 12-24 hours after activation. The expression of CD69 was not altered on $CD4^+$ or $CD8^+$ T-cells when cultured in cystine or tryptophan free media. Therefore, we determined that low tryptophan and cystine availability did not affect early activation of T-cells.

CD69 transcriptional expression is only active for the first six hours after activation. Therefore, CD69 surface expression decreases 48-72 hours after activation (Reddy et al., 2004). Seventy-two hours after activation, the CD69 expression of $CD8^+$ T-cells in R10% had been downregulated to the same level as unstimulated T-cells. However, the low cystine and tryptophan conditions caused CD69 expression to continue to be highly expressed in T-cells 72 hours after activation. It has been described previously in the literature that T-cells resident in the tumour microenvironment and tumour-draining lymph nodes have CD69 expression. CD69 expression has been shown to reduce the effector function of intra-tumoral T-cells. Sustained CD69 expression is present on resident memory T-cells and can promote Treg differentiation and suppressive function (Walsh et al., 2019, Yu et al., 2018). This suggests that the amino acid deprivation within the tumour microenvironment inhibits proliferative capacity and reduces T-cell effector function.

CD25 is the alpha chain of the IL-2 receptor that is upregulated after activation, peaking between 48-72 hours (Naghizadeh et al., 2022). IL-2 signalling through CD25 is crucial for T-cell activation and involved in a wide range of T-cell signalling through janus kinase (JAK)/STAT, mitogen-activated protein kinase (MAPK), phosphoinositide 3-kinase (PI3K), and protein kinase B (Akt)-dependent signalling pathways promoting T-cell proliferation, differentiation, cell death and responsiveness (Bachmann and Oxenius, 2007, Zhang et al., 2021a). $CD8^+$ T-

cells activated in cystine or tryptophan free environments had decreased CD25 expression. Cystine or tryptophan free media did not significantly decrease CD25 expression in $CD4^+$ T-cells.

The effects of low cystine or low tryptophan conditions on T-cell proliferation remain in CAR T-cell proliferation. CAR T-cells in cystine and tryptophan free media had reduced proliferation. CAR T-cells have been shown to lack clinical activity and have off-target effects in AML (Baumeister et al., 2019, Atilla and Benabdellah, 2023). The effect of amino acid depletion on CAR T-cells could contribute to these current results, as CAR T-cell function would be limited without effective proliferation.

The Jurkat cell line was successfully transduced with CAR constructs with additional transporter regions for SLC7A5 or SLC7A11. The successful integration of the construct was detected using a CD34 tag that was expressed on the surface of transduced cells. The cells were sorted using the CD34 tag to generate pure populations of transduced CAR Jurkat for all three constructs. The success of the transduction was further ensured by the assessment of the transporter expression using western blot. The transporter expression was demonstrated to be increased SLC7A5 and SLC7A11 in their respective anti-CD33 SLC7A5 and anti-CD33 SLC7A11 CAR Jurkat.

As described by Bloemberg et al. 2020, Jurkat do not have cytotoxic abilities, and therefore, the killing cannot be used to determine CAR Jurkat antigen recognition. Instead, activation marker CD69 expression was used as a proxy to assess the effectiveness of target recognition by the CAR receptor (Bloemberg et al., 2020). Jurkat cells have a baseline CD69 expression even without target exposure due to the nature of Jurkat cells' constitutive proliferation. Both unmodified and modified CAR Jurkat were responsive to target cells in a dose-dependent

manner, even at the lowest concentrations. This demonstrates that the CAR receptor could initiate signalling in the CAR Jurkat in response to the target antigen. The anti-CD33 SLC7A5/SLC7A11 CAR Jurkat significantly upregulated CD69 following culture with leukaemia cell lines compared to the unmodified anti-CD33 CAR Jurkat. This shows that the modified CAR could produce more potent anti-target activity than the unmodified CAR Jurkat.

An increased metabolic rate is crucial for activated T-cell survival function (Maciver et al., 2008), and therefore, assessing glycolysis and oxidative phosphorylation using Agilent seahorse technologies has been optimised to be used as indicators of T-cell performance (Mercier-Letondal et al., 2021). Anti-CD33 SLC7A5 CAR Jurkat and anti-CD33 SLC7A11 CAR Jurkat had increased ATP production rates compared to unmodified CAR Jurkat even though they were cultured in their respective starved conditions. This demonstrated that the modified CAR provides increased metabolic fitness in starved conditions, facilitating adaptation to metabolic changes. The anti-CD33 SLC7A5 CAR Jurkat had increased glycolytic proton-efflux rate in tryptophan-low conditions to achieve these increased metabolic rates. In contrast, the anti-CD33 SLC7A11 CAR Jurkat had increased basal mitochondrial respiration in low cystine conditions.

Overall, tryptophan and cystine were shown to be essential for T-cell activation, function and proliferation, and the addition of the anti-CD33 SLC7A5 and anti-CD33 SLC7A11 CAR constructs increased the metabolic fitness of CAR Jurkat in amino acid starved conditions.

4. Studying anti-CD33 CAR T-cells with the addition of SLC7A5 or SLC7A11

4.1 Overview

The results described in Chapter 3 demonstrate that the anti-CD33 SLC7A5/SLC7A11 CAR Jurkat have higher activation levels following antigen presentation, as shown by CD69 upregulation. Additionally, the CAR Jurkat have increased metabolic activation, as shown by the measurements of ATP. ATP production is linked with T-cell proliferation and activation (Holthaus et al., 2021). Increased ATP could provide essential energy for CAR T-cell activation and proliferation in low amino acid conditions. Therefore, the next step in this research was to transduce primary human T-cells with the modified construct.

4.2 Objectives

In this chapter, we aim to:

- Successfully transduce primary T-cells with the anti-CD33 SLC7A5 or anti-CD33 SLC7A11 constructs.
- Ensure the transporters are successfully expressed in the modified CAR T-cells.
- Ensure the transporters are functional within the CAR T-cells.
- Assess the anti-tumour activity of the modified CAR T-cells.
- Assess the effect of the transporter insertion on CAR T-cell phenotype and function.
- Identify whether the addition of the transporters to the anti-CD33 CAR T-cells saves T-cell proliferation in their respective low amino acid conditions.

4.3 Results

4.3.1 Transduction of primary T-cells with modified CAR constructs

To build on the evidence from Chapter 3, we inserted the amino acid transporter SLC7A5 and SLC7A11 CAR into primary T-cells. The three constructs, as described in Figure 8, were transfected separately into the Phoenix-Ampho cell line with FuGene and pCL-AMPHO plasmid for 24 hours. Primary T-cells were first activated for 48 hours with anti-CD3/CD28 Dynabeads and then incubated with harvested supernatant of the transfected Phoenix-Ampho cell, pre-coated onto RetroNectin plates for 96 hours in 37°C 5% CO_2. Flow cytometry measured the transduction efficiency on day four using an anti-CD34 antibody.

All three constructs were successfully transduced into primary T-cells (Figure 21 A). The mean transduction efficiency was 28% for anti-CD33 CAR T cells. As expected, the larger constructs of the transporter CAR T-cells had significantly lower transduction efficiencies ($p=0.002$ and $p=<0.0001$). The anti-CD33 SLC7A5 construct had a mean transduction efficiency of 13%, and the anti-CD33 SLC7A11 construct had a mean transduction efficiency of 7% (Figure 21 B).

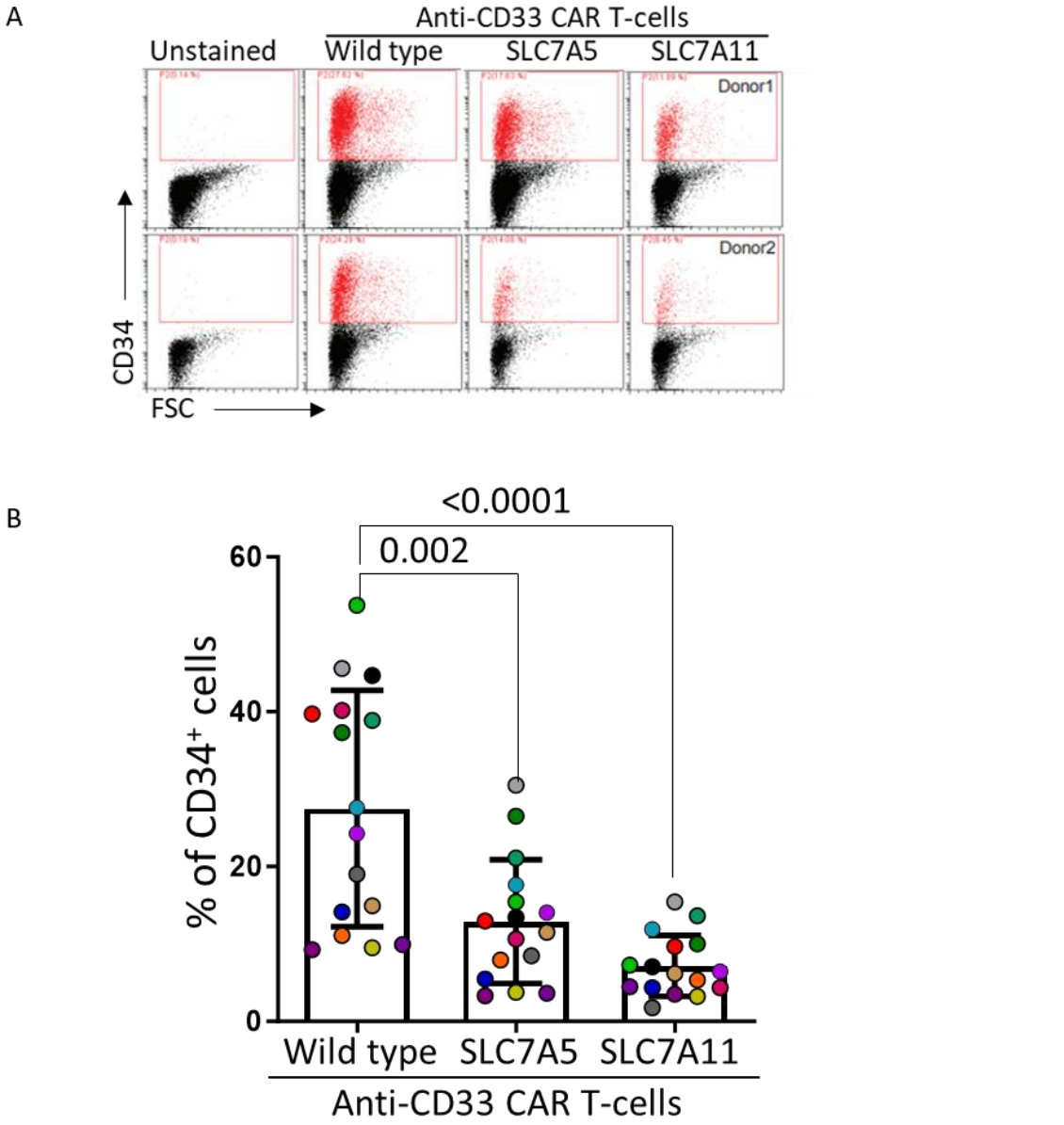

Figure 21: Transducing primary T-cells with modified anti-CD33 CAR constructs. Primary T-cells were isolated from healthy peripheral blood from human donors and activated with anti-CD3/CD28 Dynabeads for 48 hours and then incubated with the modified CAR retrovirus for 96 hours. After incubation the activated T-cells were harvested and read by flow cytometry to assess the transduction efficiency. (A) Dot plots from 2 donors representing the CD34 expression on the anti-CD33, anti-CD33 SLC7A5, and anti-CD33 SLC7A11 CAR T-cells post transduction. (B) Summary of the transduction efficiencies from all transduced donors. Parametric unpaired T-tests were used to determine statistical significance. Each point represents an individual experiment (n=16).

It has been shown in the literature that there are optimal ratios of $CD4^+$ and $CD8^+$ T-cells to enhance the anti-tumour reactivity of CAR T-cells and alter the efficiency of the therapy (Sommermeyer et al., 2016, Bove et al., 2023). In murine models, it has been shown that $CD4^+$ CAR T-cells induce severe cytokine release syndrome, which is not seen in $CD8^+$ only CAR T-cell populations. Cytokine release syndrome is a common toxicity associated with CAR T-cell treatment that can range from acute to life-threatening (Locke et al., 2019, Kumar et al., 2018). However, despite having a lower cytolytic capacity than $CD8^+$ T-cells, $CD4^+$ T-cells promote increasing proliferation activation and are required for effective anti-tumour suppression in CAR T-cell products. Therefore, we examined what proportions of $CD4^+$ and $CD8^+$ T-cells were present and whether the addition of the transporter affected the proportion of $CD4^+$ and $CD8^+$ CAR T-cells. The transduced T-cells were stained for CD34, CD4 and CD8 and analysed by flow cytometry. We observed that the insertion of transporters did not affect the percentage of $CD4^+$ and $CD8^+$ T-cells present compared to the unmodified CAR T-cells (p=ns)(Figure 22).

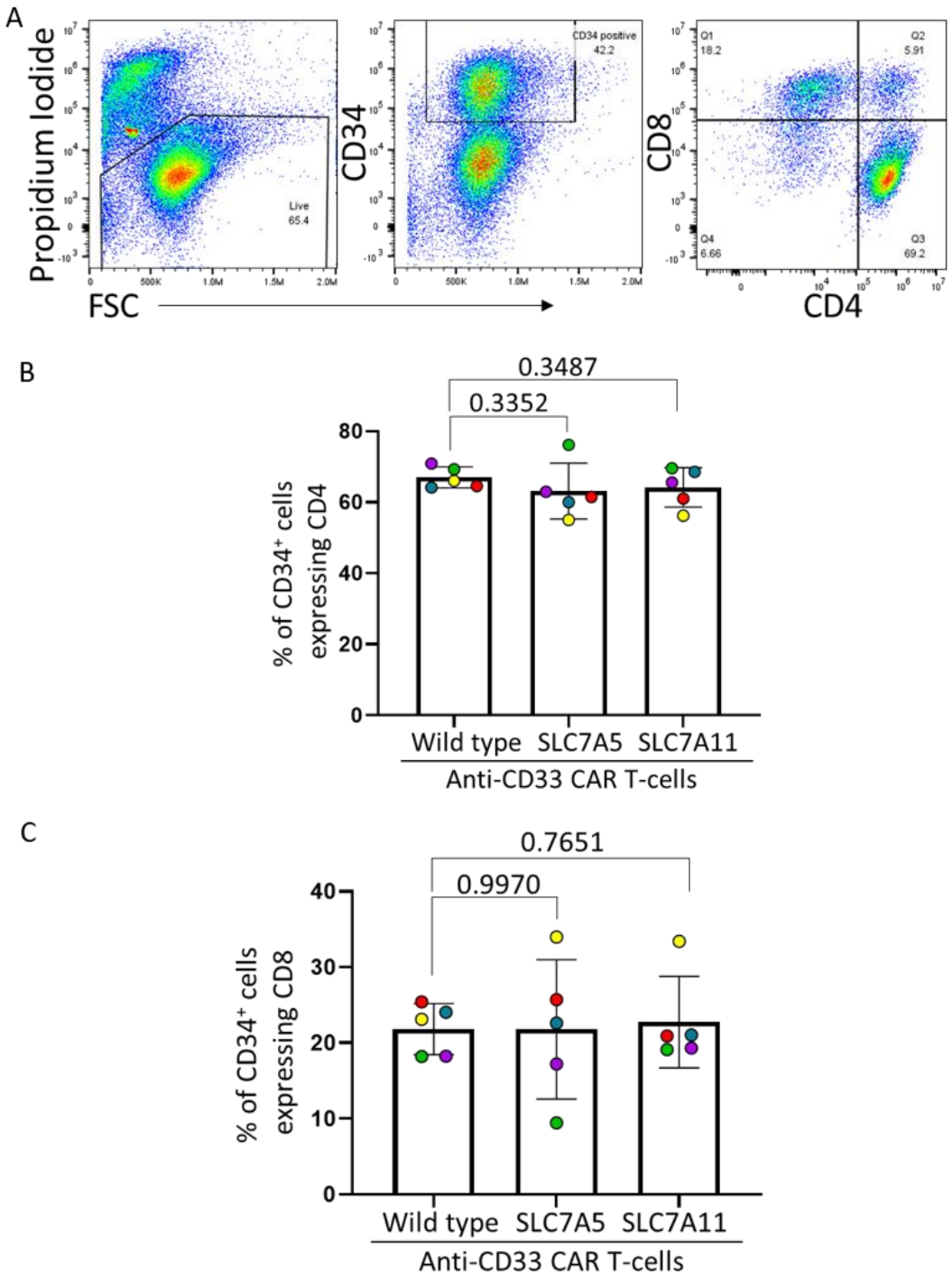

Figure 22: CD4 and CD8 T-cells had equal uptake of the CAR construct.
Human healthy T-cells were activated for 48 hours and incubated with retrovirus for 96 hours and then the transduction efficiency was assessed by flow cytometry. (A) Representative flow cytometry dot plots and the gating used to determine the desired populations. (B and C) The percentage of transduced anti-CD33 SLC7A5 and anti-CD33 SLC7A11 CAR T-cells that are CD4 or CD8 positive respective. Parametric unpaired T-tests were used to determine statistical significance. Each point represents an individual experiment (n=5).

4.3.2 Assessing the success of transporter integration

The transduced CAR T-cell populations were purified using anti-CD34 magnetic beads to ensure consistently pure populations (Figure 23 A). To understand whether the transduction efficiency, determined by CD34 expression, correlated with the successfully increased expression of the respective transporters, we assessed transporter protein levels using western blot. Following the CAR T-cell enrichment, the expression level of SLC7A5 and SLC7A11 by the respective CAR T-cell products were analysed by western blot using β-actin as a loading control (Figure 23 B). The expression of SLC7A5 and SLC7A11 was determined to be higher in anti-CD33 SLC7A5 CAR T-cells and anti-CD33 SLC7A11 CAR T-cells, respectively compared to the anti-CD33 CAR T-cells (Figure 23 B), as shown in all three transduced donors.

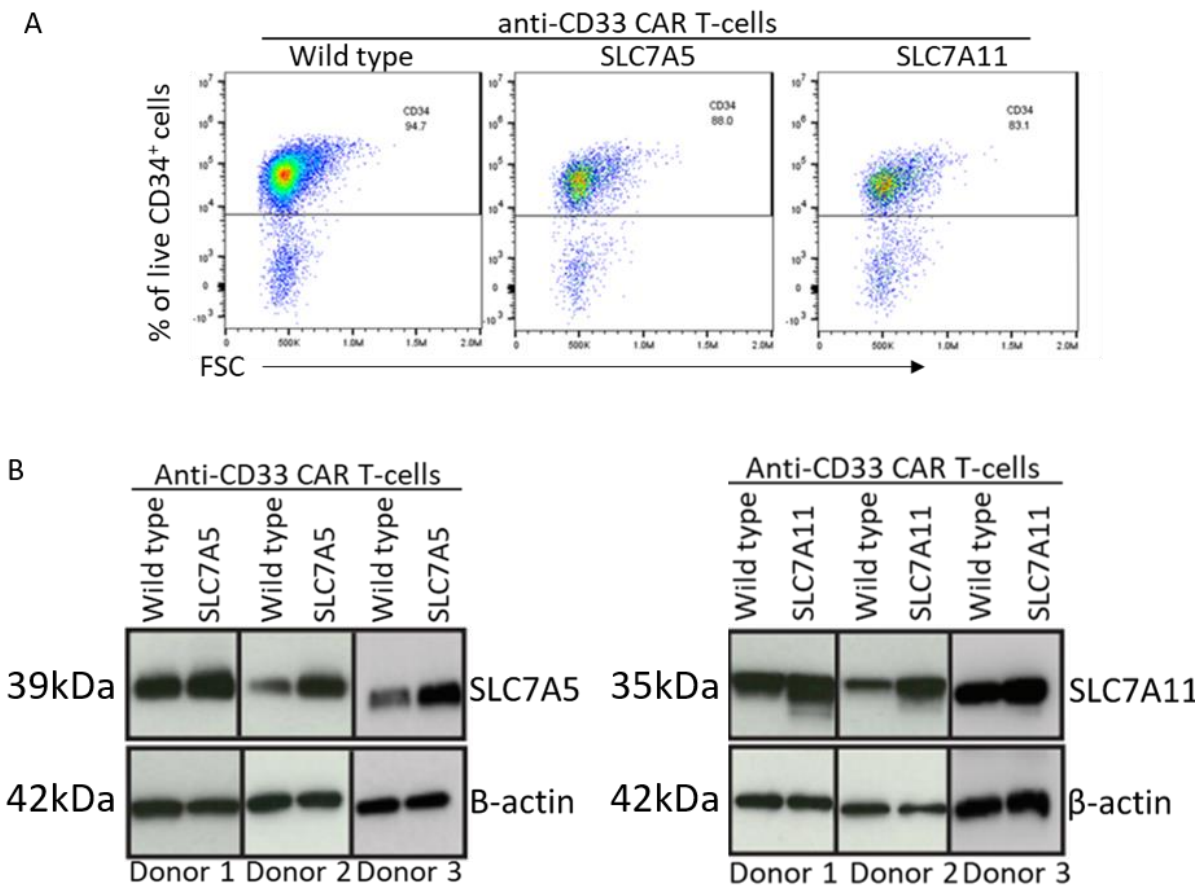

Figure 23: Transporter expression was successfully induced in transporter CAR T-cells

(A) The representative dot plots of the transduced CAR T-cells were purified using anti-CD34 magnetic beads and then assessed by flow cytometry for purity. (B) Western blot showing the expression of β-actin and the respective transporters inserted into the CAR T-cells (n=3). The protein size is indicated next to each band.

4.3.3 Modified CAR T-cell function and phenotype

To understand the ability of modified CAR T-cells to recognise and eliminate target cells, CAR T-cells were cultured with THP1 in R10% for 72 hours. The THP1 viability was assessed by flow cytometry using propidium iodide. Each type of CAR T-cells killed THP1 ($p=0.0022$) with the same efficiency ($p=ns$) (Figure 24 A).

To further confirm the effectiveness of the CAR T-cells, patient $CD33^{+}$ AML blasts were cultured for 72 hours with the three types of CAR T-cells in R10%. After 72 hours, the percentage of AML blasts was measured using flow cytometry (Figure 24 B). The percentage of AML blasts killed was significant in all CAR T-cell constructs when compared to AML alone ($p=<0.05$). No significant difference was observed in anti-AML activity between anti-CD33 SLC7A5 or anti-CD33 SLC7A11 CAR T-cells when compared to anti-CD33 CAR T-cells ($p=0.9485$ and $p=0.2967$, respectively) (Figure 24 B and C).

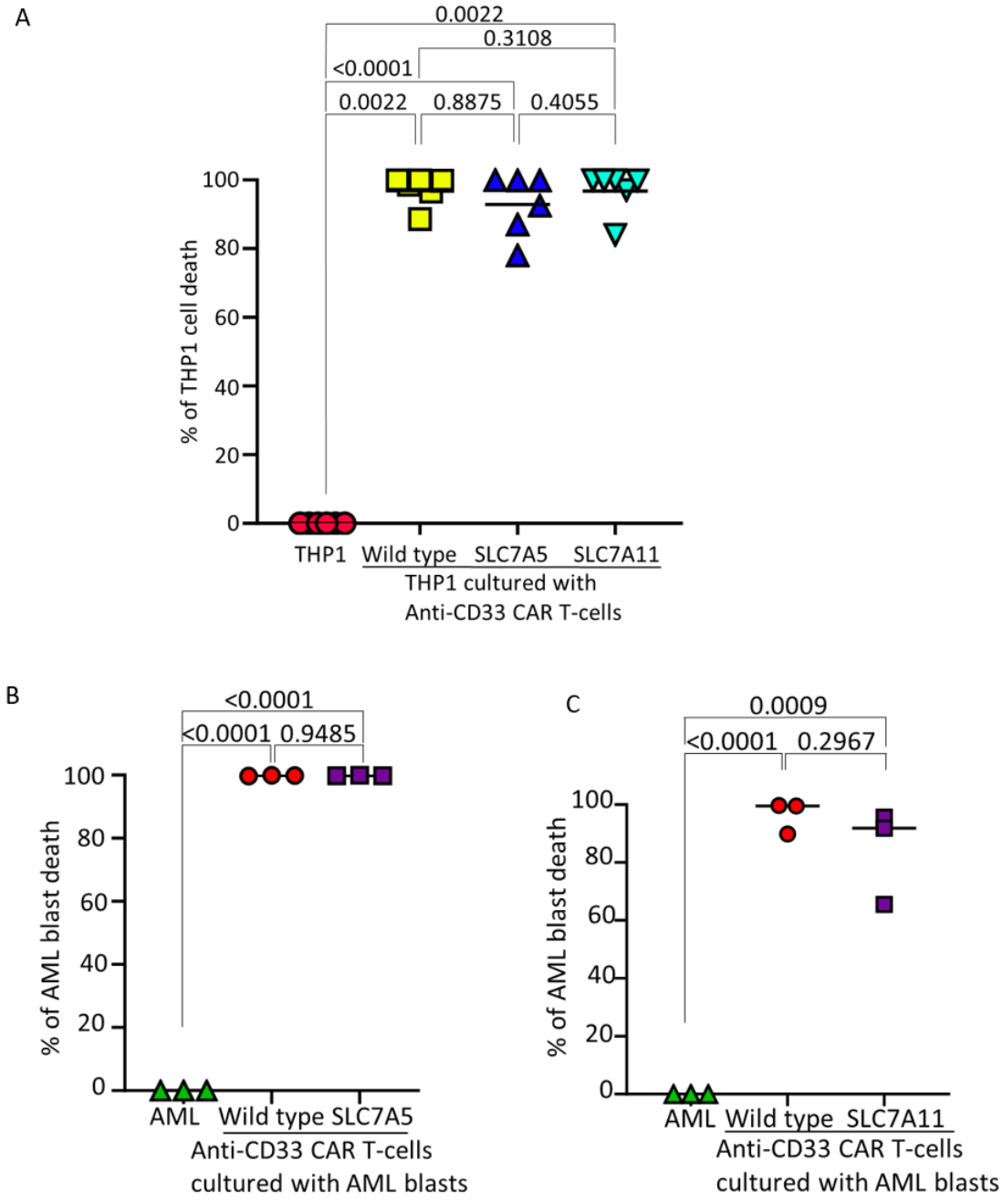

Figure 24: The addition of transporters did not affect the CAR T-cells CD33+ cell clearance.

(A) The three types of CAR T-cells were co-cultured with THP1 cells for 72 hours in R10% media. The percentage of remaining THP1 was determined by flow cytometry (n=6). (B) The CAR T-cells were co-cultured with patient derived AML blasts for 7 days for anti-CD33 SLC7A5 and anti-CD33 SLC7A11 CAR T-cell respectively (n=3). Parametric unpaired T-tests were used to determine statistical significance. Each point represents an individual experiment.

Selli et al., 2003 have shown that repeated stimulations of CAR T-cells result in T-cell exhaustion and gain a terminal effector phenotype (Selli et al., 2023). To understand whether repeated stimulations of wild-type and transporters CAR T-cells altered CAR phenotype, the CAR T-cells were stimulated with THP1 on days 1, 4 and 6. Results were analysed on days 4, 6 and 9 by flow cytometry assessing for phenotype, activation, and exhaustion markers.

The markers used to determine the CAR T-cell phenotype were CD45RA, CD45RO, CCR7, and CD62L. In Figure 25 A-B, we have depicted that the combination of specific phenotypic markers can help to differentiate central memory ($CD45RO^+$ $CD45RA^-$ $CCR7^+$ $CD62L^+$), effector memory ($CD45RO^+$ $CD45RA^-$ $CCR7^-$ $CD62L^-$), terminal effector ($CD45RO^-$ $CD45RA^+$ $CCR7^-$ $CD62L^-$) and naïve ($CD45RO^-$ $CD45RA^+$ $CCR7^+$ $CD62L^+$) T-cells. Central memory cells are described as the preferred subtype of CAR T-cells as they are considered to generate a population of CAR T-cells that is highly functional and has the potential to expand to sustain the anti-tumour response (Blaeschke et al., 2018).

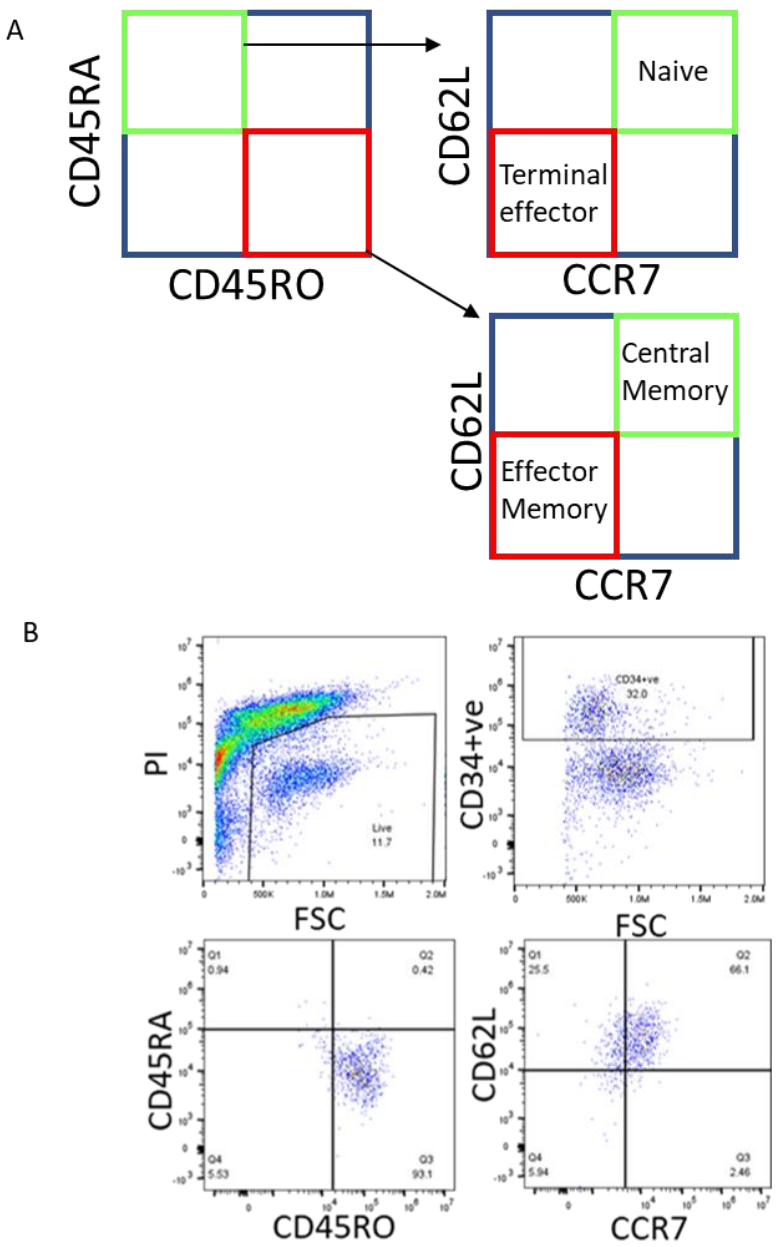

Figure 25: The gating used to determine the CAR T-cell phenotype.
(A) The representative diagram showing the gating used to determine the CAR T-cell phenotype.
(B) Representative dot plots demonstrating the gating used to determine T-cell phenotype

The phenotype of CAR T-cells is an essential factor that correlates with CAR T-cell anti-tumour function (Tantalo et al., 2021). The addition of the transporters did not affect the percentage of the central memory CAR T-cell cells (p=ns); consistently, the most prevalent phenotype of the CAR T-cells present were central memory T-cells when co-cultured with THP1 cells (Figure 26 A and B).

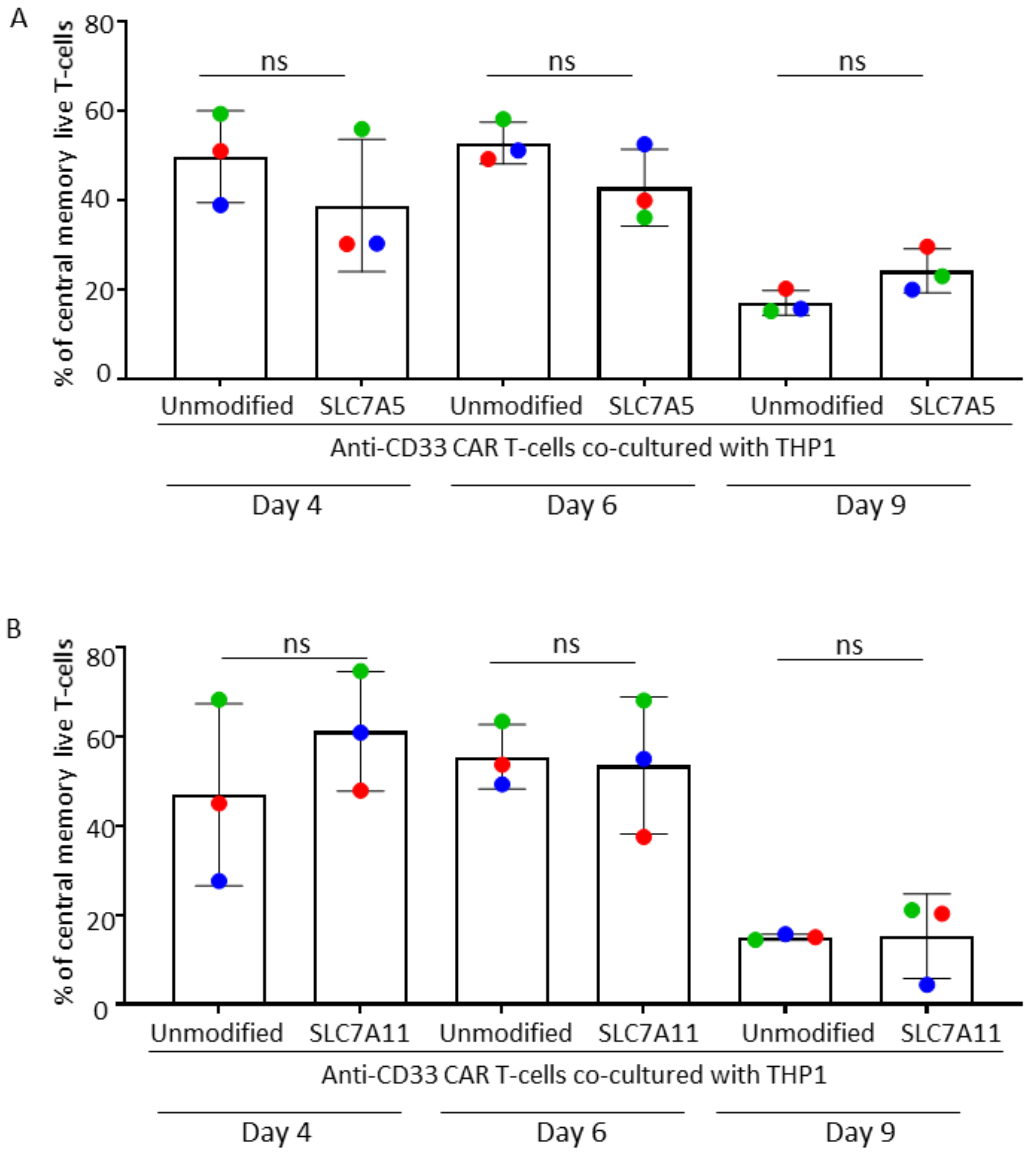

Figure 26: Phenotype of modified CAR T-cells after repeated stimulation with THP1 cells.

Anti-CD33 CAR T-cells were cultured with CD33+ THP1 cells and re-stimulated on day 4, and day 6. Samples were harvested on day 4, day 6 and day 9 and assessed by flow cytometry for phenotype. (A and B) The percentage of anti-CD33 SLC7A5 and SLC7A11 CAR T-cells which expressed a central memory phenotype (CD45RO+ CD45RA- CD62L+ CCR7+) at each time point when cultured with or without THP1 cells (n=3). Parametric unpaired T-tests were used to determine statistical significance. Each point represents an individual experiment.

The addition of the transporters did not affect the percentage of the effector memory CAR T-cell (p=ns) (Figure 27 A and B).

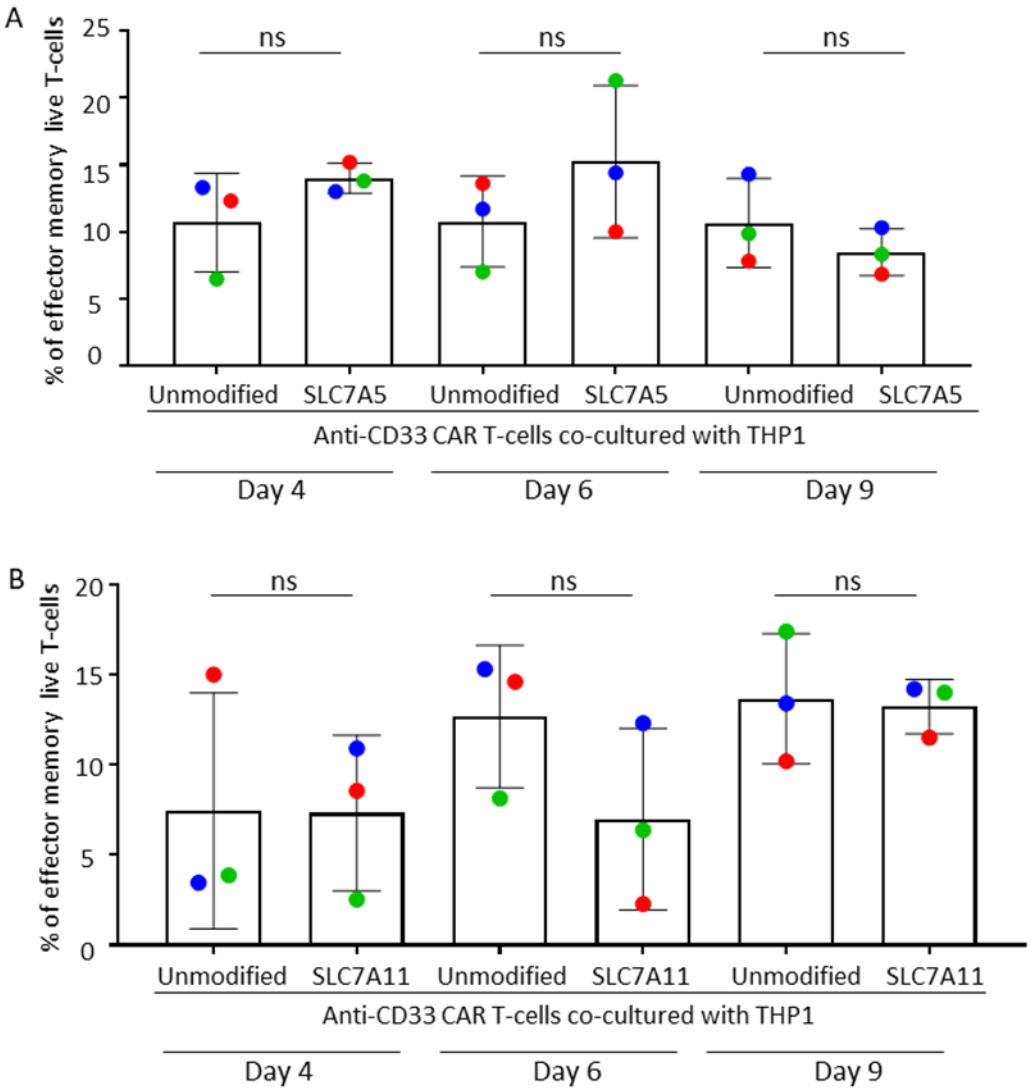

Figure 27: The addition of amino acid transporters does not alter the phenotype of the CAR T-cells

CAR T-cells were cultured with CD33+ THP1 cells and re-stimulated with THP1 on day 4, and 6. The analysis was performed on samples taken on day 4, 6, and 9 by flow cytometry.

(A and B) The percentage of anti-CD33 SLC7A5 and SLC7A11 CAR T-cells which expressed an effector memory phenotype (CD45RO+ CD45RA- CD62L+ CCR7+) at each time point when cultured with or without THP1 cells (n=3). Each colour point represents an individual experiment.

Then, we analysed the activation of the CAR T-cells following antigen stimulation. CD69 was analysed by flow cytometry on days 4, 6, and 9. Anti-CD33 SLC7A5 CAR T-cells showed a significantly increased CD69 expression when cultured with $CD33^+$ AML blasts on days 6 and 9 ($p=0.04$ and $p=0.03$, respectively) compared with anti-CD33 CAR T-cells (Figure 28 A). Instead, anti-CD33 SLC7A11 CAR T-cells significantly increased CD69 expression at day 4 but not at day 6 or 9 ($p=0.04$) (Figure 28 B).

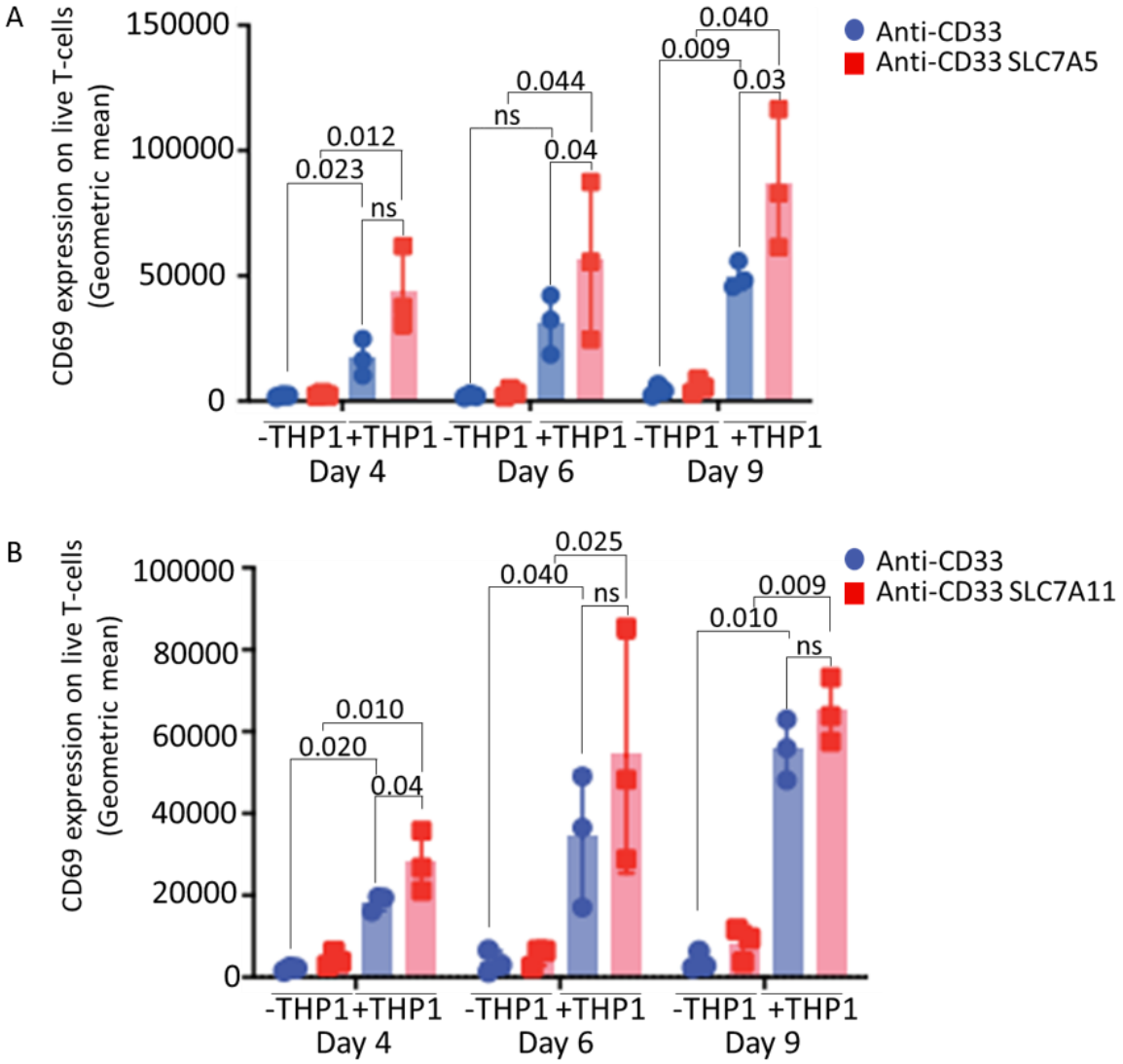

Figure 28: The activation levels of the CAR T-cells following repeated antigen presentation.

CAR T-cells were cultured with CD33^{+} THP1 cells and re-stimulated with THP1 on day 4, and 6. The analysis was performed on samples taken on day 4, 6, and 9 by flow cytometry. (A and B) The geometric mean of CD69 expressed by the CAR T-cells at each time point or anti-CD33, anti-CD33 SLC7A5, and anti-SLC7A11 CAR T-cells. Statistical analysis performed using parametric unpaired t-test. Each dot represents an individual experiment (n=3). ns=$p<0.05$.

4.3.4 Modified T-cell exhaustion markers

CAR T-cells are susceptible to becoming exhausted once injected into patients. These exhausted CAR T-cells are not functional and reduce patient treatment efficacy (Deng et al., 2020). The cause of T-cell exhaustion can be multifaceted, and previous literature has shown that CAR structure significantly influences CAR T-cell sensitivity to exhaustion. Increasing CAR T-cell resistance to exhaustion has already become essential to CAR T-cell design, such as inserting the co-stimulatory factor 41-BB into CAR T-cell constructs, reducing T-cell exhaustion (Long et al., 2015).

Therefore, it was important to confirm that the addition of the transporters did not burden the CAR T-cells, leading to increased susceptibility to T-cell exhaustion. We investigated the expression of LAG3, PD-1, and TIM3, the main markers of T-cell anergy, which causes reduced proliferation and an inability to respond to target cells. The CAR T-cells were stimulated with THP1 on days 1, 4 and 6 and assessed by flow cytometry on days 4, 6 and 9. The results showed that the addition of the transporters did not alter the expression of any of the exhaustion markers investigated (p=ns) (Figure 29).

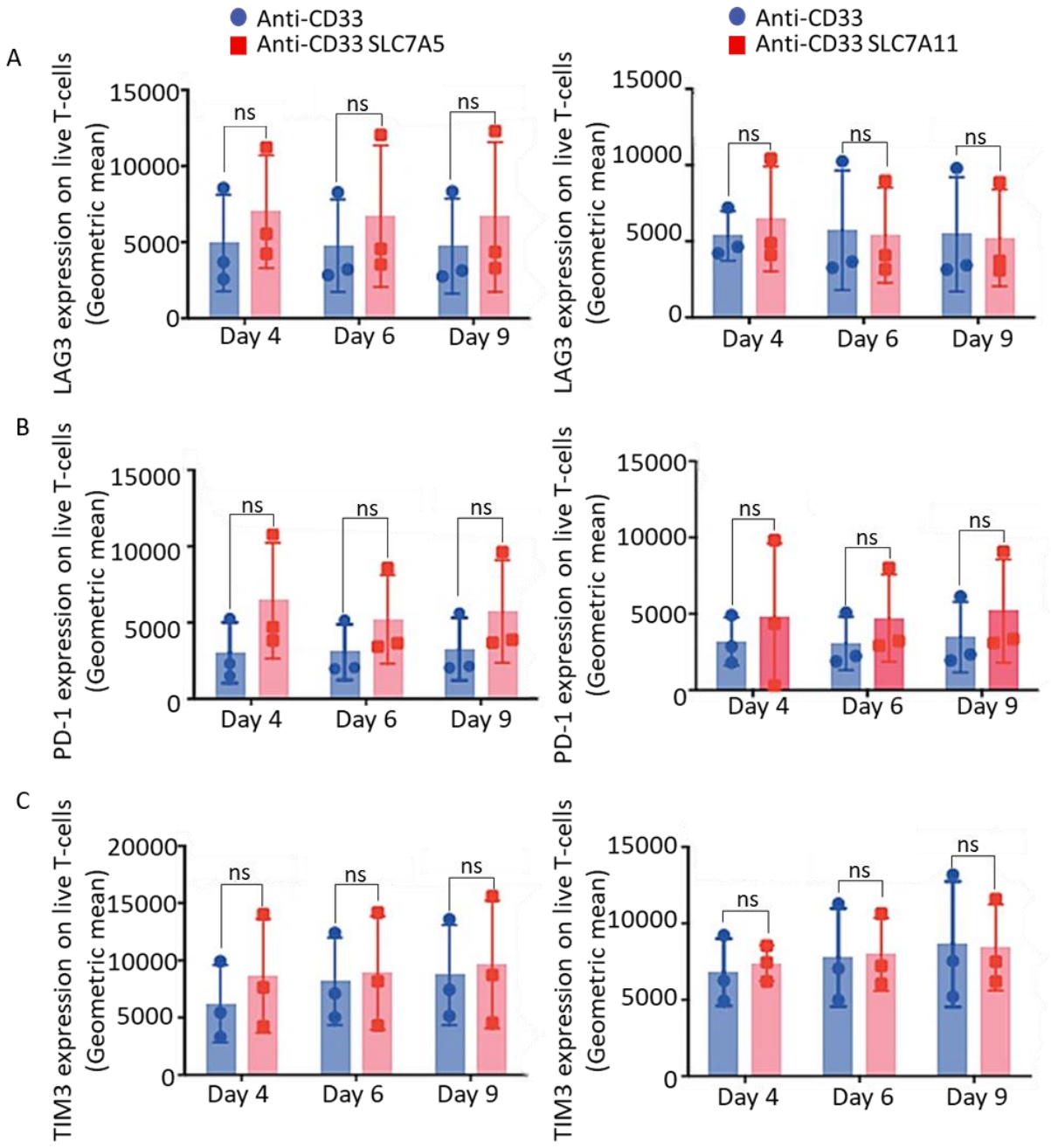

Figure 29: The CAR T-cells expression of exhaustion markers is not increased by the addition of the transporter.

Anti-CD33, anti-CD33 SLC7A5 and anti-CD33 SLC7A11 CAR T-cells were cultured in R10% with CD33+ THP1 cells and then re-stimulated on day 4, and day 6 with CD33+ THP1 cells. Results were read on day 4, 6 and 9 by flow cytometry. The markers stained were (A) LAG3 (B) PD-1 (C) TIM3. Statistical analysis performed using parametric t-test. Each dot represents an individual experiment (n=3). ns =$p<0.05$.

4.3.5 Modified CAR T-cell cytokine expression

Following the activation, T-cells start to secrete cytokines that affect T-cell differentiation and function. To understand whether the transporter CAR T-cells following co-culture with THP-1 secrete different cytokines compared to the wild-type CAR T-cells, the supernatants were harvested at days 4, 6 and 9 and analysed for tumour necrosis factor-alpha (TNF-α), IL-10 IFN-γ, IL-17a, IL-6, IFN-2a, and IL-8. The concentrations of these cytokines were measured by flow cytometry using the BioLegend LEGENDplex kit. Following antigen recognition, no difference in cytokine production was measured between anti-CD33 SLC7A5 CAR T-cells and the anti-CD33 CAR T-cells (Figure 30) (p=ns). The same results were observed for the SLC7A11 transporter; this receptor's overexpression did not affect the anti-CD33 CAR T-cells cytokine expression profile (Figure 30) (p=ns).

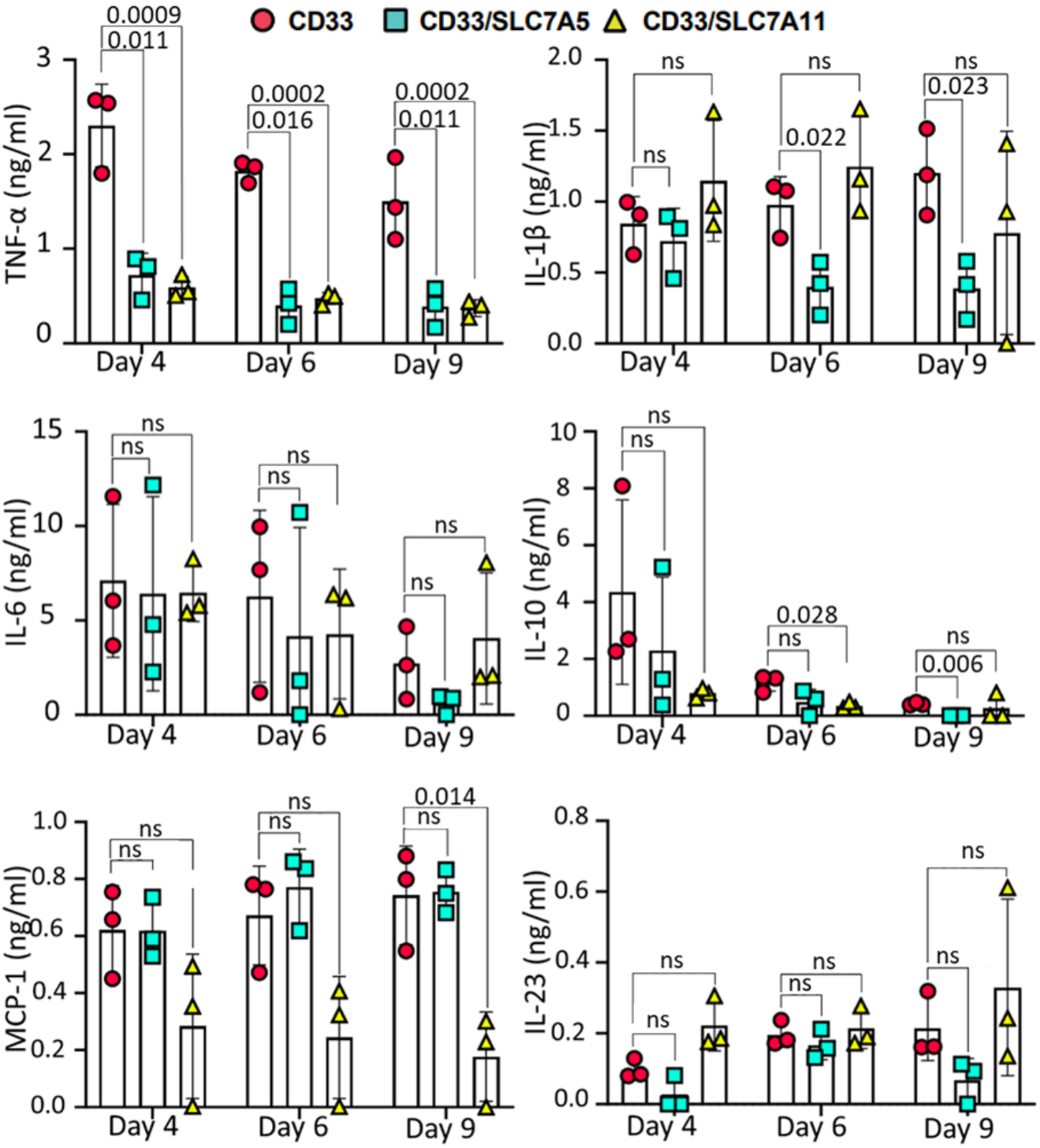

Figure 30: Addition of SLC7A5 to the CAR T-cells did not alter the cytokines the CAR T-cells produced.

Anti-CD33 CAR T-cells and anti-CD33 SLC7A5 CAR T-cells were cultured in R10% with CD33+ THP1 cells and then re-stimulated on day 4, and day 6 with CD33+ THP1 cells. The supernatant was harvested on day 4, 6, and 9. The supernatant was assessed for the cytokines IL-8, IL-10, TNF-α, IL-17a, INF-γ, IL-6, and IFN-α2 using the LegendPlex Human Inflammation panel 1 on the flow cytometer. Statistical analysis performed using parametric t-test. Each dot represents an individual experiment (n=3). Red circle represent anti-CD33 ns =$p<0.05$.

4.3.6 Modified CAR T-cell transporter functionality

To determine whether the inserted transporters were functional, we measured the concentration of tryptophan and cystine by ELISA from the supernatant of CAR T-cells cultured with THP1 for 72 hours. The anti-CD33 CAR T-cells do not decrease the tryptophan concentration compared to the R10% media and the THP1 culture alone (p=ns) (Figure 31A). The addition of the SLC7A5 transporter to the anti-CD33 CAR T-cells caused significantly increased tryptophan uptake and, therefore, decreased tryptophan levels in the supernatant compared to anti-CD33 CAR T-cells (p=0.01) (Figure 31A).

An ELISA to directly measure the cystine concentration was not available. Instead, we reduced all the present cystine in the media into its monomer form, cysteine, which was measurable. There was no detectable free cysteine in the media prior to the addition of the reduction agent (Figure 31 B). However, cysteine was detectable once the reduction agent, Tris(2-carboxyethyl) phosphine (TCEP), was introduced to the media. This detectable, reduced cysteine correlates to the levels of cystine that had been in the media before reduction, as demonstrated by the increase of cysteine levels in R10% post-adding TCEP (Figure 29B). The SLC7A11 CAR T-cells were cultured with THP1 cells for 72 hours. CAR T-cells overexpressing the SLC7A11 transporter significantly decreased the amount of cystine in the media compared to anti-CD33 CAR T-cells (p=0.02) (Figure 31 B).

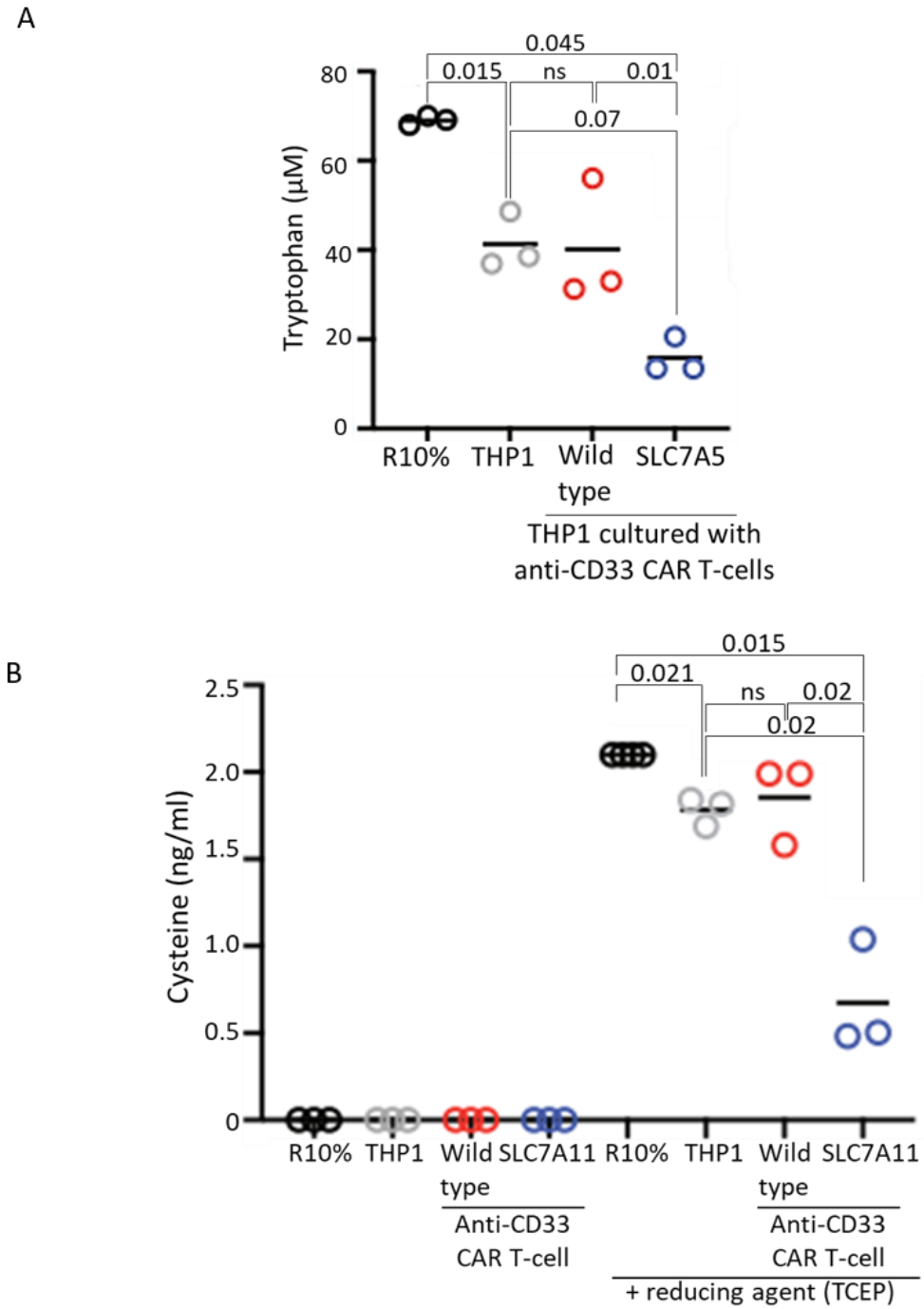

Figure 31: The transporters were functional and increased amino acid uptake
Anti-CD33 CAR T-cells, anti-CD33 SLC7A11 CAR T-cells, and anti-CD33 SLC7A5 CAR T-cells were cultured in R10% with THP1 cells for 72 hours. The supernatant was harvested and assessed for the amino acid composition (n=3). (A) The supernatants harvested from anti-CD33 CAR T-cells and anti-CD33 SLC7A5 CAR T-cells were assessed for tryptophan content by the tryptophan colorimetric assay, Tryptophan Assay kit. The results were read by a microplate reader (Biorad iMark) at 450nm absorbance. (B) The supernatants harvested from anti-CD33 CAR T-cells and anti-CD33 SLC7A11 CAR T-cells. The cystine was reduced to cysteine by TCEP where indicated and then the cysteine was measured using human cysteine ELISA kit assay (Bluegene) (n=3). Statistical analysis performed using parametric t-test. Each dot represents an individual experiment.

4.3.7 Assessing modified CAR T-cell proliferation

This chapter demonstrated that the transporters were successfully incorporated into the CAR T-cells and were functional *in vitro*. It was then essential to assess whether the addition of the transporters affected T-cell proliferation in low amino acid environments. The CAR T-cells were labelled with CFSE and cultured with THP1 cells in R10%, tryptophan low or cystine low media (Figure 32 A). After 72 hours, the CAR T-cell proliferation was analysed by flow cytometry. Anti-CD33 SLC7A5 CAR T-cells proliferated more in tryptophan low media than anti-CD33 CAR T-cells ($p=0.0286$) (Figure 32 B). The same results were observed for CAR T-cells transduced with SLC7A11 transporter; these CAR T-cells were able to proliferate more in cystine low media compared to anti-CD33 CAR T-cells ($p=0.0286$) (Figure 32 B).

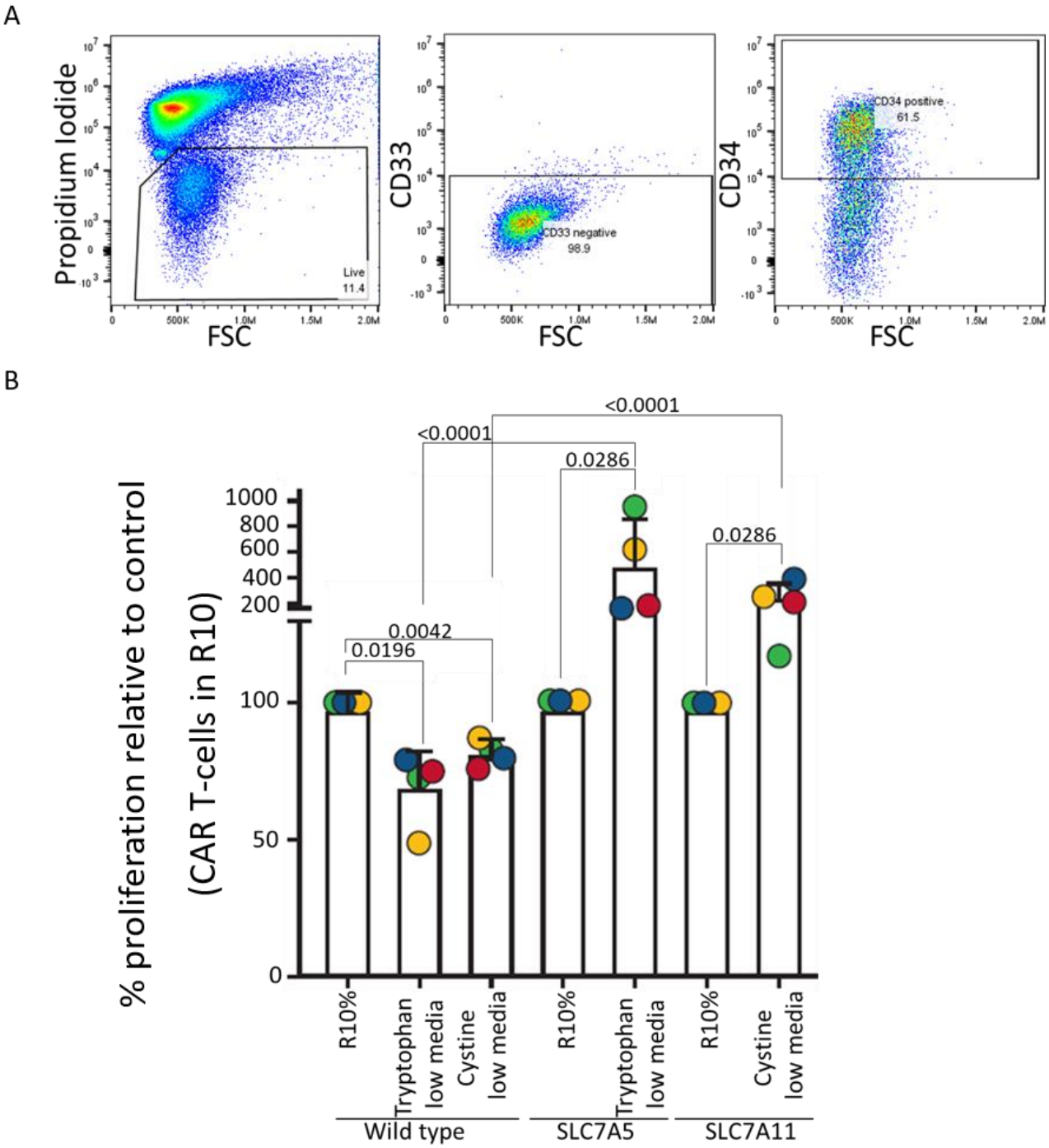

Figure 32: Addition if the transporters enabled increased proliferation in low amino acid conditions.

Anti-CD33 CAR T-cells, anti-CD33 SLC7A5 CAR T-cells, and anti-CD33 SLC7A11 CAR T-cells labelled with CSFE were cultured with THP1 cells in R10%, low tryptophan, or low cystine acid media for 72 hours as indicated and then read by flow cytometry to assess proliferation. (A) Representative dot plot of gating used to identify proliferating CAR T-cell population. (B) The percentage of proliferated anti-CD33, anti-CD33 SLC7A5 or anti-CD33 SLC7A11 CAR T-cells relative to the control when cultured with THP1 cells in R10%, low cystine or low tryptophan media. Statistical analysis performed using parametric t-test. Each dot represents an individual experiment (n=4).

4.4 Discussion

This chapter described successfully transducing the modified anti-CD33 CAR constructs containing tryptophan or cystine transporters into primary T-cells. The addition of the transporter to the CAR T-cells did not alter the $CD4^+$ to $CD8^+$ T-cell ratio. The percentage of T-cells transduced was inconsistent between constructs; therefore, successfully transduced CAR T-cells were sorted post-transduction, resulting in CAR T-cell populations of equal purity. The inserted transporter transcripts were transduced by the CAR T-cells as the anti-CD33 SLC7A5 and anti-CD33 SLC7A11 CAR T-cells had increased protein expression of their respective transporters showing that the inserted transporters were successfully integrated into the cell and translated up to the protein level. All the transduced CAR T-cells gained the ability to eliminate $CD33^+$ cells *in vitro*.

The addition of the transporters did not alter the CAR T-cell phenotype, which remained the same as non-modified CAR T-cells over repeated antigen exposure. All three CAR T-cells were demonstrated to maintain their largest present population as a central memory phenotype. At the time points measured, the CAR T-cell phenotype was $CD45RO^+$ and $CD45RA^-$. Central memory cells have a long lifespan, and despite their lower cytotoxic capacity, they still secret TNF-α and IL-2. The ability of T-cell immunotherapies to maintain a population of central memory cells enables improved persistence and more significant anti-tumour activity post-injection (Kueberuwa et al., 2017). Therefore, all the CAR T-cells maintain a population of cells with proliferative capacity *in vitro*. We did not see a population of naïve or effector T-cells, potentially because after stimulation and killing of the target cells the CAR T-cells died.

When testing the modified CAR T-cells' response to repeated antigen exposure, their CD69 expression was assessed. Both transporter CAR T-cells expressed significantly increased CD69 expression compared to anti-CD33 CAR T-cells at different time points. Anti-CD33 SLC7A5 CAR

T-cells had increased CD69 expression on days 6 and 9. Anti-CD33 SLC7A11 CAR T-cells had increased CD69 expression on day 4. The CD69 is a marker of T-cell activation as it is quickly upregulated after T-cell activation. CD69, when activated, causes the sphingosine-1-phosphate receptor 1 internalisation, leading to T-cell retention in the lymph nodes, but this can negatively regulate the intratumoral T-cell function (Koyama-Nasu et al., 2022).

After initial and repeated exposure to target antigens, the modified CAR T-cell exhaustion marker expression (PD-1, LAG3, and TIM3) was assessed. There was no increase in exhaustion marker expression following repeated antigen exposure compared to the last antigen exposure, and the addition of the transporters did not affect the expression of exhaustion markers in our *in vitro* assessment.

At all time points, there was a significant decrease in TNF-α expression found in both of the modified CAR T-cells. TNF-α has both immune-inflammatory and regulatory functions. TNF-α produced during activation of T-cells can promote T-cell activation of naïve T-cells and proliferation of T-cell populations (Alam et al., 2021). However, TNF-α also can induce the differentiation of regulatory T-cells (Yang et al., 2019). Therefore, understanding the effects of this reduced TNF-α would require further investigation such as defining the TNF-α receptors expressed on the CAR T-cell surface.

The addition of SLC7A5 and SLC7A11 constructs provided their respective anti-CD33 CAR T-cells with increased capacity to uptake their respective amino acids. This shows that the inserted transporters are not only expressed at the protein level but are also functional.

In amino acid-depleted environments in co-culture with their target cells, modified CAR T-cells have reduced proliferation, unlike the unmodified anti-CD33 CAR T-cells. Instead, the transporter CAR T-cell proliferation increased under these adverse conditions. This could be caused by the transporter CAR T-cells' increased internal reservoir of tryptophan and cystine,

allowing them to undergo proliferation even during amino acid depletion induced by tumour cells.

5. Chapter 3 Assessing the differential RNA sequences and *in vivo* function of modified CAR T-cells

5.1. Overview

The previous chapter demonstrated that the modification of the CAR by the addition of amino acid transporters increased CAR T-cell proliferation and demonstrated altered metabolic rates in CAR Jurkat. The addition of the transporters ideally enables these CAR T-cells to access amino acids despite low availability and promotes T-cell function. Tryptophan and cystine both have complex pathways associated with their metabolism that can have wide reaching effects as the availability of amino acids correlates to T-cells ability to proliferate and activate. Moreover, the knock-on effects of tryptophan and cystine availability could affect pathways not directly linked to tryptophan and cystine metabolism. Therefore, these transporters could alter the activation state and mechanisms of actions occurring within the CAR T-cells, which would be reflected in their transcriptome. RNA sequencing can generate a comprehensive snapshot of the cells transcriptome allowing us to develop a clearer understand of what pathways are altered by the transporters and increased availability of tryptophan and cystine.

A crucial part of CAR T-cell function is the complex nature of cell-to-cell and cell-to-environment interactions that occur *in vivo,* which are currently not truly replicable with *in vitro* techniques. CAR T-cells interact not only with the target cells and the tumour microenvironment but also with the host's immune system. These interactions have allowed other modified CAR T-cells to promote immune cell infiltration or alter the immune infiltrate phenotype (Chmielewski and Abken, 2017, Zhu et al., 2023). NOD SCID mice are immune-deficient mice that lack T-cells, B-cells and NK cells which allows the xerographic transplant of human cells allowing human tumour engraftment and injection of CAR T-cells without

immune rejection from the murine host. This means that tumour engraftment is possible without radio-ablation, a high-risk procedure which alters the bone marrow microenvironment and has numerous side effects such as higher risk of infections, chronic inflammation responses, cataracts, premature ageing and death. Therefore, removing this step enables the reduction of mice used in this experiment and minimises the stress and pain on the mice used within this study. However, this means that the engraftment of the tumour was not uniform across the mice and therefore the engraftment of mice was assessed prior to CAR T-cell injection and only mice with successful engraftment were used for the remainder of this experiment.

5.2 Objectives

In this chapter, we aim to,

- Understand whether the addition of the transporters to the CAR T-cells affected the transcriptome.
- Understand if the modified CAR T-cells provided better target cell clearance in vivo when compared to anti-CD33 CAR T-cells.

5.3 Results

5.3.1 Analysis of modified CAR T-cell RNA transcriptome

In the previous chapters, it was shown that the addition of the transporters to Jurkat CAR altered cell metabolism and increased the proliferation of CAR T-cells. To assess whether these changes were reflected in the transcriptome of the CAR T-cells, mRNA sequencing was performed.

T-cells from 5 human donors were transduced with the three constructs and then cultured with THP1 in low amino acid media for 72 hours. CAR-T cells were then enriched using CD34 antibody and processed for mRNA sequencing. Sequencing was performed using the Illumina HiSeq 2000 system.

Firstly, we decided to examine the top 500 differentially expressed genes. Differential gene expression analysis revealed significant changes between standard and transporter-modified CAR T cells (Figure 33 A and B).

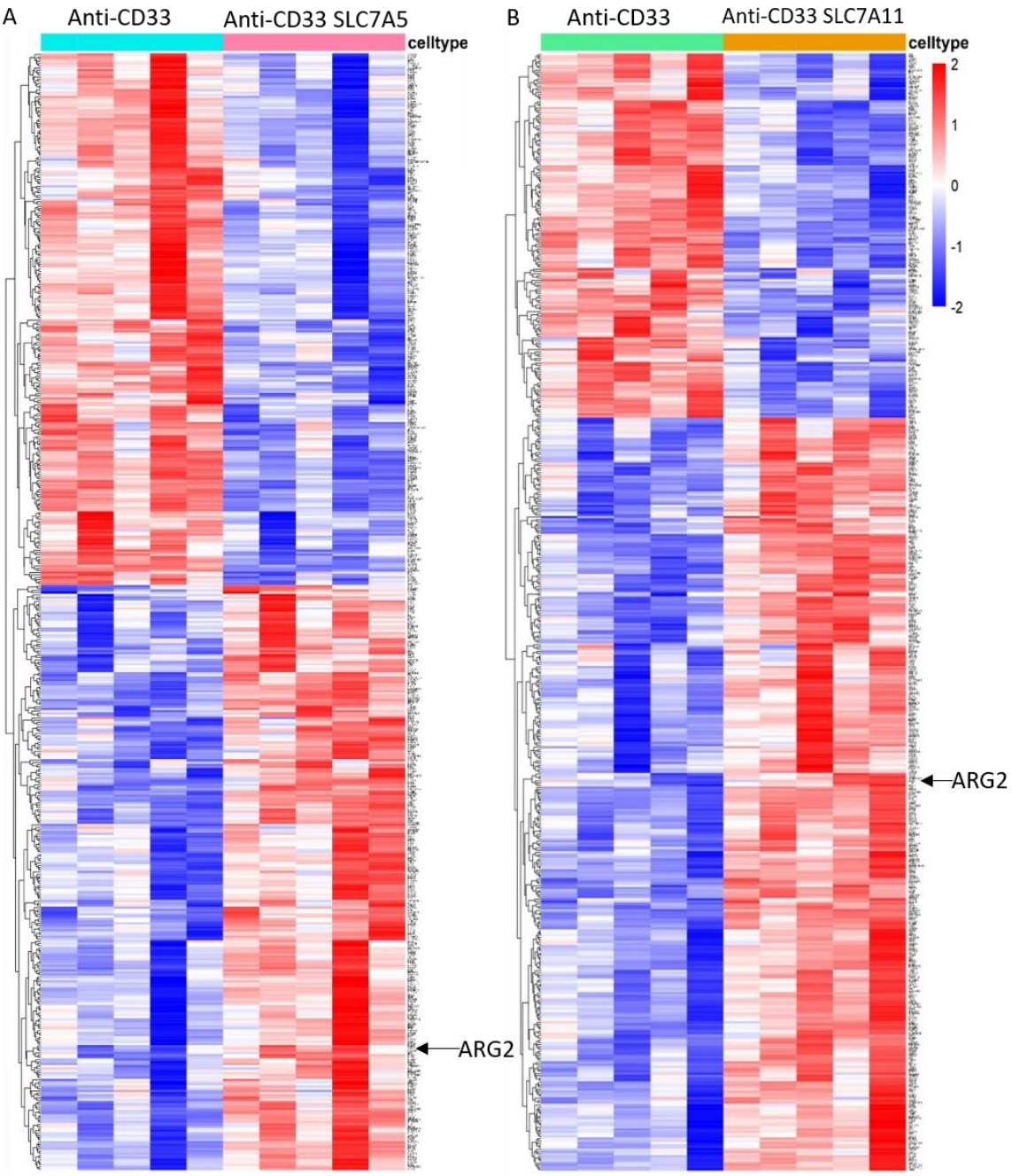

Figure 33: Top 500 differentially expressed genes between anti-CD33 CAR T-cells and anti-CD33 transporter CAR T-cells.

The CAR T-cells transduced from 5 healthy human donors were activated and cultured in 75% cystine free media with THP1 cells for 72 hours. The CAR T-cells were then isolated by FACs sorting and RNA was extracted for analysis. (A) Heat map of anti-CD33 SLC7A5 CAR T-cell top 500 differentially expressed genes compared to anti-CD33 CAR T-cells. (B) Heat map of anti-CD33 SLC7A11 CAR T-cell top 500 differentially expressed genes compared to anti-CD33 CAR T-cells. Statistical analysis was performed by CRUK Birmingham Centre bioinformaticians Noyvert B. and Pan Y.

This identified that anti-CD33 SLC7A5 CAR T-cells showed significant changes in genes associated with T-cell activation, such as chemokine ligand 3 (CCL3), a chemokine produced by activated T-cells, involved in $CD8^+$ T-cell recruitment, and promotes $CD8^+$ T-cell interactions with $CD4^+$ T-cells and DCs that primes the T-cells for activation (Castellino et al., 2006, Brewitz et al., 2017, Song et al., 2020) (Figure 35). There was the downregulation of genes such as Schlafen 5 (SLFN5), a gene that is downregulated during T-cell activation except in regulatory T-cells (Puck et al., 2015, Xu et al., 2022a) (Figure 34).

Anti-CD33 SLC7A11 upregulates genes such as SLC3A2, Lymphotoxin-α (LTA), and colony-stimulating factor-2 (CSF2) (Figure 34B). SLC3A2 is a chaperone protein required for trafficking SLC7A11 into the plasma membrane. LTA is a member of the tumour necrosis factor family that has been linked to cytotoxic capabilities, immune cell recruitment and the formation of secondary lymphoid structures (Chin et al., 2003, Borelli and Irla, 2021). Colony-stimulating factor 2 encodes granulocyte-macrophage colony-stimulating factor, promoting phagocyte inflammatory phenotypes (Rasouli et al., 2015, Inaba et al., 1992, Zhan et al., 2019).

Anti-CD33 SLC7A11 downregulates genes such as IL7R, the IL-7 receptor. IL7R is expressed on naive T-cells and is down-regulated upon T-cell activation or IL-7 binding. The downregulation is either transient or temporary, depending on the T-cell phenotype (Alves et al., 2008). This modulation of the IL7R occurs at both the protein and transcription levels. Therefore, further investigations would be required to understand the significance of IL7R downregulation by the anti-CD33 SLC7A11 CAR T-cells (Guler et al., 2020).

The top two differentially expressed transcripts included increased expression of retinol dehydrogenase 10 (RDH10) and long intergenic non-protein coding RNA 1281 (LINC01281) for both anti-CD33 SLC7A5 and anti-CD33 SLC7A11 (Figure 34). LINC01281 is a long non-coding RNA correlated with increased T-cell infiltration into cervical cancer and was deemed a protective factor in lung adenocarcinoma (Ye et al., 2021, Sun et al., 2023). RDH10 encodes for retinol dehydrogenase 10, which promotes effector T-cell differentiation (Fujiki et al., 2022). Early growth response-1 is upregulated in anti-CD33 SLC7A5 and anti-CD33 SLC7A11 CAR T-cells when compared to non-modified CAR T-cells, which stimulates T-cell activation and promotes IL-2 production (Figure 34) (Lin and Leonard, 1997, Damasio et al., 2021).

VIM, which encodes for a cytoskeletal protein called vimentin, is downregulated in anti-CD33 SLC7A5 CAR T-cells compared to anti-CD33 CAR T-cells (Figure 34 A). Vimentin may modulate lymphocyte migration and apoptosis (Su et al., 2019). E2F2, a gene associated with the regulation of T-cell activation and survival, was downregulated in the anti-CD33 SLC7A5 CAR T-cells compared to non-modified CAR T-cells (Figure 36 A)(Zhu et al., 2001, Mustafa et al., 2021). SLFN5, a gene associated with T-cell exhaustion, naive T-cells and regulatory T-cells, was downregulated in the anti-CD33 SLC7A5 CAR T-cells compared to non-modified CAR T-cells (Figure 36 A)(Xu et al., 2022a). CCL3, a chemokine associated with increased T-cell activity, was upregulated by anti-CD33 SLC7A5 CAR T-cells when compared to non-modified CAR T-cells (Figure 34 A)(Kang et al., 2021).

LTA, the gene encoding lymphotoxin-α, which promotes T-cell proliferation, was upregulated in anti-CD33 SLC7A11 CAR T-cells when compared to non-modified CAR T-cells (Figure 34 B)(Legut et al., 2022). IL7R, the gene encoding the IL-7 receptor associated with T-cell effector memory phenotype, was downregulated in anti-CD33 SLC7A11 CAR T-cells when compared

to non-modified CAR T-cells (Figure 34 B)(Zhang et al., 2021b). SLC3A2, the gene encoding for a chaperone protein that is crucial for SLC7A11 uptake into the cell membrane, is upregulated by anti-CD33 SLC7A11 CAR T-cells when compared to anti-CD33 CAR T-cells (Figure 34 B)(Parker et al., 2021).

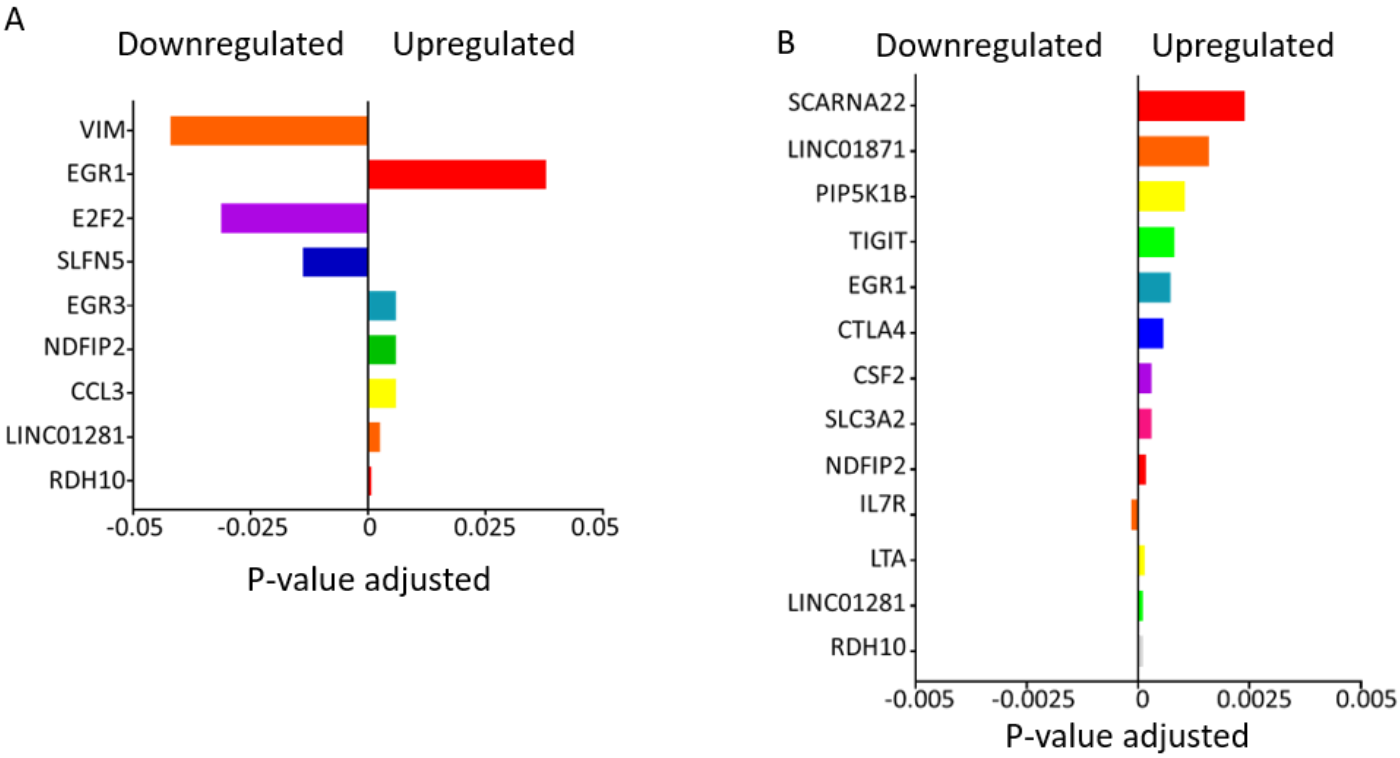

Figure 34: Differentially expressed genes in anti-CD33 CAR T-cells and anti-CD33 transporter CAR T-cells.
The CAR T-cells transduced from 5 health human donors were activated and cultured in 75% cystine free media or 75% tryptophan free media with THP1 cells for 72 hours. The CAR T-cells were then isolated by FACs sorting and RNA was extracted for analysis. (A) Plot of the differentially expressed genes between anti-CD33 SLC7A5 CAR T-cell and anti-CD33 CAR T-cells that held statistical significance. (B) Plot of the differentially expressed genes between anti-CD33 SLC7A11 CAR T-cell and anti-CD33 CAR T-cells that held statistical significance. Statistical analysis was performed by CRUK Birmingham Centre bioinformaticians Noyvert B. and Pan Y.

Interestingly, we identified that both SLC7A5- and SLC7A11-modified CAR T cells upregulated ARG2 expression. Previously this lab has shown that AML blasts cause a deprivation of arginine in AML patients due their upregulation of ARG2. A significant reduction of arginine in microenvironment decreases the ability T cell to proliferate (Mussai et al., 2015a). Arginine modulates T-cell metabolism, phenotype and anti-tumour activity. ARG2 metabolism of arginine has been shown to modulate T-cell proliferation (Mussai et al., 2019, Geiger et al., 2016). This laboratory has previously shown that the overexpression of ARG2 in CAR T-cells has improved their proliferation and anti-tumour activity (Panetti et al., 2023). Therefore, it was of interest to examine whether the upregulated ARG2 gene expression in our SLC7A5 and SLC7A11 CAR T-cells correlated to protein expression and function.

The respective unmodified and modified CAR T-cells were cultured with THP1 in R10 or low tryptophan/cystine media and then intracellularly stained with Arginase II (Figure 35A). The arginase II expression in the anti-CD33 SLC7A5 and anti-CD33 SLC7A11 CAR T-cells was significantly increased in their respective low media ($p=0.028$ and $p=0.005$, respectively) (Figure 35B).

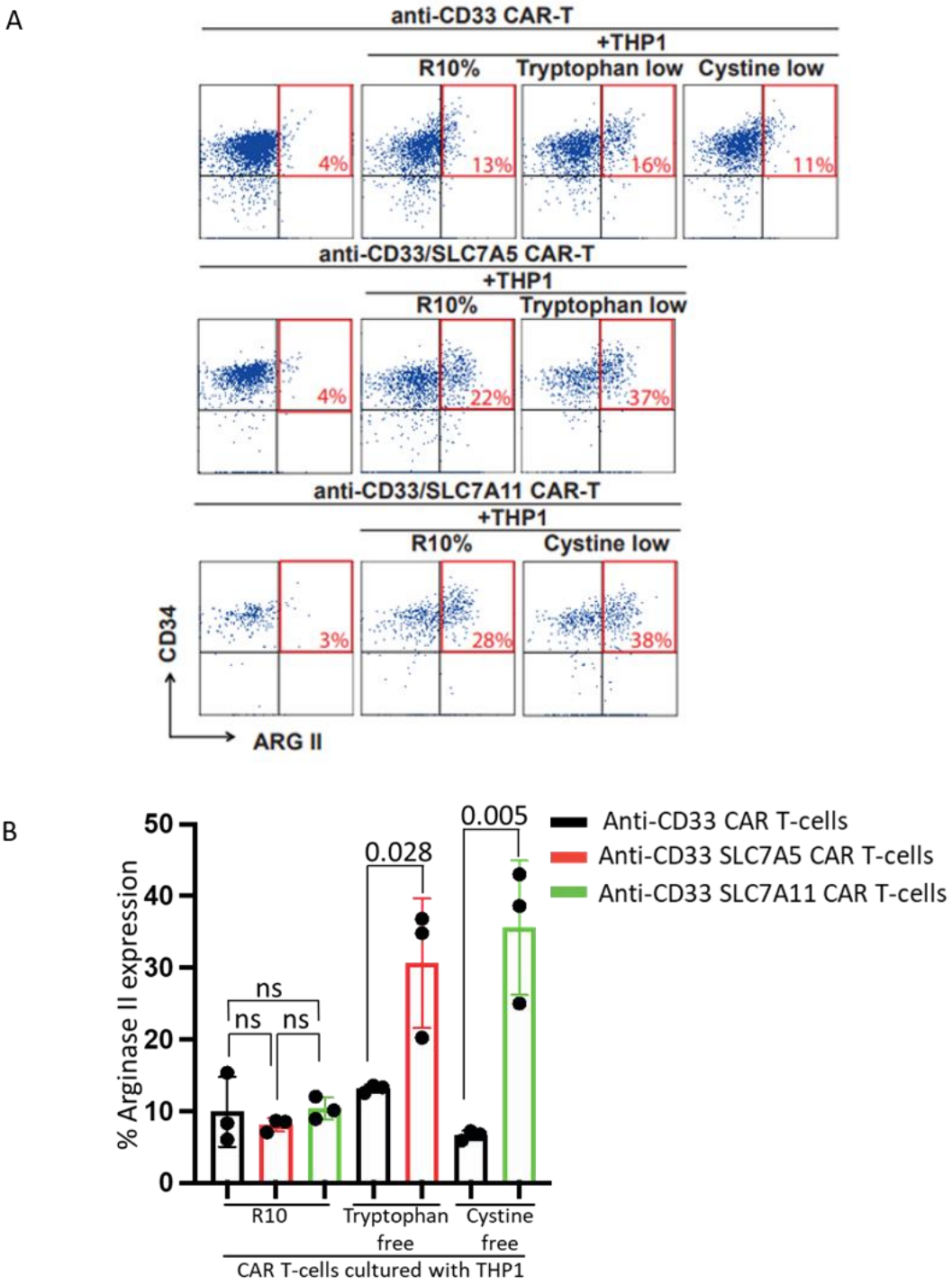

Figure 35: Measuring arginase II expression in activated CAR T-cells in low amino acids conditions

Intracellular levels of arginase II in modified CAR T-cells after being cultured in their respective 75% amino acid free for 48 hours. (A) Representative dot plots (B) Summary data of arginine expression. Each dot represents an individual experiment. Statistics performed were unpaired t-tests (n=3).

To ensure the arginase II expression shown was related to functional arginase II, the activity of arginase was measured using arginine activity assay on lysed CAR T-cells. The anti-CD33 SLC7A5 and anti-CD33 SLC7A11 CAR T-cells had significantly increased arginase activity compared to anti-CD33 CAR T-cells (Figure 36).

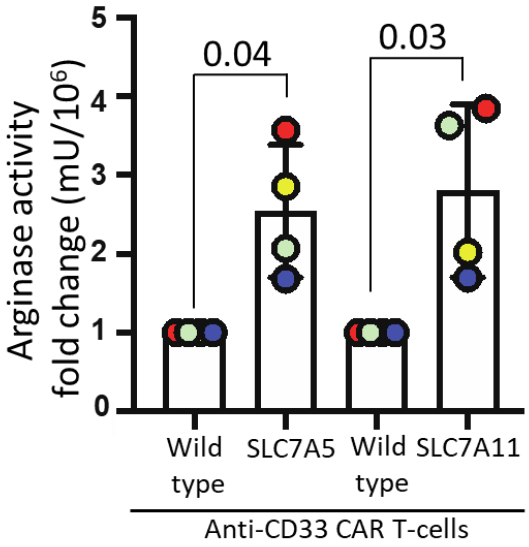

Figure 36: Arginase II expression and activity levels were elevated in modified CAR T-cells

Intracellular levels of arginase II in modified CAR T-cells after being cultured in their respective 75% amino acid free for 48 hours. CAR T-cells were lysed to assess arginase activity (mU/106 cells). Each dot represents an individual experiment. Statistical test performed were unpaired t-test (n=4).

We wanted to understand whether the addition of the amino acid transporters had altered the metabolic pathway transcriptome. The genes associated with these pathways were chosen using the Gene Set Enrichment Analysis database (MSigDB), focusing on the Hallmark gene sets for metabolism (Liberzon et al., 2015). The data sets used were Hallmark Oxidative Phosphorylation, Hallmark glycolysis, and Kegg Citrate cycle. The hypothesis was that the addition of the transporters would provide enough of the respective amino acids to inhibit the stress response by inhibiting CHOP and mTOR, thus allowing for increased metabolic rates.

The data set was obtained by comparing anti-CD33 CAR T-cells to anti-CD33 SLC7A5 CAR T-cells and anti-CD33 CAR T-cells to anti-CD33 SLC7A11 CAR T-cells. The addition of the transporter had no statistically significant effect on the RNA associated with glycolysis, oxidative phosphorylation or the citrate cycle (Figure 37 and 38).

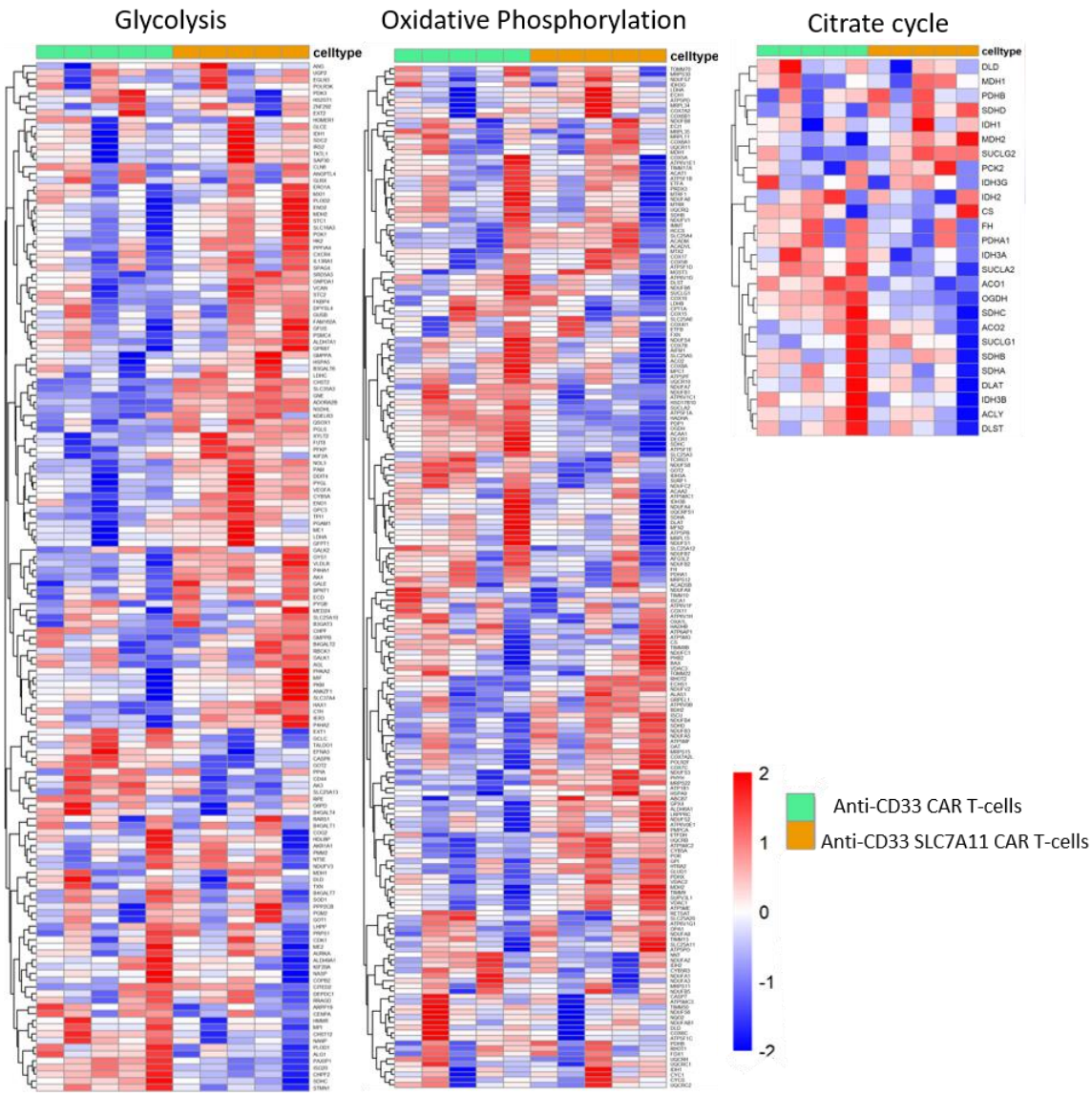

Figure 37: Differential gene expression between unmodified CAR T-cells and modified CAR T-cells on genes associated with glycolysis, oxidative phosphorylation, and the citrate cycle.

Heat maps of anti-CD33 SLC7A11 CAR T-cell gene expression compared to anti-CD33 CAR T-cells. The CAR T-cells transduced from 5 healthy human donors were activated and cultured in 75% cystine free media with THP1 cells for 72 hours. The CAR T-cells were then isolated by FACs sorting and RNA was extracted for analysis.

The data shown were chosen using the gene sets, Hallmark Oxidative Phosphorylation, Hallmark glycolysis, and Kegg Citrate cycle from the Gene Set enrichment analysis database (MSigDB). Statistical analysis was performed by CRUK Birmingham Centre bioinformaticians Noyvert B. and Pan Y.

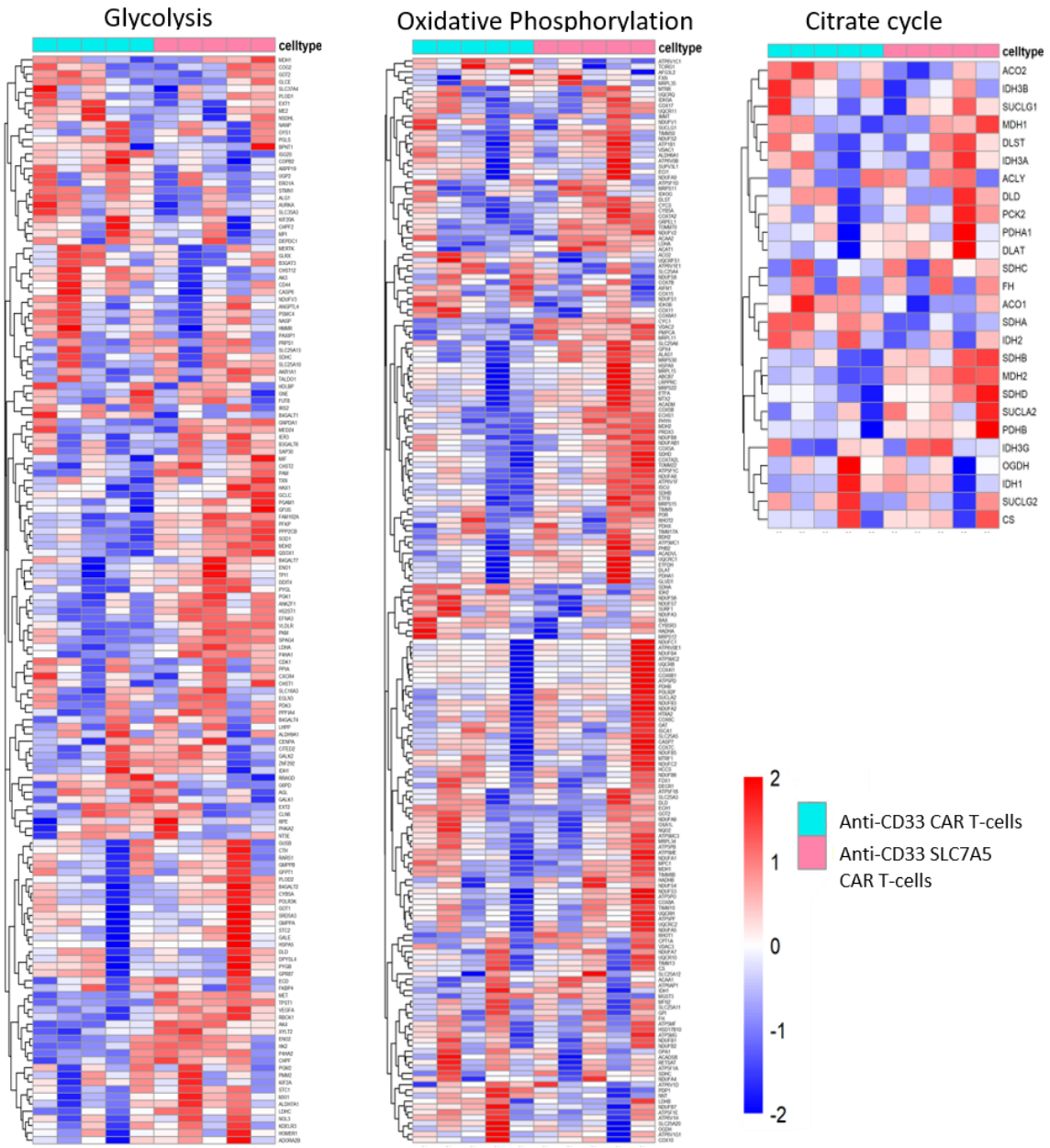

Figure 38: Differential gene expression between unmodified CAR T-cells and modified CAR T-cells on genes associated with glycolysis, oxidative phosphorylation, and the citrate cycle.

Heat maps of anti-CD33 SLC7A5 CAR T-cell gene expression compared to anti-CD33 CAR T-cells. The CAR T-cells transduced from 5 healthy human donors were activated and cultured in 75% tryptophan free media with THP1 cells for 72 hours. The CAR T-cells were then isolated by FACs sorting and RNA was extracted for analysis.

The data was generated using the gene sets: Hallmark Oxidative Phosphorylation, Hallmark glycolysis, and Kegg Citrate cycle from the Gene Set enrichment analysis database (MSigDB). Statistical analysis was performed by CRUK Birmingham Centre bioinformation's Noyvert B. and Pan Y

5.3.2 Modified CAR T-cell function in vivo

To assess if the overexpression on SLC7A5 and SLC7A11 by CAR T-cells significantly impacted tumour clearance, a xenographic model was used. $1x10^6$ cells of $CD33^+$ HL60 were intravenously injected into NOD SCID mice tail vein at 10-14 weeks of age. The engraftment into the mice's bone marrow was assessed by aspiration twenty-three days post-implantation using a CD33 antibody. The engraftment was considered successful if the bone marrow contained above a percentage of 2% HL60 cells. HL60 engrafted mice were then randomised into treatment groups (Figure 39). Twenty-four days post-HL60 injection, $2.5x10^6$ cells of unmodified and modified CAR T-cells or vehicle control were injected into the mice intravenously. The CAR T-cells were generated from 3 human donors that were cryopreserved until injection. Fourteen days and twenty-four days after CAR T-cell infusion, the mice's bone marrow was aspirated to measure the occurrence of AML Blasts by flow cytometry. Axis Bioservices, an external company, performed the *in vivo* protocol described above under the instructions of the De Santo laboratory and the guidelines stated by the Animal (Scientific Procedures) Act 1986. Post-harvest, the bone marrow was assessed by flow cytometry. Mice bone marrow was harvested either upon sacrifice due to declining health or at a maximum of 45 days.

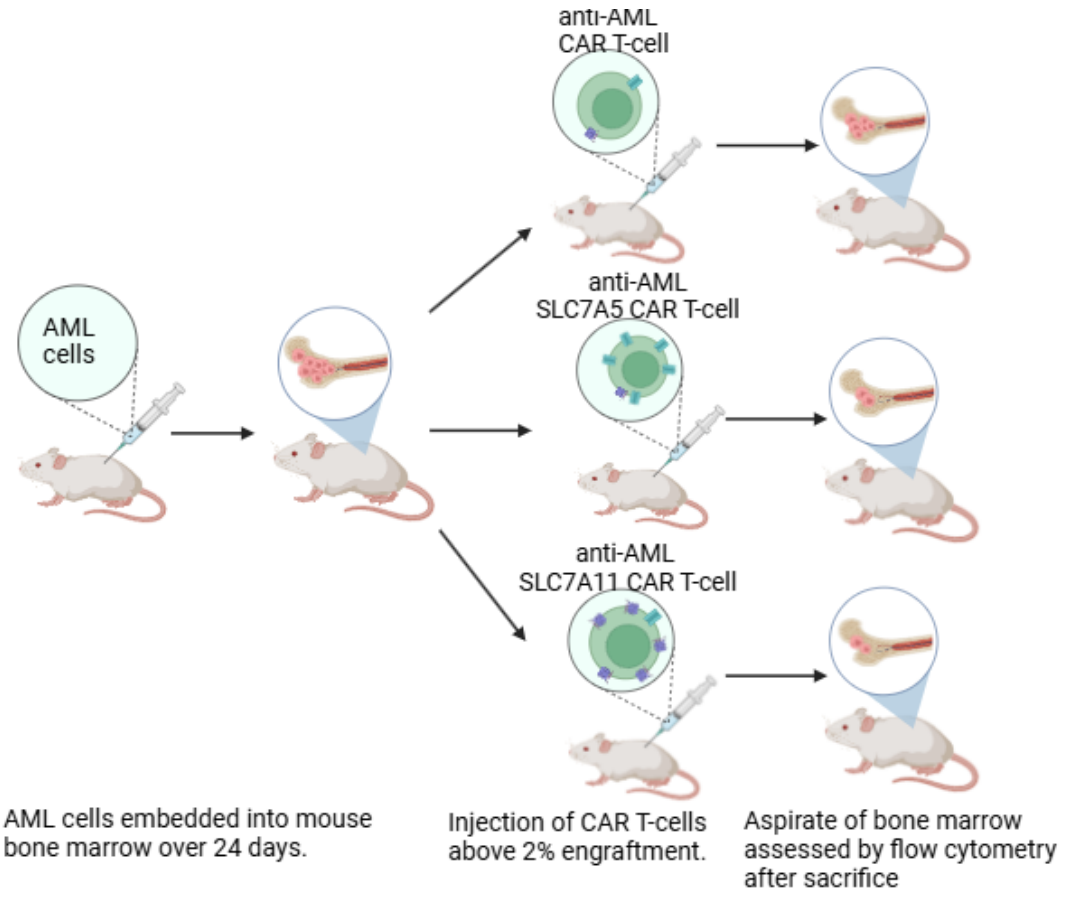

Figure 39: Design of CAR T-cell murine experiment
Mice were engrafted with HL60 AML cell line intravenously. Engrafted mice were split into 4 experiment conditions, mice intravenously injected with: Vehicle, anti-CD33 CAR T-cells, anti-CD33 SLC7A5 CAR T-cells, or anti-CD33 SLC7A11 CAR T-cells. Bone marrow was aspirated after murine sacrifice or on day 45.

The mice's body weight was regularly measured for the duration of the experiment to assess the overall health of the mice. The body weight of the mice was significantly not affected throughout the course of the experiment (Figure 40).

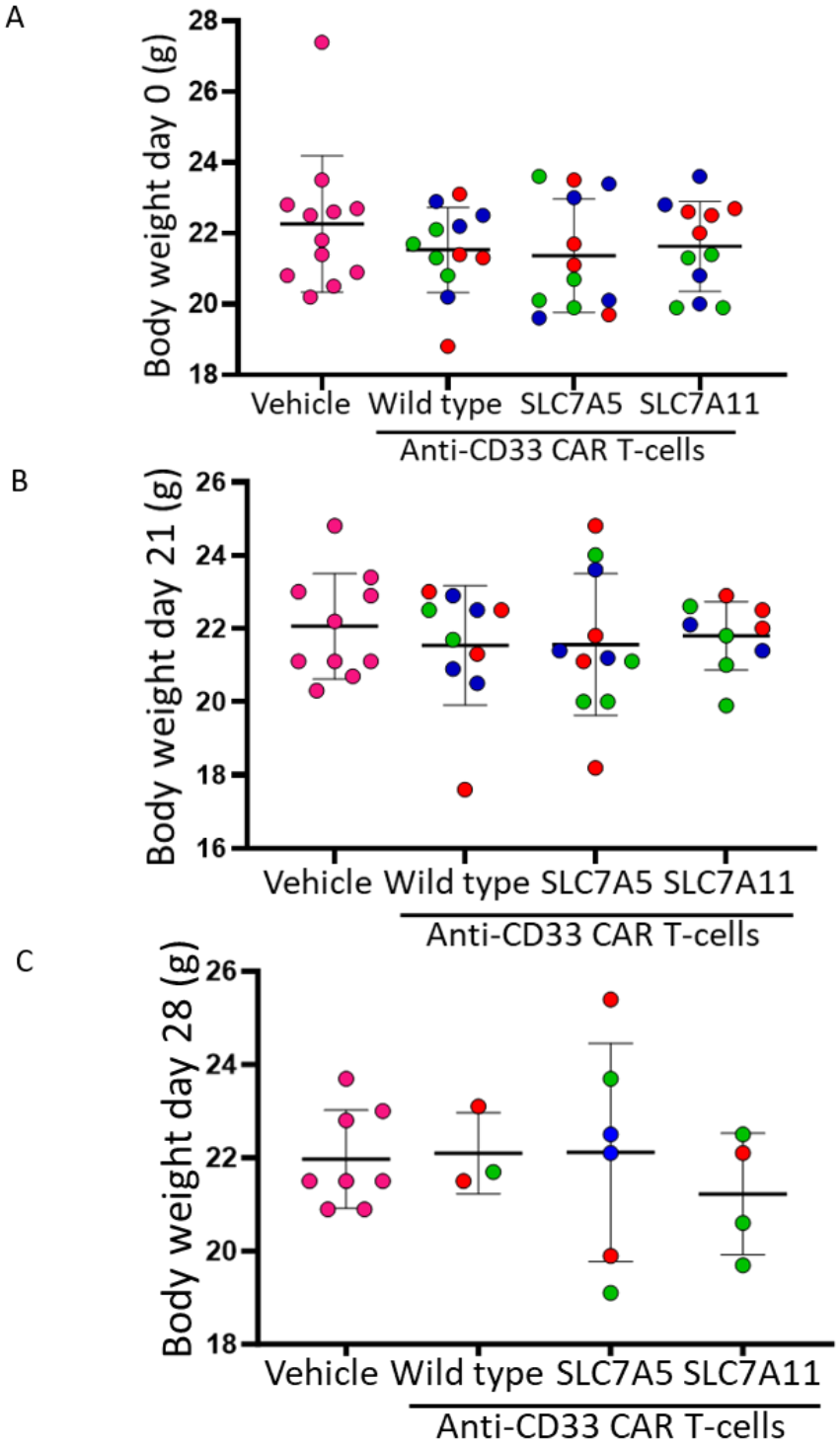

Figure 40: Summary of murine body weight for each treatment group.
The body weight in grams of the mice in all treatment groups was measured on (A) day 0, (B) day 21 and (C) day 28 (grams). Each dot represents an individual sample. Statistical test performed were unpaired t-test. Each colour dot represents a CAR T-cell donor.

The bone marrow was processed when the mice were culled to measure the frequency of CAR T-cells.

qPCR was used to measure the CAR T-cell frequency as this is the standard for detecting CAR T-cells in tissue (Narayan et al., 2022, Wang et al., 2021b). CAR T-cells were detected using a primer for the human CD34 truncated sequence (Figure 41B). There was an increase in CAR T-cells detected in all treatment groups compared to the control mice ($p=0.07$, 0.03, 0.0013) (Figure 39B). There was no significant difference in the amount of anti-CD33 SLC7A5, and anti-CD33 SLC7A11 CAR T-cells detected in the bone marrow compared to the unmodified CAR T-cells ($p=0.3$ and $p=0.17$, respectively) (Figure 41B).

Although the CAR T-cells were detected in equal amounts in the bone marrow there was significantly increased AML clearance for the anti-CD33 SLC7A5 and anti-CD33 SLC7A11 CAR T-cells ($p=0.004$ and 0.0037, respectively) (Figure 41C).

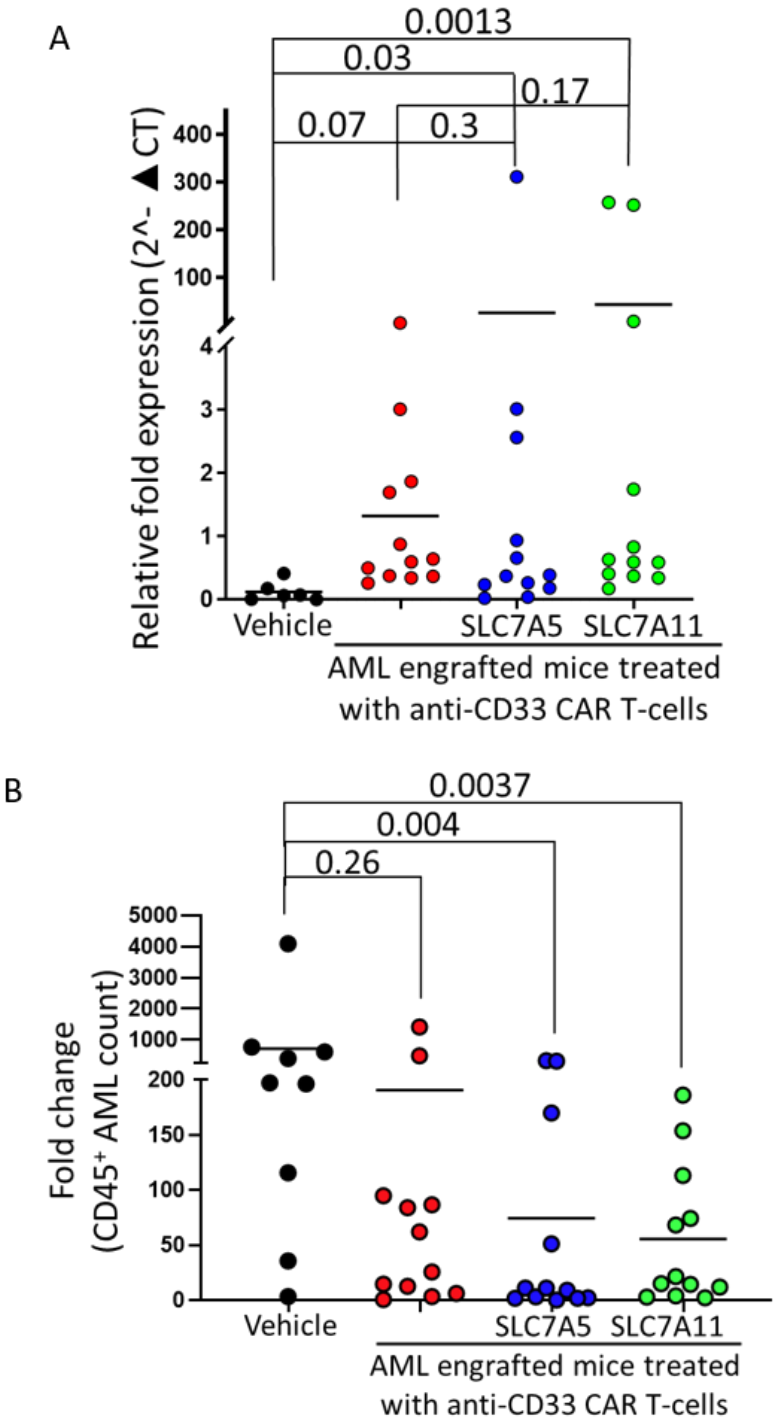

Figure 41: In vivo engraftment AML cell line HL60 into murine model
Female NOD SCID mice were implanted via intravenous injections with 1x106 HL-60 cells. Twenty-three days post implantation bone marrow aspirates were taken to ensure engraftment and engrafted mice were randomised into treatment groups. (A) CAR T-cell frequency in the bone marrow of day of harvest identified by qPCR. (B) The HL60 remaining in the bone marrow on day of harvest identified by flow cytometer. Statistical tests performed were unpaired t-tests (n=12).

5.4 Discussion

This chapter demonstrates that the modified CAR T-cells are transcriptionally and functionally different from the unmodified CAR T-cells.

Analysing the alterations in the transcriptome caused by the addition of the transporters of the CAR T-cells allowed us to identify the effect of altered amino acid availability on the pathways associated with CAR T-cell's fitness or function. The addition of the transporters did not alter the metabolic transcriptome profile of genes directly associated with glycolysis, oxidative phosphorylation, or the citrate cycle. However, there were significant alterations of RNA expression in other pathways associated with CAR T-cell function and fitness.

There was shared statistically significant upregulation of the RNA expression such as early growth response protein 1 (ERG1), RDH10, Nedd4 Family Interacting Protein 2 (NDFIP2) and LINC01281 in both anti-CD33 SLC7A5 and SLC7A11 CAR T-cells compared to anti-CD33 CAR T-cells. EGR1 is upregulated upon T-cell activation and promotes IL-2 production in T-cells (Collins et al., 2006, Waldrip et al., 2021). NDFIP2 expression is increased during T-cell activation and limits T-cell expansion to prevent excessive T-cell responses (O'Leary et al., 2016). RDH10 promotes effector T-cell differentiation (Fujiki et al., 2022). LINC01281 has been correlated with increased T-cell infiltration in some cancers (Ye et al., 2021, Sun et al., 2023). The upregulation of these genes demonstrates that the modified CAR T-cells have an increased capacity to undergo activation signalling even in low amino acid conditions. This demonstrates how the amino acid transporters have altered the CAR T-cell signalling associated with activation, expansion and differentiation.

Anti-CD33 SLC7A11 CAR T-cells upregulate SLC3A2. SLC3A2 is a chaperone protein upregulated during T-cell activation that is required for cell surface presentation of amino

acid transporters such as SLC7A5, SLC7A8, SLC7A10, and SLC7A11 (Wu et al., 2024, Jeckelmann and Fotiadis, 2019, Li et al., 2024, Ma et al., 2023a). Additional SLC3A2 protein expression allows not only increased cell surface presentation of SLC7A11 but also other amino transporters to be expressed on the cell surface, enabling increased amino acid uptake and, consequently, providing essential nutrients for anti-SLC7A11 CAR T-cells function.

In both modified CAR T-cells, the expression of other amino acid-related genes, such as ARG2 was upregulated. High expression of arginase by cancer cells, has been linked to the generation of an immunosuppressive environment due to T-cells requirement for arginine during proliferation (Mussai et al., 2015b). Further investigations into ARG2 expression were performed, demonstrating that modified CAR T-cells in low amino acid conditions increased ARG2 mRNA, resulting in increased protein expression of arginase II and increased arginase activity compared to anti-CD33 CAR T-cells. Previously, arginase II has been inserted into GD2 CAR T-cells, which provided increased proliferative capacity and tumour clearance in a murine model of neuroblastoma, demonstrating the importance of arginase II to T-cell function (Panetti et al., 2023).

Despite having no difference in the number of CAR T-cells in the bone marrow across the CAR T-cell types, the modified CAR T-cells significantly reduced the frequency of the AML blasts present in the bone marrow. Therefore, the modified CAR T-cells had increased potency against the target cells and the addition of amino acid transporters to CAR T-cells could improve patient results.

6. Final discussion

6.1 Summary

This thesis discussed designing CAR T-cell therapies to function better in low-amino acid environments generated by cancers.

- Cystine and tryptophan are essential for T-cell and CAR T-cell function.
- Inserting amino acid transporters SLC7A5 and SLC7A11 into CAR T-cells resulted in functional amino acid transporters that increased amino acid uptake in the modified CAR T-cells.
- Inserting amino acid transporters SLC7A5 and SLC7A11 into CAR T-cells increased CAR T-cell proliferation *in vitro*.
- Inserting amino acid transporters SLC7A5 and SLC7A11 into CAR T-cells increased CAR T-cell target cell clearance *in vivo*.

6.2 Discussion

CAR T-cell therapy has shown promise in haematological cancers such as B-cell lymphoma, multiple myeloma and B-cell acute lymphoblastic leukaemia. For these cancers, CAR T-cells provide complete remission for patients who previously had very limited options with dismal prognoses. Long-term follow-up of patients treated with CAR T-cells for B-cell lymphoma and multiple myeloma has shown a relapse incidence rate below 20% (Chong et al., 2021, Zhao et al., 2022a, Cappell et al., 2020). However, CAR T-cell therapy targeting AML has yet to receive approval due to limited clinical activity (Baumeister et al., 2019). The AML inhibits the function of the immune system by generating an immunosuppressive environment. AML secrete c-myc to expand MDSCs that suppress T-cell function (Pyzer et al., 2017). AML upregulates T-cell-suppressing molecules which induce T-cell exhaustion, such as PD-L1 and TIM-3 (Chen et al., 2020, Goncalves Silva et al., 2017). Importantly, AML alters the prevalence of amino acids in the TME. AML increases tryptophan metabolism, increasing the production of the immunosuppressive molecule kynurenine. Kynurenine inhibits T-cell function and promotes regulatory T-cell differentiation (Mabuchi et al., 2016, Arandi et al., 2018). AML down-regulates cystine generation from methionine. Instead, AML relies on the uptake of cystine from extracellular sources and, therefore, upregulates the cystine transporter SLC7A11 to aggressively increase cystine uptake, causing depletion of cystine levels in patient plasma (Cunningham et al., 2024, Zhou et al., 2020b).

We hypothesised that the introduction of the amino acid transporters SLC7A5 and SLC7A11 would enhance anti-CD33 CAR T-cell efficacy in the immunosuppressive environment by improving amino acid uptake. T-cells require tryptophan and cystine for T-cell proliferation. The analysis of anti-CD33 CAR T-cells in low tryptophan and cystine environments shows a

reduction in CAR T-cell proliferation. In the CAR Jurkat model, the addition of the tryptophan and cystine amino acid transporters improved ATP production and enhanced CAR Jurkat activation in low amino acid environments.

The addition of the amino acid transporters into the CAR T-cells resulted in a population of CAR T-cells that had increased protein expression of their respective transporters and increased amino acid uptake.

SLC7A5 and SLC7A11 transport other amino acids than tryptophan and cystine. SLC7A5 transports branched-chain amino acids, including leucine, isoleucine, phenylalanine, tyrosine, methionine, histidine and valine. SLC7A11 exchanges cystine uptake for glutamate export. Therefore, further analysis of the effect of the movement of the other amino acids transported by SLC7A5 and SLC7A11, for example, through metabolite labelling, could alter the perspective of how these amino acid transporters may be altering the CAR T-cell function and the surrounding cells. Studying whether CAR T-cells with increased amino acid uptake have the capability to reduce cancer cell proliferation without cell-to-cell contact through depletion of available amino acids could provide interesting insights into the effects of amino acid depletion on cancer cells.

Blocking cystine uptake and thioredoxin production from cystine causes cancer cell death (Harris et al., 2015, Cunningham et al., 2024). The inhibition of amino acid uptake via SLC7A5 by cancer cells suppresses cancer cell proliferation (Maimaiti et al., 2020). Therefore, reducing cystine and tryptophan availability to cancer cells could provide additional anti-tumour efficacy to CAR T-cells overexpressing these amino acid transporters.

Furthermore, the concept of adding amino acid transporters to CAR T-cells could be expanded beyond the amino acid transporters used here to other amino acid transporters in different CAR T-cell therapies.

The unmodified and the transporter CAR T-cells predominantly expressed a central memory phenotype, which has both proliferative capacity and the capability to differentiate into effector T-cells. This has been identified as one of the ideal phenotypes for CAR T-cells prior to use because this phenotype preserves the high proliferative capacity and effector function of the CAR T-cells (Doan et al., 2024, Arcangeli et al., 2022). It would be interesting to expand the phenotypic analysis to define further the subtype of these CAR T-cells, such as helper T-cells, type 1, 2, 17, or regulatory T-cells.

Retroviral CAR T-cells require T-cell activation to integrate CAR constructs into the T-cell genome during transduction. Therefore, the retroviral CAR T-cells injected into patients have previously been activated. The use of lentiviral vectors which do not require T-cell activation for successful transduction could provide a more naïve-like T-cell product with more functional capacity than pre-activated retroviral CAR T-cells (Ghassemi et al., 2022). The lack of expansion prior to injection would result in a smaller number of cells injected. However, the reduced manufacturing time of the CAR T-cells outside the patient has been previously shown to improve anti-cancer activity in leukaemia and would be beneficial to patients who otherwise would be waiting for treatment 7-14 days post leukapheresis (Ghassemi et al., 2018, Yang et al., 2022a). However, the use of lentiviral vectors without activation of the T-cells would not be suitable for the constructs used in this work as the larger constructs result in low transduction efficiency and, therefore, only a negligible number of CAR T-cells would be generated (Sweeney and Vink, 2021, Schambach et al., 2006).

Beyond this, the use of allogeneic CAR T-cells instead of autologous CAR T-cells could improve CAR T-cell potency. T-cells must be isolated from the patient's peripheral blood to generate autologous CAR T-cells. These patient-derived T-cells' fitness is affected by the cancer burden. Therefore, some patient's T-cells are not suitable for CAR T-cell therapy. Screening for specific T-cell phenotypes found in the leukapheresis of patients, such as increased LAG3 expression, has been shown to correlate with a lack of anti-cancer activity once injected into patients as a CAR T-cell product (Finney et al., 2019). Therefore, once the technology to prevent GVHD in allogeneic CAR T-cells has been improved, allogeneic CAR T-cell products may provide a more effective therapy for some patients. The technology of allogeneic CAR T-cells has reached phase 1 trials to be assessed for safety and cancer clearance (NCT04093596, NCT04516551) (Mailankody et al., 2023, Luo et al., 2024).

The addition of the amino acid transporters did not increase the expression of exhaustion markers PD-1, LAG3 or TIM3. Expression of these markers is expected due to prior activation during transduction, which induces the upregulation of these exhaustion markers. The upregulation of these markers by activated T-cells is often abused by cancers, including AML, to inhibit T-cell responses through cancer upregulation of the exhaustion ligands such as PD-L1, Galectin -3, and galectin-9 (Dama et al., 2019, Wang et al., 2022, Gao et al., 2017). Therefore, studying the effectiveness of anti-CD33 SLC7A5/SLC7A11 CAR T-cells when administered in combination with immune checkpoint blockades could provide essential protection for the CAR T-cell's function within the tumour microenvironment (Sailer et al., 2023, Zhou et al., 2023).

The addition of the amino acid transporters did not alter the killing capacity of the CAR T-cells *in vitro*.

The addition of the transporters reduced the expression of TNF-α. TNF-α can induce T-cell proliferation but also T-cell death (Psarras et al., 2021, Kumar et al., 2022). Therefore, the effects of the decreased TNF-α production by the CAR T-cells needs to be studied more.

Despite the increase in ATP production seen in the modified Jurkat CAR, the addition of the transporters did not affect the expression of genes associated with glycolysis, oxidative phosphorylation, and the citrate cycle in CAR T-cells. However, other genes involved in T-cell proliferation and function had altered expression.

Both transporters had differential expression of genes associated with T-cell activation, survival, proliferation and differentiation. The differential expression of the genes by the anti-CD33 transporter CAR T-cells suggests increased fitness and function in low amino acid conditions compared to anti-CD33 CAR T-cells.

Arginase II, a gene associated with amino acid metabolism, was upregulated by both modified CAR T-cells, resulting in increased expression of arginase II at the protein level and increased arginase activity in the modified CAR T-cells. Arginine is another essential amino acid for T-cell function, and therefore, the increased metabolism of arginine could provide improved CAR T-cell functions in the immunosuppressive environment. Further analysis of the protein expression levels associated with the altered RNA expression described in the transcriptome data via western blot or flow cytometry could further demonstrate how the addition of amino acid transporters exerted an effect on the CAR T-cell function.

In the *in vivo* model of leukaemia, following the injection of CAR T-cells, the frequency of the different CAR T-cells in the bone marrow was not altered. However, unlike unmodified CAR T-cells, the transporter CAR T-cells reduced the cancer burden in murine models, demonstrating increased potency of anti-tumour activity.

Armoured CAR T-cells have been discussed in the literature as potential to overcome the failures of CAR T-cell therapy (Pievani et al., 2024, Hawkins et al., 2021, Zhang et al., 2023a). Armoured CAR T-cells refer to the CAR T-cells designed with various mechanisms to overcome or target the tumour microenvironment. CAR T-cells designed to increase the production of cytokines such as IL-2 and IL-33 have been shown to have increased survival and decreased tumour growth in solid tumour mouse models compared to those that are not modified. (Brog et al., 2022). More relevantly to this thesis, the overexpression of kynurenine enzyme, kynureninase, in CAR T-cells improved anti-leukemic activity (Yang et al., 2022b). Further *in vivo* testing and clinical trials would be required to prove the efficacy of these armoured CAR T-cells within the solid microenvironment.

In the future, combining these armoured CAR T-cells and adding amino acid transporters could provide resistance to the TME, tailoring CAR design to individual TME types and protecting against CAR function from the heterogeneity of the TME. Combining the kynurenine-clearing ability of kynureninase-producing CAR T-cells with increased tryptophan uptake could provide a robust response to cancers with altered tryptophan metabolism within the TME. Additionally, in TMEs identified to have increased ROS production, CAR T-cells with increased catalase expression to protect from increased ROS exposure could be combined with increased cystine uptake as cystine is utilised to protect against ROS species could provide resistance against the TME (Ligtenberg et al., 2016, Han et al., 2024). Conversely, an amalgamation of these designs targeting a combination of pathways could provide protection in heterogeneous TMEs and prevent tumour escape via cancer upregulation of alternative mechanisms of immunosuppression.

6.3 Limitations

As discussed in the previous chapter, one of the difficulties with the transduction efficiency of the modified CAR T-cells was the construct's size. The insertion of the transporters to the construct adds significant length to the construct, decreasing the transduction efficiency. This significantly decreases the number of cells obtained following the CAR T-cell enrichment. Optimisation and upscaling of the transduction process would enable additional work to be carried out to allow experiments which require a larger cell count to be completed. Optimisation of the process, such as altering media composition, transduction enhancer type or concentration, and cytokine exposure, all have been shown in other CAR T-cell models to alter transduction efficiency (Ghassemi et al., 2020, Nasiri et al., 2023, Du et al., 2021).

6.5 Conclusion

This thesis demonstrated that the addition of amino acid transporters to CAR T-cells is viable and can result in functional amino acid transporters that increase CAR T-cell uptake of available amino acids. Therefore, this could be an avenue of CAR T-cell design that could unlock improved results within CAR T-cell therapy, especially within cancer microenvironments where the amino acid availability is altered. Considerable expansion upon the results described here would need to be completed before clinical application to develop the most effective amino acid transporter CAR T-cells and assess which patients they would benefit most. However, these results show proof of concept that CAR T-cell design benefits from metabolic considerations.

7. References

ALAM, M. S., OTSUKA, S., WONG, N., ABBASI, A., GAIDA, M. M., FAN, Y., MEERZAMAN, D. & ASHWELL, J. D. 2021. TNF plays a crucial role in inflammation by signaling via T cell TNFR2. *Proc Natl Acad Sci U S A,* 118.

ALTER, B. P. 2014. Fanconi anemia and the development of leukemia. *Best Pract Res Clin Haematol,* 27**,** 214-21.

ALTMAN, B. J., STINE, Z. E. & DANG, C. V. 2016. From Krebs to clinic: glutamine metabolism to cancer therapy. *Nat Rev Cancer,* 16**,** 773.

ALVES, N. L., VAN LEEUWEN, E. M., DERKS, I. A. & VAN LIER, R. A. 2008. Differential regulation of human IL-7 receptor alpha expression by IL-7 and TCR signaling. *J Immunol,* 180**,** 5201-10.

ANAGNOSTOU, T., RIAZ, I. B., HASHMI, S. K., MURAD, M. H. & KENDERIAN, S. S. 2020. Anti-CD19 chimeric antigen receptor T-cell therapy in acute lymphocytic leukaemia: a systematic review and meta-analysis. *Lancet Haematol,* 7**,** e816-e826.

ANDREASSEN, P. R., SEO, J., WIEK, C. & HANENBERG, H. 2021. Understanding BRCA2 Function as a Tumor Suppressor Based on Domain-Specific Activities in DNA Damage Responses. *Genes (Basel),* 12.

APERT, C., GALINDO-ALBARRAN, A. O., CASTAN, S., DETRAVES, C., MICHAUD, H., MCJANNETT, N., HAEGEMAN, B., FILLATREAU, S., MALISSEN, B., HOLLANDER, G., ZUKLYS, S., SANTAMARIA, J. C., JOFFRE, O. P., ROMAGNOLI, P. & VAN MEERWIJK, J. P. M. 2022. IL-2 and IL-15 drive intrathymic development of distinct periphery-seeding CD4(+)Foxp3(+) regulatory T lymphocytes. *Front Immunol,* 13**,** 965303.

ARANDI, N., RAMZI, M., SAFAEI, F. & MONABATI, A. 2018. Overexpression of indoleamine 2,3-dioxygenase correlates with regulatory T cell phenotype in acute myeloid leukemia patients with normal karyotype. *Blood Res,* 53**,** 294-298.

ARCANGELI, S., BOVE, C., MEZZANOTTE, C., CAMISA, B., FALCONE, L., MANFREDI, F., BEZZECCHI, E., EL KHOURY, R., NORATA, R., SANVITO, F., PONZONI, M., GRECO, B., MORESCO, M. A., CARRABBA, M. G., CICERI, F., BONINI, C., BONDANZA, A. & CASUCCI, M. 2022. CAR T cell manufacturing from naive/stem memory T lymphocytes enhances antitumor responses while curtailing cytokine release syndrome. *J Clin Invest,* 132.

ARNOLD, D. E., MAUDE, S. L., CALLAHAN, C. A., DINOFIA, A. M., GRUPP, S. A. & HEIMALL, J. R. 2020. Subcutaneous immunoglobulin replacement following CD19-specific chimeric antigen receptor T-cell therapy for B-cell acute lymphoblastic leukemia in pediatric patients. *Pediatr Blood Cancer,* 67**,** e28092.

ATILLA, E. & BENABDELLAH, K. 2023. The Black Hole: CAR T Cell Therapy in AML. *Cancers (Basel),* 15.

ATKINS, M. B., LOTZE, M. T., DUTCHER, J. P., FISHER, R. I., WEISS, G., MARGOLIN, K., ABRAMS, J., SZNOL, M., PARKINSON, D., HAWKINS, M., PARADISE, C., KUNKEL, L. & ROSENBERG, S. A. 1999. High-dose recombinant interleukin 2 therapy for patients with metastatic melanoma: analysis of 270 patients treated between 1985 and 1993. *J Clin Oncol,* 17**,** 2105-16.

AYYADURAI, V. A. S., DEONIKAR, P., MCLURE, K. G. & SAKAMOTO, K. M. 2022. Molecular Systems Architecture of Interactome in the Acute Myeloid Leukemia Microenvironment. *Cancers (Basel),* 14.

BACHMANN, M. F. & OXENIUS, A. 2007. Interleukin 2: from immunostimulation to immunoregulation and back again. *EMBO Rep,* 8**,** 1142-8.
BADER, P. 2023. Allo or auto CAR-T cells for refractory BCP-ALL? *Blood,* 142**,** 122-124.
BAKHTIYARI, M., LIAGHAT, M., AZIZIYAN, F., SHAPOURIAN, H., YAHYAZADEH, S., ALIPOUR, M., SHAHVEH, S., MALEKI-SHEIKHABADI, F., HALIMI, H., FORGHANIESFIDVAJANI, R., ZALPOOR, H., NABI-AFJADI, M. & PORNOUR, M. 2023. The role of bone marrow microenvironment (BMM) cells in acute myeloid leukemia (AML) progression: immune checkpoints, metabolic checkpoints, and signaling pathways. *Cell Commun Signal,* 21**,** 252.
BANNOUD, N., DALOTTO-MORENO, T., KINDGARD, L., GARCIA, P. A., BLIDNER, A. G., MARINO, K. V., RABINOVICH, G. A. & CROCI, D. O. 2021. Hypoxia Supports Differentiation of Terminally Exhausted CD8 T Cells. *Front Immunol,* 12**,** 660944.
BAUMEISTER, S. H., MURAD, J., WERNER, L., DALEY, H., TREBEDEN-NEGRE, H., GICOBI, J. K., SCHMUCKER, A., REDER, J., SENTMAN, C. L., GILHAM, D. E., LEHMANN, F. F., GALINSKY, I., DIPIETRO, H., CUMMINGS, K., MUNSHI, N. C., STONE, R. M., NEUBERG, D. S., SOIFFER, R., DRANOFF, G., RITZ, J. & NIKIFOROW, S. 2019. Phase I Trial of Autologous CAR T Cells Targeting NKG2D Ligands in Patients with AML/MDS and Multiple Myeloma. *Cancer Immunol Res,* 7**,** 100-112.
BERGSLAND, C. H., JEANMOUGIN, M., MOOSAVI, S. H., SVINDLAND, A., BRUUN, J., NESBAKKEN, A., SVEEN, A. & LOTHE, R. A. 2022. Spatial analysis and CD25-expression identify regulatory T cells as predictors of a poor prognosis in colorectal cancer. *Mod Pathol,* 35**,** 1236-1246.
BERRAONDO, P., SANMAMED, M. F., OCHOA, M. C., ETXEBERRIA, I., AZNAR, M. A., PEREZ-GRACIA, J. L., RODRIGUEZ-RUIZ, M. E., PONZ-SARVISE, M., CASTANON, E. & MELERO, I. 2019. Cytokines in clinical cancer immunotherapy. *Br J Cancer,* 120**,** 6-15.
BLAESCHKE, F., STENGER, D., KAEUFERLE, T., WILLIER, S., LOTFI, R., KAISER, A. D., ASSENMACHER, M., DORING, M., FEUCHT, J. & FEUCHTINGER, T. 2018. Induction of a central memory and stem cell memory phenotype in functionally active CD4(+) and CD8(+) CAR T cells produced in an automated good manufacturing practice system for the treatment of CD19(+) acute lymphoblastic leukemia. *Cancer Immunol Immunother,* 67**,** 1053-1066.
BLOEMBERG, D., NGUYEN, T., MACLEAN, S., ZAFER, A., GADOURY, C., GURNANI, K., CHATTOPADHYAY, A., ASH, J., LIPPENS, J., HARCUS, D., PAGE, M., FORTIN, A., PON, R. A., GILBERT, R., MARCIL, A., WEERATNA, R. D. & MCCOMB, S. 2020. A High-Throughput Method for Characterizing Novel Chimeric Antigen Receptors in Jurkat Cells. *Mol Ther Methods Clin Dev,* 16**,** 238-254.
BORELLI, A. & IRLA, M. 2021. Lymphotoxin: from the physiology to the regeneration of the thymic function. *Cell Death Differ,* 28**,** 2305-2314.
BOVE, C., ARCANGELI, S., FALCONE, L., CAMISA, B., EL KHOURY, R., GRECO, B., DE LUCIA, A., BERGAMINI, A., BONDANZA, A., CICERI, F., BONINI, C. & CASUCCI, M. 2023. CD4 CAR-T cells targeting CD19 play a key role in exacerbating cytokine release syndrome, while maintaining long-term responses. *J Immunother Cancer,* 11.
BRACHO-SANCHEZ, E., HASSANZADEH, A., BRUSKO, M. A., WALLET, M. A. & KESELOWSKY, B. G. 2019. Dendritic Cells Treated with Exogenous Indoleamine 2,3-Dioxygenase Maintain an Immature Phenotype and Suppress Antigen-specific T cell Proliferation. *J Immunol Regen Med,* 5.

BRAY, F., LAVERSANNE, M., WEIDERPASS, E. & SOERJOMATARAM, I. 2021. The ever-increasing importance of cancer as a leading cause of premature death worldwide. *Cancer,* 127**,** 3029-3030.

BREWITZ, A., EICKHOFF, S., DAHLING, S., QUAST, T., BEDOUI, S., KROCZEK, R. A., KURTS, C., GARBI, N., BARCHET, W., IANNACONE, M., KLAUSCHEN, F., KOLANUS, W., KAISHO, T., COLONNA, M., GERMAIN, R. N. & KASTENMULLER, W. 2017. CD8(+) T Cells Orchestrate pDC-XCR1(+) Dendritic Cell Spatial and Functional Cooperativity to Optimize Priming. *Immunity,* 46**,** 205-219.

BRINCKS, E. L., ADAMS, J., WANG, L., TURNER, B., MARCINOWICZ, A., KE, J., ESSMANN, M., MAUTINO, L. M., ALLEN, C. V., KUMAR, S., VAHANIAN, N., LINK, C. & MAUTINO, M. R. 2020. Indoximod opposes the immunosuppressive effects mediated by IDO and TDO via modulation of AhR function and activation of mTORC1. *Oncotarget,* 11**,** 2438-2461.

BROG, R. A., FERRY, S. L., SCHIEBOUT, C. T., MESSIER, C. M., COOK, W. J., ABDULLAH, L., ZOU, J., KUMAR, P., SENTMAN, C. L., FROST, H. R. & HUANG, Y. H. 2022. Superkine IL-2 and IL-33 Armored CAR T Cells Reshape the Tumor Microenvironment and Reduce Growth of Multiple Solid Tumors. *Cancer Immunol Res,* 10**,** 962-977.

BRUCK, O., DUFVA, O., HOHTARI, H., BLOM, S., TURKKI, R., ILANDER, M., KOVANEN, P., PALLAUD, C., RAMOS, P. M., LAHTEENMAKI, H., VALIMAKI, K., EL MISSIRY, M., RIBEIRO, A., KALLIONIEMI, O., PORKKA, K., PELLINEN, T. & MUSTJOKI, S. 2020. Immune profiles in acute myeloid leukemia bone marrow associate with patient age, T-cell receptor clonality, and survival. *Blood Adv,* 4**,** 274-286.

CAIMI, P. F., PACHECO SANCHEZ, G., SHARMA, A., OTEGBEYE, F., AHMED, N., ROJAS, P., PATEL, S., KLEINSORGE BLOCK, S., SCHIAVONE, J., ZAMBORSKY, K., BOUGHAN, K., HILLIAN, A., REESE-KOC, J., MASCHAN, M., DROPULIC, B., SEKALY, R. P. & DE LIMA, M. 2021. Prophylactic Tocilizumab Prior to Anti-CD19 CAR-T Cell Therapy for Non-Hodgkin Lymphoma. *Front Immunol,* 12**,** 745320.

CAMPBELL, C., MCKENNEY, P. T., KONSTANTINOVSKY, D., ISAEVA, O. I., SCHIZAS, M., VERTER, J., MAI, C., JIN, W. B., GUO, C. J., VIOLANTE, S., RAMOS, R. J., CROSS, J. R., KADAVERU, K., HAMBOR, J. & RUDENSKY, A. Y. 2020. Bacterial metabolism of bile acids promotes generation of peripheral regulatory T cells. *Nature,* 581**,** 475-479.

CAPPELL, K. M., SHERRY, R. M., YANG, J. C., GOFF, S. L., VANASSE, D. A., MCINTYRE, L., ROSENBERG, S. A. & KOCHENDERFER, J. N. 2020. Long-Term Follow-Up of Anti-CD19 Chimeric Antigen Receptor T-Cell Therapy. *J Clin Oncol,* 38**,** 3805-3815.

CASTELLINO, F., HUANG, A. Y., ALTAN-BONNET, G., STOLL, S., SCHEINECKER, C. & GERMAIN, R. N. 2006. Chemokines enhance immunity by guiding naive CD8+ T cells to sites of CD4+ T cell-dendritic cell interaction. *Nature,* 440**,** 890-5.

CASUCCI, M., FALCONE, L., CAMISA, B., NORELLI, M., PORCELLINI, S., STORNAIUOLO, A., CICERI, F., TRAVERSARI, C., BORDIGNON, C., BONINI, C. & BONDANZA, A. 2018. Extracellular NGFR Spacers Allow Efficient Tracking and Enrichment of Fully Functional CAR-T Cells Co-Expressing a Suicide Gene. *Front Immunol,* 9**,** 507.

CHAE, S., BAE, J., YOUN, N., LOPEZ, K. D., SUTAMTEWAGUL, G. & RAKEL, B. 2024. Agreement between patient-reported and clinically documented symptoms of acute myeloid leukemia: Study protocol. *J Adv Nurs*.

CHAE, Y. K., CHOI, W. M., BAE, W. H., ANKER, J., DAVIS, A. A., AGTE, S., IAMS, W. T., CRUZ, M., MATSANGOU, M. & GILES, F. J. 2018. Overexpression of adhesion molecules and

barrier molecules is associated with differential infiltration of immune cells in non-small cell lung cancer. *Sci Rep,* 8**,** 1023.
CHAMBERS, C. A. & ALLISON, J. P. 1997. Co-stimulation in T cell responses. *Curr Opin Immunol,* 9**,** 396-404.
CHANG, C. H., CURTIS, J. D., MAGGI, L. B., JR., FAUBERT, B., VILLARINO, A. V., O'SULLIVAN, D., HUANG, S. C., VAN DER WINDT, G. J., BLAGIH, J., QIU, J., WEBER, J. D., PEARCE, E. J., JONES, R. G. & PEARCE, E. L. 2013. Posttranscriptional control of T cell effector function by aerobic glycolysis. *Cell,* 153**,** 1239-51.
CHEN, C., LIANG, C., WANG, S., CHIO, C. L., ZHANG, Y., ZENG, C., CHEN, S., WANG, C. & LI, Y. 2020. Expression patterns of immune checkpoints in acute myeloid leukemia. *J Hematol Oncol,* 13**,** 28.
CHEN, H., BEARDSLEY, G. P. & COEN, D. M. 2014. Mechanism of ganciclovir-induced chain termination revealed by resistant viral polymerase mutants with reduced exonuclease activity. *Proc Natl Acad Sci U S A,* 111**,** 17462-7.
CHEN, X., DU, Y., HU, Q. & HUANG, Z. 2017. Tumor-derived CD4+CD25+regulatory T cells inhibit dendritic cells function by CTLA-4. *Pathol Res Pract,* 213**,** 245-249.
CHEN, Y. J., ABILA, B. & MOSTAFA KAMEL, Y. 2023. CAR-T: What Is Next? *Cancers (Basel),* 15.
CHEUNG, H. L., WONG, Y. H., LI, Y. Y., YANG, X., KO, L. H., TAN KABIGTING, J. E., CHAN, K. C., LEUNG, A. Y. H. & CHAN, B. P. 2024. Microenvironment matters: In vitro 3D bone marrow niches differentially modulate survival, phenotype and drug responses of acute myeloid leukemia (AML) cells. *Biomaterials,* 312**,** 122719.
CHIA, W. K., WANG, W. W., TEO, M., TAI, W. M., LIM, W. T., TAN, E. H., LEONG, S. S., SUN, L., CHEN, J. J., GOTTSCHALK, S. & TOH, H. C. 2012. A phase II study evaluating the safety and efficacy of an adenovirus-DeltaLMP1-LMP2 transduced dendritic cell vaccine in patients with advanced metastatic nasopharyngeal carcinoma. *Ann Oncol,* 23**,** 997-1005.
CHIN, R. K., LO, J. C., KIM, O., BLINK, S. E., CHRISTIANSEN, P. A., PETERSON, P., WANG, Y., WARE, C. & FU, Y. X. 2003. Lymphotoxin pathway directs thymic Aire expression. *Nat Immunol,* 4**,** 1121-7.
CHMIELEWSKI, M. & ABKEN, H. 2017. CAR T Cells Releasing IL-18 Convert to T-Bet(high) FoxO1(low) Effectors that Exhibit Augmented Activity against Advanced Solid Tumors. *Cell Rep,* 21**,** 3205-3219.
CHOCARRO, L., BOCANEGRA, A., BLANCO, E., FERNANDEZ-RUBIO, L., ARASANZ, H., ECHAIDE, M., GARNICA, M., RAMOS, P., PINEIRO-HERMIDA, S., VERA, R., ESCORS, D. & KOCHAN, G. 2022. Cutting-Edge: Preclinical and Clinical Development of the First Approved Lag-3 Inhibitor. *Cells,* 11.
CHONG, E. A., RUELLA, M., SCHUSTER, S. J. & LYMPHOMA PROGRAM INVESTIGATORS AT THE UNIVERSITY OF, P. 2021. Five-Year Outcomes for Refractory B-Cell Lymphomas with CAR T-Cell Therapy. *N Engl J Med,* 384**,** 673-674.
CHOW, V. A., SHADMAN, M. & GOPAL, A. K. 2018. Translating anti-CD19 CAR T-cell therapy into clinical practice for relapsed/refractory diffuse large B-cell lymphoma. *Blood,* 132**,** 777-781.
CHRISTEN, F., HOYER, K., YOSHIDA, K., HOU, H. A., WALDHUETER, N., HEUSER, M., HILLS, R. K., CHAN, W., HABLESREITER, R., BLAU, O., OCHI, Y., KLEMENT, P., CHOU, W. C., BLAU, I. W., TANG, J. L., ZEMOJTEL, T., SHIRAISHI, Y., SHIOZAWA, Y., THOL, F., GANSER, A., LOWENBERG, B., LINCH, D. C., BULLINGER, L., VALK, P. J. M., TIEN, H. F., GALE, R. E., OGAWA, S. & DAMM, F. 2019. Genomic landscape and clonal evolution

of acute myeloid leukemia with t(8;21): an international study on 331 patients. *Blood,* 133**,** 1140-1151.

CLAYTON, K. L., HAALAND, M. S., DOUGLAS-VAIL, M. B., MUJIB, S., CHEW, G. M., NDHLOVU, L. C. & OSTROWSKI, M. A. 2014. T cell Ig and mucin domain-containing protein 3 is recruited to the immune synapse, disrupts stable synapse formation, and associates with receptor phosphatases. *J Immunol,* 192**,** 782-91.

COLD, S., COLD, F., JENSEN, M. B., CRONIN-FENTON, D., CHRISTIANSEN, P. & EJLERTSEN, B. 2022. Systemic or Vaginal Hormone Therapy After Early Breast Cancer: A Danish Observational Cohort Study. *J Natl Cancer Inst,* 114**,** 1347-1354.

COLLINS, S., WOLFRAIM, L. A., DRAKE, C. G., HORTON, M. R. & POWELL, J. D. 2006. Cutting Edge: TCR-induced NAB2 enhances T cell function by coactivating IL-2 transcription. *J Immunol,* 177**,** 8301-5.

COLLISON, L. W., WORKMAN, C. J., KUO, T. T., BOYD, K., WANG, Y., VIGNALI, K. M., CROSS, R., SEHY, D., BLUMBERG, R. S. & VIGNALI, D. A. 2007. The inhibitory cytokine IL-35 contributes to regulatory T-cell function. *Nature,* 450**,** 566-9.

CRAMER, S. L., SAHA, A., LIU, J., TADI, S., TIZIANI, S., YAN, W., TRIPLETT, K., LAMB, C., ALTERS, S. E., ROWLINSON, S., ZHANG, Y. J., KEATING, M. J., HUANG, P., DIGIOVANNI, J., GEORGIOU, G. & STONE, E. 2017. Systemic depletion of L-cyst(e)ine with cyst(e)inase increases reactive oxygen species and suppresses tumor growth. *Nat Med,* 23**,** 120-127.

CUNNINGHAM, A., ERDEM, A., ALSHAMLEH, I., GEUGIEN, M., PRUIS, M., PEREIRA-MARTINS, D. A., VAN DEN HEUVEL, F. A. J., WIERENGA, A. T. J., TEN BERGE, H., DENNEBOS, R., VAN DEN BOOM, V., HOGELING, S. M., WEINHAUSER, I., KNOPS, R., DE BLAAUW, P., HEINER-FOKKEMA, M. R., WOOLTHUIS, C., GUNTHER, U. L., REGO, E. M., MARTENS, J. H. A., JANSEN, J. H., SCHWALBE, H., HULS, G. & SCHURINGA, J. J. 2022. Dietary methionine starvation impairs acute myeloid leukemia progression. *Blood,* 140**,** 2037-2052.

CUNNINGHAM, A., OUDEJANS, L. L., GEUGIEN, M., PEREIRA-MARTINS, D. A., WIERENGA, A. T. J., ERDEM, A., STERNADT, D., HULS, G. & SCHURINGA, J. J. 2024. The nonessential amino acid cysteine is required to prevent ferroptosis in acute myeloid leukemia. *Blood Adv,* 8**,** 56-69.

CURTI, A., PANDOLFI, S., VALZASINA, B., ALUIGI, M., ISIDORI, A., FERRI, E., SALVESTRINI, V., BONANNO, G., RUTELLA, S., DURELLI, I., HORENSTEIN, A. L., FIORE, F., MASSAIA, M., COLOMBO, M. P., BACCARANI, M. & LEMOLI, R. M. 2007. Modulation of tryptophan catabolism by human leukemic cells results in the conversion of CD25- into CD25+ T regulatory cells. *Blood,* 109**,** 2871-7.

CURTIS, M., KENNY, H. A., ASHCROFT, B., MUKHERJEE, A., JOHNSON, A., ZHANG, Y., HELOU, Y., BATLLE, R., LIU, X., GUTIERREZ, N., GAO, X., YAMADA, S. D., LASTRA, R., MONTAG, A., AHSAN, N., LOCASALE, J. W., SALOMON, A. R., NEBREDA, A. R. & LENGYEL, E. 2019. Fibroblasts Mobilize Tumor Cell Glycogen to Promote Proliferation and Metastasis. *Cell Metab,* 29**,** 141-155 e9.

DAMA, P., TANG, M., FULTON, N., KLINE, J. & LIU, H. 2019. Gal9/Tim-3 expression level is higher in AML patients who fail chemotherapy. *J Immunother Cancer,* 7**,** 175.

DAMASIO, M. P., MARCHINGO, J. M., SPINELLI, L., HUKELMANN, J. L., CANTRELL, D. A. & HOWDEN, A. J. M. 2021. Extracellular signal-regulated kinase (ERK) pathway control of CD8+ T cell differentiation. *Biochem J,* 478**,** 79-98.

DE KOUCHKOVSKY, I. & ABDUL-HAY, M. 2016. 'Acute myeloid leukemia: a comprehensive review and 2016 update'. *Blood Cancer J,* 6**,** e441.

DE SANTO, C., BOOTH, S., VARDON, A., COUSINS, A., TUBB, V., PERRY, T., NOYVERT, B., BEGGS, A., NG, M., HALSEY, C., KEARNS, P., CHENG, P. & MUSSAI, F. 2018. The arginine metabolome in acute lymphoblastic leukemia can be targeted by the pegylated-recombinant arginase I BCT-100. *Int J Cancer,* 142**,** 1490-1502.

DEL BUFALO, F., DE ANGELIS, B., CARUANA, I., DEL BALDO, G., DE IORIS, M. A., SERRA, A., MASTRONUZZI, A., CEFALO, M. G., PAGLIARA, D., AMICUCCI, M., LI PIRA, G., LEONE, G., BERTAINA, V., SINIBALDI, M., DI CECCA, S., GUERCIO, M., ABBASZADEH, Z., IAFFALDANO, L., GUNETTI, M., IACOVELLI, S., BUGIANESI, R., MACCHIA, S., ALGERI, M., MERLI, P., GALAVERNA, F., ABBAS, R., GARGANESE, M. C., VILLANI, M. F., COLAFATI, G. S., BONETTI, F., RABUSIN, M., PERRUCCIO, K., FOLSI, V., QUINTARELLI, C., LOCATELLI, F. & PRECISION MEDICINE TEAM, I. O. P. B. G. 2023. GD2-CART01 for Relapsed or Refractory High-Risk Neuroblastoma. *N Engl J Med,* 388**,** 1284-1295.

DENG, Q., HAN, G., PUEBLA-OSORIO, N., MA, M. C. J., STRATI, P., CHASEN, B., DAI, E., DANG, M., JAIN, N., YANG, H., WANG, Y., ZHANG, S., WANG, R., CHEN, R., SHOWELL, J., GHOSH, S., PATCHVA, S., ZHANG, Q., SUN, R., HAGEMEISTER, F., FAYAD, L., SAMANIEGO, F., LEE, H. C., NASTOUPIL, L. J., FOWLER, N., ERIC DAVIS, R., WESTIN, J., NEELAPU, S. S., WANG, L. & GREEN, M. R. 2020. Characteristics of anti-CD19 CAR T cell infusion products associated with efficacy and toxicity in patients with large B cell lymphomas. *Nat Med,* 26**,** 1878-1887.

DENNEY, H., CLENCH, M. R. & WOODROOFE, M. N. 2009. Cleavage of chemokines CCL2 and CXCL10 by matrix metalloproteinases-2 and -9: implications for chemotaxis. *Biochem Biophys Res Commun,* 382**,** 341-7.

DESCHLER, B. & LUBBERT, M. 2006. Acute myeloid leukemia: epidemiology and etiology. *Cancer,* 107**,** 2099-107.

DI STASI, A., TEY, S. K., DOTTI, G., FUJITA, Y., KENNEDY-NASSER, A., MARTINEZ, C., STRAATHOF, K., LIU, E., DURETT, A. G., GRILLEY, B., LIU, H., CRUZ, C. R., SAVOLDO, B., GEE, A. P., SCHINDLER, J., KRANCE, R. A., HESLOP, H. E., SPENCER, D. M., ROONEY, C. M. & BRENNER, M. K. 2011. Inducible apoptosis as a safety switch for adoptive cell therapy. *N Engl J Med,* 365**,** 1673-83.

DIAZ-BEYA, M., LABOPIN, M., MAERTENS, J., ALJURF, M., PASSWEG, J., DIETRICH, B., SCHOUTEN, H., SOCIE, G., SCHAAP, N., SCHWERDTFEGER, R., VOLIN, L., MICHALLET, M., POLGE, E., SIERRA, J., MOHTY, M., ESTEVE, J., NAGLER, A., ACUTE LEUKAEMIA WORKING PARTY OF THE EUROPEAN SOCIETY FOR, B. & MARROW, T. 2020. Allogeneic stem cell transplantation in AML with t(6;9)(p23;q34);DEK-NUP214 shows a favourable outcome when performed in first complete remission. *Br J Haematol,* 189**,** 920-925.

DIAZ DE LA GUARDIA, R., LOPEZ-MILLAN, B., LAVOIE, J. R., BUENO, C., CASTANO, J., GOMEZ-CASARES, M., VIVES, S., PALOMO, L., JUAN, M., DELGADO, J., BLANCO, M. L., NOMDEDEU, J., CHAPARRO, A., FUSTER, J. L., ANGUITA, E., ROSU-MYLES, M. & MENENDEZ, P. 2017. Detailed Characterization of Mesenchymal Stem/Stromal Cells from a Large Cohort of AML Patients Demonstrates a Definitive Link to Treatment Outcomes. *Stem Cell Reports,* 8**,** 1573-1586.

DIMELOE, S., BURGENER, A. V., GRAHLERT, J. & HESS, C. 2017. T-cell metabolism governing activation, proliferation and differentiation; a modular view. *Immunology,* 150**,** 35-44.

DOAN, A. E., MUELLER, K. P., CHEN, A. Y., ROUIN, G. T., CHEN, Y., DANIEL, B., LATTIN, J., MARKOVSKA, M., MOZARSKY, B., ARIAS-UMANA, J., HAPKE, R., JUNG, I. Y., WANG, A., XU, P., KLYSZ, D., ZUERN, G., BASHTI, M., QUINN, P. J., MIAO, Z., SANDOR, K., ZHANG, W., CHEN, G. M., RYU, F., LOGUN, M., HALL, J., TAN, K., GRUPP, S. A., MCCLORY, S. E., LAREAU, C. A., FRAIETTA, J. A., SOTILLO, E., SATPATHY, A. T., MACKALL, C. L. & WEBER, E. W. 2024. FOXO1 is a master regulator of memory programming in CAR T cells. *Nature,* 629**,** 211-218.

DOLGALEV, I. & TIKHONOVA, A. N. 2021. Connecting the Dots: Resolving the Bone Marrow Niche Heterogeneity. *Front Cell Dev Biol,* 9**,** 622519.

DOMBRET, H. & GARDIN, C. 2016. An update of current treatments for adult acute myeloid leukemia. *Blood,* 127**,** 53-61.

DONG, Y., HAN, Y., HUANG, Y., JIANG, S., HUANG, Z., CHEN, R., YU, Z., YU, K. & ZHANG, S. 2020a. PD-L1 Is Expressed and Promotes the Expansion of Regulatory T Cells in Acute Myeloid Leukemia. *Front Immunol,* 11**,** 1710.

DONG, Y., SHI, O., ZENG, Q., LU, X., WANG, W., LI, Y. & WANG, Q. 2020b. Leukemia incidence trends at the global, regional, and national level between 1990 and 2017. *Exp Hematol Oncol,* 9**,** 14.

DU, L., NAI, Y., SHEN, M., LI, T., HUANG, J., HAN, X., WANG, W., PANG, D. & JIN, A. 2021. IL-21 Optimizes the CAR-T Cell Preparation Through Improving Lentivirus Mediated Transfection Efficiency of T Cells and Enhancing CAR-T Cell Cytotoxic Activities. *Front Mol Biosci,* 8**,** 675179.

DUNN, G. P., OLD, L. J. & SCHREIBER, R. D. 2004. The three Es of cancer immunoediting. *Annu Rev Immunol,* 22**,** 329-60.

EDINGER, A. L. & THOMPSON, C. B. 2002. Antigen-presenting cells control T cell proliferation by regulating amino acid availability. *Proc Natl Acad Sci U S A,* 99**,** 1107-9.

EHNINGER, A., KRAMER, M., ROLLIG, C., THIEDE, C., BORNHAUSER, M., VON BONIN, M., WERMKE, M., FELDMANN, A., BACHMANN, M., EHNINGER, G. & OELSCHLAGEL, U. 2014. Distribution and levels of cell surface expression of CD33 and CD123 in acute myeloid leukemia. *Blood Cancer J,* 4**,** e218.

EMADI, A., DUONG, V. H., PANTIN, J., IMRAN, M., KOKA, R., SINGH, Z., SAUSVILLE, E. A., LAW, J. Y., LEE, S. T., SHI, H., KOLHE, R., BAER, M. R., LOKEN, M. R., KENNEDY, E. P., LINK, C. & MUNN, D. H. 2018a. Indoximod Combined with Standard Induction Chemotherapy

Is Well Tolerated and Induces a High Rate of Complete

Remission with MRD-Negativity in Patients with

Newly Diagnosed AML: Results from a Phase 1 Trial. *Blood,* 132**,** 332.

EMADI, A., LAW, J. Y., STROVEL, E. T., LAPIDUS, R. G., JENG, L. J. B., LEE, M., BLITZER, M. G., CARTER-COOPER, B. A., SEWELL, D., VAN DER MERWE, I., PHILIP, S., IMRAN, M., YU, S. L., LI, H., AMREIN, P. C., DUONG, V. H., SAUSVILLE, E. A., BAER, M. R., FATHI, A. T., SINGH, Z. & BENTZEN, S. M. 2018b. Asparaginase Erwinia chrysanthemi effectively depletes plasma glutamine in adult patients with relapsed/refractory acute myeloid leukemia. *Cancer Chemother Pharmacol,* 81**,** 217-222.

ESTEY, E., HASSERJIAN, R. P. & DOHNER, H. 2022. Distinguishing AML from MDS: a fixed blast percentage may no longer be optimal. *Blood,* 139**,** 323-332.

FALLARINO, F., GROHMANN, U., VACCA, C., BIANCHI, R., ORABONA, C., SPRECA, A., FIORETTI, M. C. & PUCCETTI, P. 2002. T cell apoptosis by tryptophan catabolism. *Cell Death Differ,* 9**,** 1069-77.

FENWICK, N., WESTON, R., WHEATLEY, K., HODGSON, J., MARSHALL, L., ELLIOTT, M., MAKIN, G., NG, A., BRENNAN, B., LOWIS, S., ADAMSKI, J., KILDAY, J. P., COX, R., GATTENS, M., MOORE, A., TRAHAIR, T., RONGHE, M., CAMPBELL, M., CAMPBELL, H., WILLIAMS, M. W., KIRBY, M., VAN EIJKELENBURG, N., KEELY, J., SCARPA, U., STAVROU, V., FULTANG, L., BOOTH, S., CHENG, P., DE SANTO, C. & MUSSAI, F. 2024. PARC: a phase I/II study evaluating the safety and activity of pegylated recombinant human arginase BCT-100 in relapsed/refractory cancers of children and young adults. *Front Oncol,* 14**,** 1296576.

FINNEY, O. C., BRAKKE, H. M., RAWLINGS-RHEA, S., HICKS, R., DOOLITTLE, D., LOPEZ, M., FUTRELL, R. B., ORENTAS, R. J., LI, D., GARDNER, R. A. & JENSEN, M. C. 2019. CD19 CAR T cell product and disease attributes predict leukemia remission durability. *J Clin Invest,* 129**,** 2123-2132.

FOLGER, O., JERBY, L., FREZZA, C., GOTTLIEB, E., RUPPIN, E. & SHLOMI, T. 2011. Predicting selective drug targets in cancer through metabolic networks. *Mol Syst Biol,* 7**,** 501.

FREEMAN, G. J., LONG, A. J., IWAI, Y., BOURQUE, K., CHERNOVA, T., NISHIMURA, H., FITZ, L. J., MALENKOVICH, N., OKAZAKI, T., BYRNE, M. C., HORTON, H. F., FOUSER, L., CARTER, L., LING, V., BOWMAN, M. R., CARRENO, B. M., COLLINS, M., WOOD, C. R. & HONJO, T. 2000. Engagement of the PD-1 immunoinhibitory receptor by a novel B7 family member leads to negative regulation of lymphocyte activation. *J Exp Med,* 192**,** 1027-34.

FRITAH, H., ROVELLI, R., CHIANG, C. L. & KANDALAFT, L. E. 2022. The current clinical landscape of personalized cancer vaccines. *Cancer Treat Rev,* 106**,** 102383.

FROBEL, J., LANDSPERSKY, T., PERCIN, G., SCHRECK, C., RAHMIG, S., ORI, A., NOWAK, D., ESSERS, M., WASKOW, C. & OOSTENDORP, R. A. J. 2021. The Hematopoietic Bone Marrow Niche Ecosystem. *Front Cell Dev Biol,* 9**,** 705410.

FU, H., VUONONVIRTA, J., FANTI, S., BONACINA, F., D'AMATI, A., WANG, G., POOBALASINGAM, T., FANKHAENEL, M., LUCCHESI, D., COLEBY, R., TARUSSIO, D., THORENS, B., HEARNDEN, R. J., LONGHI, M. P., GREVITT, P., SHEIKH, M. H., SOLITO, E., GODINHO, S. A., BOMBARDIERI, M., SMITH, D. M., COOPER, D., IQBAL, A. J., RATHMELL, J. C., SCHAEFER, S., MORALES, V., BIANCHI, K., NORATA, G. D. & MARELLI-BERG, F. M. 2023. The glucose transporter 2 regulates CD8(+) T cell function via environment sensing. *Nat Metab,* 5**,** 1969-1985.

FUERTES MARRACO, S. A., SONESON, C., CAGNON, L., GANNON, P. O., ALLARD, M., ABED MAILLARD, S., MONTANDON, N., RUFER, N., WALDVOGEL, S., DELORENZI, M. & SPEISER, D. E. 2015. Long-lasting stem cell-like memory CD8+ T cells with a naive-like profile upon yellow fever vaccination. *Sci Transl Med,* 7**,** 282ra48.

FUJIKI, F., MORIMOTO, S., KATSUHARA, A., OKUDA, A., OGAWA, S., UEDA, E., MIYAZAKI, M., ISOTANI, A., IKAWA, M., NISHIDA, S., NAKAJIMA, H., TSUBOI, A., OKA, Y., NAKATA, J., HOSEN, N., KUMANOGOH, A., OJI, Y. & SUGIYAMA, H. 2022. T Cell-Intrinsic Vitamin A Metabolism and Its Signaling Are Targets for Memory T Cell-Based Cancer Immunotherapy. *Front Immunol,* 13**,** 935465.

FULTANG, L., GNEO, L., DE SANTO, C. & MUSSAI, F. J. 2021. Targeting Amino Acid Metabolic Vulnerabilities in Myeloid Malignancies. *Front Oncol,* 11**,** 674720.

FULTANG, L., PANETTI, S., NG, M., COLLINS, P., GRAEF, S., RIZKALLA, N., BOOTH, S., LENTON, R., NOYVERT, B., SHANNON-LOWE, C., MIDDLETON, G., MUSSAI, F. & DE SANTO, C. 2019. MDSC targeting with Gemtuzumab ozogamicin restores T cell immunity and immunotherapy against cancers. *EBioMedicine,* 47**,** 235-246.

FYFE, G., FISHER, R. I., ROSENBERG, S. A., SZNOL, M., PARKINSON, D. R. & LOUIE, A. C. 1995. Results of treatment of 255 patients with metastatic renal cell carcinoma who received high-dose recombinant interleukin-2 therapy. *J Clin Oncol,* 13**,** 688-96.

GABELLI, M., OPORTO-ESPUELAS, M., BURRIDGE, S., CHU, J., FARISH, S., HEDGES, E., WARE, K., WILLIAMS, L., YOUNG, L., ALAJANGI, R., ANCLIFF, P., BARTRAM, J., BONNEY, D., CHENCHARA, L., CHIESA, R., CUGNO, C., HODBY, K., JALOWIEC, K. A., LAZAREVA, A., LUCCHINI, G., MIRCI-DANICAR, O. C., MULLANFIROZE, K., PAVASOVIC, V., RAO, A., RAO, K., RILEY, L., SAMARASINGHE, S., SHENTON, G., SILVA, J., VORA, A., HOUGH, R., AMROLIA, P. J. & GHORASHIAN, S. 2024. Maintenance therapy for early loss of B-cell aplasia after anti-CD19 CAR T-cell therapy. *Blood Adv,* 8**,** 1959-1963.

GAO, N., YU, W. Z., GUO, N. J., WANG, X. X. & SUN, J. R. 2017. Clinical significance of galectin-3 in patients with adult acute myeloid leukemia: a retrospective cohort study with long-term follow-up and formulation of risk scoring system. *Leuk Lymphoma,* 58**,** 1394-1402.

GARG, A., GANGULY, S., VISHNUBHATLA, S., CHOPRA, A. & BAKHSHI, S. 2020. Outpatient ADE (cytarabine, daunorubicin, and etoposide) is feasible and effective for the first relapse of pediatric acute myeloid leukemia: A prospective, phase II study. *Pediatr Blood Cancer,* 67**,** e28404.

GARG, S. K., YAN, Z., VITVITSKY, V. & BANERJEE, R. 2011. Differential dependence on cysteine from transsulfuration versus transport during T cell activation. *Antioxid Redox Signal,* 15**,** 39-47.

GEIGER, R., RIECKMANN, J. C., WOLF, T., BASSO, C., FENG, Y., FUHRER, T., KOGADEEVA, M., PICOTTI, P., MEISSNER, F., MANN, M., ZAMBONI, N., SALLUSTO, F. & LANZAVECCHIA, A. 2016. L-Arginine Modulates T Cell Metabolism and Enhances Survival and Anti-tumor Activity. *Cell,* 167**,** 829-842 e13.

GHASSEMI, S., DURGIN, J. S., NUNEZ-CRUZ, S., PATEL, J., LEFEROVICH, J., PINZONE, M., SHEN, F., CUMMINS, K. D., PLESA, G., CANTU, V. A., REDDY, S., BUSHMAN, F. D., GILL, S. I., O'DOHERTY, U., O'CONNOR, R. S. & MILONE, M. C. 2022. Rapid manufacturing of non-activated potent CAR T cells. *Nat Biomed Eng,* 6**,** 118-128.

GHASSEMI, S., MARTINEZ-BECERRA, F. J., MASTER, A. M., RICHMAN, S. A., HEO, D., LEFEROVICH, J., TU, Y., GARCIA-CANAVERAS, J. C., AYARI, A., LU, Y., WANG, A., RABINOWITZ, J. D., MILONE, M. C., JUNE, C. H. & O'CONNOR, R. S. 2020. Enhancing Chimeric Antigen Receptor T Cell Anti-tumor Function through Advanced Media Design. *Mol Ther Methods Clin Dev,* 18**,** 595-606.

GHASSEMI, S., NUNEZ-CRUZ, S., O'CONNOR, R. S., FRAIETTA, J. A., PATEL, P. R., SCHOLLER, J., BARRETT, D. M., LUNDH, S. M., DAVIS, M. M., BEDOYA, F., ZHANG, C., LEFEROVICH, J., LACEY, S. F., LEVINE, B. L., GRUPP, S. A., JUNE, C. H., MELENHORST, J. J. & MILONE, M. C. 2018. Reducing Ex Vivo Culture Improves the Antileukemic Activity of Chimeric Antigen Receptor (CAR) T Cells. *Cancer Immunol Res,* 6**,** 1100-1109.

GOLUBOVSKAYA, V. & WU, L. 2016. Different Subsets of T Cells, Memory, Effector Functions, and CAR-T Immunotherapy. *Cancers (Basel),* 8.

GONCALVES SILVA, I., YASINSKA, I. M., SAKHNEVYCH, S. S., FIEDLER, W., WELLBROCK, J., BARDELLI, M., VARANI, L., HUSSAIN, R., SILIGARDI, G., CECCONE, G., BERGER, S. M.,

USHKARYOV, Y. A., GIBBS, B. F., FASLER-KAN, E. & SUMBAYEV, V. V. 2017. The Tim-3-galectin-9 Secretory Pathway is Involved in the Immune Escape of Human Acute Myeloid Leukemia Cells. *EBioMedicine,* 22**,** 44-57.

GREEN, A. M., DIFAZIO, R. & FLYNN, J. L. 2013. IFN-gamma from CD4 T cells is essential for host survival and enhances CD8 T cell function during Mycobacterium tuberculosis infection. *J Immunol,* 190**,** 270-7.

GREGORY, M. A., NEMKOV, T., PARK, H. J., ZABEREZHNYY, V., GEHRKE, S., ADANE, B., JORDAN, C. T., HANSEN, K. C., D'ALESSANDRO, A. & DEGREGORI, J. 2019. Targeting Glutamine Metabolism and Redox State for Leukemia Therapy. *Clin Cancer Res,* 25**,** 4079-4090.

GROB, T., AL HINAI, A. S. A., SANDERS, M. A., KAVELAARS, F. G., RIJKEN, M., GRADOWSKA, P. L., BIEMOND, B. J., BREEMS, D. A., MAERTENS, J., VAN MARWIJK KOOY, M., PABST, T., DE WEERDT, O., OSSENKOPPELE, G. J., VAN DE LOOSDRECHT, A. A., HULS, G. A., CORNELISSEN, J. J., BEVERLOO, H. B., LOWENBERG, B., JONGEN-LAVRENCIC, M. & VALK, P. J. M. 2022. Molecular characterization of mutant TP53 acute myeloid leukemia and high-risk myelodysplastic syndrome. *Blood,* 139**,** 2347-2354.

GROSS, G., WAKS, T. & ESHHAR, Z. 1989. Expression of immunoglobulin-T-cell receptor chimeric molecules as functional receptors with antibody-type specificity. *Proc Natl Acad Sci U S A,* 86**,** 10024-8.

GULER, A., LOPEZ VENEGAS, M., ADANKWAH, E., MAYATEPEK, E., NAUSCH, N. & JACOBSEN, M. 2020. Suppressor of cytokine signalling 3 is crucial for interleukin-7 receptor re-expression after T-cell activation and interleukin-7 dependent proliferation. *Eur J Immunol,* 50**,** 234-244.

GUMBER, D. & WANG, L. D. 2022. Improving CAR-T immunotherapy: Overcoming the challenges of T cell exhaustion. *EBioMedicine,* 77**,** 103941.

GWANGWA, M. V., JOUBERT, A. M. & VISAGIE, M. H. 2019. Effects of glutamine deprivation on oxidative stress and cell survival in breast cell lines. *Biol Res,* 52**,** 15.

HAFLIGER, P., GRAFF, J., RUBIN, M., STOOSS, A., DETTMER, M. S., ALTMANN, K. H., GERTSCH, J. & CHARLES, R. P. 2018. The LAT1 inhibitor JPH203 reduces growth of thyroid carcinoma in a fully immunocompetent mouse model. *J Exp Clin Cancer Res,* 37**,** 234.

HALL, M. S., MULLINAX, J. E., COX, C. A., HALL, A. M., BEATTY, M. S., BLAUVELT, J., INNAMARATO, P., NAGLE, L., BRANTHOOVER, H., WIENER, D., SCHACHNER, B., MARTINEZ, A. J., RICHARDS, A. D., RICH, C. J., COLON COLON, M., SCHELL, M. J., TEER, J. K., KHUSHALANI, N. I., WEBER, J. S., MULE, J. J., SONDAK, V. K., PILON-THOMAS, S. & SARNAIK, A. A. 2022. Combination Nivolumab, CD137 Agonism, and Adoptive Cell Therapy with Tumor-Infiltrating Lymphocytes for Patients with Metastatic Melanoma. *Clin Cancer Res,* 28**,** 5317-5329.

HAN, C., GE, M., XING, P., XIA, T., ZHANG, C., MA, K., MA, Y., LI, S., LI, W., LIU, X., ZHANG, B., ZHANG, L. & ZHANG, L. 2024. Cystine deprivation triggers CD36-mediated ferroptosis and dysfunction of tumor infiltrating CD8(+) T cells. *Cell Death Dis,* 15**,** 145.

HAN, W., CHEN, S., YUAN, W., FAN, Q., TIAN, J., WANG, X., CHEN, L., ZHANG, X., WEI, W., LIU, R., QU, J., JIAO, Y., AUSTIN, R. H. & LIU, L. 2016. Oriented collagen fibers direct tumor cell intravasation. *Proc Natl Acad Sci U S A,* 113**,** 11208-11213.

HAN, X., WANG, Y., WEI, J. & HAN, W. 2019. Multi-antigen-targeted chimeric antigen receptor T cells for cancer therapy. *J Hematol Oncol,* 12**,** 128.

HAN, Y., DONG, Y., YANG, Q., XU, W., JIANG, S., YU, Z., YU, K. & ZHANG, S. 2018. Acute Myeloid Leukemia Cells Express ICOS Ligand to Promote the Expansion of Regulatory T Cells. *Front Immunol,* 9**,** 2227.

HANAHAN, D. & WEINBERG, R. A. 2000. The hallmarks of cancer. *Cell,* 100**,** 57-70.

HANAHAN, D. & WEINBERG, R. A. 2011. Hallmarks of cancer: the next generation. *Cell,* 144**,** 646-74.

HARA, T., MATSUMOTO, T., SHIBATA, Y., NAKAMURA, N., NAKAMURA, H., NINOMIYA, S., KITAGAWA, J., NANNYA, Y., SHIMIZU, M., ITO, H., SAITO, K. & TSURUMI, H. 2016. Prognostic value of the combination of serum l-kynurenine level and indoleamine 2,3-dioxygenase mRNA expression in acute myeloid leukemia. *Leuk Lymphoma,* 57**,** 2208-11.

HARRIS, I. S., TRELOAR, A. E., INOUE, S., SASAKI, M., GORRINI, C., LEE, K. C., YUNG, K. Y., BRENNER, D., KNOBBE-THOMSEN, C. B., COX, M. A., ELIA, A., BERGER, T., CESCON, D. W., ADEOYE, A., BRUSTLE, A., MOLYNEUX, S. D., MASON, J. M., LI, W. Y., YAMAMOTO, K., WAKEHAM, A., BERMAN, H. K., KHOKHA, R., DONE, S. J., KAVANAGH, T. J., LAM, C. W. & MAK, T. W. 2015. Glutathione and thioredoxin antioxidant pathways synergize to drive cancer initiation and progression. *Cancer Cell,* 27**,** 211-22.

HASAN, M. M., RAGNARSSON, L., CARDOSO, F. C. & LEWIS, R. J. 2021. Transfection methods for high-throughput cellular assays of voltage-gated calcium and sodium channels involved in pain. *PLoS One,* 16**,** e0243645.

HAWKINS, E. R., D'SOUZA, R. R. & KLAMPATSA, A. 2021. Armored CAR T-Cells: The Next Chapter in T-Cell Cancer Immunotherapy. *Biologics,* 15**,** 95-105.

HAYASHI, K., JUTABHA, P., ENDOU, H., SAGARA, H. & ANZAI, N. 2013. LAT1 is a critical transporter of essential amino acids for immune reactions in activated human T cells. *J Immunol,* 191**,** 4080-5.

HE, Y., PEI, J. H., LI, X. Q. & CHI, G. 2021. IL-35 promotes EMT through STAT3 activation and induces MET by promoting M2 macrophage polarization in HCC. *Biochem Biophys Res Commun,* 559**,** 35-41.

HEIL, J., OLSAVSZKY, V., BUSCH, K., KLAPPROTH, K., DE LA TORRE, C., STICHT, C., SANDORSKI, K., HOFFMANN, J., SCHONHABER, H., ZIEROW, J., WINKLER, M., SCHMID, C. D., STANICZEK, T., DANIELS, D. E., FRAYNE, J., METZGEROTH, G., NOWAK, D., SCHNEIDER, S., NEUMAIER, M., WEYER, V., GRODEN, C., GRONE, H. J., RICHTER, K., MOGLER, C., TAKETO, M. M., SCHLEDZEWSKI, K., GERAUD, C., GOERDT, S. & KOCH, P. S. 2021. Bone marrow sinusoidal endothelium controls terminal erythroid differentiation and reticulocyte maturation. *Nat Commun,* 12**,** 6963.

HERNDON, T. M., DEMKO, S. G., JIANG, X., HE, K., GOOTENBERG, J. E., COHEN, M. H., KEEGAN, P. & PAZDUR, R. 2012. U.S. Food and Drug Administration Approval: peginterferon-alfa-2b for the adjuvant treatment of patients with melanoma. *Oncologist,* 17**,** 1323-8.

HEROLD, T., ROTHENBERG-THURLEY, M., GRUNWALD, V. V., JANKE, H., GOERLICH, D., SAUERLAND, M. C., KONSTANDIN, N. P., DUFOUR, A., SCHNEIDER, S., NEUSSER, M., KSIENZYK, B., GREIF, P. A., SUBKLEWE, M., FALDUM, A., BOHLANDER, S. K., BRAESS, J., WORMANN, B., KRUG, U., BERDEL, W. E., HIDDEMANN, W., SPIEKERMANN, K. & METZELER, K. H. 2020. Validation and refinement of the revised 2017 European LeukemiaNet genetic risk stratification of acute myeloid leukemia. *Leukemia,* 34**,** 3161-3172.

HIGUCHI, K., SAKAMOTO, S., ANDO, K., MAIMAITI, M., TAKESHITA, N., OKUNUSHI, K., REIEN, Y., IMAMURA, Y., SAZUKA, T., NAKAMURA, K., MATSUSHIMA, J., FURIHATA, T., IKEHARA, Y., ICHIKAWA, T. & ANZAI, N. 2019. Characterization of the expression of LAT1 as a prognostic indicator and a therapeutic target in renal cell carcinoma. *Sci Rep,* 9**,** 16776.

HINO, C., PHAM, B., PARK, D., YANG, C., NGUYEN, M. H. K., KAUR, S., REEVES, M. E., XU, Y., NISHINO, K., PU, L., KWON, S. M., ZHONG, J. F., ZHANG, K. K., XIE, L., CHONG, E. G., CHEN, C. S., NGUYEN, V., CASTILLO, D. R. & CAO, H. 2022. Targeting the Tumor Microenvironment in Acute Myeloid Leukemia: The Future of Immunotherapy and Natural Products. *Biomedicines,* 10.

HOLLINGSWORTH, R. E. & JANSEN, K. 2019. Turning the corner on therapeutic cancer vaccines. *NPJ Vaccines,* 4**,** 7.

HOLTHAUS, L., SHARMA, V., BRANDT, D., ZIEGLER, A. G., JASTROCH, M. & BONIFACIO, E. 2021. Functional and metabolic fitness of human CD4(+) T lymphocytes during metabolic stress. *Life Sci Alliance,* 4.

HU, Y., ZHANG, M., YANG, T., MO, Z., WEI, G., JING, R., ZHAO, H., CHEN, R., ZU, C., GU, T., XIAO, P., HONG, R., FENG, J., FU, S., KONG, D., XU, H., CUI, J., HUANG, S., LIANG, B., YUAN, X., CUI, Q., GUO, H., YU, Y., FENG, Y., JIN, C., REN, J., CHANG, A. H., WANG, D. & HUANG, H. 2024. Sequential CD7 CAR T-Cell Therapy and Allogeneic HSCT without GVHD Prophylaxis. *N Engl J Med,* 390**,** 1467-1480.

HUANG, C., LI, N., LI, Z., CHANG, A., CHEN, Y., ZHAO, T., LI, Y., WANG, X., ZHANG, W., WANG, Z., LUO, L., SHI, J., YANG, S., REN, H. & HAO, J. 2017. Tumour-derived Interleukin 35 promotes pancreatic ductal adenocarcinoma cell extravasation and metastasis by inducing ICAM1 expression. *Nat Commun,* 8**,** 14035.

HUANG, R., WEN, Q. & ZHANG, X. 2023. CAR-NK cell therapy for hematological malignancies: recent updates from ASH 2022. *J Hematol Oncol,* 16**,** 35.

HUBER, S., BAER, C., HUTTER, S., DICKER, F., MEGGENDORFER, M., POHLKAMP, C., KERN, W., HAFERLACH, T., HAFERLACH, C. & HOERMANN, G. 2023. AML classification in the year 2023: How to avoid a Babylonian confusion of languages. *Leukemia,* 37**,** 1413-1420.

HUO, J. L., WANG, Y. T., FU, W. J., LU, N. & LIU, Z. S. 2022. The promising immune checkpoint LAG-3 in cancer immunotherapy: from basic research to clinical application. *Front Immunol,* 13**,** 956090.

HUPPA, J. B. & DAVIS, M. M. 2003. T-cell-antigen recognition and the immunological synapse. *Nat Rev Immunol,* 3**,** 973-83.

INABA, K., INABA, M., ROMANI, N., AYA, H., DEGUCHI, M., IKEHARA, S., MURAMATSU, S. & STEINMAN, R. M. 1992. Generation of large numbers of dendritic cells from mouse bone marrow cultures supplemented with granulocyte/macrophage colony-stimulating factor. *J Exp Med,* 176**,** 1693-702.

IWASAKI, A. & MEDZHITOV, R. 2015. Control of adaptive immunity by the innate immune system. *Nat Immunol,* 16**,** 343-53.

JAIN, A. G., BALL, S., AGUIRRE, L., AL ALI, N., KALDAS, D., TINSLEY-VANCE, S., KUYKENDALL, A., CHAN, O., SWEET, K., LANCET, J. E., PADRON, E., SALLMAN, D. A. & KOMROKJI, R. 2024. Patterns of lower risk myelodysplastic syndrome progression: factors predicting progression to high-risk myelodysplastic syndrome and acute myeloid leukemia. *Haematologica,* 109**,** 2157-2164.

JAIN, M. D., SMITH, M. & SHAH, N. N. 2023. How I treat refractory CRS and ICANS after CAR T-cell therapy. *Blood,* 141**,** 2430-2442.

JAN, M., LEVENTHAL, M. J., MORGAN, E. A., WENGROD, J. C., NAG, A., DRINAN, S. D., WOLLISON, B. M., DUCAR, M. D., THORNER, A. R., LEPPANEN, S., BARONAS, J., STEVENS, J., LANE, W. J., KEKRE, N., HO, V. T., KORETH, J., CUTLER, C. S., NIKIFOROW, S., ALYEA, E. P., 3RD, ANTIN, J. H., SOIFFER, R. J., RITZ, J., LINDSLEY, R. C. & EBERT, B. L. 2019. Recurrent genetic HLA loss in AML relapsed after matched unrelated allogeneic hematopoietic cell transplantation. *Blood Adv,* 3**,** 2199-2204.

JARNICKI, A. G., LYSAGHT, J., TODRYK, S. & MILLS, K. H. 2006. Suppression of antitumor immunity by IL-10 and TGF-beta-producing T cells infiltrating the growing tumor: influence of tumor environment on the induction of CD4+ and CD8+ regulatory T cells. *J Immunol,* 177**,** 896-904.

JECKELMANN, J. M. & FOTIADIS, D. 2019. Volta Phase Plate Cryo-EM Structure of the Human Heterodimeric Amino Acid Transporter 4F2hc-LAT2. *Int J Mol Sci,* 20.

JIANG, N., HUANG, J., EDWARDS, L. J., LIU, B., ZHANG, Y., BEAL, C. D., EVAVOLD, B. D. & ZHU, C. 2011. Two-stage cooperative T cell receptor-peptide major histocompatibility complex-CD8 trimolecular interactions amplify antigen discrimination. *Immunity,* 34**,** 13-23.

JONES, C. L., STEVENS, B. M., D'ALESSANDRO, A., CULP-HILL, R., REISZ, J. A., PEI, S., GUSTAFSON, A., KHAN, N., DEGREGORI, J., POLLYEA, D. A. & JORDAN, C. T. 2019. Cysteine depletion targets leukemia stem cells through inhibition of electron transport complex II. *Blood,* 134**,** 389-394.

JONES, D. S., 2ND, NARDOZZI, J. D., SACKTON, K. L., AHMAD, G., CHRISTENSEN, E., RINGGAARD, L., CHANG, D. K., JAEHGER, D. E., KONAKONDLA, J. V., WIINBERG, M., STOKES, K. L., PRATAMA, A., SAUER, K. & ANDRESEN, T. L. 2022. Cell surface-tethered IL-12 repolarizes the tumor immune microenvironment to enhance the efficacy of adoptive T cell therapy. *Sci Adv,* 8**,** eabi8075.

JULIER, Z., PARK, A. J., BRIQUEZ, P. S. & MARTINO, M. M. 2017. Promoting tissue regeneration by modulating the immune system. *Acta Biomater,* 53**,** 13-28.

KANG, T. G., PARK, H. J., MOON, J., LEE, J. H. & HA, S. J. 2021. Enriching CCL3 in the Tumor Microenvironment Facilitates T cell Responses and Improves the Efficacy of Anti-PD-1 Therapy. *Immune Netw,* 21**,** e23.

KAYSER, S., HILLS, R. K., LUSKIN, M. R., BRUNNER, A. M., TERRE, C., WESTERMANN, J., MENGHRAJANI, K., SHAW, C., BAER, M. R., ELLIOTT, M. A., PERL, A. E., RACIL, Z., MAYER, J., ZAK, P., SZOTKOWSKI, T., DE BOTTON, S., GRIMWADE, D., MAYER, K., WALTER, R. B., KRAMER, A., BURNETT, A. K., HO, A. D., PLATZBECKER, U., THIEDE, C., EHNINGER, G., STONE, R. M., ROLLIG, C., TALLMAN, M. S., ESTEY, E. H., MULLER-TIDOW, C., RUSSELL, N. H., SCHLENK, R. F. & LEVIS, M. J. 2020. Allogeneic hematopoietic cell transplantation improves outcome of adults with t(6;9) acute myeloid leukemia: results from an international collaborative study. *Haematologica,* 105**,** 161-169.

KEATING, G. M. 2013. Asparaginase Erwinia chrysanthemi (Erwinaze(R)): a guide to its use in acute lymphoblastic leukemia in the USA. *BioDrugs,* 27**,** 413-8.

KIERDORF, F., ZIMMER, P., JOISTEN, N., KIESL, D., WINKER, M., RIGOUX, L. & ELTER, T. 2022. L-kynurenine as a prognostic marker for early mortality in patients with acute myeloid leukemia. *Leuk Lymphoma,* 63**,** 2001-2004.

KIM, M. J. & HA, S. J. 2021. Differential Role of PD-1 Expressed by Various Immune and Tumor Cells in the Tumor Immune Microenvironment: Expression, Function, Therapeutic Efficacy, and Resistance to Cancer Immunotherapy. *Front Cell Dev Biol,* 9**,** 767466.

KLEIN, L., KYEWSKI, B., ALLEN, P. M. & HOGQUIST, K. A. 2014. Positive and negative selection of the T cell repertoire: what thymocytes see (and don't see). *Nat Rev Immunol,* 14**,** 377-91.

KOCHENDERFER, J. N., WILSON, W. H., JANIK, J. E., DUDLEY, M. E., STETLER-STEVENSON, M., FELDMAN, S. A., MARIC, I., RAFFELD, M., NATHAN, D. A., LANIER, B. J., MORGAN, R. A. & ROSENBERG, S. A. 2010. Eradication of B-lineage cells and regression of lymphoma in a patient treated with autologous T cells genetically engineered to recognize CD19. *Blood,* 116**,** 4099-102.

KOMROKJI, R. S., WEI, S., MAILLOUX, A. W., ZHANG, L., PADRON, E., SALLMAN, D., LANCET, J. E., TINSLEY, S., NARDELLI, L. A., PINILLA-IBARZ, J., EPLING-BURNETTE, P. K. & LIST, A. F. 2019. A Phase II Study to Determine the Safety and Efficacy of the Oral Inhibitor of Indoleamine 2,3-Dioxygenase (IDO) Enzyme INCB024360 in Patients with Myelodysplastic Syndromes. *Clin Lymphoma Myeloma Leuk,* 19**,** 157-161.

KONDOH, M., OHGA, N., AKIYAMA, K., HIDA, Y., MAISHI, N., TOWFIK, A. M., INOUE, N., SHINDOH, M. & HIDA, K. 2013. Hypoxia-induced reactive oxygen species cause chromosomal abnormalities in endothelial cells in the tumor microenvironment. *PLoS One,* 8**,** e80349.

KONG, Y., TANG, L., YOU, Y., LI, Q. & ZHU, X. 2023. Analysis of causes for poor persistence of CAR-T cell therapy in vivo. *Front Immunol,* 14**,** 1063454.

KONGPRACHA, P., NAGAMORI, S., WIRIYASERMKUL, P., TANAKA, Y., KANEDA, K., OKUDA, S., OHGAKI, R. & KANAI, Y. 2017. Structure-activity relationship of a novel series of inhibitors for cancer type transporter L-type amino acid transporter 1 (LAT1). *J Pharmacol Sci,* 133**,** 96-102.

KOOSHKAKI, O., DERAKHSHANI, A., HOSSEINKHANI, N., TORABI, M., SAFAEI, S., BRUNETTI, O., RACANELLI, V., SILVESTRIS, N. & BARADARAN, B. 2020. Combination of Ipilimumab and Nivolumab in Cancers: From Clinical Practice to Ongoing Clinical Trials. *Int J Mol Sci,* 21.

KOYAMA-NASU, R., WANG, Y., HASEGAWA, I., ENDO, Y., NAKAYAMA, T. & KIMURA, M. Y. 2022. The cellular and molecular basis of CD69 function in anti-tumor immunity. *Int Immunol,* 34**,** 555-561.

KRALL, A. S., MULLEN, P. J., SURJONO, F., MOMCILOVIC, M., SCHMID, E. W., HALBROOK, C. J., THAMBUNDIT, A., MITTELMAN, S. D., LYSSIOTIS, C. A., SHACKELFORD, D. B., KNOTT, S. R. V. & CHRISTOFK, H. R. 2021. Asparagine couples mitochondrial respiration to ATF4 activity and tumor growth. *Cell Metab,* 33**,** 1013-1026 e6.

KRALL, A. S., XU, S., GRAEBER, T. G., BRAAS, D. & CHRISTOFK, H. R. 2016. Asparagine promotes cancer cell proliferation through use as an amino acid exchange factor. *Nat Commun,* 7**,** 11457.

KRESLAVSKY, T., GLEIMER, M., MIYAZAKI, M., CHOI, Y., GAGNON, E., MURRE, C., SICINSKI, P. & VON BOEHMER, H. 2012. beta-Selection-induced proliferation is required for alphabeta T cell differentiation. *Immunity,* 37**,** 840-53.

KUCZEK, D. E., LARSEN, A. M. H., THORSETH, M. L., CARRETTA, M., KALVISA, A., SIERSBAEK, M. S., SIMOES, A. M. C., ROSLIND, A., ENGELHOLM, L. H., NOESSNER, E., DONIA, M.,

SVANE, I. M., STRATEN, P. T., GRONTVED, L. & MADSEN, D. H. 2019. Collagen density regulates the activity of tumor-infiltrating T cells. *J Immunother Cancer,* 7**,** 68.
KUEBERUWA, G., GORNALL, H., ALCANTAR-OROZCO, E. M., BOUVIER, D., KAPACEE, Z. A., HAWKINS, R. E. & GILHAM, D. E. 2017. CCR7(+) selected gene-modified T cells maintain a central memory phenotype and display enhanced persistence in peripheral blood in vivo. *J Immunother Cancer,* 5**,** 14.
KUMAR, B., GARCIA, M., WENG, L., JUNG, X., MURAKAMI, J. L., HU, X., MCDONALD, T., LIN, A., KUMAR, A. R., DIGIUSTO, D. L., STEIN, A. S., PULLARKAT, V. A., HUI, S. K., CARLESSO, N., KUO, Y. H., BHATIA, R., MARCUCCI, G. & CHEN, C. C. 2018. Acute myeloid leukemia transforms the bone marrow niche into a leukemia-permissive microenvironment through exosome secretion. *Leukemia,* 32**,** 575-587.
KUMAR, J., PATEL, S., CHANG, A., MUKHERJEE, S., SMALL, C., GOLLAPUDI, S., BUTZMANN, A., JANGAM, D., WEINBERG, O. K., GEORGE, T. I., ZEHNDER, J. L. & OHGAMI, R. S. 2023. Smoking status in acute myeloid leukemia is associated with worse overall survival and independent of prior nonhematopoietic malignancies, cytogenetic abnormalities, and WHO category. *Hum Pathol,* 135**,** 45-53.
KUMAR, V., ROSENZWEIG, R., ASALLA, S., NEHRA, S., PRABHU, S. D. & BANSAL, S. S. 2022. TNFR1 Contributes to Activation-Induced Cell Death of Pathological CD4(+) T Lymphocytes During Ischemic Heart Failure. *JACC Basic Transl Sci,* 7**,** 1038-1049.
KUWANA, Y., ASAKURA, Y., UTSUNOMIYA, N., NAKANISHI, M., ARATA, Y., ITOH, S., NAGASE, F. & KUROSAWA, Y. 1987. Expression of chimeric receptor composed of immunoglobulin-derived V regions and T-cell receptor-derived C regions. *Biochem Biophys Res Commun,* 149**,** 960-8.
LANCET, J. E., UY, G. L., NEWELL, L. F., LIN, T. L., RITCHIE, E. K., STUART, R. K., STRICKLAND, S. A., HOGGE, D., SOLOMON, S. R., BIXBY, D. L., KOLITZ, J. E., SCHILLER, G. J., WIEDUWILT, M. J., RYAN, D. H., FADERL, S. & CORTES, J. E. 2021. CPX-351 versus 7+3 cytarabine and daunorubicin chemotherapy in older adults with newly diagnosed high-risk or secondary acute myeloid leukaemia: 5-year results of a randomised, open-label, multicentre, phase 3 trial. *Lancet Haematol,* 8**,** e481-e491.
LEE, G. K., PARK, H. J., MACLEOD, M., CHANDLER, P., MUNN, D. H. & MELLOR, A. L. 2002. Tryptophan deprivation sensitizes activated T cells to apoptosis prior to cell division. *Immunology,* 107**,** 452-60.
LEE, W. S., LEE, S. M., KIM, M. K., PARK, S. G., CHOI, I. W., CHOI, I., JOO, Y. D., PARK, S. J., KANG, S. W. & SEO, S. K. 2013. The tryptophan metabolite 3-hydroxyanthranilic acid suppresses T cell responses by inhibiting dendritic cell activation. *Int Immunopharmacol,* 17**,** 721-6.
LEGUT, M., GAJIC, Z., GUARINO, M., DANILOSKI, Z., RAHMAN, J. A., XUE, X., LU, C., LU, L., MIMITOU, E. P., HAO, S., DAVOLI, T., DIEFENBACH, C., SMIBERT, P. & SANJANA, N. E. 2022. A genome-scale screen for synthetic drivers of T cell proliferation. *Nature,* 603**,** 728-735.
LI, J., CHEN, Z., KIM, G., LUO, J., HORI, S. & WU, C. 2023. Cathepsin W restrains peripheral regulatory T cells for mucosal immune quiescence. *Sci Adv,* 9**,** eadf3924.
LI, K., YUAN, Z., LYU, J., AHN, E., DAVIS, S. J., AHMED, R. & ZHU, C. 2021. PD-1 suppresses TCR-CD8 cooperativity during T-cell antigen recognition. *Nat Commun,* 12**,** 2746.
LI, Q., ZHU, C. C., NI, B., ZHANG, Z. Z., JIANG, S. H., HU, L. P., WANG, X., ZHANG, X. X., HUANG, P. Q., YANG, Q., LI, J., GU, J. R., XU, J., LUO, K. Q., ZHAO, G. & ZHANG, Z. G. 2019. Lysyl oxidase promotes liver metastasis of gastric cancer via facilitating the

reciprocal interactions between tumor cells and cancer associated fibroblasts. *EBioMedicine,* 49**,** 157-171.

LI, Y., GUO, Y., BROER, A., DAI, L., BRÖER, S. & YAN, R. 2024. Cryo-EM structure of the human Asc-1 transporter complex. *Nat Commun,* 15**,** 3036.

LIBERZON, A., BIRGER, C., THORVALDSDOTTIR, H., GHANDI, M., MESIROV, J. P. & TAMAYO, P. 2015. The Molecular Signatures Database (MSigDB) hallmark gene set collection. *Cell Syst,* 1**,** 417-425.

LIGTENBERG, M. A., MOUGIAKAKOS, D., MUKHOPADHYAY, M., WITT, K., LLADSER, A., CHMIELEWSKI, M., RIET, T., ABKEN, H. & KIESSLING, R. 2016. Coexpressed Catalase Protects Chimeric Antigen Receptor-Redirected T Cells as well as Bystander Cells from Oxidative Stress-Induced Loss of Antitumor Activity. *J Immunol,* 196**,** 759-66.

LIN, J. X. & LEONARD, W. J. 1997. The immediate-early gene product Egr-1 regulates the human interleukin-2 receptor beta-chain promoter through noncanonical Egr and Sp1 binding sites. *Mol Cell Biol,* 17**,** 3714-22.

LIN, M. J., SVENSSON-ARVELUND, J., LUBITZ, G. S., MARABELLE, A., MELERO, I., BROWN, B. D. & BRODY, J. D. 2022. Cancer vaccines: the next immunotherapy frontier. *Nat Cancer,* 3**,** 911-926.

LIU, J., TONG, J. & YANG, H. 2022. Targeting CD33 for acute myeloid leukemia therapy. *BMC Cancer,* 22**,** 24.

LIU, W., YAO, Y., LIU, X., LIU, Y. & ZHANG, G. M. 2021. Neoadjuvant hormone therapy for patients with high-risk prostate cancer: a systematic review and meta-analysis. *Asian J Androl,* 23**,** 429-436.

LIU, X., JIANG, S., FANG, C., YANG, S., OLALERE, D., PEQUIGNOT, E. C., COGDILL, A. P., LI, N., RAMONES, M., GRANDA, B., ZHOU, L., LOEW, A., YOUNG, R. M., JUNE, C. H. & ZHAO, Y. 2015. Affinity-Tuned ErbB2 or EGFR Chimeric Antigen Receptor T Cells Exhibit an Increased Therapeutic Index against Tumors in Mice. *Cancer Res,* 75**,** 3596-607.

LIU, Y. N., YANG, J. F., HUANG, D. J., NI, H. H., ZHANG, C. X., ZHANG, L., HE, J., GU, J. M., CHEN, H. X., MAI, H. Q., CHEN, Q. Y., ZHANG, X. S., GAO, S. & LI, J. 2020. Hypoxia Induces Mitochondrial Defect That Promotes T Cell Exhaustion in Tumor Microenvironment Through MYC-Regulated Pathways. *Front Immunol,* 11**,** 1906.

LOCKE, F. L., GHOBADI, A., JACOBSON, C. A., MIKLOS, D. B., LEKAKIS, L. J., OLUWOLE, O. O., LIN, Y., BRAUNSCHWEIG, I., HILL, B. T., TIMMERMAN, J. M., DEOL, A., REAGAN, P. M., STIFF, P., FLINN, I. W., FAROOQ, U., GOY, A., MCSWEENEY, P. A., MUNOZ, J., SIDDIQI, T., CHAVEZ, J. C., HERRERA, A. F., BARTLETT, N. L., WIEZOREK, J. S., NAVALE, L., XUE, A., JIANG, Y., BOT, A., ROSSI, J. M., KIM, J. J., GO, W. Y. & NEELAPU, S. S. 2019. Long-term safety and activity of axicabtagene ciloleucel in refractory large B-cell lymphoma (ZUMA-1): a single-arm, multicentre, phase 1-2 trial. *Lancet Oncol,* 20**,** 31-42.

LOEBBERMANN, J., THORNTON, H., DURANT, L., SPARWASSER, T., WEBSTER, K. E., SPRENT, J., CULLEY, F. J., JOHANSSON, C. & OPENSHAW, P. J. 2012. Regulatory T cells expressing granzyme B play a critical role in controlling lung inflammation during acute viral infection. *Mucosal Immunol,* 5**,** 161-72.

LONETTI, A., INDIO, V., LAGINESTRA, M. A., TARANTINO, G., CHIARINI, F., ASTOLFI, A., BERTUCCIO, S. N., MARTELLI, A. M., LOCATELLI, F., PESSION, A. & MASETTI, R. 2020. Inhibition of Methyltransferase DOT1L Sensitizes to Sorafenib Treatment AML Cells Irrespective of MLL-Rearrangements: A Novel Therapeutic Strategy for Pediatric AML. *Cancers (Basel),* 12.

LONG, A. H., HASO, W. M., SHERN, J. F., WANHAINEN, K. M., MURGAI, M., INGARAMO, M., SMITH, J. P., WALKER, A. J., KOHLER, M. E., VENKATESHWARA, V. R., KAPLAN, R. N., PATTERSON, G. H., FRY, T. J., ORENTAS, R. J. & MACKALL, C. L. 2015. 4-1BB costimulation ameliorates T cell exhaustion induced by tonic signaling of chimeric antigen receptors. *Nat Med,* 21**,** 581-90.

LOWE, M. M., BOOTHBY, I., CLANCY, S., AHN, R. S., LIAO, W., NGUYEN, D. N., SCHUMANN, K., MARSON, A., MAHURON, K. M., KINGSBURY, G. A., LIU, Z., MUNOZ SANDOVAL, P., RODRIGUEZ, R. S., PAULI, M. L., TARAVATI, K., ARRON, S. T., NEUHAUS, I. M., HARRIS, H. W., KIM, E. A., SHIN, U. S., KRUMMEL, M. F., DAUD, A., SCHARSCHMIDT, T. C. & ROSENBLUM, M. D. 2019. Regulatory T cells use arginase 2 to enhance their metabolic fitness in tissues. *JCI Insight,* 4.

LU, L., ZHAN, M., LI, X. Y., ZHANG, H., DAUPHARS, D. J., JIANG, J., YIN, H., LI, S. Y., LUO, S., LI, Y. & HE, Y. W. 2022. Clinically approved combination immunotherapy: Current status, limitations, and future perspective. *Curr Res Immunol,* 3**,** 118-127.

LU, Y., WANG, W., WANG, J., YANG, C., MAO, H., FU, X., WU, Y., CAI, J., HAN, J., XU, Z., ZHUANG, Z., LIU, Z., HU, H. & CHEN, B. 2013. Overexpression of arginine transporter CAT-1 is associated with accumulation of L-arginine and cell growth in human colorectal cancer tissue. *PLoS One,* 8**,** e73866.

LUO, Y., GAO, L., LIU, J., YANG, L., WANG, L., LAI, X., GAO, S., LIU, L., ZHAO, L., YE, Y., WANG, M., SHEN, L., CAO, W. W., WANG, D., LI, W., ZHANG, X. & HUANG, H. 2024. Donor-derived Anti-CD19 CAR T cells GC007g for relapsed or refractory B-cell acute lymphoblastic leukemia after allogeneic HSCT: a phase 1 trial. *EClinicalMedicine,* 67**,** 102377.

MA, H., CHEN, X., MO, S., ZHANG, Y., MAO, X., CHEN, J., LIU, Y., TONG, W. M., LU, Z., YU, S. & CHEN, J. 2023a. Targeting N-glycosylation of 4F2hc mediated by glycosyltransferase B3GNT3 sensitizes ferroptosis of pancreatic ductal adenocarcinoma. *Cell Death Differ,* 30**,** 1988-2004.

MA, J., HU, W., LIU, Y., DUAN, C., ZHANG, D., WANG, Y., CHENG, K., YANG, L., WU, S., JIN, B., ZHANG, Y. & ZHUANG, R. 2023b. CD226 maintains regulatory T cell phenotype stability and metabolism by the mTOR/Myc pathway under inflammatory conditions. *Cell Rep,* 42**,** 113306.

MA, V. P., HU, Y., KELLNER, A. V., BROCKMAN, J. M., VELUSAMY, A., BLANCHARD, A. T., EVAVOLD, B. D., ALON, R. & SALAITA, K. 2022. The magnitude of LFA-1/ICAM-1 forces fine-tune TCR-triggered T cell activation. *Sci Adv,* 8**,** eabg4485.

MABUCHI, R., HARA, T., MATSUMOTO, T., SHIBATA, Y., NAKAMURA, N., NAKAMURA, H., KITAGAWA, J., KANEMURA, N., GOTO, N., SHIMIZU, M., ITO, H., YAMAMOTO, Y., SAITO, K., MORIWAKI, H. & TSURUMI, H. 2016. High serum concentration of L-kynurenine predicts unfavorable outcomes in patients with acute myeloid leukemia. *Leuk Lymphoma,* 57**,** 92-8.

MACIVER, N. J., JACOBS, S. R., WIEMAN, H. L., WOFFORD, J. A., COLOFF, J. L. & RATHMELL, J. C. 2008. Glucose metabolism in lymphocytes is a regulated process with significant effects on immune cell function and survival. *J Leukoc Biol,* 84**,** 949-57.

MACK, P. C., BANKS, K. C., ESPENSCHIED, C. R., BURICH, R. A., ZILL, O. A., LEE, C. E., RIESS, J. W., MORTIMER, S. A., TALASAZ, A., LANMAN, R. B. & GANDARA, D. R. 2020. Spectrum of driver mutations and clinical impact of circulating tumor DNA analysis in non-small cell lung cancer: Analysis of over 8000 cases. *Cancer,* 126**,** 3219-3228.

MAILANKODY, S., MATOUS, J. V., CHHABRA, S., LIEDTKE, M., SIDANA, S., OLUWOLE, O. O., MALIK, S., NATH, R., ANWER, F., CRUZ, J. C., HTUT, M., KARSKI, E. E., LOVELACE, W., DILLON, M., BUTZ, E., YING, W., BALAKUMARAN, A. & KUMAR, S. K. 2023. Allogeneic BCMA-targeting CAR T cells in relapsed/refractory multiple myeloma: phase 1 UNIVERSAL trial interim results. *Nat Med,* 29**,** 422-429.

MAIMAITI, M., SAKAMOTO, S., YAMADA, Y., SUGIURA, M., RII, J., TAKEUCHI, N., IMAMURA, Y., FURIHATA, T., ANDO, K., HIGUCHI, K., XU, M., SAZUKA, T., NAKAMURA, K., KANEDA, A., KANAI, Y., KYPRIANOU, N., IKEHARA, Y., ANZAI, N. & ICHIKAWA, T. 2020. Expression of L-type amino acid transporter 1 as a molecular target for prognostic and therapeutic indicators in bladder carcinoma. *Sci Rep,* 10**,** 1292.

MAJETI, R., CHAO, M. P., ALIZADEH, A. A., PANG, W. W., JAISWAL, S., GIBBS, K. D., JR., VAN ROOIJEN, N. & WEISSMAN, I. L. 2009. CD47 is an adverse prognostic factor and therapeutic antibody target on human acute myeloid leukemia stem cells. *Cell,* 138**,** 286-99.

MAK, T. W., GRUSDAT, M., DUNCAN, G. S., DOSTERT, C., NONNENMACHER, Y., COX, M., BINSFELD, C., HAO, Z., BRUSTLE, A., ITSUMI, M., JAGER, C., CHEN, Y., PINKENBURG, O., CAMARA, B., OLLERT, M., BINDSLEV-JENSEN, C., VASILIOU, V., GORRINI, C., LANG, P. A., LOHOFF, M., HARRIS, I. S., HILLER, K. & BRENNER, D. 2017. Glutathione Primes T Cell Metabolism for Inflammation. *Immunity,* 46**,** 675-689.

MAO, Y., WANG, Y., DONG, L., ZHANG, Y., ZHANG, Y., WANG, C., ZHANG, Q., YANG, S., CAO, L., ZHANG, X., LI, X. & FU, Z. 2019. Hypoxic exosomes facilitate angiogenesis and metastasis in esophageal squamous cell carcinoma through altering the phenotype and transcriptome of endothelial cells. *J Exp Clin Cancer Res,* 38**,** 389.

MARKEL, G., SEIDMAN, R., STERN, N., COHEN-SINAI, T., IZHAKI, O., KATZ, G., BESSER, M., TREVES, A. J., BLUMBERG, R. S., LOEWENTHAL, R., MANDELBOIM, O., ORENSTEIN, A. & SCHACHTER, J. 2006. Inhibition of human tumor-infiltrating lymphocyte effector functions by the homophilic carcinoembryonic cell adhesion molecule 1 interactions. *J Immunol,* 177**,** 6062-71.

MARSHALL, J. S., WARRINGTON, R., WATSON, W. & KIM, H. L. 2018. An introduction to immunology and immunopathology. *Allergy Asthma Clin Immunol,* 14**,** 49.

MARTINEZ-MENDEZ, D., HUERTA, L. & VILLARREAL, C. 2022. Modeling the effect of environmental cytokines, nutrient conditions and hypoxia on CD4(+) T cell differentiation. *Front Immunol,* 13**,** 962175.

MARTINEZ BEDOYA, D., DUTOIT, V. & MIGLIORINI, D. 2021. Allogeneic CAR T Cells: An Alternative to Overcome Challenges of CAR T Cell Therapy in Glioblastoma. *Front Immunol,* 12**,** 640082.

MARTINS, Y. C., RIBEIRO-GOMES, F. L. & DANIEL-RIBEIRO, C. T. 2023. A short history of innate immunity. *Mem Inst Oswaldo Cruz,* 118**,** e230023.

MARUHASHI, T., OKAZAKI, I. M., SUGIURA, D., TAKAHASHI, S., MAEDA, T. K., SHIMIZU, K. & OKAZAKI, T. 2018. LAG-3 inhibits the activation of CD4(+) T cells that recognize stable pMHCII through its conformation-dependent recognition of pMHCII. *Nat Immunol,* 19**,** 1415-1426.

MAYER, S., MILO, T., ISAACSON, A., HALPERIN, C., MIYARA, S., STEIN, Y., LIOR, C., PEVSNER-FISCHER, M., TZAHOR, E., MAYO, A., ALON, U. & SCHERZ-SHOUVAL, R. 2023. The tumor microenvironment shows a hierarchy of cell-cell interactions dominated by fibroblasts. *Nat Commun,* 14**,** 5810.

MCCARTHY, E. F. 2006. The toxins of William B. Coley and the treatment of bone and soft-tissue sarcomas. *Iowa Orthop J,* 26**,** 154-8.
MENTER, T. & TZANKOV, A. 2022. Tumor Microenvironment in Acute Myeloid Leukemia: Adjusting Niches. *Front Immunol,* 13**,** 811144.
MERCIER-LETONDAL, P., MARTON, C., GODET, Y. & GALAINE, J. 2021. Validation of a method evaluating T cell metabolic potential in compliance with ICH Q2 (R1). *J Transl Med,* 19**,** 21.
MIRCHANDANI, A. S., BESNARD, A. G., YIP, E., SCOTT, C., BAIN, C. C., CEROVIC, V., SALMOND, R. J. & LIEW, F. Y. 2014. Type 2 innate lymphoid cells drive CD4+ Th2 cell responses. *J Immunol,* 192**,** 2442-8.
MOGHANLOO, E., MOLLANOORI, H., TALEBI, M., PASHANGZADEH, S., FARAJI, F., HADJILOOEI, F. & MAHMOODZADEH, H. 2021. Remote controlling of CAR-T cells and toxicity management: Molecular switches and next generation CARs. *Transl Oncol,* 14**,** 101070.
MOTZER, R. J., TANNIR, N. M., MCDERMOTT, D. F., AREN FRONTERA, O., MELICHAR, B., CHOUEIRI, T. K., PLIMACK, E. R., BARTHELEMY, P., PORTA, C., GEORGE, S., POWLES, T., DONSKOV, F., NEIMAN, V., KOLLMANNSBERGER, C. K., SALMAN, P., GURNEY, H., HAWKINS, R., RAVAUD, A., GRIMM, M. O., BRACARDA, S., BARRIOS, C. H., TOMITA, Y., CASTELLANO, D., RINI, B. I., CHEN, A. C., MEKAN, S., MCHENRY, M. B., WIND-ROTOLO, M., DOAN, J., SHARMA, P., HAMMERS, H. J., ESCUDIER, B. & CHECKMATE, I. 2018. Nivolumab plus Ipilimumab versus Sunitinib in Advanced Renal-Cell Carcinoma. *N Engl J Med,* 378**,** 1277-1290.
MULLER-THOMAS, C., HEIDER, M., PIONTEK, G., SCHLENSOG, M., BASSERMANN, F., KIRCHNER, T., GERMING, U., GOTZE, K. S. & RUDELIUS, M. 2020. Prognostic value of indoleamine 2,3 dioxygenase in patients with higher-risk myelodysplastic syndromes treated with azacytidine. *Br J Haematol,* 190**,** 361-370.
MUNN, D. H., SHAFIZADEH, E., ATTWOOD, J. T., BONDAREV, I., PASHINE, A. & MELLOR, A. L. 1999. Inhibition of T cell proliferation by macrophage tryptophan catabolism. *J Exp Med,* 189**,** 1363-72.
MUNZ, C. 2011. Antigen processing by macroautophagy for MHC presentation. *Front Immunol,* 2**,** 42.
MUSCARITOLI, M., CONVERSANO, L., PETTI, M. C., TORELLI, G. F., CASCINO, A., MECAROCCI, S., ANNICCHIARICO, M. A. & ROSSI FANELLI, F. 1999. Plasma amino acid concentrations in patients with acute myelogenous leukemia. *Nutrition,* 15**,** 195-9.
MUSSAI, F., DE SANTO, C., ABU-DAYYEH, I., BOOTH, S., QUEK, L., MCEWEN-SMITH, R. M., QURESHI, A., DAZZI, F., VYAS, P. & CERUNDOLO, V. 2013. Acute myeloid leukemia creates an arginase-dependent immunosuppressive microenvironment. *Blood,* 122**,** 749-58.
MUSSAI, F., DE SANTO, C., CHENG, P., THOMAS, I. F., ARITI, C., UPTON, L., SCARPA, U., STAVROU, V., SYDENHAM, M., BURNETT, A. K., KNAPPER, S. K., MEHTA, P., MCMULLIN, M. F., COPLAND, M., RUSSELL, N. H. & DENNIS, M. 2023. A randomised evaluation of low-dose Ara-C plus pegylated recombinant arginase BCT-100 versus low dose Ara-C in older unfit patients with acute myeloid leukaemia: Results from the LI-1 trial. *Br J Haematol,* 200**,** 573-578.
MUSSAI, F., EGAN, S., HIGGINBOTHAM-JONES, J., PERRY, T., BEGGS, A., ODINTSOVA, E., LOKE, J., PRATT, G., U, K. P., LO, A., NG, M., KEARNS, P., CHENG, P. & DE SANTO, C.

2015a. Arginine dependence of acute myeloid leukemia blast proliferation: a novel therapeutic target. *Blood,* 125**,** 2386-96.
MUSSAI, F., EGAN, S., HUNTER, S., WEBBER, H., FISHER, J., WHEAT, R., MCCONVILLE, C., SBIRKOV, Y., WHEELER, K., BENDLE, G., PETRIE, K., ANDERSON, J., CHESLER, L. & DE SANTO, C. 2015b. Neuroblastoma Arginase Activity Creates an Immunosuppressive Microenvironment That Impairs Autologous and Engineered Immunity. *Cancer Res,* 75**,** 3043-53.
MUSSAI, F., WHEAT, R., SARROU, E., BOOTH, S., STAVROU, V., FULTANG, L., PERRY, T., KEARNS, P., CHENG, P., KEESHAN, K., CRADDOCK, C. & DE SANTO, C. 2019. Targeting the arginine metabolic brake enhances immunotherapy for leukaemia. *Int J Cancer,* 145**,** 2201-2208.
MUSTAFA, N., MITXELENA, J., INFANTE, A., ZENARRUZABEITIA, O., ERIZ, A., IGLESIAS-ARA, A. & ZUBIAGA, A. M. 2021. E2f2 Attenuates Apoptosis of Activated T Lymphocytes and Protects from Immune-Mediated Injury through Repression of Fas and FasL. *Int J Mol Sci,* 23.
MYERS, K. C., FURUTANI, E., WELLER, E., SIEGELE, B., GALVIN, A., ARSENAULT, V., ALTER, B. P., BOULAD, F., BUESO-RAMOS, C., BURROUGHS, L., CASTILLO, P., CONNELLY, J., DAVIES, S. M., DINARDO, C. D., HANIF, I., HO, R. H., KARRAS, N., MANALANG, M., MCREYNOLDS, L. J., NAKANO, T. A., NALEPA, G., NORKIN, M., OBERLEY, M. J., ORGEL, E., PASTORE, Y. D., ROSENTHAL, J., WALKOVICH, K., LARSON, J., MALSCH, M., ELGHETANY, M. T., FLEMING, M. D. & SHIMAMURA, A. 2020. Clinical features and outcomes of patients with Shwachman-Diamond syndrome and myelodysplastic syndrome or acute myeloid leukaemia: a multicentre, retrospective, cohort study. *Lancet Haematol,* 7**,** e238-e246.
NAGHIZADEH, M., HATAMZADE, N., LARSEN, F. T., KJAERUP, R. B., WATTRANG, E. & DALGAARD, T. S. 2022. Kinetics of activation marker expression after in vitro polyclonal stimulation of chicken peripheral T cells. *Cytometry A,* 101**,** 45-56.
NARAYAN, V., BARBER-ROTENBERG, J. S., JUNG, I. Y., LACEY, S. F., RECH, A. J., DAVIS, M. M., HWANG, W. T., LAL, P., CARPENTER, E. L., MAUDE, S. L., PLESA, G., VAPIWALA, N., CHEW, A., MONIAK, M., SEBRO, R. A., FARWELL, M. D., MARSHALL, A., GILMORE, J., LLEDO, L., DENGEL, K., CHURCH, S. E., HETHER, T. D., XU, J., GOHIL, M., BUCKINGHAM, T. H., YEE, S. S., GONZALEZ, V. E., KULIKOVSKAYA, I., CHEN, F., TIAN, L., TIEN, K., GLADNEY, W., NOBLES, C. L., RAYMOND, H. E., PROSTATE CANCER CELLULAR THERAPY PROGRAM, I., HEXNER, E. O., SIEGEL, D. L., BUSHMAN, F. D., JUNE, C. H., FRAIETTA, J. A. & HAAS, N. B. 2022. PSMA-targeting TGFbeta-insensitive armored CAR T cells in metastatic castration-resistant prostate cancer: a phase 1 trial. *Nat Med,* 28**,** 724-734.
NASIRI, F., MUHAMMADNEJAD, S. & RAHBARIZADEH, F. 2023. Effects of polybrene and retronectin as transduction enhancers on the development and phenotypic characteristics of VHH-based CD19-redirected CAR T cells: a comparative investigation. *Clin Exp Med,* 23**,** 2535-2549.
NAVIAUX, R. K., COSTANZI, E., HAAS, M. & VERMA, I. M. 1996. The pCL vector system: rapid production of helper-free, high-titer, recombinant retroviruses. *J Virol,* 70**,** 5701-5.
NESS, S., LIN, S. & GORDON, J. R. 2021. Regulatory Dendritic Cells, T Cell Tolerance, and Dendritic Cell Therapy for Immunologic Disease. *Front Immunol,* 12**,** 633436.
NEWMAN, J. H., CHESSON, C. B., HERZOG, N. L., BOMMAREDDY, P. K., ASPROMONTE, S. M., PEPE, R., ESTUPINIAN, R., ABOELATTA, M. M., BUDDHADEV, S., TARABICHI, S., LEE,

M., LI, S., MEDINA, D. J., GIURINI, E. F., GUPTA, K. H., GUEVARA-ALEMAN, G., ROSSI, M., NOWICKI, C., ABED, A., GOLDUFSKY, J. W., BROUCEK, J. R., REDONDO, R. E., ROTTER, D., JHAWAR, S. R., WANG, S. J., KOHLHAPP, F. J., KAUFMAN, H. L., THOMAS, P. G., GUPTA, V., KUZEL, T. M., REISER, J., PARAS, J., KANE, M. P., SINGER, E. A., MALHOTRA, J., DENZIN, L. K., SANT'ANGELO, D. B., RABSON, A. B., LEE, L. Y., LASFAR, A., LANGENFELD, J., SCHENKEL, J. M., FIDLER, M. J., RUIZ, E. S., MARZO, A. L., RUDRA, J. S., SILK, A. W. & ZLOZA, A. 2020. Intratumoral injection of the seasonal flu shot converts immunologically cold tumors to hot and serves as an immunotherapy for cancer. *Proc Natl Acad Sci U S A,* 117**,** 1119-1128.

NILSSON, A., HAANSTRA, J. R., ENGQVIST, M., GERDING, A., BAKKER, B. M., KLINGMULLER, U., TEUSINK, B. & NIELSEN, J. 2020. Quantitative analysis of amino acid metabolism in liver cancer links glutamate excretion to nucleotide synthesis. *Proc Natl Acad Sci U S A,* 117**,** 10294-10304.

O'LEARY, C. E., RILING, C. R., SPRUCE, L. A., DING, H., KUMAR, S., DENG, G., LIU, Y., SEEHOLZER, S. H. & OLIVER, P. M. 2016. Ndfip-mediated degradation of Jak1 tunes cytokine signalling to limit expansion of CD4+ effector T cells. *Nat Commun,* 7**,** 11226.

OGAWA, S., WATANABE, M., SAKURAI, Y., INUTAKE, Y., WATANABE, S., TAI, X. & ABE, R. 2013. CD28 signaling in primary CD4(+) T cells: identification of both tyrosine phosphorylation-dependent and phosphorylation-independent pathways. *Int Immunol,* 25**,** 671-81.

OKANO, N., NARUGE, D., KAWAI, K., KOBAYASHI, T., NAGASHIMA, F., ENDOU, H. & FURUSE, J. 2020. First-in-human phase I study of JPH203, an L-type amino acid transporter 1 inhibitor, in patients with advanced solid tumors. *Invest New Drugs,* 38**,** 1495-1506.

OLIVIER, M., HOLLSTEIN, M. & HAINAUT, P. 2010. TP53 mutations in human cancers: origins, consequences, and clinical use. *Cold Spring Harb Perspect Biol,* 2**,** a001008.

ORLANDO, E. J., HAN, X., TRIBOULEY, C., WOOD, P. A., LEARY, R. J., RIESTER, M., LEVINE, J. E., QAYED, M., GRUPP, S. A., BOYER, M., DE MOERLOOSE, B., NEMECEK, E. R., BITTENCOURT, H., HIRAMATSU, H., BUECHNER, J., DAVIES, S. M., VERNERIS, M. R., NGUYEN, K., BROGDON, J. L., BITTER, H., MORRISSEY, M., PIEROG, P., PANTANO, S., ENGELMAN, J. A. & WINCKLER, W. 2018. Genetic mechanisms of target antigen loss in CAR19 therapy of acute lymphoblastic leukemia. *Nat Med,* 24**,** 1504-1506.

OTHUS, M., GARCIA-MANERO, G., GODWIN, J. E., WEICK, J. K., APPELBAUM, F. R., ERBA, H. P. & ESTEY, E. H. 2023. Improved outcomes with "7+3" induction chemotherapy for acute myeloid leukemia over the past four decades: analysis of SWOG trial data. *Haematologica,* 108**,** 42-47.

OTTAIANO, A., SCALA, S., D'ALTERIO, C., TROTTA, A., BELLO, A., REA, G., PICONE, C., SANTORSOLA, M., PETRILLO, A. & NASTI, G. 2021. Unexpected tumor reduction in metastatic colorectal cancer patients during SARS-Cov-2 infection. *Ther Adv Med Oncol,* 13**,** 17588359211011455.

PAN, J., ZHANG, Y. Y., JIAO, X. X., SONG, L. N., LIN, C. Q., WANG, S. L., ZHU, B., PAN, S. Y., DING, Z. Y. & ZHAO, W. L. 2022. [Correlation between Expression of CD47 Molecule in Patients with Newly Diagnosed Adult Acute Myeloid Leukemia and Clinical Prognosis]. *Zhongguo Shi Yan Xue Ye Xue Za Zhi,* 30**,** 1071-1078.

PANETTI, S., MCJANNETT, N., FULTANG, L., BOOTH, S., GNEO, L., SCARPA, U., SMITH, C., VARDON, A., VETTORE, L., WHALLEY, C., PAN, Y., VARNAI, C., ENDOU, H., BARLOW, J., TENNANT, D., BEGGS, A., MUSSAI, F. & DE SANTO, C. 2023. Engineering amino acid

uptake or catabolism promotes CAR T-cell adaption to the tumor environment. *Blood Adv,* 7**,** 1754-1761.

PARDIEU, B., PASANISI, J., LING, F., DAL BELLO, R., PENNEROUX, J., SU, A., JOUDINAUD, R., CHAT, L., WU, H. C., DUCHMANN, M., SODARO, G., CHAUVEL, C., CASTELLI, F. A., VASSEUR, L., PACCHIARDI, K., BELLOUCIF, Y., LAIGUILLON, M. C., MEDURI, E., VAGANAY, C., ALEXE, G., BERROU, J., BENAKSAS, C., FORGET, A., BRAUN, T., GARDIN, C., RAFFOUX, E., CLAPPIER, E., ADES, L., DE THE, H., FENAILLE, F., HUNTLY, B. J., STEGMAIER, K., DOMBRET, H., FENOUILLE, N., LOBRY, C., PUISSANT, A. & ITZYKSON, R. 2022. Cystine uptake inhibition potentiates front-line therapies in acute myeloid leukemia. *Leukemia,* 36**,** 1585-1595.

PARKER, J. L., DEME, J. C., KOLOKOURIS, D., KUTEYI, G., BIGGIN, P. C., LEA, S. M. & NEWSTEAD, S. 2021. Molecular basis for redox control by the human cystine/glutamate antiporter system xc(). *Nat Commun,* 12**,** 7147.

PASZEK, M. J., DUFORT, C. C., ROSSIER, O., BAINER, R., MOUW, J. K., GODULA, K., HUDAK, J. E., LAKINS, J. N., WIJEKOON, A. C., CASSEREAU, L., RUBASHKIN, M. G., MAGBANUA, M. J., THORN, K. S., DAVIDSON, M. W., RUGO, H. S., PARK, J. W., HAMMER, D. A., GIANNONE, G., BERTOZZI, C. R. & WEAVER, V. M. 2014. The cancer glycocalyx mechanically primes integrin-mediated growth and survival. *Nature,* 511**,** 319-25.

PEARSON, A. D., ROSSIG, C., MACKALL, C., SHAH, N. N., BARUCHEL, A., REAMAN, G., RICAFORT, R., HEENEN, D., BASSAN, A., BERNTGEN, M., BIRD, N., BLEICKARDT, E., BOUCHKOUJ, N., BROSS, P., BROWNSTEIN, C., COHEN, S. B., DE ROJAS, T., EHRLICH, L., FOX, E., GOTTSCHALK, S., HANSSENS, L., HAWKINS, D. S., HORAK, I. D., TAYLOR, D. H., JOHNSON, C., KARRES, D., LIGAS, F., LUDWINSKI, D., MAMONKIN, M., MARSHALL, L., MASOULEH, B. K., MATLOUB, Y., MAUDE, S., MCDONOUGH, J., MINARD-COLIN, V., NORGA, K., NYSOM, K., PAPPO, A., PEARCE, L., PIETERS, R., PULE, M., QUINTAS-CARDAMA, A., RICHARDSON, N., SCHUSSLER-LENZ, M., SCOBIE, N., SERSCH, M. A., SMITH, M. A., STERBA, J., TASIAN, S. K., WEIGEL, B., WEINER, S. L., ZWAAN, C. M., LESA, G. & VASSAL, G. 2022. Paediatric Strategy Forum for medicinal product development of chimeric antigen receptor T-cells in children and adolescents with cancer: ACCELERATE in collaboration with the European Medicines Agency with participation of the Food and Drug Administration. *Eur J Cancer,* 160**,** 112-133.

PHILIP, B., KOKALAKI, E., MEKKAOUI, L., THOMAS, S., STRAATHOF, K., FLUTTER, B., MARIN, V., MARAFIOTI, T., CHAKRAVERTY, R., LINCH, D., QUEZADA, S. A., PEGGS, K. S. & PULE, M. 2014. A highly compact epitope-based marker/suicide gene for easier and safer T-cell therapy. *Blood,* 124**,** 1277-87.

PIEVANI, A., BIONDI, M., TETTAMANTI, S., BIONDI, A., DOTTI, G. & SERAFINI, M. 2024. CARs are sharpening their weapons. *J Immunother Cancer,* 12.

PORTER, D. L., HWANG, W. T., FREY, N. V., LACEY, S. F., SHAW, P. A., LOREN, A. W., BAGG, A., MARCUCCI, K. T., SHEN, A., GONZALEZ, V., AMBROSE, D., GRUPP, S. A., CHEW, A., ZHENG, Z., MILONE, M. C., LEVINE, B. L., MELENHORST, J. J. & JUNE, C. H. 2015. Chimeric antigen receptor T cells persist and induce sustained remissions in relapsed refractory chronic lymphocytic leukemia. *Sci Transl Med,* 7**,** 303ra139.

PSARRAS, A., ANTANAVICIUTE, A., ALASE, A., CARR, I., WITTMANN, M., EMERY, P., TSOKOS, G. C. & VITAL, E. M. 2021. TNF-alpha Regulates Human Plasmacytoid Dendritic Cells by Suppressing IFN-alpha Production and Enhancing T Cell Activation. *J Immunol,* 206**,** 785-796.

PUCK, A., AIGNER, R., MODAK, M., CEJKA, P., BLAAS, D. & STOCKL, J. 2015. Expression and regulation of Schlafen (SLFN) family members in primary human monocytes, monocyte-derived dendritic cells and T cells. *Results Immunol,* 5**,** 23-32.

PUGLISI, C., GIUFFRIDA, R., BORZI, G., DI MATTIA, P., COSTA, A., COLAROSSI, C., DEIANA, E., PICARDO, M. C., COLAROSSI, L., MARE, M., MARINO, L., DI GRAZIA, A. & FORTE, S. 2020. Radiosensitivity of Cancer Stem Cells Has Potential Predictive Value for Individual Responses to Radiotherapy in Locally Advanced Rectal Cancer. *Cancers (Basel),* 12.

PYZER, A. R., STROOPINSKY, D., RAJABI, H., WASHINGTON, A., TAGDE, A., COLL, M., FUNG, J., BRYANT, M. P., COLE, L., PALMER, K., SOMAIYA, P., KARP LEAF, R., NAHAS, M., APEL, A., JAIN, S., MCMASTERS, M., MENDEZ, L., LEVINE, J., JOYCE, R., ARNASON, J., PANDOLFI, P. P., KUFE, D., ROSENBLATT, J. & AVIGAN, D. 2017. MUC1-mediated induction of myeloid-derived suppressor cells in patients with acute myeloid leukemia. *Blood,* 129**,** 1791-1801.

QIN, H., YANG, L., CHUKINAS, J. A., SHAH, N., TARUN, S., POUZOLLES, M., CHIEN, C. D., NISWANDER, L. M., WELCH, A. R., TAYLOR, N., TASIAN, S. K. & FRY, T. J. 2021. Systematic preclinical evaluation of CD33-directed chimeric antigen receptor T cell immunotherapy for acute myeloid leukemia defines optimized construct design. *J Immunother Cancer,* 9.

RADWAN, S. M., ELLEBOUDY, N. S., NABIH, N. A. & KAMAL, A. M. 2020. The immune checkpoints Cytotoxic T lymphocyte antigen-4 and Lymphocyte activation gene-3 expression is up-regulated in acute myeloid leukemia. *HLA,* 96**,** 3-12.

RAFIQ, S., HACKETT, C. S. & BRENTJENS, R. J. 2020. Engineering strategies to overcome the current roadblocks in CAR T cell therapy. *Nat Rev Clin Oncol,* 17**,** 147-167.

RAMOS, S., FERREIRA, S., FERNANDES, A. S. & SARAIVA, N. 2022. Lysyl Oxidases Expression and Breast Cancer Progression: A Bioinformatic Analysis. *Front Pharmacol,* 13**,** 883998.

RASHIDI, A., MISKA, J., LEE-CHANG, C., KANOJIA, D., PANEK, W. K., LOPEZ-ROSAS, A., ZHANG, P., HAN, Y., XIAO, T., PITUCH, K. C., KIM, J. W., TALEBIAN, M., FARES, J. & LESNIAK, M. S. 2020. GCN2 is essential for CD8(+) T cell survival and function in murine models of malignant glioma. *Cancer Immunol Immunother,* 69**,** 81-94.

RASKOV, H., ORHAN, A., CHRISTENSEN, J. P. & GOGENUR, I. 2021. Cytotoxic CD8(+) T cells in cancer and cancer immunotherapy. *Br J Cancer,* 124**,** 359-367.

RASOULI, J., CIRIC, B., IMITOLA, J., GONNELLA, P., HWANG, D., MAHAJAN, K., MARI, E. R., SAFAVI, F., LEIST, T. P., ZHANG, G. X. & ROSTAMI, A. 2015. Expression of GM-CSF in T Cells Is Increased in Multiple Sclerosis and Suppressed by IFN-beta Therapy. *J Immunol,* 194**,** 5085-93.

REDDY, M., EIRIKIS, E., DAVIS, C., DAVIS, H. M. & PRABHAKAR, U. 2004. Comparative analysis of lymphocyte activation marker expression and cytokine secretion profile in stimulated human peripheral blood mononuclear cell cultures: an in vitro model to monitor cellular immune function. *J Immunol Methods,* 293**,** 127-42.

REN, H., LIU, X., XU, Q., LI, W. & ZHAO, N. 2023. Interleukin-35 expression promotes hepatocellular carcinogenesis by inducing gammadelta T-cell exhaustion. *Genomics,* 115**,** 110639.

RITCHIE, D. S., NEESON, P. J., KHOT, A., PEINERT, S., TAI, T., TAINTON, K., CHEN, K., SHIN, M., WALL, D. M., HONEMANN, D., GAMBELL, P., WESTERMAN, D. A., HAURAT, J., WESTWOOD, J. A., SCOTT, A. M., KRAVETS, L., DICKINSON, M., TRAPANI, J. A.,

SMYTH, M. J., DARCY, P. K., KERSHAW, M. H. & PRINCE, H. M. 2013. Persistence and efficacy of second generation CAR T cell against the LeY antigen in acute myeloid leukemia. *Mol Ther,* 21**,** 2122-9.

ROSSY, J., WILLIAMSON, D. J. & GAUS, K. 2012. How does the kinase Lck phosphorylate the T cell receptor? Spatial organization as a regulatory mechanism. *Front Immunol,* 3**,** 167.

RUSHDI, M. N., PAN, V., LI, K., CHOI, H. K., TRAVAGLINO, S., HONG, J., GRIFFITTS, F., AGNIHOTRI, P., MARIUZZA, R. A., KE, Y. & ZHU, C. 2022. Cooperative binding of T cell receptor and CD4 to peptide-MHC enhances antigen sensitivity. *Nat Commun,* 13**,** 7055.

SAILER, C. J., HONG, Y., DAHAL, A., RYAN, A. T., MIR, S., GERBER, S. A., REAGAN, P. M. & KIM, M. 2023. PD-1(Hi) CAR-T cells provide superior protection against solid tumors. *Front Immunol,* 14**,** 1187850.

SAITO, K., ZHANG, Q., YANG, H., YAMATANI, K., AI, T., RUVOLO, V., BARAN, N., CAI, T., MA, H., JACAMO, R., KURUVILLA, V., IMOTO, J., KINJO, S., IKEO, K., MORIYA, K., SUZUKI, K., MIIDA, T., KIM, Y. M., VELLANO, C. P., ANDREEFF, M., MARSZALEK, J. R., TABE, Y. & KONOPLEVA, M. 2021. Exogenous mitochondrial transfer and endogenous mitochondrial fission facilitate AML resistance to OxPhos inhibition. *Blood Adv,* 5**,** 4233-4255.

SALTER, A. I., IVEY, R. G., KENNEDY, J. J., VOILLET, V., RAJAN, A., ALDERMAN, E. J., VOYTOVICH, U. J., LIN, C., SOMMERMEYER, D., LIU, L., WHITEAKER, J. R., GOTTARDO, R., PAULOVICH, A. G. & RIDDELL, S. R. 2018. Phosphoproteomic analysis of chimeric antigen receptor signaling reveals kinetic and quantitative differences that affect cell function. *Sci Signal,* 11.

SANTOMASSO, B. D., PARK, J. H., SALLOUM, D., RIVIERE, I., FLYNN, J., MEAD, E., HALTON, E., WANG, X., SENECHAL, B., PURDON, T., CROSS, J. R., LIU, H., VACHHA, B., CHEN, X., DEANGELIS, L. M., LI, D., BERNAL, Y., GONEN, M., WENDEL, H. G., SADELAIN, M. & BRENTJENS, R. J. 2018. Clinical and Biological Correlates of Neurotoxicity Associated with CAR T-cell Therapy in Patients with B-cell Acute Lymphoblastic Leukemia. *Cancer Discov,* 8**,** 958-971.

SCHAMBACH, A., BOHNE, J., CHANDRA, S., WILL, E., MARGISON, G. P., WILLIAMS, D. A. & BAUM, C. 2006. Equal potency of gammaretroviral and lentiviral SIN vectors for expression of O6-methylguanine-DNA methyltransferase in hematopoietic cells. *Mol Ther,* 13**,** 391-400.

SCHARPING, N. E., RIVADENEIRA, D. B., MENK, A. V., VIGNALI, P. D. A., FORD, B. R., RITTENHOUSE, N. L., PERALTA, R., WANG, Y., WANG, Y., DEPEAUX, K., POHOLEK, A. C. & DELGOFFE, G. M. 2021. Mitochondrial stress induced by continuous stimulation under hypoxia rapidly drives T cell exhaustion. *Nat Immunol,* 22**,** 205-215.

SCHATZ, D. G. & SWANSON, P. C. 2011. V(D)J recombination: mechanisms of initiation. *Annu Rev Genet,* 45**,** 167-202.

SCHRAW, J. M., BAILEY, H. D., BONAVENTURE, A., MORA, A. M., ROMAN, E., MUELLER, B. A., CLAVEL, J., PETRIDOU, E. T., KARALEXI, M., NTZANI, E., EZZAT, S., RASHED, W. M., MARCOTTE, E. L., SPECTOR, L. G., METAYER, C., KANG, A. Y., MAGNANI, C., MILIGI, L., DOCKERTY, J. D., MEJIOTAA-ARANGURE, J. M., NUNEZ-ENRIQUEZ, J. C., INFANTE-RIVARD, C., MILNE, E. & SCHEURER, M. E. 2022. Infant feeding practices and childhood acute leukemia: Findings from the Childhood Cancer & Leukemia International Consortium. *Int J Cancer,* 151**,** 1013-1023.

SCHUMACHER, B., POTHOF, J., VIJG, J. & HOEIJMAKERS, J. H. J. 2021. The central role of DNA damage in the ageing process. *Nature,* 592**,** 695-703.

SCHUSTER, S. J., SVOBODA, J., CHONG, E. A., NASTA, S. D., MATO, A. R., ANAK, O., BROGDON, J. L., PRUTEANU-MALINICI, I., BHOJ, V., LANDSBURG, D., WASIK, M., LEVINE, B. L., LACEY, S. F., MELENHORST, J. J., PORTER, D. L. & JUNE, C. H. 2017. Chimeric Antigen Receptor T Cells in Refractory B-Cell Lymphomas. *N Engl J Med,* 377**,** 2545-2554.

SELLI, M. E., LANDMANN, J. H., ARVESETH, C. & SINGH, N. 2023. Inducing T cell dysfunction by chronic stimulation of CAR-engineered T cells targeting cancer cells in suspension cultures. *STAR Protoc,* 4**,** 101954.

SENA, L. A., LI, S., JAIRAMAN, A., PRAKRIYA, M., EZPONDA, T., HILDEMAN, D. A., WANG, C. R., SCHUMACKER, P. T., LICHT, J. D., PERLMAN, H., BRYCE, P. J. & CHANDEL, N. S. 2013. Mitochondria are required for antigen-specific T cell activation through reactive oxygen species signaling. *Immunity,* 38**,** 225-36.

SHAH, D. K. & ZUNIGA-PFLUCKER, J. C. 2014. An overview of the intrathymic intricacies of T cell development. *J Immunol,* 192**,** 4017-23.

SHAH, K., AL-HAIDARI, A., SUN, J. & KAZI, J. U. 2021a. T cell receptor (TCR) signaling in health and disease. *Signal Transduct Target Ther,* 6**,** 412.

SHAH, N. N., LEE, D. W., YATES, B., YUAN, C. M., SHALABI, H., MARTIN, S., WOLTERS, P. L., STEINBERG, S. M., BAKER, E. H., DELBROOK, C. P., STETLER-STEVENSON, M., FRY, T. J., STRONCEK, D. F. & MACKALL, C. L. 2021b. Long-Term Follow-Up of CD19-CAR T-Cell Therapy in Children and Young Adults With B-ALL. *J Clin Oncol,* 39**,** 1650-1659.

SHAHZAD, M., HUSSAIN, A., SIDDIQUI, R. S., SHAH, A. Y., FAISAL, M. S., ANWAR, I., TUN, A. M., HOFFMANN, M., BANSAL, R., SHUNE, L., MOHYUDDIN, G. R., MUSHTAQ, M. U., MCGUIRK, J. P. & AHMED, N. 2021. Comparison of Efficacy and Safety Profile of Allogeneic Versus Autologous CD19 Chimeric Antigen Receptor T Cell Therapy in Hematological Malignancies: A Systematic Review and Meta-Analysis. *Blood,* 138**,** 4824-4824.

SHIBASAKI, Y., YOKOBORI, T., SOHDA, M., SHIOI, I., OZAWA, N., KOMINE, C., SUGA, K., NAKAZAWA, N., OSONE, K., SHIRAISHI, T., OKADA, T., SANO, A., SAKAI, M., OGAWA, H., KAIRA, K., SHIRABE, K. & SAEKI, H. 2023. Association of High LAT1 Expression with Poor Prognosis and Recurrence in Colorectal Cancer Patients Treated with Oxaliplatin-Based Adjuvant Chemotherapy. *Int J Mol Sci,* 24.

SHIMABUKURO-VORNHAGEN, A., GODEL, P., SUBKLEWE, M., STEMMLER, H. J., SCHLOSSER, H. A., SCHLAAK, M., KOCHANEK, M., BOLL, B. & VON BERGWELT-BAILDON, M. S. 2018. Cytokine release syndrome. *J Immunother Cancer,* 6**,** 56.

SHU, X. O., ROSS, J. A., PENDERGRASS, T. W., REAMAN, G. H., LAMPKIN, B. & ROBISON, L. L. 1996. Parental alcohol consumption, cigarette smoking, and risk of infant leukemia: a Childrens Cancer Group study. *J Natl Cancer Inst,* 88**,** 24-31.

SISKA, P. J., JIAO, J., MATOS, C., SINGER, K., BERGER, R. S., DETTMER, K., OEFNER, P. J., CULLY, M. D., WANG, Z., QUINN, I. W., OLIFF, K. N., WILKINS, B. J., CHRISTENSEN, L. M., WANG, L., HANCOCK, W. W., BAUR, J. A., LEVINE, M. H., UGELE, I., MAYR, R., RENNER, K., ZHOU, L., KREUTZ, M. & BEIER, U. H. 2021. Kynurenine induces T cell fat catabolism and has limited suppressive effects in vivo. *EBioMedicine,* 74**,** 103734.

SISKA, P. J., KIM, B., JI, X., HOEKSEMA, M. D., MASSION, P. P., BECKERMANN, K. E., WU, J., CHI, J. T., HONG, J. & RATHMELL, J. C. 2016. Fluorescence-based measurement of

cystine uptake through xCT shows requirement for ROS detoxification in activated lymphocytes. *J Immunol Methods,* 438**,** 51-58.

SMYTH, M. J., KELLY, J. M., SUTTON, V. R., DAVIS, J. E., BROWNE, K. A., SAYERS, T. J. & TRAPANI, J. A. 2001. Unlocking the secrets of cytotoxic granule proteins. *J Leukoc Biol,* 70**,** 18-29.

SOLIMAN, H. H., JACKSON, E., NEUGER, T., DEES, E. C., HARVEY, R. D., HAN, H., ISMAIL-KHAN, R., MINTON, S., VAHANIAN, N. N., LINK, C., SULLIVAN, D. M. & ANTONIA, S. 2014. A first in man phase I trial of the oral immunomodulator, indoximod, combined with docetaxel in patients with metastatic solid tumors. *Oncotarget,* 5**,** 8136-46.

SOMMERMEYER, D., HUDECEK, M., KOSASIH, P. L., GOGISHVILI, T., MALONEY, D. G., TURTLE, C. J. & RIDDELL, S. R. 2016. Chimeric antigen receptor-modified T cells derived from defined CD8+ and CD4+ subsets confer superior antitumor reactivity in vivo. *Leukemia,* 30**,** 492-500.

SONG, Q., SHANG, J., ZHANG, C., CHEN, J., ZHANG, L. & WU, X. 2020. Transcription factor RUNX3 promotes CD8(+) T cell recruitment by CCL3 and CCL20 in lung adenocarcinoma immune microenvironment. *J Cell Biochem,* 121**,** 3208-3220.

SRIVASTAVA, M. K., SINHA, P., CLEMENTS, V. K., RODRIGUEZ, P. & OSTRAND-ROSENBERG, S. 2010. Myeloid-derived suppressor cells inhibit T-cell activation by depleting cystine and cysteine. *Cancer Res,* 70**,** 68-77.

SROUR, S. A., SINGH, H., MCCARTY, J., DE GROOT, E., HULS, H., RONDON, G., QAZILBASH, M., CIUREA, S., BARDELLI, G., BUCK, J., ALOUSI, A., NIETO, Y., REZVANI, K., MARIN, D., POPAT, U., HOSING, C., SHPALL, E. J., WIERDA, W. G., KANTARJIAN, H., CHAMPLIN, R. E., COOPER, L. J. & KEBRIAEI, P. 2020. Long-term outcomes of Sleeping Beauty-generated CD19-specific CAR T-cell therapy for relapsed-refractory B-cell lymphomas. *Blood,* 135**,** 862-865.

STEIN, E. M., GARCIA-MANERO, G., RIZZIERI, D. A., TIBES, R., BERDEJA, J. G., SAVONA, M. R., JONGEN-LAVRENIC, M., ALTMAN, J. K., THOMSON, B., BLAKEMORE, S. J., DAIGLE, S. R., WATERS, N. J., SUTTLE, A. B., CLAWSON, A., POLLOCK, R., KRIVTSOV, A., ARMSTRONG, S. A., DIMARTINO, J., HEDRICK, E., LOWENBERG, B. & TALLMAN, M. S. 2018. The DOT1L inhibitor pinometostat reduces H3K79 methylation and has modest clinical activity in adult acute leukemia. *Blood,* 131**,** 2661-2669.

STERNER, R. C. & STERNER, R. M. 2021. CAR-T cell therapy: current limitations and potential strategies. *Blood Cancer J,* 11**,** 69.

STERNER, R. C. & STERNER, R. M. 2022. Immune effector cell associated neurotoxicity syndrome in chimeric antigen receptor-T cell therapy. *Front Immunol,* 13**,** 879608.

STEVANOVIC, S., DRAPER, L. M., LANGHAN, M. M., CAMPBELL, T. E., KWONG, M. L., WUNDERLICH, J. R., DUDLEY, M. E., YANG, J. C., SHERRY, R. M., KAMMULA, U. S., RESTIFO, N. P., ROSENBERG, S. A. & HINRICHS, C. S. 2015. Complete regression of metastatic cervical cancer after treatment with human papillomavirus-targeted tumor-infiltrating T cells. *J Clin Oncol,* 33**,** 1543-50.

STEVENS, A. M., HORTON, T. M., GLASSER, C. L., GERBING, R. B., APLENC, R., ALONZO, T. A. & REDELL, M. S. 2023. IL-10 and TNFalpha are associated with decreased survival in low-risk pediatric acute myeloid leukemia; a children's oncology group report. *Pediatr Hematol Oncol,* 40**,** 147-158.

SU, L., PAN, P., YAN, P., LONG, Y., ZHOU, X., WANG, X., ZHOU, R., WEN, B., XIE, L. & LIU, D. 2019. Role of vimentin in modulating immune cell apoptosis and inflammatory responses in sepsis. *Sci Rep,* 9**,** 5747.

SUAREZ, E. R., CHANG DE, K., SUN, J., SUI, J., FREEMAN, G. J., SIGNORETTI, S., ZHU, Q. & MARASCO, W. A. 2016. Chimeric antigen receptor T cells secreting anti-PD-L1 antibodies more effectively regress renal cell carcinoma in a humanized mouse model. *Oncotarget,* 7**,** 34341-55.

SULLIVAN, J. A., TOMITA, Y., JANKOWSKA-GAN, E., LEMA, D. A., ARVEDSON, M. P., NAIR, A., BRACAMONTE-BARAN, W., ZHOU, Y., MEYER, K. K., ZHONG, W., SAWANT, D. V., SZYMCZAK-WORKMAN, A. L., ZHANG, Q., WORKMAN, C. J., HONG, S., VIGNALI, D. A. A. & BURLINGHAM, W. J. 2020. Treg-Cell-Derived IL-35-Coated Extracellular Vesicles Promote Infectious Tolerance. *Cell Rep,* 30**,** 1039-1051 e5.

SUN, L., HE, C., NAIR, L., YEUNG, J. & EGWUAGU, C. E. 2015. Interleukin 12 (IL-12) family cytokines: Role in immune pathogenesis and treatment of CNS autoimmune disease. *Cytokine,* 75**,** 249-55.

SUN, L. U., TAN, H., YU, T. & LIANG, R. 2023. Identification of lncRNAs associated with T cells as potential biomarkers and therapeutic targets in lung adenocarcinoma. *Oncol Res,* 31**,** 967-988.

SUN, Y., YAO, L., WANG, C., XIONG, B., GUO, J., WANG, L., ZHU, J., CHENG, Z. & LIU, S. 2022. Involvement of Cancer Stem Cells in Chemoresistant Relapse of Epithelial Ovarian Cancer Identified by Transcriptome Analysis. *J Oncol,* 2022**,** 6406122.

SWAMINATHAN, M. & CORTES, J. E. 2023. Update on the role of gemtuzumab-ozogamicin in the treatment of acute myeloid leukemia. *Ther Adv Hematol,* 14**,** 20406207231154708.

SWEENEY, N. P. & VINK, C. A. 2021. The impact of lentiviral vector genome size and producer cell genomic to gag-pol mRNA ratios on packaging efficiency and titre. *Mol Ther Methods Clin Dev,* 21**,** 574-584.

TAGUCHI, A., KAWANA, K., TOMIO, K., YAMASHITA, A., ISOBE, Y., NAGASAKA, K., KOGA, K., INOUE, T., NISHIDA, H., KOJIMA, S., ADACHI, K., MATSUMOTO, Y., ARIMOTO, T., WADA-HIRAIKE, O., ODA, K., KANG, J. X., ARAI, H., ARITA, M., OSUGA, Y. & FUJII, T. 2014. Matrix metalloproteinase (MMP)-9 in cancer-associated fibroblasts (CAFs) is suppressed by omega-3 polyunsaturated fatty acids in vitro and in vivo. *PLoS One,* 9**,** e89605.

TAKAHASHI, H., SAKAKURA, K., KUDO, T., TOYODA, M., KAIRA, K., OYAMA, T. & CHIKAMATSU, K. 2017. Cancer-associated fibroblasts promote an immunosuppressive microenvironment through the induction and accumulation of protumoral macrophages. *Oncotarget,* 8**,** 8633-8647.

TAKEHARA, T., WAKAMATSU, E., MACHIYAMA, H., NISHI, W., EMOTO, K., AZUMA, M., SOEJIMA, K., FUKUNAGA, K. & YOKOSUKA, T. 2021. PD-L2 suppresses T cell signaling via coinhibitory microcluster formation and SHP2 phosphatase recruitment. *Commun Biol,* 4**,** 581.

TAMBARO, F. P., SINGH, H., JONES, E., RYTTING, M., MAHADEO, K. M., THOMPSON, P., DAVER, N., DINARDO, C., KADIA, T., GARCIA-MANERO, G., CHAN, T., SHAH, R. R. & WIERDA, W. G. 2021. Autologous CD33-CAR-T cells for treatment of relapsed/refractory acute myelogenous leukemia. *Leukemia*.

TANG, J., XIE, J., CHEN, W., TANG, C., WU, J., WANG, Y., ZHOU, X. D., ZHOU, H. D. & LI, Y. P. 2020. Runt-related transcription factor 1 is required for murine osteoblast differentiation and bone formation. *J Biol Chem,* 295**,** 11669-11681.

TANTALO, D. G., OLIVER, A. J., VON SCHEIDT, B., HARRISON, A. J., MUELLER, S. N., KERSHAW, M. H. & SLANEY, C. Y. 2021. Understanding T cell phenotype for the design of effective chimeric antigen receptor T cell therapies. *J Immunother Cancer,* 9.

TCHOU, J., ZHAO, Y., LEVINE, B. L., ZHANG, P. J., DAVIS, M. M., MELENHORST, J. J., KULIKOVSKAYA, I., BRENNAN, A. L., LIU, X., LACEY, S. F., POSEY, A. D., JR., WILLIAMS, A. D., SO, A., CONEJO-GARCIA, J. R., PLESA, G., YOUNG, R. M., MCGETTIGAN, S., CAMPBELL, J., PIERCE, R. H., MATRO, J. M., DEMICHELE, A. M., CLARK, A. S., COOPER, L. J., SCHUCHTER, L. M., VONDERHEIDE, R. H. & JUNE, C. H. 2017. Safety and Efficacy of Intratumoral Injections of Chimeric Antigen Receptor (CAR) T Cells in Metastatic Breast Cancer. *Cancer Immunol Res,* 5**,** 1152-1161.

TETTAMANTI, S., PIEVANI, A., BIONDI, A., DOTTI, G. & SERAFINI, M. 2022. Catch me if you can: how AML and its niche escape immunotherapy. *Leukemia,* 36**,** 13-22.

THOM, J. T., WEBER, T. C., WALTON, S. M., TORTI, N. & OXENIUS, A. 2015. The Salivary Gland Acts as a Sink for Tissue-Resident Memory CD8(+) T Cells, Facilitating Protection from Local Cytomegalovirus Infection. *Cell Rep,* 13**,** 1125-1136.

TIKHONOVA, A. N., DOLGALEV, I., HU, H., SIVARAJ, K. K., HOXHA, E., CUESTA-DOMINGUEZ, A., PINHO, S., AKHMETZYANOVA, I., GAO, J., WITKOWSKI, M., GUILLAMOT, M., GUTKIN, M. C., ZHANG, Y., MARIER, C., DIEFENBACH, C., KOUSTENI, S., HEGUY, A., ZHONG, H., FOOKSMAN, D. R., BUTLER, J. M., ECONOMIDES, A., FRENETTE, P. S., ADAMS, R. H., SATIJA, R., TSIRIGOS, A. & AIFANTIS, I. 2019. The bone marrow microenvironment at single-cell resolution. *Nature,* 569**,** 222-228.

TOFFALORI, C., ZITO, L., GAMBACORTA, V., RIBA, M., OLIVEIRA, G., BUCCI, G., BARCELLA, M., SPINELLI, O., GRECO, R., CRUCITTI, L., CIERI, N., NOVIELLO, M., MANFREDI, F., MONTALDO, E., OSTUNI, R., NALDINI, M. M., GENTNER, B., WATERHOUSE, M., ZEISER, R., FINKE, J., HANOUN, M., BEELEN, D. W., GOJO, I., LUZNIK, L., ONOZAWA, M., TESHIMA, T., DEVILLIER, R., BLAISE, D., HALKES, C. J. M., GRIFFIOEN, M., CARRABBA, M. G., BERNARDI, M., PECCATORI, J., BARLASSINA, C., STUPKA, E., LAZAREVIC, D., TONON, G., RAMBALDI, A., CITTARO, D., BONINI, C., FLEISCHHAUER, K., CICERI, F. & VAGO, L. 2019. Immune signature drives leukemia escape and relapse after hematopoietic cell transplantation. *Nat Med,* 25**,** 603-611.

TOWERS, R., TROMBELLO, L., FUSENIG, M., TUNGER, A., BAUMANN, A. L., SAVOLDELLI, R., WEHNER, R., FASSLRINNER, F., ARNDT, C., DAZZI, F., VON BONIN, M., FELDMANN, A., BACHMANN, M. P., WOBUS, M., SCHMITZ, M. & BORNHAUSER, M. 2024. Bone marrow-derived mesenchymal stromal cells obstruct AML-targeting CD8(+) clonal effector and CAR T-cell function while promoting a senescence-associated phenotype. *Cancer Immunol Immunother,* 73**,** 8.

ULBAR, F., VILLANOVA, I., GIANCOLA, R., BALDONI, S., GUARDALUPI, F., FABI, B., OLIOSO, P., CAPONE, A., SOLA, R., CIARDELLI, S., DEL PAPA, B., BRATTELLI, A., RICCIARDI, I., TARICANI, S., SABBATINELLI, G., IULIANI, O., PASSERI, C., SPORTOLETTI, P., SANTARONE, S., PIERINI, A., CALABRESE, G., FALZETTI, F., BONFINI, T., ACCORSI, P., RUGGERI, L., MARTELLI, M. F., VELARDI, A. & DI IANNI, M. 2020. Clinical-Grade Expanded Regulatory T Cells Are Enriched with Highly Suppressive Cells Producing IL-10, Granzyme B, and IL-35. *Biol Blood Marrow Transplant,* 26**,** 2204-2210.

VAN DEN BERG, J. H., HEEMSKERK, B., VAN ROOIJ, N., GOMEZ-EERLAND, R., MICHELS, S., VAN ZON, M., DE BOER, R., BAKKER, N. A. M., JORRITSMA-SMIT, A., VAN BUUREN, M. M., KVISTBORG, P., SPITS, H., SCHOTTE, R., MALLO, H., KARGER, M., VAN DER HAGE, J. A., WOUTERS, M., PRONK, L. M., GEUKES FOPPEN, M. H., BLANK, C. U., BEIJNEN, J.

H., NUIJEN, B., SCHUMACHER, T. N. & HAANEN, J. 2020. Tumor infiltrating lymphocytes (TIL) therapy in metastatic melanoma: boosting of neoantigen-specific T cell reactivity and long-term follow-up. *J Immunother Cancer,* 8.

VAN DER VELDEN, V. H., TE MARVELDE, J. G., HOOGEVEEN, P. G., BERNSTEIN, I. D., HOUTSMULLER, A. B., BERGER, M. S. & VAN DONGEN, J. J. 2001. Targeting of the CD33-calicheamicin immunoconjugate Mylotarg (CMA-676) in acute myeloid leukemia: in vivo and in vitro saturation and internalization by leukemic and normal myeloid cells. *Blood,* 97**,** 3197-204.

VANDER MAUSE, E. R., BAKER, J. M., DIETZE, K. A., RADHAKRISHNAN, S. V., IRAGUHA, T., OMILI, D., DAVIS, P., CHIDESTER, S. L., MODZELEWSKA, K., PANSE, J., MARVIN, J. E., OLSON, M. L., STEINBACH, M., NG, D. P., LIM, C. S., ATANACKOVIC, D. & LUETKENS, T. 2023. Systematic single amino acid affinity tuning of CD229 CAR T cells retains efficacy against multiple myeloma and eliminates on-target off-tumor toxicity. *Sci Transl Med,* 15**,** eadd7900.

VIGNALI, D. A., COLLISON, L. W. & WORKMAN, C. J. 2008. How regulatory T cells work. *Nat Rev Immunol,* 8**,** 523-32.

WALDRIP, Z. J., BURDINE, L., HARRISON, D. K., AZEVEDO-POULY, A. C., STOREY, A. J., MOFFETT, O. G., MACKINTOSH, S. G. & BURDINE, M. S. 2021. DNA-PKcs kinase activity stabilizes the transcription factor Egr1 in activated immune cells. *J Biol Chem,* 297**,** 101209.

WALSH, D. A., BORGES DA SILVA, H., BEURA, L. K., PENG, C., HAMILTON, S. E., MASOPUST, D. & JAMESON, S. C. 2019. The Functional Requirement for CD69 in Establishment of Resident Memory CD8(+) T Cells Varies with Tissue Location. *J Immunol,* 203**,** 946-955.

WAN, Y., ZHANG, C., XU, Y., WANG, M., RAO, Q., XING, H., TIAN, Z., TANG, K., MI, Y., WANG, Y. & WANG, J. 2020. Hyperfunction of CD4 CD25 regulatory T cells in de novo acute myeloid leukemia. *BMC Cancer,* 20**,** 472.

WANG, C., SUN, C., LI, M., XIA, B., WANG, Y., ZHANG, L., ZHANG, Y., WANG, J., SUN, F., LU, S., ZHU, J., HUANG, J. & ZHANG, Y. 2021a. Novel fully human anti-CD47 antibodies stimulate phagocytosis and promote elimination of AML cells. *J Cell Physiol,* 236**,** 4470-4481.

WANG, F., YANG, L., XIAO, M., ZHANG, Z., SHEN, J., ANUCHAPREEDA, S., TIMA, S., CHIAMPANICHAYAKUL, S. & XIAO, Z. 2022. PD-L1 regulates cell proliferation and apoptosis in acute myeloid leukemia by activating PI3K-AKT signaling pathway. *Sci Rep,* 12**,** 11444.

WANG, Z., LI, N., FENG, K., CHEN, M., ZHANG, Y., LIU, Y., YANG, Q., NIE, J., TANG, N., ZHANG, X., CHENG, C., SHEN, L., HE, J., YE, X., CAO, W., WANG, H. & HAN, W. 2021b. Phase I study of CAR-T cells with PD-1 and TCR disruption in mesothelin-positive solid tumors. *Cell Mol Immunol,* 18**,** 2188-2198.

WATANABE, N., MO, F. & MCKENNA, M. K. 2022. Impact of Manufacturing Procedures on CAR T Cell Functionality. *Front Immunol,* 13**,** 876339.

WEI, J., HAN, X., BO, J. & HAN, W. 2019. Target selection for CAR-T therapy. *J Hematol Oncol,* 12**,** 62.

WELLS, G., KENNEDY, P. T. & DAHAL, L. N. 2021. Investigating the Role of Indoleamine 2,3-Dioxygenase in Acute Myeloid Leukemia: A Systematic Review. *Front Immunol,* 12**,** 651687.

WERNER, A., PIEH, D., ECHCHANNAOUI, H., RUPP, J., RAJALINGAM, K., THEOBALD, M., CLOSS, E. I. & MUNDER, M. 2019. Cationic Amino Acid Transporter-1-Mediated Arginine Uptake Is Essential for Chronic Lymphocytic Leukemia Cell Proliferation and Viability. *Front Oncol,* 9**,** 1268.

WEST, R. R., STAFFORD, D. A., WHITE, A. D., BOWEN, D. T. & PADUA, R. A. 2000. Cytogenetic abnormalities in the myelodysplastic syndromes and occupational or environmental exposure. *Blood,* 95**,** 2093-7.

WILKINSON, E. 2023. NICE approves routine NHS use of CAR-T for diffuse large B-cell lymphoma. *Lancet Oncol,* 24**,** 208.

WOLF, Y., ANDERSON, A. C. & KUCHROO, V. K. 2020. TIM3 comes of age as an inhibitory receptor. *Nat Rev Immunol,* 20**,** 173-185.

WONG, H. S., PARK, K., GOLA, A., BAPTISTA, A. P., MILLER, C. H., DEEP, D., LOU, M., BOYD, L. F., RUDENSKY, A. Y., SAVAGE, P. A., ALTAN-BONNET, G., TSANG, J. S. & GERMAIN, R. N. 2021. A local regulatory T cell feedback circuit maintains immune homeostasis by pruning self-activated T cells. *Cell,* 184**,** 3981-3997 e22.

WU, D., YAN, R., SONG, S., SWANSIGER, A. K., LI, Y., PRELL, J. S., ZHOU, Q. & ROBINSON, C. V. 2024. The complete assembly of human LAT1-4F2hc complex provides insights into its regulation, function and localisation. *Nat Commun,* 15**,** 3711.

WU, D. & ZHU, Y. 2021. Role of kynurenine in promoting the generation of exhausted CD8(+) T cells in colorectal cancer. *Am J Transl Res,* 13**,** 1535-1547.

WU, H., LI, P., SHAO, N., MA, J., JI, M., SUN, X., MA, D. & JI, C. 2012. Aberrant expression of Treg-associated cytokine IL-35 along with IL-10 and TGF-beta in acute myeloid leukemia. *Oncol Lett,* 3**,** 1119-1123.

XIA, Y., JIN, S. & WU, Y. 2023. Small-molecule BCL6 inhibitor protects chronic cardiac transplant rejection and inhibits T follicular helper cell expansion and humoral response. *Front Pharmacol,* 14**,** 1140703.

XU, J., CHEN, S., LIANG, J., HAO, T., WANG, H., LIU, G., JIN, X., LI, H., ZHANG, J., ZHANG, C. & HE, Y. 2022a. Schlafen family is a prognostic biomarker and corresponds with immune infiltration in gastric cancer. *Front Immunol,* 13**,** 922138.

XU, L., ZHAO, B., BUTLER, W., XU, H., SONG, N., CHEN, X., SPENCER HAUCK, J., GAO, X., ZHANG, H., GROTH, J., YANG, Q., ZHAO, Y., MOON, D., GEORGE, D., ZHOU, Y., HE, Y. & HUANG, J. 2022b. Targeting glutamine metabolism network for the treatment of therapy-resistant prostate cancer. *Oncogene,* 41**,** 1140-1154.

XU, X., SUN, Q., LIANG, X., CHEN, Z., ZHANG, X., ZHOU, X., LI, M., TU, H., LIU, Y., TU, S. & LI, Y. 2019. Mechanisms of Relapse After CD19 CAR T-Cell Therapy for Acute Lymphoblastic Leukemia and Its Prevention and Treatment Strategies. *Front Immunol,* 10**,** 2664.

YANAGISAWA, N., HANA, K., NAKADA, N., ICHINOE, M., KOIZUMI, W., ENDOU, H., OKAYASU, I. & MURAKUMO, Y. 2014. High expression of L-type amino acid transporter 1 as a prognostic marker in bile duct adenocarcinomas. *Cancer Med,* 3**,** 1246-55.

YANG, J., HE, J., ZHANG, X., LI, J., WANG, Z., ZHANG, Y., QIU, L., WU, Q., SUN, Z., YE, X., YIN, W., CAO, W., SHEN, L., SERSCH, M. & LU, P. 2022a. Next-day manufacture of a novel anti-CD19 CAR-T therapy for B-cell acute lymphoblastic leukemia: first-in-human clinical study. *Blood Cancer J,* 12**,** 104.

YANG, Q., HAO, J., CHI, M., WANG, Y., XIN, B., HUANG, J., LU, J., LI, J., SUN, X., LI, C., HUO, Y., ZHANG, J., HAN, Y. & GUO, C. 2022b. Superior antitumor immunotherapy efficacy of

kynureninase modified CAR-T cells through targeting kynurenine metabolism. *Oncoimmunology,* 11**,** 2055703.
YANG, S., XIE, C., CHEN, Y., WANG, J., CHEN, X., LU, Z., JUNE, R. R. & ZHENG, S. G. 2019. Differential roles of TNFalpha-TNFR1 and TNFalpha-TNFR2 in the differentiation and function of CD4(+)Foxp3(+) induced Treg cells in vitro and in vivo periphery in autoimmune diseases. *Cell Death Dis,* 10**,** 27.
YARDEN, R. I., PARDO-REOYO, S., SGAGIAS, M., COWAN, K. H. & BRODY, L. C. 2002. BRCA1 regulates the G2/M checkpoint by activating Chk1 kinase upon DNA damage. *Nat Genet,* 30**,** 285-9.
YE, J., CHEN, X. & LU, W. 2021. Identification and Experimental Validation of Immune-Associate lncRNAs for Predicting Prognosis in Cervical Cancer. *Onco Targets Ther,* 14**,** 4721-4734.
YING, Z., HE, T., WANG, X., ZHENG, W., LIN, N., TU, M., XIE, Y., PING, L., ZHANG, C., LIU, W., DENG, L., QI, F., DING, Y., LU, X. A., SONG, Y. & ZHU, J. 2019. Parallel Comparison of 4-1BB or CD28 Co-stimulated CD19-Targeted CAR-T Cells for B Cell Non-Hodgkin's Lymphoma. *Mol Ther Oncolytics,* 15**,** 60-68.
YOKOSUKA, T., TAKAMATSU, M., KOBAYASHI-IMANISHI, W., HASHIMOTO-TANE, A., AZUMA, M. & SAITO, T. 2012. Programmed cell death 1 forms negative costimulatory microclusters that directly inhibit T cell receptor signaling by recruiting phosphatase SHP2. *J Exp Med,* 209**,** 1201-17.
YOO, H. J. & HARAPAN, B. N. 2021. Chimeric antigen receptor (CAR) immunotherapy: basic principles, current advances, and future prospects in neuro-oncology. *Immunol Res*.
YOON, H., TANG, C. M., BANERJEE, S., DELGADO, A. L., YEBRA, M., DAVIS, J. & SICKLICK, J. K. 2021. TGF-beta1-mediated transition of resident fibroblasts to cancer-associated fibroblasts promotes cancer metastasis in gastrointestinal stromal tumor. *Oncogenesis,* 10**,** 13.
YOU, S., ZHU, X., YANG, Y., DU, X., SONG, K., ZHENG, Q., ZENG, P. & YAO, Q. 2022. SLC7A1 Overexpression Is Involved in Energy Metabolism Reprogramming to Induce Tumor Progression in Epithelial Ovarian Cancer and Is Associated with Immune-Infiltrating Cells. *J Oncol,* 2022**,** 5864826.
YU, L., HUANG, L., LIN, D., LAI, X., WU, L., LIAO, X., LIU, J., ZENG, Y., LIANG, L., ZHANG, G., WANG, B., WU, Z., TAO, S., LIU, Y., JIAO, C., CHANG, L. J. & YANG, L. 2022. GD2-specific chimeric antigen receptor-modified T cells for the treatment of refractory and/or recurrent neuroblastoma in pediatric patients. *J Cancer Res Clin Oncol,* 148**,** 2643-2652.
YU, L., YANG, F., ZHANG, F., GUO, D., LI, L., WANG, X., LIANG, T., WANG, J., CAI, Z. & JIN, H. 2018. CD69 enhances immunosuppressive function of regulatory T-cells and attenuates colitis by prompting IL-10 production. *Cell Death Dis,* 9**,** 905.
YU, S., YI, M., QIN, S. & WU, K. 2019. Next generation chimeric antigen receptor T cells: safety strategies to overcome toxicity. *Mol Cancer,* 18**,** 125.
ZAMBRANO, A., MOLT, M., URIBE, E. & SALAS, M. 2019. Glut 1 in Cancer Cells and the Inhibitory Action of Resveratrol as A Potential Therapeutic Strategy. *Int J Mol Sci,* 20.
ZHAN, Y., LEW, A. M. & CHOPIN, M. 2019. The Pleiotropic Effects of the GM-CSF Rheostat on Myeloid Cell Differentiation and Function: More Than a Numbers Game. *Front Immunol,* 10**,** 2679.
ZHANG, K., CHEN, H., LI, F., HUANG, S., CHEN, F. & LI, Y. 2023a. Bright future or blind alley? CAR-T cell therapy for solid tumors. *Front Immunol,* 14**,** 1045024.

ZHANG, Q., HRESKO, M. E., PICTON, L. K., SU, L., HOLLANDER, M. J., NUNEZ-CRUZ, S., ZHANG, Z., ASSENMACHER, C. A., SOCKOLOSKY, J. T., GARCIA, K. C. & MILONE, M. C. 2021a. A human orthogonal IL-2 and IL-2Rbeta system enhances CAR T cell expansion and antitumor activity in a murine model of leukemia. *Sci Transl Med,* 13**,** eabg6986.

ZHANG, S., KOHLI, K., BLACK, R. G., YAO, L., SPADINGER, S. M., HE, Q., PILLARISETTY, V. G., CRANMER, L. D., VAN TINE, B. A., YEE, C., PIERCE, R. H., RIDDELL, S. R., JONES, R. L. & POLLACK, S. M. 2019. Systemic Interferon-gamma Increases MHC Class I Expression and T-cell Infiltration in Cold Tumors: Results of a Phase 0 Clinical Trial. *Cancer Immunol Res,* 7**,** 1237-1243.

ZHANG, W., CAO, X., ZHONG, X., WU, H., SHI, Y., FENG, M., WANG, Y. C., ANN, D., GWACK, Y., YUAN, Y. C., SHANG, W. & SUN, Z. 2023b. SRC2 controls CD4(+) T cell activation via stimulating c-Myc-mediated upregulation of amino acid transporter Slc7a5. *Proc Natl Acad Sci U S A,* 120**,** e2221352120.

ZHANG, X., LU, X. A., YANG, J., ZHANG, G., LI, J., SONG, L., SU, Y., SHI, Y., ZHANG, M., HE, J., SONG, D., LV, F., LI, W., WU, Y., WANG, H., LIU, H., ZHOU, X., HE, T. & LU, P. 2020a. Efficacy and safety of anti-CD19 CAR T-cell therapy in 110 patients with B-cell acute lymphoblastic leukemia with high-risk features. *Blood Adv,* 4**,** 2325-2338.

ZHANG, X., ZHENG, P., PRESTWOOD, T. R., ZHANG, H., CARMI, Y., TOLENTINO, L. L., WU, N., CHOI, O., WINER, D. A., STROBER, S., KANG, E. S., ALONSO, M. N. & ENGLEMAN, E. G. 2020b. Human Regulatory Dendritic Cells Develop From Monocytes in Response to Signals From Regulatory and Helper T Cells. *Front Immunol,* 11**,** 1982.

ZHANG, Y., LI, B., BAI, Q., WANG, P., WEI, G., LI, Z., HU, L., TIAN, Q., ZHOU, J., HUANG, Q., WANG, Z., YUE, S., WU, J., YANG, L., ZHOU, X., JIANG, L., NI, T., YE, L. & WU, Y. 2021b. The lncRNA Snhg1-Vps13D vesicle trafficking system promotes memory CD8 T cell establishment via regulating the dual effects of IL-7 signaling. *Signal Transduct Target Ther,* 6**,** 126.

ZHANG, Y., LI, C., DU, M., JIANG, H., LUO, W., TANG, L., KANG, Y., XU, J., WU, Z., WANG, X., HUANG, Z., ZHANG, Y., WU, D., CHANG, A. H., HU, Y. & MEI, H. 2023c. Allogenic and autologous anti-CD7 CAR-T cell therapies in relapsed or refractory T-cell malignancies. *Blood Cancer J,* 13**,** 61.

ZHAO, C., YANG, S., LU, W., LIU, J., WEI, Y., GUO, H., ZHANG, Y. & SHI, J. 2020. Increased NFATC4 Correlates With Poor Prognosis of AML Through Recruiting Regulatory T Cells. *Front Genet,* 11**,** 573124.

ZHAO, W. H., WANG, B. Y., CHEN, L. J., FU, W. J., XU, J., LIU, J., JIN, S. W., CHEN, Y. X., CAO, X. M., YANG, Y., ZHANG, Y. L., WANG, F. X., ZHANG, P. Y., LEI, B., GU, L. F., WANG, J. L., ZHANG, H., BAI, J., XU, Y., ZHU, H., DU, J., JIANG, H., FAN, X. H., LI, J. Y., HOU, J., CHEN, Z., ZHANG, W. G., MI, J. Q., CHEN, S. J. & HE, A. L. 2022a. Four-year follow-up of LCAR-B38M in relapsed or refractory multiple myeloma: a phase 1, single-arm, open-label, multicenter study in China (LEGEND-2). *J Hematol Oncol,* 15**,** 86.

ZHAO, X., LI, Y. & WU, H. 2018. A novel scoring system for acute myeloid leukemia risk assessment based on the expression levels of six genes. *Int J Mol Med,* 42**,** 1495-1507.

ZHAO, Y., DENG, J., RAO, S., GUO, S., SHEN, J., DU, F., WU, X., CHEN, Y., LI, M., CHEN, M., LI, X., LI, W., GU, L., SUN, Y., ZHANG, Z., WEN, Q., XIAO, Z. & LI, J. 2022b. Tumor Infiltrating Lymphocyte (TIL) Therapy for Solid Tumor Treatment: Progressions and Challenges. *Cancers (Basel),* 14.

ZHAO, Z., DING, H., LIN, Z. B., QIU, S. H., ZHANG, Y. R., GUO, Y. G., CHU, X. D., SAM, L. I., PAN, J. H. & PAN, Y. L. 2021. Relationship between Tertiary Lymphoid Structure and the Prognosis and Clinicopathologic Characteristics in Solid Tumors. *Int J Med Sci,* 18**,** 2327-2338.

ZHOU, J., ZHU, J., YU, S. J., MA, H. L., CHEN, J., DING, X. F., CHEN, G., LIANG, Y. & ZHANG, Q. 2020a. Sodium-glucose co-transporter-2 (SGLT-2) inhibition reduces glucose uptake to induce breast cancer cell growth arrest through AMPK/mTOR pathway. *Biomed Pharmacother,* 132**,** 110821.

ZHOU, X., ZHENG, M., WANG, Q., AA, J., CAO, B. & LI, J. 2020b. Metabolomics analysis identifies lysine and taurine as candidate prognostic biomarkers for AML-M2 patients. *Int J Hematol,* 111**,** 761-770.

ZHOU, Y., MU, W., WANG, C., ZHUO, Z., XIN, Y., LI, H. & WANG, C. 2023. Ray of dawn: Anti-PD-1 immunotherapy enhances the chimeric antigen receptor T-cell therapy in Lymphoma patients. *BMC Cancer,* 23**,** 1019.

ZHU, C., ZHAO, Y., HE, J., ZHAO, H., NI, L., CHENG, X., CHEN, Y., MU, L., ZHOU, X., SHI, Q. & SUN, J. 2023. TIL-Derived CAR T Cells Improve Immune Cell Infiltration and Survival in the Treatment of CD19-Humanized Mouse Colorectal Cancer. *Cancers (Basel),* 15.

ZHU, J. W., FIELD, S. J., GORE, L., THOMPSON, M., YANG, H., FUJIWARA, Y., CARDIFF, R. D., GREENBERG, M., ORKIN, S. H. & DEGREGORI, J. 2001. E2F1 and E2F2 determine thresholds for antigen-induced T-cell proliferation and suppress tumorigenesis. *Mol Cell Biol,* 21**,** 8547-64.

8. Supplementary data

8.1 anti-CD33 SLC7A5 CAR T-cell sequence

This is the code for the following components: truncated CD34, F2A peptide linker, CD8 signal peptide, CD33 ScFV, CD8 Hinge/transmembrane, 4-1BB intracellular signalling domain, CD3zeta intracellular signalling domain, P2A peptide linker, and SLC7A5.

ATGCCTCGCGGCTGGACAGCCCTGTGCCTGCTGTCTCTGCTGCCATCCGGCTTCATGAGCCTGGATA
ATAACGGCACAGCCACCCCAGAGCTGCCTACACAGGGCACCTTCAGCAATGTGTCCACAAACGTGA
GCTATCAGGAGACCACAACCCCTTCTACCCTGGGATCCACAAGCCTGCACCCCGTGTCTCAGCACGG
CAACGAAGCCACCACCAACATCACCGAGACCACAGTGAAGTTTACCTCCACCTCTGTGATTACCTCTG
TGTACGGAAATACAAACTCCAGCGTGCAGTCTCAGACATCTGTGATCTCCACAGTGTTTACAACACCT
GCCAATGTGTCCACCCCAGAGACAACCCTGAAGCCCAGCCTGTCTCCTGGAAATGTGTCCGATCTGT
CTACCACCTCCACCAGCCTGGCCACCTCTCCCACCAAGCCCTATACCTCCTCTTCTCCCATCCTGAGCG
ATATCAAAGCCGAGATCAAATGCAGCGGGATTCGGGAAGTGAAACTGACACAGGGCATCTGCCTGG
AACAGAATAAGACATCCAGCTGCGCCGAGTTTAAGAAAGATAGAGGAGAGGGACTGGCCAGGGTG
CTGTGTGGCGAAGAGCAGGCCGACGCCGATGCCGGCGCCCAGGTGTGTTCCCTGCTGCTGGCCCAG
TCTGAGGTGCGCCCCCAGTGCCTGCTGCTGGTGCTGGCCAATCGGACAGAAATTAGCAGCAAGCTG
CAGCTGATGAAAAAACACCAGAGCGATCTGAAAAAGCTGGGCATCCTGGACTTTACCGAGCAGGAC
GTGGCCTCTCACCAGAGCTACAGCCAGAAAACACTGATCGCCCTGGTGACCAGCGGAGCCCTGCTG
GCCGTGCTGGGCATCACCGGATATTTCCTGATGAATAGGCGCAGCTGGAGCCCCACCGGCGAACGG
CTGGAGCTGGAGCCTGTCGACCGAGTGAAGCAGACCCTGAACTTTGATCTGCTGAAGCTGGCCGGC
GACGTGGAGTCCAACCCCGGGCCAGGGAATATGGCCTTACCAGTGACCGCCTTGCTCCTGCCGCTG
GCCTTGCTGCTCCACGCCGCCAGGCCGGGATCCAACATCATGCTGACCCAGAGCCCTAGCAGCCTGG
CCGTGTCTGCCGGCGAGAAAGTGACCATGAGCTGCAAGAGCAGCCAGAGCGTGTTCTTCAGCAGCT
CCCAGAAGAACTACCTAGCCTGGTATCAGCAGATCCCAGGCCAGAGCCCTAAGCTGCTGATCTACTG
GGCCAGCACCAGAGAAAGCGGCGTGCCCGATAGATTCACCGGAAGCGGTTCTGGCACCGACTTCAC
CCTGACAATCAGCAGCGTGCAGAGCGAGGACCTGGCCATCTACTACTGCCACCAGTACCTGAGCAG
CCGGACCTTTGGCGGAGGCACCAAGCTGGAAATCAAGAGAGGCGGCGGAGGCTCAGGCGGAGGC
GGATCTAGTGGCGGAGGATCTCAGGTGCAGCTGCAGCAGCCAGGCGCCGAGGTCGTGAAACCTGG
CGCCTCTGTGAAGATGTCCTGCAAGGCCAGCGGCTACACCTTCACCAGCTACTACATCCACTGGATC
AAGCAGACCCCTGGACAGGGCCTGGAATGGGTGGGAGTGATCTACCCCGGCAACGACGACATCAG
CTACAACCAGAAGTTCAAGGGCAAGGCCACCCTGACCGCCGACAAGTCTAGCACCACCGCCTACAT
GCAGCTGTCCAGCCTGACCAGCGAGGACAGCGCCGTGTACTACTGCGCCAGAGAAGTGCGGCTGC
GGTACTTCGATGTGTGGGGAGCCGGCACCACCGTGACCGTGTCATCTACCACGACGCCAGCACCGC
GACCACCAACACCGGCGCCAACCATCGCATCGCAGCCCCTGTCCCTGCGCCCAGAGGCGTGCCGACC
AGCGGCGGGGGGCGCAGTGCACACGAGGGGGCTGGACTTCGCCTGTGATATCTACATCTGGGCGC
CCTTGGCCGGGACTTGTGGGGTCCTTCTCCTGTCACTGGTTATCACCCTTTACTGCAAACGGGGCAG
AAAGAAACTCCTGTATATATTCAAACAACCATTTATGAGACCAGTACAAACTACTCAAGAGGAAGAT
GGCTGTAGCTGCCGATTTCCAGAAGAAGAAGAAGGAGGATGTGAACTGAGAGTGAAGTTCAGCAG
GAGCGCAGACGCCCCCGCGTACAAGCAGGGCCAGAACCAGCTCTATAACGAGCTCAATCTAGGACG
AAGAGAGGAGTACGATGTTTTGGACAAGAGACGTGGCCGGGACCCTGAGATGGGGGGAAAGCCG
AGAAGGAAGAACCCTCAGGAAGGCCTGTACAATGAACTGCAGAAAGATAAGATGGCGGAGGCCTA

CAGTGAGATTGGGATGAAAGGCGAGCGCCGGAGGGGCAAGGGGCACGATGGCCTTTACCAGGGT
CTCAGTACAGCCACCAAGGACACCTACGACGCCCTTCACATGCAGGCCCTGCCCCCTCGCGCCACCA
ACTTCAGCCTGCTGAAGCAGGCCGGCGACGTGGAGGAAAACCCTGGCCCCATGGCCGGCGCTGGA
CCTAAGAGAAGGGCTCTGGCTGCTCCCGCTGCTGAGGAGAAAGAAGAGGCTAGAGAGAAGATGCT
GGCTGCTAAGAGCGCCGATGGCTCCGCTCCCGCCGGAGAAGGAGAGGGCGTGACACTGCAGAGGA
ACATCACACTGCTCAACGGCGTCGCCATTATCGTGGGCACCATCATTGGAAGCGGCATCTTCGTGAC
CCCCACCGGCGTGCTGAAGGAGGCTGGATCCCCCGGACTGGCTCTGGTGGTCTGGGCTGCTTGCGG
CGTGTTCAGCATTGTGGGCGCTCTGTGTTACGCCGAACTGGGCACCACCATTAGCAAAAGCGGAGG
AGACTACGCCTACATGCTGGAAGTGTACGGAAGCCTCCCCGCCTTCCTCAAGCTGTGGATCGAGCTG
CTGATCATTAGGCCTTCCAGCCAGTACATCGTCGCCCTCGTCTTCGCCACATATCTGCTCAAGCCTCT
GTTTCCCACATGCCCCGTGCCCGAGGAGGCTGCTAAACTGGTCGCTTGTCTCTGTGTGCTGCTGCTG
ACAGCCGTCAATTGTTACAGCGTCAAGGCTGCCACAAGAGTGCAAGACGCTTTTGCCGCCGCTAAGC
TGCTCGCCCTCGCTCTGATCATTCTGCTGGGCTTCGTCCAAATTGGCAAGGGCGATGTCAGCAATCT
GGACCCCAACTTCTCCTTCGAGGGCACCAAACTCGACGTGGGCAACATCGTGCTCGCTCTGTATTCC
GGACTGTTCGCTTACGGAGGCTGGAACTATCTGAACTTCGTCACCGAGGAGATGATCAACCCCTATA
GAAATCTGCCTCTGGCTATCATCATCTCTCTGCCCATCGTCACACTGGTGTATGTGCTCACCAATCTG
GCCTACTTCACCACACTGAGCACAGAACAGATGCTGTCCAGCGAAGCCGTCGCCGTGGACTTTGGCA
ACTATCATCTGGGCGTGATGAGCTGGATCATCCCCGTGTTCGTCGGACTGAGCTGCTTCGGCTCCGT
GAATGGATCCCTCTTTACAAGCTCTAGACTCTTCTTCGTGGGCTCTAGAGAGGGACATCTGCCTAGC
ATCCTCAGCATGATTCACCCTCAGCTGCTGACCCCCGTGCCCTCTCTGGTGTTCACATGCGTGATGAC
ACTGCTGTACGCCTTCAGCAAGGATATCTTCAGCGTGATTAATTTTTTTAGCTTTTTCAACTGGCTCTG
CGTGGCTCTGGCCATCATTGGCATGATTTGGCTGAGACATAGAAAACCCGAGCTGGAGAGGCCCAT
CAAAGTGAATCTGGCTCTGCCCGTGTTCTTCATTCTCGCTTGTCTGTTTCTGATTGCCGTGTCCTTCTG
GAAGACCCCCGTGGAATGCGGCATTGGCTTCACCATCATTCTGTCCGGCCTCCCCGTGTACTTCTTCG
GCGTCTGGTGGAAGAACAAGCCCAAGTGGCTGCTGCAAGGCATCTTCAGCACCACAGTGCTGTGCC
AAAAGCTGATGCAAGTGGTGCCCCAAGAGACATGA

8.2 anti-CD33 SLC7A11 CAR T-cell sequence

This is the code for the following components: Truncated CD34, F2A peptide linker, CD8 signal peptide, CD33 ScFV, CD8 Hinge/transmembrane, 4-1BB intrcellular signalling domain, CD3z signalling domain, P2A peptide linker, and SLC7A11 transporter.

ATGCCTCGCGGCTGGACAGCCCTGTGCCTGCTGTCTCTGCTGCCATCCGGCTTCATGAGCCTGGATA
ATAACGGCACAGCCACCCCAGAGCTGCCTACACAGGGCACCTTCAGCAATGTGTCCACAAACGTGA
GCTATCAGGAGACCACAACCCCTTCTACCCTGGGATCCACAAGCCTGCACCCCGTGTCTCAGCACGG
CAACGAAGCCACCACCAACATCACCGAGACCACAGTGAAGTTTACCTCCACCTCTGTGATTACCTCTG
TGTACGGAAATACAAACTCCAGCGTGCAGTCTCAGACATCTGTGATCTCCACAGTGTTTACAACACCT
GCCAATGTGTCCACCCCAGAGACAACCCTGAAGCCCAGCCTGTCTCCTGGAAATGTGTCCGATCTGT
CTACCACCTCCACCAGCCTGGCCACCTCTCCCACCAAGCCCTATACCTCCTCTTCTCCCATCCTGAGCG
ATATCAAAGCCGAGATCAAATGCAGCGGGATTCGGGAAGTGAAACTGACACAGGGCATCTGCCTGG
AACAGAATAAGACATCCAGCTGCGCCGAGTTTAAGAAAGATAGAGGAGAGGGACTGGCCAGGGTG
CTGTGTGGCGAAGAGCAGGCCGACGCCGATGCCGGCGCCCAGGTGTGTTCCCTGCTGCTGGCCCAG
TCTGAGGTGCGCCCCCAGTGCCTGCTGCTGGTGCTGGCCAATCGGACAGAAATTAGCAGCAAGCTG
CAGCTGATGAAAAAACACCAGAGCGATCTGAAAAAGCTGGGCATCCTGGACTTTACCGAGCAGGAC
GTGGCCTCTCACCAGAGCTACAGCCAGAAAACACTGATCGCCCTGGTGACCAGCGGAGCCCTGCTG
GCCGTGCTGGGCATCACCGGATATTTCCTGATGAATAGGCGCAGCTGGAGCCCCACCGGCGAACGG
CTGGAGCTGGAGCCTGTCGACCGAGTGAAGCAGACCCTGAACTTTGATCTGCTGAAGCTGGCCGGC
GACGTGGAGTCCAACCCCGGGCCAGGGAATATGGCCTTACCAGTGACCGCCTTGCTCCTGCCGCTG
GCCTTGCTGCTCCACGCCGCCAGGCCGGGATCCAACATCATGCTGACCCAGAGCCCTAGCAGCCTGG
CCGTGTCTGCCGGCGAGAAAGTGACCATGAGCTGCAAGAGCAGCCAGAGCGTGTTCTTCAGCAGCT
CCCAGAAGAACTACCTAGCCTGGTATCAGCAGATCCCAGGCCAGAGCCCTAAGCTGCTGATCTACTG
GGCCAGCACCAGAGAAAGCGGCGTGCCCGATAGATTCACCGGAAGCGGTTCTGGCACCGACTTCAC
CCTGACAATCAGCAGCGTGCAGAGCGAGGACCTGGCCATCTACTACTGCCACCAGTACCTGAGCAG
CCGGACCTTTGGCGGAGGCACCAAGCTGGAAATCAAGAGAGGCGGCGGAGGCTCAGGCGGAGGC
GGATCTAGTGGCGGAGGATCTCAGGTGCAGCTGCAGCAGCCAGGCGCCGAGGTCGTGAAACCTGG
CGCCTCTGTGAAGATGTCCTGCAAGGCCAGCGGCTACACCTTCACCAGCTACTACATCCACTGGATC
AAGCAGACCCCTGGACAGGGCCTGGAATGGGTGGGAGTGATCTACCCCGGCAACGACGACATCAG
CTACAACCAGAAGTTCAAGGGCAAGGCCACCCTGACCGCCGACAAGTCTAGCACCACCGCCTACAT
GCAGCTGTCCAGCCTGACCAGCGAGGACAGCGCCGTGTACTACTGCGCCAGAGAAGTGCGGCTGC
GGTACTTCGATGTGTGGGGAGCCGGCACCACCGTGACCGTGTCATCTACCACGACGCCAGCACCGC
GACCACCAACACCGGCGCCAACCATCGCATCGCAGCCCCTGTCCCTGCGCCCAGAGGCGTGCCGACC
AGCGGCGGGGGGCGCAGTGCACACGAGGGGGCTGGACTTCGCCTGTGATATCTACATCTGGGCGC
CCTTGGCCGGGACTTGTGGGGTCCTTCTCCTGTCACTGGTTATCACCCTTTACTGCAAACGGGGCAG
AAAGAAACTCCTGTATATATTCAAACAACCATTTATGAGACCAGTACAAACTACTCAAGAGGAAGAT
GGCTGTAGCTGCCGATTTCCAGAAGAAGAAGAAGGAGGATGTGAACTGAGAGTGAAGTTCAGCAG
GAGCGCAGACGCCCCCGCGTACAAGCAGGGCCAGAACCAGCTCTATAACGAGCTCAATCTAGGACG
AAGAGAGGAGTACGATGTTTTGGACAAGAGACGTGGCCGGGACCCTGAGATGGGGGGAAAGCCG
AGAAGGAAGAACCCTCAGGAAGGCCTGTACAATGAACTGCAGAAAGATAAGATGGCGGAGGCCTA
CAGTGAGATTGGGATGAAAGGCGAGCGCCGGAGGGGCAAGGGGCACGATGGCCTTTACCAGGGT
CTCAGTACAGCCACCAAGGACACCTACGACGCCCTTCACATGCAGGCCCTGCCCCCTCGCGCCACCA

ACTTCAGCCTGCTGAAGCAGGCCGGCGACGTGGAGGAAAACCCTGGCCCCATGGTGAGGAAACCC
GTGGTGTCCACAATCAGCAAGGGCGGCTATCTGCAAGGCAATGTGAACGGCAGACTGCCTAGCCTC
GGAAACAAGGAACCCCCCGGCCAAGAGAAGGTGCAGCTGAAGAGGAAAGTGACACTGCTGAGAG
GCGTCTCCATCATTATCGGCACCATCATCGGAGCTGGCATCTTCATCAGCCCTAAGGGCGTGCTCCA
GAACACCGGATCCGTCGGCATGTCTCTGACCATCTGGACCGTCTGCGGCGTGCTGTCTCTGTTTGGC
GCCCTCTCCTACGCCGAGCTGGGAACAACCATCAAGAAGTCCGGCGGCCACTATACCTACATTCTGG
AAGTCTTCGGCCCTCTGCCCGCCTTTGTGAGAGTGTGGGTGGAGCTGCTGATCATTAGACCCGCCGC
CACCGCTGTCATTTCTCTGGCTTTCGGAAGGTACATTCTGGAGCCCTTCTTCATCCAGTGTGAGATCC
CCGAGCTGGCTATCAAGCTGATCACCGCTGTCGGCATCACCGTGGTCATGGTCCTCAACAGCATGAG
CGTGAGCTGGAGCGCTAGGATCCAGATCTTTCTGACCTTCTGCAAGCTGACAGCCATTCTGATCATC
ATTGTCCCCGGAGTCATGCAGCTGATTAAGGGCCAGACCCAGAACTTTAAGGACGCCTTTAGCGGA
AGAGACAGCAGCATCACAAGGCTGCCCCTCGCCTTTTACTACGGCATGTACGCCTATGCCGGCTGGT
TTTATCTGAACTTCGTCACCGAGGAGGTGGAGAACCCCGAGAAGACCATCCCTCTGGCCATCTGCAT
CTCCATGGCCATCGTGACAATCGGATACGTGCTCACCAACGTCGCCTACTTTACCACCATCAATGCCG
AAGAGCTGCTGCTCTCCAATGCTGTCGCCGTCACATTTTCCGAAAGGCTGCTGGGCAATTTCTCTCTG
GCCGTGCCTATCTTTGTGGCTCTGAGCTGTTTCGGCAGCATGAACGGCGGAGTGTTCGCCGTGTCTA
GACTGTTCTACGTGGCCTCCAGAGAGGGACATCTGCCCGAGATCCTCTCCATGATCCACGTGAGGAA
GCACACCCCTCTGCCCGCCGTGATCGTGCTCCACCCTCTGACCATGATCATGCTCTTTTCCGGAGATC
TGGATTCTCTGCTGAACTTTCTGTCCTTCGCTAGATGGCTGTTTATCGGACTGGCTGTGGCCGGACTG
ATTTATCTGAGATACAAGTGCCCCGACATGCACAGACCCTTTAAGGTGCCTCTGTTTATCCCCGCTCT
GTTCAGCTTCACATGTCTGTTCATGGTCGCCCTCTCCCTCTACAGCGACCCCTTCTCCACCGGCATCGG
ATTCGTCATTACACTGACCGGCGTGCCCGCCTATTACCTCTTTATCATCTGGGACAAGAAGCCTAGAT
GGTTTAGGATCATGAGCGAGAAGATCACAAGAACCCTCCAAATCATTCTCGAGGTGGTCCCCGAGG
AAGATAAGCTGTGA